

國立臺灣大學醫學院臨床醫學研究所

博士論文

Graduate Institute of Clinical Medicine

College of Medicine

National Taiwan University

Doctoral dissertation



膽汁傳輸蛋白之肝細胞分布與膽汁滯留疾病之相關機轉

The subcellular trafficking and targeting of bile salt export pump in
hepatocytes and related mechanisms in cholestatic liver diseases

吳上欣

Shang-Hsin Wu

指導教授：張美惠教授 陳惠玲博士

Advisor: Mei-Hwei Chang, M.D. Hui-Ling Chen, Ph.D.

中華民國 108 年 9 月

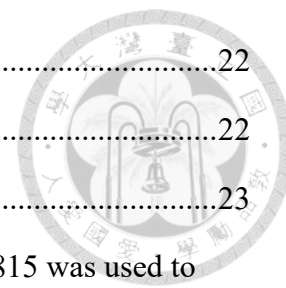
September, 2019



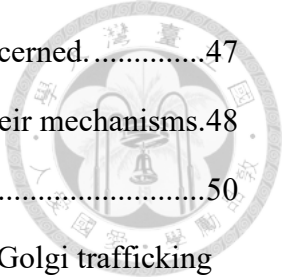
Contents

| | |
|---|------|
| Contents..... | i |
| 誌謝..... | viii |
| 摘要..... | x |
| ABSTRACT..... | xii |
| Chapter 1 Background and specific aims..... | 1 |
| 1.1. Cholestatic liver diseases..... | 1 |
| 1.2. The function and composition of bile..... | 1 |
| 1.3. Biosynthesis, homeostasis, and the enterohepatic circulation of bile acids..... | 2 |
| 1.4. The transporters mediating the transfer of bile acids and other bile ingredients...5 | |
| 1.5. Progressive intrahepatic cholestasis (PFIC)..... | 6 |
| 1.6. The bile salt export pump (BSEP) is the canalicular bile acid transporter. | 7 |
| 1.7. Developmental expression of BSEP/Bsep orthologs..... | 11 |
| 1.8. Bile salt preferences of BSEP/Bsep orthologs..... | 11 |
| 1.9. <i>Abcb11/Bsep</i> knockout animal models..... | 12 |
| 1.10. Subcellular trafficking of BSEP..... | 15 |
| 1.11. BSEP interacting proteins that participate in subcellular trafficking of BSEP.. | 16 |
| 1.12. Research Questions and Niches..... | 17 |
| 1.13. Hypothesis and specific aims..... | 18 |
| Chapter 2 Identification of BSEP-interacting proteins..... | 20 |
| 2.1. Introduction..... | 20 |
| 2.2. Materials and Methods..... | 20 |
| 2.2.1. Reagents and chemicals..... | 20 |
| 2.2.2. Plasmid construction..... | 21 |
| 2.2.3. Yeast transformation, protein extraction, and 3-AT titration..... | 21 |
| 2.2.4. The human fetal liver cDNA library..... | 21 |

| | |
|--|----|
| 2.2.5. Yeast two-hybrid and β -galactosidase filter assays..... | 22 |
| 2.2.6. Determination of cDNA identities | 22 |
| 2.3. Results | 23 |
| 2.3.1. The human BSEP polypeptide spanning amino acid 270-815 was used to search the BSEP-interacting proteins through yeast two-hybrid assays. | 23 |
| 2.3.2. Approximate 15% of yeast colonies identified from yeast two-hybrid screening reveals strong β -galactosidase activity..... | 24 |
| 2.3.3. Analysis of yeast plasmid inserts by polymerase chain reaction | 24 |
| 2.4. Summary | 25 |
| Chapter 3 The ESCRT machinery participates the post-Golgi trafficking of BSEP | 26 |
| 3.1. Introduction | 26 |
| 3.2. Materials and Methods | 27 |
| 3.2.1. Human liver samples | 27 |
| 3.2.2. Plasmid construction and transfection..... | 27 |
| 3.2.3. Hydrodynamic injection of mice | 28 |
| 3.2.4. Yeast two-hybrid screen and interaction assay | 29 |
| 3.2.5. Cell culture | 29 |
| 3.2.6. Temperature shift assay..... | 29 |
| 3.2.7. Protein extraction and subcellular fractionation..... | 29 |
| 3.2.8. Antibodies, immunoprecipitation, Western blotting and immunostaining ... | 30 |
| 3.2.9. RNA interference and quantitative RT-PCR..... | 31 |
| 3.2.10. Determination of total bile acids | 32 |
| 3.2.11. Image acquisition and processing | 32 |
| 3.2.12. Subcellular distribution index and canalicular targeting index..... | 32 |
| 3.2.13. Statistical analysis | 33 |
| 3.3. Results | 33 |
| 3.3.1. The ESCRT-III CHMP5 interacts with BSEP. | 33 |
| 3.3.2. Subapical BSEP localizes in CHMP5-positive subapical compartments. | 34 |

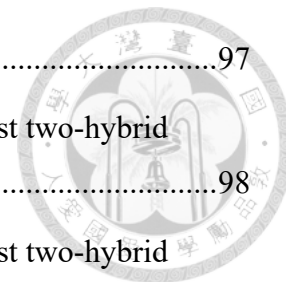


| | |
|--|----|
| 3.3.3. Cholestatic human livers demonstrate aberrant subapical BSEP vesicles. | 35 |
| 3.3.4. The canalicular targeting of BSEP is developmentally associated with CHMP5..... | 35 |
| 3.3.5. Aberrant interaction between BSEP mutants and CHMP5 affects the polarized trafficking of BSEP mutants..... | 36 |
| 3.3.6. CHMP5 regulates the apical targeting of BSEP and BSEP-mediated bile acid secretion. | 38 |
| 3.3.7. K63-linked ubiquitination of BSEP is required for the BSEP apical-targeting via CHMP5 associated ESCRT machinery. | 39 |
| 3.3.8. The ESCRT machinery affects the polarized trafficking of BSEP. | 40 |
| 3.3.9. The ESCRT machinery is upstream of Rab11A to affect the post-Golgi trafficking of BSEP. | 40 |
| 3.4. Summary | 41 |
| Chapter 4 Plectin mutations in progressive familial intrahepatic cholestasis | 42 |
| 4.1. Introduction | 42 |
| 4.2. Materials and Methods | 43 |
| 4.2.1. Antibodies and Reagents | 43 |
| 4.2.2. Immunofluorescence staining | 43 |
| 4.2.3. Image acquisition | 43 |
| 4.2.4. Analysis and Statistics of PLEC-K8 colocalization..... | 44 |
| 4.3. Results | 44 |
| 4.3.1. Case description | 44 |
| 4.3.2. Plectin mutations are associated to PFIC | 45 |
| 4.3.3. Decreased colocalization of PLEC and Keratin 8 (K8) in the liver samples of PLEC mutations | 45 |
| 4.3.4. PLEC mutated livers show impaired canalicular expression of BSEP, dilated bile canaliculi, and distorted bile ducts. | 46 |
| 4.4. Summary | 46 |
| Chapter 5 Discussion..... | 47 |



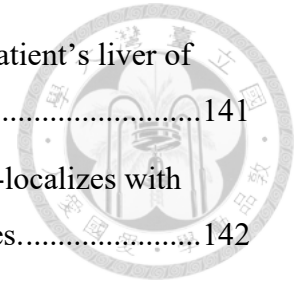
| | |
|---|----|
| 5.1. Some underlying factors in human <i>BSEP</i> cDNA should be concerned..... | 47 |
| 5.2. Limited information of BSEP-interacting proteins as well as their mechanisms..... | 48 |
| 5.3. ESCRTs involve in post-Golgi trafficking of BSEP..... | 50 |
| 5.4. Both ESCRTs and endosomal Rab proteins participate in post-Golgi trafficking of apical proteins. | 51 |
| 5.5. Defects in canalicular sorting of BSEP mutants may be caused by aberrant association with ESCRTs. | 52 |
| 5.6. A proposed model of ESCRTs regulating the apical targeting of BSEP | 54 |
| 5.7. Cholestatic liver diseases may be tangled with cytoskeleton disorganization and mis-sorting of canalicular transporters. | 55 |
| Chapter 6 Perspectives | 59 |
| 6.1. Ubiquitination and deubiquitination of BSEP..... | 59 |
| 6.2. The role of autophagy in canalicular expression of BSEP..... | 60 |
| 6.3. COPA may mediate BSEP between ER and Golgi..... | 61 |
| 6.4. The cytoskeleton network and cytoskeleton-associated proteins in BSEP trafficking..... | 61 |
| 6.5. To search underlying cholestasis-associated genes and to generate <i>in vitro</i> and <i>in vivo</i> models for studying BSEP and cholestasis are essential not only to disease mechanism but also to drug screening. | 62 |
| References | 63 |
| Tables | 91 |
| Table 1 Progressive familial intrahepatic cholestasis (PFIC)* | 91 |
| Table 2 A comparison of human, rat, mouse and skate BSEP/Bsep orthologs..... | 93 |
| Table 3 Comparison of Km/*Ki values and bile salt transport between human, rat, mouse and skate membrane vesicles from the liver and the cell with ectopic BSEP/Bsep expression. | 94 |
| Table 4 The rank order of different bile salts transported by the Bsep ortholog of human, rat, mouse, and skate. | 95 |
| Table 5 A comarison of <i>Abcb11/abcb11b</i> knockout (KO) animal models..... | 96 |

| | |
|--|-----|
| Table 6 Statistics and classification of β -galactosidase assays | 97 |
| Table 7 Classification of the cDNA inserts identified from the yeast two-hybrid screen for BSEP-interacting proteins. | 98 |
| Table 8 Classification of the cDNA inserts identified from the yeast two-hybrid screen for BSEP-interacting proteins. | 100 |
| Table 9 Clinical characteristics with serial laboratory data | 101 |
| Table 10 Jaundice-associated gene panel for target-gene enriched next-generation sequencing..... | 102 |
| Table 11 The Variants of the Five Genes Identified Using the Whole-Exome Sequencing from the Family Suspected of PFIC | 103 |
| Table 12 The Protein Encoded, Functions, Tissue Expression and Disease Association of the Gene Variants Identified in The Family of Progressive Familial Intrahepatic Cholestasis..... | 104 |
| Figures..... | 105 |
| Figure 1 Etiologies of intrahepatic and extrahepatic cholestasis of congenital or acquired causes..... | 105 |
| Figure 2 Functions of PFIC- and other cholestasis-associated proteins..... | 106 |
| Figure 3 The synthesis pathways of bile acids..... | 107 |
| Figure 4 The enterohepatic circulation and homeostasis of bile acids..... | 108 |
| Figure 5 Milestones of BSEP/Bsep being characterized as the canalicular bile acid transporter (cBAT). | 110 |
| Figure 6 The line graph illustrates developmental expression of rat hepatic transporters. | 112 |
| Figure 7 Graphic illustration of subcellular trafficking of BSEP in hepatocytes..... | 113 |
| Figure 8 The protein alignment of human, rat, and mouse BSEP orthologs spanning amino acids from 270 to 815..... | 114 |
| Figure 9 The bait protein, BSEP (270-815), is unstable in yeast competent cells.... | 115 |
| Figure 10 The bait protein, BSEP (270-815), is unstable in yeast competent cells.. | 116 |
| Figure 11 The flow chart illustrates the search of BSEP-interacting proteins..... | 117 |



| | |
|---|-----|
| Figure 12 A representative result of β -galactosidase filter assays. | 118 |
| Figure 13 The ESCRT-III subunit CHMP5 co-localizes with BSEP in the subapical compartments of hepatocytes. | 120 |
| Figure 14 Aberrant subapical BSEP compartments in cholestatic human livers are CHMP5 positive. | 122 |
| Figure 15 Impaired polarized trafficking of BSEP-R487H and BSEP-N490D mutants <i>in vivo</i> and <i>in vitro</i> | 123 |
| Figure 16 Aberrant association between CHMP5 and the two BSEP-R487H and BSEP-N490D mutants. | 125 |
| Figure 17 The protein expression and turnover of BSEP is unaffected with CHMP5 knockdown. | 126 |
| Figure 18 CHMP5 regulates the apical targeting of BSEP <i>in vivo</i> and <i>in vitro</i> | 127 |
| Figure 19 CHMP5 indirectly regulates BSEP-mediated bile acid secretion. | 129 |
| Figure 20 BSEP is abundantly modified with K63-linked ubiquitination. | 130 |
| Figure 21 Both VPS4 molecules affect post-Golgi trafficking of BSEP. | 132 |
| Figure 22 VPS4 affecting apical targeting of BSEP is upstream of Rab11a. | 133 |
| Figure 23 The subapical compartments at which BSEP and CHMP5 are colocalized are Rab5 and Rab11 positive. | 134 |
| Figure 24 Proposed model of CHMP5-associated ESCRTs in BSEP canalicular-targeting. | 135 |
| Figure 25 The flow chart of whole-exome sequencing to explore novel PFIC-associated candidate genes. | 136 |
| Figure 26 The <i>PLEC</i> (NM_000436) mutations identified from the PFIC family. | 137 |
| Figure 27 Decreased colocalization of <i>PLEC</i> and K8 in the cholestatic liver samples of <i>PLEC</i> mutations. | 138 |
| Figure 28 The distorted bile ducts, disturbed canalicular targeting of BSEP and dilated ZO-1 positive bile canaliculi in the livers with <i>PLEC</i> mutation. | 140 |
| Appendix | 141 |

| | |
|---|-----|
| Appendix Figure 1 Aberrant subapical BSEP compartments in a patient’s liver of neonatal hepatitis..... | 141 |
| Appendix Figure 2 The ESCRT-III subunits CHMP5 and LIP5 co-localizes with BSEP-resident subapical compartments in adult human hepatocytes..... | 142 |
| Appendix Figure 3 The total membrane-protein fraction contains the plasma-membrane plus organelle-membrane protein fractions. | 143 |
| Appendix Figure 4 BSEP is retained at aberrant CHMP5-positive subapical compartments in a transient cholestatic human liver sample. (Related to Figure 14D) | 144 |
| Appendix Figure 5 The canalicular targeting of BSEP is developmentally regulated and very likely associated with CHMP5 in human livers. | 146 |
| Appendix Figure 6 The glycosylation patterns of BSEP-R487H and BSEP-N490D are different from that of wild type BSEP..... | 147 |
| Appendix Figure 7 CHMP5 might regulate BSEP ubiquitination in an indirect manner..... | 148 |
| Appendix Table 1. The primer list | 149 |
| Appendix Table 2. All plasmids constructed and used in the dissertation..... | 157 |
| Appendix Table 3. The publication during the PhD program..... | 161 |
| Abbreviations | 162 |





誌謝

經過數載的日月起落，終於走完這條漫長的道路。心中有無限的感懷與謝意。很感謝我的父母能包容與陪我走過這段歲月。

首先要感謝兩位指導教授：張美惠教授與陳惠玲老師。非常謝謝張教授一直以來在實驗上的支持、鼓勵與指導。在我的實驗過於離散失焦時，總能將我拉回一條主軸而不至偏離。而且張教授一直以來在研究上的熱忱也是學生的我深刻敬仰與學習的模範。謝謝陳老師多年來的信任及給了我自由，讓我做了很多我想做的實驗。我要特別感謝陳慧玲教授/醫師。自我回到台大這個環境由助理轉換成學生，一直給予我的鼓勵、指導、信任與協助，讓我有機會能循序漸進地在研究這條路上前行與成長，讓我在這份研究裡有許多的自主性與發揮，也讓我有機會出國參與學術交流活動，一窺這世界的多元與壯闊。真的非常非常謝謝慧玲醫師。同時也要特別謝謝吳慧琳老師，在一次次我的實驗與研究陷入困境時，總能在討論後給我一些可行的方向並給予我關懷與鼓勵。

另外要感謝這一路走來一起努力的夥伴與朋友們。謝謝張教授及陳老師實驗室的雅惠及錦松學長，自我從助理、博士班學生到此刻，許許多多在實驗上的合作、幫作與討論。真的很謝謝你們。還有慧玲醫師的助理宇恩及邦渝，很謝謝你們在很多的實驗上的幫助。沒有你們，我一個真的無法完那麼多複雜的實驗。也要感謝張教授實驗室的蔡慧慧博士以崔道貞博士，在我陷入實驗方向無所適從時，給了我許多寶貴的建議。要特別感謝吳慧琳老師實驗室的泳聰、雪琍、惠珠及立峰，除了帶給我許多實驗上的幫助外，也給了諸多的溫暖與觀笑。在實驗室之外的朋友們，我要特別謝謝在 Johns Hopkins University 的庭育，真的很感謝庭育給了我很多在細胞生物學實驗方面的建議與指導。近二十年的相識，沒想到會在研究的主題上有如此多的交流。真的很獲益良多與感懷在心。其他的朋友們，包括馬丁、風木、Vic、小勇、逸仲等等，又有多少人能一起這樣走過這樣長的歲月呢？

在這段的歲月裡，有實驗方向陷入困境時的低潮，也有發現新的實驗成果的

喜悅。我一直很喜歡神話學大師 Joseph Campbell 的一部著作《The Hero with a Thousand Faces》(中譯本名為千面英雄)。每個人都是自己生命中孤獨的英雄，經歷著諸多考驗、挫折、失落、成功、自我質疑、自滿等，最後在這些磨難後成長，走出那黑洞、幽谷等等，迎向下一段的旅程。此刻，僅僅是一個階段的結束，也將是另一段生命旅程的開始。帶著這些感懷，我將踏上下一段的旅程。

上欣 謹誌

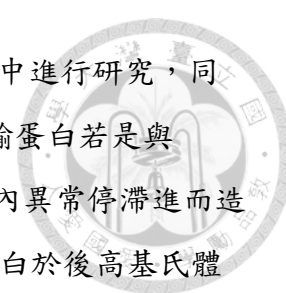
2019 年歲末

摘要



人類的膽汁傳輸蛋白 (Bile salt export pump, BSEP; 基因為 *ABCB11*) 是一個具有十二個穿膜區塊 (transmembrane domain) 的膜蛋白, 主要分布在肝細胞的膽小管膜 (canalicular/apical membrane) 上將膽鹽自肝細胞輸送進入膽道系統 (biliary system)。相較於大、小鼠有其他的分子能代償其膽汁傳輸蛋白的功能缺損, 人類的膽汁傳輸蛋白是膽小管膜上唯一能傳輸膽鹽的蛋白質。當人類的膽汁傳輸蛋白異常或功能缺損時, 會造成一系列不同嚴重程度的膽汁滯留症 (cholestasis), 包括: 第二型進行性家族性肝內膽汁滯留 (progressive familial intrahepatic cholestasis type 2, PFIC2)、第二型良性反覆性肝內膽汁滯留 (benign recurrent intrahepatic cholestasis type 2, BRIC2)、妊娠期肝內膽汁滯留症 (intrahepatic cholestasis in pregnancy, ICP), 以及藥物引起的肝臟受損 (drug-induced liver injuries)。在許多藥物開發過程中, 若會造成膽汁傳輸蛋白功能受到抑制或是影響膽汁傳輸蛋白在膽小管膜上表現時, 也是造成該藥物開發失敗的主因之一。然而目前關於膽汁傳輸蛋白造成膽汁滯留的機制所知不多, 特別是在臨上可以發現許多病人的膽汁傳輸蛋白無法在膽小管膜上表現, 但是卻沒有膽汁傳輸蛋白基因上的突變。此外, 在人類胎兒肝臟裡的膽汁傳輸蛋白分布與成人有顯著地不同。相較於成人肝細胞內的膽汁傳輸蛋白主要分布在膽小管膜上, 胎兒肝細胞裡的膽汁傳輸蛋白卻只有部份在膽小管膜上, 其他則散布在細胞質中。由這些觀察可以推測有些潛在的因子能直接或間接地調控膽汁傳輸蛋白在細胞內的分布與膽小管膜的定位 (canalicular/apical targeting)。但是在這部分的相關研究相當有限。

本論文試圖探索能調控膽汁傳輸蛋白於細胞內的移動 (subcellular trafficking) 可能的膽汁傳輸蛋白交互作用蛋白分子 (interacting proteins), 同時也企圖從疑似患有進行性家族性肝內膽汁滯留的病人檢體來找尋潛在的致病基因。在找尋可能的膽汁傳輸蛋白交互作用蛋白分子部份, 利用人類膽汁傳輸蛋白的片段分子於人類胎兒肝臟 cDNA 基因庫 (human fetal liver cDNA library) 中進行酵母菌雙雜交系統分析, 進而找到 CHMP5 為可能的膽汁傳輸蛋白交互作用分子。CHMP5 已知參與細胞內 endosomal sorting complex required for transport



(ESCRT) subcomplex-III 的組成。在體外培養細胞株以及小鼠中進行研究，同時以人類的胎兒肝臟與患有膽汁滯留的肝臟染色發現：膽汁運輸蛋白若是與 ESCRT 的交互作用異常，很可能是導致膽汁運輸蛋白於細胞質內異常停滯進而造成膽汁滯留疾病。同時這也是首次發現 ESCRT 參與膽汁運輸蛋白於後高基氏體的傳送 (post-Golgi trafficking)，而且是在已知的 Rab11 上游。更進一步地發現肝細胞內已知膽汁運輸蛋白所停留的胞器 (subapical compartments, SACs)，除了會有 CHMP5 以及另一個 ESCRT-III 分子 LIP5 外，這個仍諸多未知的胞器同時也有 Rab5 及 Rab11 的表現，所以這個胞器極有可能是所謂的早期/轉運胞內體 (early/sorting endosome)。因此可以推測 ESCRT 所參與的膽汁運輸蛋白於細胞內的移動是在膽汁運輸蛋白離開高基氏體至轉運胞內體之間。

另一方面在找尋可能造成進行性家族性肝內膽汁滯留的基因部分，自一對膽汁滯留手足中發現一個全新的膽汁滯留基因 *PLEC*。Plectin (PLEC，基因為 *PLEC*) 是一個細胞骨架連接蛋白 (cytoskeleton linker protein)。膽汁運輸蛋白在細胞內的運輸已知會受到細胞骨架以及細胞骨架上相關蛋白分子 (cytoskeleton-associated proteins) 影響。Plectin 能聯結不同的細胞骨架 (例如：角質蛋白) 以維持肝細胞的結構。在帶有 PLEC 突變的膽汁滯留病人肝臟中發現其膽汁運輸蛋白在膽小管膜上的表現嚴重受到影響，同時 PLEC 與角質蛋白第八型 (Keratin 8, K8) 的共同分布 (co-localization) 也降低。由膽汁運輸蛋白於膽小管膜上的分布異常，同時血清中的膽鹽濃度異常增加，意味著 PLEC 突變可能藉由影響膽汁運輸蛋白的膽小管膜定位或是可能扮演疾病修飾角色，進而造成膽汁滯留。

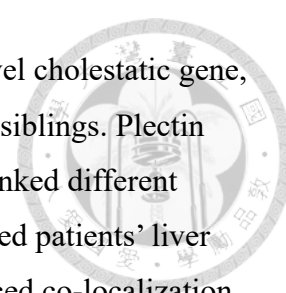
膽汁運輸蛋白於膽小管膜上表現對其功能極為重要。本論文所運用的一些研究方式亦能應用於其他的膜蛋白的細胞內運輸與相關疾病的機制探索。同時，本論文中所發現的一些其他膽汁運輸蛋白交互作用分子及 PLEC 對膽汁滯留的機制值得更深入的探討與研究。

關鍵字：膽汁運輸蛋白; ESCRT; 胞內體; 後高基氏體傳送; PLEC

ABSTRACT

The bile salt export pump (BSEP), encoded by the *ABCB11* gene, is an apical/canalicular protein with 12 transmembrane domains and mediates bile salts from hepatocytes into the biliary system. BSEP is the only apical transporter for the bile salts in humans and, unlike rodents, no other genes could compensate for the loss of BSEP functions. Abnormalities of BSEP could lead to a spectrum of cholestatic diseases including the progressive familial intrahepatic cholestasis type 2, benign recurrent intrahepatic cholestasis, intrahepatic cholestasis in pregnancy, and drug-induced liver injuries. Defects in BSEP function and canalicular expression, such as cytoplasmic accumulation, are also pivotal events that have caused the failure of many newly developed drugs. However, the mechanism of BSEP-associated cholestasis is poorly understood, especially in patients with no detected *BSEP* mutations in the coding regions but having impaired apical targeting of BSEP. Moreover, BSEP in human fetal livers partially expressed at the canalicular membrane and in the cytoplasm, rather than majorly at the canalicular membrane in adult. These data suggested some underlying factors regulate the distribution and apical targeting of BSEP directly or in an indirect manner.

In this dissertation, I aimed to discover BSEP-interacting proteins that modulates the subcellular trafficking of BSEP and to search novel PFIC-associated genes. I used a human BSEP polypeptide as a bait to screen the human fetal liver cDNA library through yeast two-hybrid systems. Several BSEP-interacting candidates were uncovered. One of the BSEP-interacting candidates is charged multivesicular body protein 5 (CHMP5), a key endosomal protein complex required for transport subcomplex-III (ESCRT-III). Using *in vitro* and *in vivo* modals, cholestatic, and developmental human liver samples, BSEP aberrantly associating with ESCRTs may cause cytoplasmic retention of BSEP at the subapical compartments (SACs) in cholestatic diseases. These BSEP locating SACs had the expression of not only ESCRT molecules but also the two endosomal proteins Rab5 and Rab11. These findings suggested that these SACs are the early/sorting endosomes. Moreover, I provided the first example and new function of ESCRTs, in which ESCRTs involved in the post-Golgi trafficking of BSEP, which was upstream of Rab11 regulated apical cycling of BSEP. Therefore, ESCRTs mediated BSEP sorting from the *trans*-Golgi to the sorting endosomes.



The last part of the dissertation described the discovery of a novel cholestatic gene, *PLEC*, associated by studying the samples from a pair of cholestasis siblings. Plectin (PLEC), encoded by *PLEC*, is a cytoskeleton linker protein, which linked different cytoskeletons to sustain the architecture of hepatocytes. PLEC mutated patients' liver samples revealed impaired canalicular expression of BSEP and reduced co-localization of PLEC and the keratin 8 (K8). The impaired BSEP canalicular expression and elevated bile acid levels suggested that the PLEC mutations may either affect BSEP targeting and cause cholestasis, or be a disease modifier gene.

Canalicular expression of BSEP is critical to BSEP function. The modus operandi of my work on the trafficking mechanism of BSEP could be easily applied to study all other transmembrane proteins for uncovering the etiologies of other important diseases. Besides, several BSEP-interacting candidates and the diseased mechanism of impaired BSEP trafficking in PLEC mutations are worthy to further study.

Keywords: BSEP; ESCRT; early/sorting endosome; post-Golgi trafficking; plectin



Chapter 1 Background and specific aims

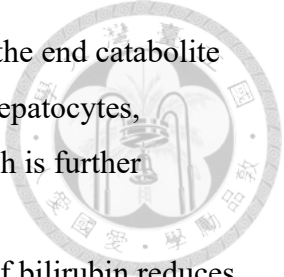
1.1. Cholestatic liver diseases

Cholestasis is one of the most common liver diseases and is also the leading cause of liver transplantation in children (Chen, Wu et al. 2018, Sticova, Jirsa et al. 2018). Cholestasis is caused by disturbances in bile flow resulted from inherited or acquired mechanisms (Chen, Wu et al. 2018). The disturbance in bile flow may occur within the liver (intrahepatic cholestasis) or the biliary tract (extrahepatic cholestasis) (Figure 1). Neonates and infants are substantially susceptible to cholestatic liver diseases due to infections, gene mutations, the developmental immaturity or abnormality of the liver, impaired metabolism of bile acids, drugs or toxins (Roberts 2003, Samyn and Mieli-Vergani 2007, Hunt, Papay et al. 2017, Bezerra, Wells et al. 2018, Chen, Wu et al. 2018, Vijayvargiya and Camilleri 2018). Hence, clinical diagnosis of cholestasis in infancy is challenged. Target enrichment next-generation sequencing for 42 cholestasis-associated genes has been developed to improve inherited cholestasis. However, 15% of cholestatic patients still lacked genetic disorders in these defined cholestasis-associated genes (Chen, Li et al. 2019). To search undefined cholestatic genes is in need.

1.2. The function and composition of bile

Bile is generated in the biliary system that comprises the livers, bile ducts, and the gall bladder. Hepatocytes synthesize and secrete most of bile ingredients into bile-canaliculi to generate the bile flow. Flowing through the bile duct, bile is stored in the gall bladder and finally drained into the duodenum after ingestion. The main physiological function of bile is to emulsify the lipid content of food for advanced digestion and absorption of lipids and lipid-soluble substances. Additionally, bile is an important route to regulate cholesterol homeostasis, hemoglobin catabolism, and xenobiotics elimination (Esteller 2008).

Bile is a yellow-to-greenish amalgam of water, bile acids (BAs), ions, phospholipids (phosphatidylcholine [PC]), cholesterol, bilirubin, proteins (such as glutathione and peptides), and the other xenobiotics (Figure 2) (Esteller 2008). Bilirubin



and its derivatives contribute the color of bile and stools. Bilirubin is the end catabolite of heme-containing proteins such as hemoglobin and myoglobin. In hepatocytes, catabolism of heme molecules generates unconjugated bilirubin, which is further glucuronidated to conjugated bilirubin by the enzyme uridine diphosphoglucuronosyltransferase 1A1 (UGT-1A). Glucuronidation of bilirubin reduces the hydrophobicity and cytotoxicity of bilirubin molecules. Conjugated bilirubin is the major form of bilirubin in bile and eliminated with stools. Lower UGT-1A activity in infancy results in frequent occurrence of hyperbilirubinemia in human neonates (Fujiwara, Haag et al. 2018). However, neonates or adults with hyperbilirubinemia were associated with lower risks of metabolic diseases and asthma, suggesting hyperbilirubinemia may have antioxidation functions (Sedlak, Saleh et al. 2009, Sticova and Jirsa 2013, Fujiwara, Haag et al. 2018).

In contrast to the colored molecule bilirubin, BAs are colorless and are the most abundant organic ingredient of bile. BAs are synthesized from cholesterol and associated with sodium or potassium ion in bile. BAs or bile salts (Na^+ or K^+ associated BAs) contribute the lipid-emulsion function of bile and act as signaling molecules to regulate gene expression (Chiang 2002, Martinot, Sedes et al. 2017, Molinaro, Wahlstrom et al. 2018). The emulsion ability of bile salts may also injure those cells exposed to bile. Phospholipids and cholesterol, the second and the third abundant organic composition of bile, protect those cells from the injury of bile acids (Esteller 2008). Therefore, insufficient phospholipids and cholesterol in bile will damage livers and cause diseases.

1.3. Biosynthesis, homeostasis, and the enterohepatic circulation of bile acids

Bile acids are the catabolic derivative of cholesterol. There are two pathways to synthesize bile acids: the classic (neutral) pathway and the alternative (acidic) pathway (Figure 3). The classic pathway is occurred in the hepatocytes and is initiated by the rate-limiting cytochrome P450 (CYP) enzyme cholesterol 7 α -hydroxylase (CYP7A1), which hydroxylates the seventh carbon (C-7) of cholesterol to generate 7 α -hydroxycholesterol. The downstream key enzyme of the classic pathway is the sterol

12 α -hydroxylase (CYP8B1), which hydroxylates at C-12 of the cholesterol backbone. With CYP8B1-mediated 12 α -hydroxylation, the product of the classic pathway is cholic acid (CA). On the other hand, chenodeoxycholic acid (CDCA) is synthesized when 12 α -hydroxylation is bypassed. Hence, there are more hydroxyl groups in CA (C-3, C-7, and C-12) than in CDCA (C-3 and C-7).

In the alternative pathway, the catabolism of cholesterol is initiated either by CYP27A1 in the liver, macrophages, and adrenal glands, or by CYP46A1 in the brain. The bile acid generated through the alternative pathway is only CDCA. Both CA and CDCA are the primary BAs in humans. In addition to CA and CDCA, mice contain another two primary BAs, α -muricholic acid (α -MCA) and β -muricholic acid (β -MCA), which are converted from CDCA by rodent-specific enzymes (Russell 2003, Chiang and Ferrell 2019). The primary BAs are conjugated with either taurine or glycine in hepatocytes. The dominant conjugate is different among species. In humans, glycine conjugates are more abundant than taurine ones (taurine : glycine = 1 : 3 ~ 1 : 5), but nearly taurine conjugates only in rats and mice (Hofmann 1999, Linton 2015, Thakare, Alamoudi et al. 2018, Thakare, Alamoudi et al. 2018, Chiang and Ferrell 2019). Tauro- or glyco-conjugation transforms BAs from weak acid to strong acid and makes conjugated BAs impermeable to the cell membrane.

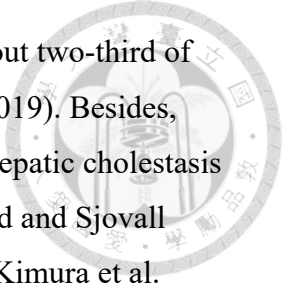
BAs are actively transported by the bile salt export pump (BSEP/Bsep) protein at the canalicular/apical membrane of hepatocytes (Figure 4). This ATP-dependent transport of BAs is the major driving force to generate bile flow. Conjugated primary BAs will be further processed by intestinal bacteria in the distal intestine or the large intestine, including deconjugation, 7-dehydroxylation, and epimerization (Figure 3). Some of unconjugated BAs are absorbed directly and return to hepatocytes for the next cycle of conjugation and secretion. Other unconjugated CDCA and CA are 7-dehydroxylated to lithocholic acid (LCA) and deoxycholic acid (DCA), respectively. Trace amount of CDCA (~2%) is transformed to ursodeoxycholic acid (UDCA) by bacterial epimerization. LCA, DCA and UDCA, which are termed secondary BAs, are absorbed from the intestines and returned to the liver. Secondary BAs, as the primary bile acids, are conjugated with glycine or taurine in hepatocytes and excreted in bile. LCA could be additionally sulfonated at the C-3, which results LCA with double conjugation and reduces the reabsorption of LCA (Hofmann 1999). Sulfation of BAs is an important mechanism to reduce toxicity and to eliminate these toxic BAs (Alnouti

2009). Primary and secondary BAs are secreted by BSEP/Bsep into bile-canaliculi. In human bile, approximate 20% of BAs is DCA, and the others are CDCA and CA in roughly equal percentage (Hofmann 1999, Russell 2003, Reshetnyak 2013, Linton 2015).

BAs are re-absorbed from the ileum and returned to the liver in a highly efficient manner. This is so-called the enterohepatic circulation (Figure 4). In humans, the bile salt pool is approximately 2-3 g, and *de novo* synthesized bile salts are 500-600 mg. However, 20-30 g of BAs are secreted every day (Chan and Vandeberg 2012). More than 90% of BAs are re-absorbed at the intestine and returned to the liver through circulation systems for the next cycle. Bile salts cycle 6- to 10-times daily. Besides, *de novo* synthesis and elimination of BAs is regulated by a group of BA receptors (Chiang and Ferrell 2019). Unconjugated primary and secondary BAs are the potent ligand for BA receptors, especially receptor farnesoid X receptor (FXR) (Matsubara, Li et al. 2013, Hiebl, Ladurner et al. 2018, Ikegami and Honda 2018, Molinaro, Wahlstrom et al. 2018).

FXR is the first identified BA receptor, which is expressed in both hepatocytes and enterocytes. After binding with BAs, FXR forms heterodimers with the retinoid X receptor (RXR), and translocates into the nucleus of hepatocytes or enterocytes. Efflux transporters will be upregulated, and influx transporters will be downregulated. This mechanism could reduce the intracellular loading of BAs. Moreover, the expression of enzymes for BA synthesis in hepatocytes is also repressed by the BA-FXR signaling (Jurica, Dovrtelova et al. 2016). In addition to FXR, other BA receptors participating in the BA homeostasis include the pregnane X receptor (PXR), vitamin D receptor (VDR), Takeda G-protein-coupled receptor 5 (TGR5; also known as G protein-coupled bile acid receptor-1, or GPBAR-1), and sphingosine-1-phosphate receptor (S1PR2) (Matsubara, Li et al. 2013, Deutschmann, Reich et al. 2018, Hiebl, Ladurner et al. 2018, Molinaro, Wahlstrom et al. 2018, Chiang and Ferrell 2019). Hence, the bile pool could be maintained (Malhi and Camilleri 2017, Chiang and Ferrell 2019).

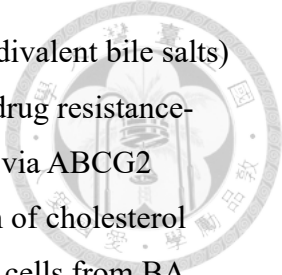
The composition and conjugation of BAs is fluctuated with animal species, physiological or diseased conditions, and developmental stages (Hofmann, Hagey et al. 2010, Thakare, Alamoudi et al. 2018, Thakare, Alamoudi et al. 2018, Chiang and Ferrell 2019). For example, CA and CDCA are the most abundant bile acids in human bile, and



each occupies approximately two-fifth of total bile acids. In mice, about two-third of total bile acids is CA (Fickert and Wagner 2017, Chiang and Ferrell 2019). Besides, more hydroxylated bile acids could be detected in patients with intrahepatic cholestasis and in animal models with defective bile-salt transport (Bremmelgaard and Sjøvall 1980, Wang, Salem et al. 2001, Fuchs, Paumgartner et al. 2017, Lee, Kimura et al. 2017, Liu, Wang et al. 2018). In human fetus after 22- and 26-weeks' gestation, taurine-conjugated di-hydroxyl BAs could be detected in the gallbladder. After 28 weeks, small amounts of glycine conjugates are synthesized. In postnatal stages, the ratio of CA to CDCA falls from 2.5 to 1.2 (Murphy and Signer 1974). These findings suggest that the bile acid pool is highly diverse.

1.4. The transporters mediating the transfer of bile acids and other bile ingredients

Bile flow is dominantly driven by the excretion of BAs (the bile acid-dependent bile flow) and, to a lesser extent, by osmotic pressure (the bile acid-independent bile flow) at the canalicular membrane of hepatocytes (Hofmann 1999, Kullak-Ublick, Stieger et al. 2000). Both driving forces are mediated by a group of membrane transporters, *i.e.* ATP-binding cassette (ABC) family proteins (Figure 2) (Vasiliou, Vasiliou et al. 2009). Bile salt export pump (BSEP encoded by *ABCB11*) is the critical canalicular transporter and exclusively expresses in hepatocytes to mediate monovalent BAs transport into bile canaliculi. In the intestines, BAs are absorbed into enterocytes by the apical sodium-dependent bile acid transporter (ASBT encoded by *SLC10A2*), and delivered into the circulation system through the basolateral heterodimeric transporter organic solute transporter α/β (OST α/β encoded by *OSTA/B*) (Figure 4) (Dawson, Hubbert et al. 2010, Ballatori, Christian et al. 2013, Claro da Silva, Polli et al. 2013). At the basolateral/sinusoidal membrane of hepatocytes, the uptake of BAs is sodium, rather than ATP, dependent. The Na⁺-taurocholate co-transporting polypeptide (NTCP/SLC10A1 encoded by *SLA10A1*) is the major transporter for BA uptake. The heterodimeric transporter organic-anion-transporting polypeptide 1B1/3 (OATP1B1/3 encoded by *SLCO1B1/3*) transports BAs in less degree, and also mediates the uptake of unconjugated bilirubin (Claro da Silva, Polli et al. 2013, Suga, Yamaguchi et al. 2017).



Canalicular excretion of bilirubin and organic anions (including divalent bile salts) generates the osmotic force to bile flow, and is mediated by the multidrug resistance-associated protein 2 (MRP2 encoded by *ABCC2*) and, a lesser extent, via ABCG2 (Sticova and Jirsa 2013, Keppler 2014). Besides, canalicular secretion of cholesterol and phospholipids could maintain the membrane integrity and protect cells from BA injuries. The heterodimeric transporter ABCG5/G8 mediates cholesterol excretion. The multidrug resistance P-glycoprotein 3 (MDR3/ABCB4 encoded by *ABCB4*) flops the lipid PC to the outer lipid leaflet. PC is extracted by and formed micelles with bile salts in bile. The canalicular membrane becomes unstable and vulnerable due to the flop of phosphatidylserine (PS) accompanied with PC loss. The flippase ATP8B1 (encoded by *FIC1*) flips PS back for stabilizing the integrity of the canalicular membrane (Linton 2015). ATP8B1 is also necessary for functional expression of MDR3 (Groen, Romero et al. 2011). Therefore, the cytoprotective mechanism of hepatocytes from the BA injuries is not only dependent on the BA efflux mediated by BSEP but also required the cooperation of MDR3 and ATP8B1.

1.5. Progressive intrahepatic cholestasis (PFIC)

Patients with either *FIC1*, *ABCB11*, or *ABCB4* mutations result in progressive familial intrahepatic cholestasis (PFIC) (Figure 2 and Table 1) (Bull, van Eijk et al. 1998, de Vree, Jacquemin et al. 1998, Strautnieks, Bull et al. 1998). Besides, mutations in either the tight junction protein Zona Occludens-2 (*ZO-2/TJP2* encoded by *TJP2*) (Sambrotta, Strautnieks et al. 2014) or FXR (Gomez-Ospina, Potter et al. 2016) have been referred to PFIC4 and PFIC5, respectively, due to the similar phenotypes of PFIC. Patients with PFIC types 1, 2, 4, or 5 mutants demonstrate with low level of BAs in bile and with reduction in gamma-glutamyl transpeptidase (GGT) in their serum (Bull, van Eijk et al. 1998, Strautnieks, Bull et al. 1998, Gomez-Ospina, Potter et al. 2016). On the contrary, PFIC3 displays with high GGT level that is usually observed in other cholestatic diseases (de Vree, Jacquemin et al. 1998, Morotti, Suchy et al. 2011). Mutations in one of these genes are the most severe cause for inherited cholestasis. For those with totally dysfunctional or nonsense mutants, these patients usually display severe symptoms since the first few years of life. Nevertheless, mild or recurrent phenotypes also occur, which may result from missense mutations or genetic

polymorphisms that causes partial or transient loss of function, including benign recurrent intrahepatic cholestasis (BRIC), intrahepatic cholestasis of pregnancy (ICP), predisposition to cholelithiasis and drug-induced liver injury (DILI) (Morotti, Suchy et al. 2011).

Despite of the above-mentioned PFIC genetic mutations, many cholestatic patients who reveal inherited cholestasis have neither mutation in these cholestatic genes nor other identifiable cause of cholestasis (idiopathic cholestasis). One explanation is some cholestasis-associated genes that have not been discovered. Another possibility is some *trans* factors that disturber the protein involved in bile transport. One example of the *trans* factor inducing cholestasis is the arthrogyrosis, renal dysfunction and cholestasis (ARC) syndrome (MIM 208085) (Gissen, Tee et al. 2006, Golachowska, Hoekstra et al. 2010). ARC syndrome is associated to *VPS33B* mutations and typically presented with neonatal cholestasis. *VPS33B* participates in regulation of vesicular membrane fusion and the sorting process of Rab11-positive recycling endosomes. *VPS33B* mutations disturb the polarized targeting of membrane-associated proteins and mis-sorting the apical proteins, including BSEP (Figure 2). Another example is the motor protein myosin VB (*MYO5B*, encoded by the *MYO5B* gene), which and the small GTPase protein Rab11a are required for bile canaliculi formation (Figure 2 and Table 1) (Wakabayashi, Dutt et al. 2005). Mutations in *MYO5B* result in microvillus inclusion diseases (MVID; MIM 606540) (Muller, Hess et al. 2008) and cholestasis (Girard, Lacaille et al. 2014, Gonzales, Taylor et al. 2017). It is possible that many undiscovered molecules are participating in bile transport and regulation in physiological and diseased status, which may be targets for diagnostic and therapeutic approaches.

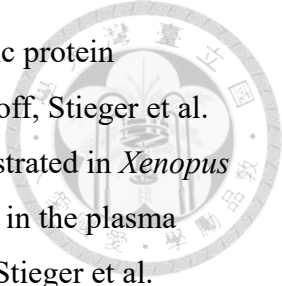
1.6. The bile salt export pump (BSEP) is the canalicular bile acid transporter.

The major driving force for bile flow is ATP-dependent transport of bile salts at the canalicular membrane of hepatocytes. BSEP/Bsep, encoded by the *ABCB11/Abcb11* gene, is finally recognized as the canalicular bile acid transporter (cBAT) from laboratory findings and clinical observation (Figure 5). The *ABCB11/abcb11* orthologs of human, two rodents, and skate have been cloned (Table 2), assayed for their transport

activities (Table 3) and substrate preferences (Table 4) for different bile salts. Animal models with *Abcb11* knockout have been generated for studying Bsep *in vivo* (Table 5).

Canalicular transport of bile acids is ATP dependent, which was evidenced by taurocholate (TC) transport in canalicular membrane vesicles from rat (Adachi, Kobayashi et al. 1991, Muller, Ishikawa et al. 1991, Nishida, Gatmaitan et al. 1991, Stieger, O'Neill et al. 1992) and human (Wolters, Kuipers et al. 1992) livers in early 1990s. The ATP-dependent TC transport was not only competitively inhibited by other bile salts (Stieger, O'Neill et al. 1992), but also decreased in several animal modes of cholestasis (Bossard, Stieger et al. 1993, Bohme, Muller et al. 1994, Moseley, Wang et al. 1996, Bolder, Ton-Nu et al. 1997). Notably, kinetic assays revealed the decrease in TC transport was caused by a reduction in the number of functional TC transporters at the canalicular membrane rather than functional inhibition (Bossard, Stieger et al. 1993, Moseley, Wang et al. 1996), suggesting the existence of a putative cBAT. The first cBAT candidate was the $\text{Ca}^{2+}/\text{Mg}^{2+}$ -ecto-ATPase/cCAM-105 due to its canalicular expression, ATPase activity (Muller, Ishikawa et al. 1991), and downregulation in sepsis-induced cholestasis models (Moseley, Wang et al. 1996). The domain prediction and biochemical assays of ecto-ATPase excluded the possibility of ecto-ATPase being a cBAT (reviewed in (Trauner 1997)). The yeast Bat1p, encoded by the *BAT1* (bile acid transporter) gene, was another cBAT candidate, which transported several bile salts in ATP-dependent manner. Nevertheless, Bat1p is homologous in its protein sequence to the basolateral transporter MRP1 (encoded by *ABCB1*), and has an extremely low affinity for TC, suggesting Bat1p is a functional analog of cBAT (Ortiz, St Pierre et al. 1997). On the other hand, the molecular identification and characterization of the *Abcb11/ABCB11* gene in laboratories and clinics were validated to be the cBAT (Gerloff, Stieger et al. 1998, Strautnieks, Bull et al. 1998, Jansen, Strautnieks et al. 1999, Green, Hoda et al. 2000, Lecureur, Sun et al. 2000, Noe, Hagenbuch et al. 2001, Byrne, Strautnieks et al. 2002, Noe, Stieger et al. 2002).

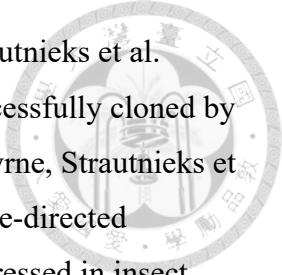
The gene encoding BSEP/Bsep was first identified in pig liver from a partial cDNA sequence and denominated the *Sister gene of P-glycoprotein (Spgp)* due to its protein sequence and signature, specifically the ATPase motif, closely related to the P-glycoprotein (P-gp) multigene family proteins (Childs, Yeh et al. 1995). The partial *Spgp/Bsep/Abcb11* gene exclusively expressed in the liver of rat tissue panels and corresponded to a single gene in the genome (Childs, Yeh et al. 1995). The full-length



rat *Bsep* (*rBsep*) cDNA was further cloned and encoded a liver specific protein expressing at the canalicular membrane (Childs, Yeh et al. 1998, Gerloff, Stieger et al. 1998). The *rBsep* mediating ATP-dependent TC transport was demonstrated in *Xenopus* oocytes with the injection of rat *Bsep* capped sense RNA (cRNA) and in the plasma membrane vesicle from insect cells with *rBsep* transfection (Gerloff, Stieger et al. 1998). The transport of other bile salts by *rBsep* was in line with the same rank order of that by the canalicular membrane (cLPM) vesicle prepared from rat livers (Childs, Yeh et al. 1998, Gerloff, Stieger et al. 1998). Defined in a latter study, monoanionic bile salt derivatives are the specific substrate of *rBsep*, and *rBsep* has the greatest activities for taurochenodeoxycholate (TCDC) and glycochenodeoxycholate (GCDC) (Stieger, Fattinger et al. 2000, Hayashi, Takada et al. 2005).

During the same time of *rBsep* being cloned and identified, the second locus for PFIC (*PFIC2*) was mapped to chromosome 2q24 from six PFIC families that were with excluded linkage to the chromosome 18q21-22, *i.e.* the *PFIC1* locus (Strautnieks, Kagalwalla et al. 1997). Using *rBsep* cDNA as a probe, the human *BSEP* ortholog was mapped to chromosome 2q31 (Childs, Yeh et al. 1998), which is very close to the *PFIC2* locus. The *PFIC2* locus was refined and mapped to the *BSEP/ABCB11* gene, encoded by which the human BSEP shared an 82% amino acid identity and 88% similarity with *rBsep* (Strautnieks, Bull et al. 1998). The *PFIC2*-linked patients were associated with mutations in the *BSEP/ABCB11* gene (Strautnieks, Bull et al. 1998), and demonstrated functional defects in canalicular expression of BSEP as well as in biliary excretion of bile salts (Jansen, Strautnieks et al. 1999), suggesting the function of BSEP from clinical aspects. In addition to *PFIC2*, BSEP mutations were linked to *BRIC2*, who demonstrated BRIC symptom but harbored no *ATP8B1* mutations (van Mil, van der Woerd et al. 2004).

The full-length *BSEP/ABCB11* cDNA was successfully cloned from human livers until 2002 because the intrinsically toxic nature of the human *BSEP* cDNA hindered its cloning (Byrne, Strautnieks et al. 2002, Noe, Stieger et al. 2002). The nucleotide sequences of the human *BSEP* cDNA at positions 59-64 (TTGAGT) and 76-81 (TATAAT) downstream of the translation start site are highly homologous with the consensus sequences, *i.e.* the -35 (TTGACA) and the -10 (TATAAT) elements, of bacterial promoters (Noe, Stieger et al. 2002). The unique existence of the cryptic prokaryotic promoter in the human *BSEP* cDNA seemed extremely toxic to the



Escherichia coli competent cell in the process of cloning (Byrne, Strautnieks et al. 2002, Noe, Stieger et al. 2002). The full-length *BSEP* cDNA was successfully cloned by either performing gene recombination bypassing *E. coli* host cells (Byrne, Strautnieks et al. 2002) or inactivating the putative prokaryotic promoter through site-directed mutagenesis (Noe, Stieger et al. 2002). Human BSEP ectopically expressed in insect cells demonstrated high ATPase activity (Byrne, Strautnieks et al. 2002) and ATP-dependent TC transport (Noe, Stieger et al. 2002). The Michaelis constant (K_m) for TC in human BSEP expressing membrane vesicles was very close to that in human cLPM vesicles (Wolters, Kuipers et al. 1992, Byrne, Strautnieks et al. 2002, Noe, Stieger et al. 2002, Hayashi, Takada et al. 2005) (Table 3). Human BSEP has a high affinity for conjugated primary bile salts, especially TCDC and GCDC, which explained the extremely low amount of chenodeoxycholate in PFIC2 patients' bile (Jansen, Strautnieks et al. 1999).

Another mammalian *Bsep* that has been cloned and well characterized is the mouse *Bsep* (*mBsep*) (Green, Hoda et al. 2000, Lecureur, Sun et al. 2000, Hayashi, Takada et al. 2005). The *mBsep* is localized at mouse chromosome 2C13 (Lecureur, Sun et al. 2000). The deduced amino acid identity of *mBsep* between either *rBsep* or BSEP was 90% and 81%, and the similarity was 94% and 89%, respectively. Some features are shared among BSEP, *rBsep*, and *mBsep*, including canalicular expression, transport of various bile salts, and the transport function inhibited by cholestatic stimuli (Childs, Yeh et al. 1998, Gerloff, Stieger et al. 1998, Green, Hoda et al. 2000, Lecureur, Sun et al. 2000, Stieger, Fattinger et al. 2000, Byrne, Strautnieks et al. 2002, Noe, Stieger et al. 2002, Hayashi, Takada et al. 2005).

Besides of mammalian vertebrates, the fish *Bsep* ortholog of the skate (*Raja erinacea*) has been studied (Ballatori, Rebbeor et al. 2000, Cai, Wang et al. 2001), and that (encoded by *abcb11b*) of the zebrafish (*Danio rerio*) has been genetically depleted to generate the disease model (Ellis, Bove et al. 2018). The mRNAs of chicken and turtle livers were also positive for the *Abcb11* gene hybridization by rat *Abcb11* cDNA probe (Gerloff, Stieger et al. 1998). Table 2 summarizes the information of the four *ABCB11/Abcb11* orthologs that has been cloned and functionally characterized, including human, rat, mouse, and skate. *In vitro* assays and clinical observation of BSEP/*Bsep* orthologs concluded that BSEP/*Bsep* is the cBAT (Gerloff, Stieger et al. 1998, Strautnieks, Bull et al. 1998, Jansen, Strautnieks et al. 1999, Ballatori, Rebbeor et

al. 2000, Green, Hoda et al. 2000, Lecureur, Sun et al. 2000, Cai, Wang et al. 2001, Noe, Hagenbuch et al. 2001, Hayashi, Takada et al. 2005).

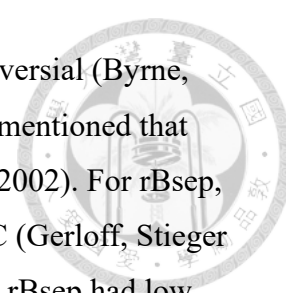


1.7. Developmental expression of BSEP/Bsep orthologs

Scanty reports conduct BSEP/Bsep expression in developmental stages, especially in humans. BSEP, like some hepatic transporters and regulators, is expressed in early gestation of human fetuses. However, the expression pattern of BSEP in fetal livers are different from that in adult. Immunohistochemical staining of BSEP in adult human liver samples exhibited strong BSEP signals on the canalicular membrane as branched lines. The BSEP signals in fetal liver samples, by contrast, were partially at the cytoplasm and partially at the canalicular membrane (Chen, Chen et al. 2005). It seems like some uncharacterized mechanisms to “trap” BSEP in the cytoplasm. Compared to human liver investigations of transporters, studies conducting rodents’ Bsep and other transporters in developmental stage are more comprehensive (Tomer, Ananthanarayanan et al. 2003, Gao, St Pierre et al. 2004, Cheng, Buckley et al. 2007). As shown in Figure 6, rat *Bsep* mRNA could be detected as late as on the embryonic day (E) 20, which is the same to *Ntcp* but latter than *Mrp2* (E16) (Gao, St Pierre et al. 2004). Unlike human transporters with early expression, rodents’ transporters express at the time before or closed to birth (Tomer, Ananthanarayanan et al. 2003, Gao, St Pierre et al. 2004, Chen, Chen et al. 2005, Cheng, Buckley et al. 2007).

1.8. Bile salt preferences of BSEP/Bsep orthologs

Human, rat, mouse, and skate BSEP/Bsep proteins have been studied for their own preferences for bile salts, in which individual bile salt was used as a substrate or a TC competitor in Bsep/BSEP-mediated transport assays (Table 3 and Table 4). The K_m/K_i value or the rank of inhibition efficacy may be divergent, and not the same bile salts were analyzed in the literatures (Gerloff, Stieger et al. 1998, Green, Hoda et al. 2000, Stieger, Fattinger et al. 2000, Cai, Wang et al. 2001, Noe, Hagenbuch et al. 2001, Byrne, Strautnieks et al. 2002, Noe, Stieger et al. 2002, Hayashi, Takada et al. 2005). Human BSEP has a highest activity for TC, and followed with GC and TUDC in a similar



degree. The transport activity for TCDC by human BSEP was controversial (Byrne, Strautnieks et al. 2002, Noe, Stieger et al. 2002). Besides, Noe et al. mentioned that human BSEP did not transport unconjugated CA (Noe, Stieger et al. 2002). For rBsep, the rank order of bile-salt transport was TCDC > TC ≥ TDC > TUDC (Gerloff, Stieger et al. 1998, Stieger, Fattinger et al. 2000, Cai, Wang et al. 2001). The rBsep had low activities for GC or CA (Gerloff, Stieger et al. 1998), and no for the sulfated secondary bile salt tauroolithosulfocholate (Stieger, Fattinger et al. 2000). Like rBsep, mBsep also had a high activity for TCDC, and then for GC as well as TC (Noe, Hagenbuch et al. 2001). Taurodeoxycholate (TDC) and chenodeoxycholate (CDC) probably had higher affinities for mBsep than TCDC (Green, Hoda et al. 2000). The sulfated bile alcohol, scymnol sulfate (ScyS), has a highest affinity for sBsep than other bile acids that were analyzed in sBsep expressing vesicles (Cai, Wang et al. 2001).

As mentioned in the section 1.3, bile acids in humans are conjugated with glycine or taurine in an approximate ratio of five to one, but almost exclusively with taurine in rats as well as mice. Glycine conjugated bile salts are capably transported by rat and mouse Bsep as that by human BSEP. Human BSEP transports glycine-conjugated bile salts to a greater extent than rodent Bsep (Green, Hoda et al. 2000, Stieger, Fattinger et al. 2000, Cai, Wang et al. 2001, Noe, Hagenbuch et al. 2001, Hayashi, Takada et al. 2005). Moreover, bile alcohols, such as ScyS, are nearly absent in rat or mouse bile, but are the major bile salt in fish bile (Hofmann, Hagey et al. 2010, Thakare, Alamoudi et al. 2018). Interestingly, the TC transport by rBsep could be markedly inhibited by ScyS (23.9% of the control) (Cai, Wang et al. 2001), suggesting the Bsep protein was initially evolved for transport of bile alcohols. In conclusion, these Bsep proteins generally preferred the bile salts that were taurine conjugates, chenodeoxycholate derivatives, and primary bile acids (Table 4).

1.9. *Abcb11/Bsep* knockout animal models

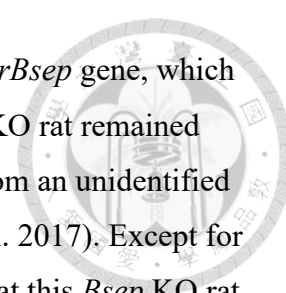
PFIC2 is an early onset of a fatal liver disease in humans. To study BSEP and imitate its functional loss in PFIC2 patients, an animal model with a systemic knockout (KO) of the *Abcb11* gene has been generated chronologically in mice (Wang, Salem et al. 2001), rats (Cheng, Freeden et al. 2016), and zebrafish (Ellis, Bove et al. 2018). However, either the phenotypes being less severe or divergent preferences for bile salts

in these *Abcb11* KO animals rendered the representative of PFIC2 models.

The knockout of the *Abcb11* gene in mice resulted in growth retardation and enlarged livers (~5% of body weight in wild-type but ~10% in KO mice), intrahepatic cholestasis, greatly reduced canalicular excretion of bile salts, especially cholate conjugates (Wang, Salem et al. 2001), and elevation of cholestasis-induced oxidative stress in the brains, hearts as well as kidneys (Ljubuncic, Yousef et al. 2004). Surprisingly, *Abcb11* null mice had a normal lifespan, no advanced cholestasis in a follow-up to 1 year, no significant reduction in bile flow rate, about 60% decrease in bile salt output in comparison of wild type littermates (Wang, Salem et al. 2001). Cholestasis-induced oxidative stress in the livers of *Abcb11* KO mice was comparable to that of the wild-type and the heterozygous littermates (Ljubuncic, Yousef et al. 2004). Besides, *Abcb11* KO mice increased the canalicular excretion of cholesterol, phospholipids, and the more hydrophilic bile salts, especially tetra-hydroxylated bile salts that were extremely few or absent in the wild type littermate (Wang, Salem et al. 2001, Lam, Wang et al. 2005).

Observations on *Abcb11* KO mice suggested several things underlying mBsep and bile physiology. First, hydrophobic bile salts (*i.e.* taurine or glycine conjugates) are the major substrate of mBsep, which was in accordance with the findings in kinetic assays using mBsep expressing membrane vesicles (Green, Hoda et al. 2000, Lecqueur, Sun et al. 2000, Hayashi, Takada et al. 2005). Next, an increase in hydroxylation to decrease hydrophobicity of bile salts reduced the injuries from hydrophobic bile salts in *Abcb11* KO mice. Finally, an alternative canalicular transporter(s) in existence could transport bile salts because the bile flow was affected slightly in *Abcb11* KO mice. Further studies of *Abcb11* KO mice discovered that mouse *Mdr1* is the alternative bile-acid transporter, which together with mBsep mediated bile salt transport in mutually compensatory mechanisms in mice (Lam, Wang et al. 2005, Wang, Chen et al. 2009). However, there is no compensatory elevation of the human *MDR1* mRNA in PFIC2 livers (Keitel, Burdelski et al. 2005). On the contrary, abundant MDR1 aggregates were observed in the cytoplasm of PFIC2 patient's hepatocytes, in which BSEP expression is completely absent (Ellis, Bove et al. 2018).

The *Abcb11* KO rat demonstrated more minor cholestatic phenotypes than *Abcb11* KO mice (Cheng, Freeden et al. 2016). Using zinc finger nuclease technology, a



premature stop codon was theologically introduced on exon 5 of the *rBsep* gene, which resulted in a nonfunctional truncated protein. However, the *Abcb11* KO rat remained 15% of rBsep proteins relative to wild type rats, which may come from an unidentified variant of *rBsep* gene (Cheng, Freeden et al. 2016, Cheng, Chen et al. 2017). Except for reduced liver efflux of TC, results from several assayed suggested that this *Bsep* KO rat was nearly normal in comparison to the wild-type rat (Cheng, Freeden et al. 2016, Cheng, Chen et al. 2017, Patel, Johnson et al. 2018). The mRNA level of *Mdr1* was significantly elevated in the *Bsep* KO rat livers in compared to the wild-type in a Troglitazone study (Cheng, Chen et al. 2017), but the protein level was so far unknown (Cheng, Freeden et al. 2016). Besides, the rat Mdr1 protein has been reported to transport fluorescein isothiocyanate-conjugated glycocholate in cell-based assays (Sai, Nies et al. 1999). Hence, merely low rBsep proteins in the liver and/or the rat Mdr1 may sufficiently sustain the physiological functions.

Different from two *Bsep* KO rodent models, knockout of the *abcb11b* gene in zebrafish revealed phenotypes that were more comparable to PFIC2 patients (Ellis, Bove et al. 2018). Zebrafish exhibits two orthologs of the human *ABCB11* gene, which are expressed in different organs. The *abcb11a* transcript was abundant in the intestine, and the *abcb11b* was exclusively expressed in the liver. Zebrafish *abcb11b* protein shares 70% and 67% identities to human BSEP and mBsep, respectively. CRISPR/Cas9 mediated knockout of the *abcb11b* gene in zebrafish resulted in PFIC2-like phenotypes, including premature death, aberrant liver histology, impaired bile secretion, an increase in hepatic autophagy, and mislocalization of zebrafish Mdr1/*abcb4* in the hepatocyte cytoplasm. Notably, *abcb11b* KO zebrafish treated with autophagy inducers, rapamycin or trehalose, could restore canalicular targeting of Mdr1 and a part of BA excretion, which resulted in more mutants survived (Ellis, Bove et al. 2018), suggesting the possibility of Mdr1 being an BA transporter. Moreover, the molecules involved in autophagy pathway may be the therapeutic target of PFIC2. Although the *abcb11b* KO zebrafish revealed many PFIC2-like phenotypes, the composition of bile and preference for bile salts between human and fish should be concerned because sulfated bile alcohols are the predominant bile salts in fish bile (Cai, Wang et al. 2001, Reschly, Ai et al. 2008) but extremely rare in human and mammals (Kuroki, Shimazu et al. 1985, Hofmann, Hagey et al. 2010).

Table 5 summarized three *Abcb11* KO animal models. Two *Abcb11* KO rodent

models revealed less severe or no cholestatic phenotypes, in which the murine Mdr1 or low amount of rBsep from an unidentified rat *Abcb11* variant contributed to bile acid transport, respectively. The *abcb11b* KO zebrafish closely resembled PFIC2, and revealed defect in canalicular targeting of Mdr1. The degree of canalicular targeting of Mdr1 may determine how these *Bsep* KO models are comparable to PFIC2.

1.10. Subcellular trafficking of BSEP

BSEP/Bsep is an apical transport protein with 12-transmembrane domains and is localized at the subapical compartments (SACs) in the cytoplasm and at the canalicular/apical membrane of hepatocytes (Figure 7A) (Gerloff, Stieger et al. 1998). The plasma membrane of hepatocytes is divided into the apical (the canalicular) domain and the basal-lateral (the sinusoidal) domain by tight junctions (Figure 2) (Treyer and Musch 2013, Musch 2014). A group of molecules, such as Rab GTPases, adaptor proteins, cytoskeletons, junctional proteins, and bile acids, has contributed to the establishment of hepatocyte polarity and the subcellular trafficking of BSEP as well as other membrane proteins (Delacour and Jacob 2006, Cresawn, Potter et al. 2007, Weisz and Rodriguez-Boulan 2009, Golachowska, Hoekstra et al. 2010, Fu, Lippincott-Schwartz et al. 2011, Lobert and Stenmark 2011, Bonifacino 2014, Musch 2014, Xie, Miao et al. 2018). The loss of hepatocyte polarity have been documented in cholestasis and liver cancers (Muthuswamy and Xue 2012).

Newly synthesized membrane proteins at the *trans*-Golgi network (TGN) route through two pathways to their destined membrane domain of polarized cells (Folsch, Mattila et al. 2009, Weisz and Rodriguez-Boulan 2009). Most of canalicular proteins, including dipeptidyl peptidase IV (DPPIV), polymeric immunoglobulin A receptor (pIgA-R) and the glycosyl-phosphatidylinositol (GPI)-anchored proteins like 5-nucleotidase (5-NT), are initially transferred to the basolateral membrane, which is followed by endocytosis to the canalicular membrane (the indirect pathway or transcytosis). On the other hand, sinusoidal proteins and a few apical transporters, including BSEP and MDR1/2, target the destined domain directly from the Golgi and bypass the transcytosis (the direct pathway, also known as the vectorial pathway) (Kipp and Arias 2000, Kipp and Arias 2000, Kipp, Pichetshote et al. 2001, Kipp and Arias 2002, Wakabayashi, Kipp et al. 2006, Decaens, Durand et al. 2008, Weisz and

Rodriguez-Boulan 2009). In contrast to Mdr1/2, assays using rat livers with *in vivo* pulse-chase labeling and cLPM preparation demonstrated that the direct targeting of BSEP/Bsep was more complicated (Kipp and Arias 2000, Kipp, Pichetshote et al. 2001).



Canalicular targeting of rBsep was initially transferred from the Golgi to an intracellular pool, from which approximate half of rBsep was further translocated to the canalicular membrane (Kipp and Arias 2000, Kipp, Pichetshote et al. 2001). This intracellular pool was enriched with endosome markers, including Rab5 (early/sorting endosomes) and Rab11 (apical/slow recycling endosomes) (Kipp and Arias 2000). At steady state, BSEP/Bsep constitutively cycled between Rab11-positive compartments and the canalicular membrane in polarized hepatic cells (Wakabayashi, Lippincott-Schwartz et al. 2004, Wakabayashi, Dutt et al. 2005). Moreover, the half-life of rBsep in the cLPM and in the whole liver homogenate was approximately 4 days and 6 days, respectively (Kipp, Pichetshote et al. 2001). The half-life discrepancy of rBsep between the cLPM and the liver homogenate suggested an underlying mechanism of BSEP/Bsep trafficking at the post-Golgi network, especially at the SACs.

The movement of Bsep from the SACs to the canalicular membrane is microtubule (MT)-dependent, and the retrieval of BSEP from the canalicular membrane to the SACs is MT- and actin-dependent (Misra, Varticovski et al. 2003, Wakabayashi, Lippincott-Schwartz et al. 2004). Several physical stimuli and chemical substances, through some common signaling pathways, modulate BSEP/Bsep translocation, which is followed by changes in bile salt secretion. These stimuli, substances, and signaling pathways are illustrated in Figure 7B.

1.11. BSEP interacting proteins that participate in subcellular trafficking of BSEP

There have been very limited studies regarding to BSEP-interacting proteins and their roles on the subcellular transfer of BSEP, especially on canalicular targeting (Ortiz, Moseley et al. 2004, Chan, Calderon et al. 2005, Hayashi, Inamura et al. 2012, Lam, Xu et al. 2012, Przybylla, Stindt et al. 2016). HAX-1 is the first protein identified via genetic approach to involve the BSEP internalization. HAX-1 can interact with cortactin

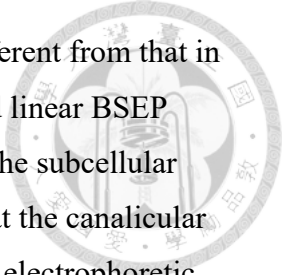
that has been implicated in clathrin-mediated endocytosis (Ortiz, Moseley et al. 2004). Hayashi *et al.* demonstrated that AP2 adaptor complex, an adaptor protein mediating clathrin-mediated endocytosis, could bind BSEP directly through a tyrosine motif at the carboxyl terminus of BSEP (Hayashi, Inamura et al. 2012). Lam *et al.* discovered the canonical tyrosine-base motif ¹³¹⁰YYKLV¹³¹⁴ of BSEP was sufficient to internalize BSEP and to sort it to the endosomal pathway (Lam, Xu et al. 2012).

In comparison with several Bsep-interacting proteins involving in Bsep retrieval, the non-muscle myosin II regulatory light chain (MLC2) is so far the only Bsep-interacting protein known to influence the apical targeting of Bsep (Chan, Calderon et al. 2005). MLC2 is a subunit of the non-muscle myosin II, which mediates cell polarization, migration, and cell-cell adhesion (Conti and Adelstein 2008). MLC2 and Bsep were dominantly presented in a cLMP fraction prepared from rat livers, and were colocalized at the canalicular membrane of several polarized cell lines with ectopically expressing both proteins. Treatment with myosin II specific inhibitor or co-expression with dominant negative MLC2 severely impaired the apical targeting and reduced the canalicular abundancy, respectively, of Bsep (Chan, Calderon et al. 2005).

In addition to HAX-1 and MLC2, Przybylla *et al.* have reported several BSEP-interacting proteins, but their functions or impacts on BSEP were not further characterized (Przybylla and Schmitt 2014). In these studies, the mechanisms of BSEP internalization was elucidated, but the significance of these interacting proteins in liver diseases has not been reported (Ortiz, Moseley et al. 2004, Hayashi, Inamura et al. 2012, Lam, Xu et al. 2012).

1.12. Research Questions and Niches

The mechanisms of BSEP apical targeting during fetal development as well as mechanisms of disturbances of BSEP targeting in intrahepatic cholestasis such as intrahepatic cholestasis of pregnancy, neonatal and infantile cholestasis, drug-induced cholestasis are still unknown. No mutations of those BSEP-interacting molecules above mentioned were so far found in clinical samples. Therefore, it is important to identify the key molecules participate in the BSEP sorting from intracellular compartments to the canalicular membrane of hepatocytes.



The subcellular distribution of BSEP in fetal human livers is different from that in adult (Chen, Chen et al. 2005). Adult human livers revealed sharp and linear BSEP signals at the canalicular membrane of hepatocytes. On the contrary, the subcellular location of BSEP in fetal livers is partially intracellular and partially at the canalicular membrane. Western blot of BSEP showed no significant difference in electrophoretic migration of adult and fetal BSEP (Chen, Chen et al. 2005). Besides, I have stained BSEP in several human liver specimens that is come from an infant with transient cholestasis and without BSEP mutations. As shown in Appendix Figure 1, the hepatocytes in patients' liver samples demonstrated aberrant intracellular BSEP signals compared to normal adult human hepatocytes (Figure 7A). According to the observation in fetal and transient cholestatic human liver samples, it suggested some underlying *trans* factors that may cause the intracellular retention of BSEP. Besides, more than one hundred of BSEP mutations have been identified, but a few BSEP mutants have been dissected for the disease mechanism (Kubitz, Droge et al. 2012, Droge, Bonus et al. 2017). BSEP mutants may be mediated through a similar or the same targeting machinery used in development livers but disturbed due to BSEP mutations.

Besides, a significant ratio of PFIC patients do not have mutations in those known cholestasis-associated genes (Chen, Li et al. 2019). What underlying genetic disorders result in PFIC is still a tough task required to be identified. Therefore, it is import to uncover the underlying *trans* factors that may regulate BSEP trafficking and function. Besides, searching unknown disease-associated genes from clinical patients' samples is another approach.

1.13. Hypothesis and specific aims

Identification of cholestasis-associated genes from clinical samples and BSEP-interacting proteins may help us to know the trafficking mechanism of BSEP. In this study, I hypothesized that aberrant subapical BSEP compartments observed in cholestatic liver samples were caused by unidentified *trans*-factors and their associated mechanisms. To test the hypothesis, I proposed two research aims in this study.

To explore the BSEP-interacting proteins and to characterize their impacts on BSEP sorting

To approach this aim, I would use a fragment of human BSEP as the bait to search

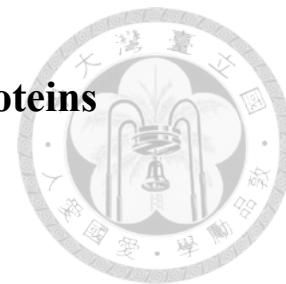
BSEP-interacting proteins through yeast two-hybrid assays. A BSEP-interacting candidate, which has been known to participate in cargo sorting, would be characterized for its impacts on BSEP sorting *in vitro* and *in vivo*. I believe that some BSEP-interacting candidates discovered in these assays will help us to realize the trafficking mechanism of BSEP.

To search novel PFIC-associated genes from cholestatic patients and to dissect their subcellular distribution of BSEP

The clinical samples from cholestatic patients without associations with those known cholestatic genes will be subjected to the whole exome sequencing. The cholestasis-associated gene candidate will be analyzed for its distribution and the BSEP subcellular localization in cholestatic patients' liver samples. I believe this approach will discover some underlying cholestasis-associated genes, which could be directly linked to clinical diseases.

Through the forward and reverse genetic approaches, I believe that the sorting mechanism of BSEP will be elucidated. The findings of this study may also provide new aspects of treatment options and novel drugs development for BSEP-associated diseases.

Chapter 2 Identification of BSEP-interacting proteins



2.1. Introduction

BSEP, encoded by the gene *ABCB11*, is the key molecule mediating translocation of bile salts from hepatocytes into the bile canaliculi, and contribute to the major driving force for bile flow. Chen *et al.* and Lu *et al.* have identified genetic disorder and abnormal protein expression of BSEP in Taiwanese patients with PFIC and cholestasis in infancy (Chen, Chang *et al.* 2002, Chen, Liu *et al.* 2008, Lu, Wu *et al.* 2014). Among those PFIC patients with low GGT level, merely about half of these patients being identified had mutations in FIC1 or BSEP (Chen, Chang *et al.* 2002, Chen, Liu *et al.* 2008). In the study of intrahepatic cholestasis in infancy, as high as 45% of patients did not have identifiable causes of cholestasis (Lu, Wu *et al.* 2014). I have also found that some patients are without BSEP mutations but with abnormal (partial or transient) expressions of BSEP in their livers (Appendix Figure 1A). Besides, the mechanism of BSEP membrane targeting and subcellular trafficking are poorly understood, especially during liver development. Chen *et al.* reported a very distinct pattern of BSEP in fetal livers, in which the BSEP was localized at the cytoplasm diffusely in contrast to at the cytoplasm as speckles and at the canalicular membrane as lines in the adult liver (Chen, Chen *et al.* 2005). Therefore, it is important to identify the key molecules participate in BSEP sorting from the intracellular compartment to the canalicular membrane of hepatocytes.

The object of this study is to search BSEP interacting proteins through genetic assays. I used the human BSEP polypeptide as a bait to screen the human fetal liver cDNA library through yeast two-hybrid systems. Several BSEP-interacting candidates were uncovered.

2.2. Materials and Methods

2.2.1. Reagents and chemicals

Yeast Nitrogen Base (YNB) with ammonium sulfate (Q300-09) or without ammonium sulfate (233520) was purchased from Thermo Fisher Scientific and BD

Difco, respectively. Chemicals were purchased from Sigma-Aldrich (Sigma-Aldrich, Inc., Missouri, USA), including adenine (A8626), uracil (U1128), tryptophan (T0254), histidine (H8000), arginine (A8094), methionine (M9625), tyrosine (T8566), isoleucine (I2752), valine (V0500), lysine (L5501), phenylalanine (P5482), glutamic acid (G1251), aspartic acid (A8949), threonine (T8625), serine (S4311), leucine (L8000), 5-bromo-4-chloro-3-indolyl- β -D-galactopyranoside (X-Gal; B5252), and β -mercaptoethanol (M6250).

2.2.2. Plasmid construction

A frozen human liver sample with neither BSEP deficiency nor *ABCB11* mutation was used to extract total RNA by RNeasy kit (Qiagen GmbH, Hilden, Germany). A PCR DNA fragment coding for amino acids 270-815 of human BSEP was cloned into the BamHI/Sall site of pBTM116, a bait plasmid containing LexA DNA-binding domain and tryptophan genes. All primer sequences used for cloning and site-directed mutagenesis were listed in Appendix Table 1. All constructs were confirmed via sequencing and listed in Appendix Table 2.

2.2.3. Yeast transformation, protein extraction, and 3-AT titration

The bait plasmid was transformed into *Saccharomyces cerevisiae* strain L40 (*MATa trp1 leu2 his3 LYS::(lexAop)4-HIS3 URA3::(lexAop)8-lac*) through electroporation. The transformed yeast was cultured in YPD medium supplement with tryptophan-free Dropout (DO) solution. Yeast protein was extracted from broth after 5 days of culture for immunoblotting. The transformed yeast was cultured on YPD/-Trp/-His plates containing 0, 0.5, 1, 2, 5, and 10 mM of 3-amino-1,2,4-triazole (3-AT). The concentration of 3-AT was optimized to suppress background growth on SD medium lacking His.

2.2.4. The human fetal liver cDNA library

The Human Fetal Liver MATCHMAKER cDNA Library (638805, Clontech Laboratories, Inc., CA) was provided by the Biomedical Resource Core of the First Core Laboratory, National Taiwan University College of Medicine. The human fetal liver cDNA was derived from a normal fetal liver pool, in which contained 32 whole livers from spontaneously aborted Caucasian fetuses at gestational age from 18 to 24 weeks. The cDNA library was constructed in the pACT2 vector, which contains the

yeast *LEU2* gene for leucine selection.

The cDNA library amplification through bacterial competent cells (DH5 α) followed the instruction of “Matchmaker™ GAL4 Two-Hybrid System 3 & Libraries User Manual (Clontech Laboratories, Inc., CA).” The cDNA library was titrated to be higher than 1×10^4 independent colonies per microgram of DNA, and more than 1×10^7 independent colonies to achieve the coverage at least three times of total cDNA library.

2.2.5. Yeast two-hybrid and β -galactosidase filter assays

The yeast two-hybrid screen and interaction assay were performed using the “interaction-trap” system (Li, Chiang et al. 2007). In brief, *S. cerevisiae* strain L40 was transformed with LexA-expressing pBTM116 carrying BSEP (270-815). A human fetal liver cDNA library in pACT2 was screened using BSEP (270-815) as the bait through histidine auxotrophy (YPD/-Ura/-Lys/-Trp/-Leu/-His). With nutritional selection for 1 week, the yeast colonies growing in histidine auxotrophy were transferred to the keeping/master plate (YPD/-Ura/-Lys/-Trp/-Leu).

Histidine auxotrophic colonies were assayed for β -galactosidase activity using a colony-lift filter assay. The protocol was followed the instruction of “Yeast Protocols Handbook (Clontech Laboratories).” Briefly, yeast colonies on master plates were sub-cultured on interaction plates, and the yeast colony with human lamin expression was as the negative control for β -galactosidase assay. X-gal, the β -gal substrate, was freshly prepared. Yeast colonies were lifted off from the plate to nitrocellulose (NC) membranes (Immobilon® Transfer membrane, Millipore Corporation, MA), and permeabilized through freeze-and-thaw cycles. After incubated with the β -gal substrate at 30°C, colonies on NC membranes were classified as levels 1 to 6 according to the appearance of blue in 0.5, 1, 2, 4, 5 hours, or overnight.

2.2.6. Determination of cDNA identities

The yeast cells were cultured in nutrition-limiting broth (YPD/-Ura/-Lys/-Trp/-Leu) for plasmid extraction by Zymoprep™ Yeast Plasmid Miniprep II (D2004, ZYMO RESEARCH, CA). The cDNA fragments in pACT2 were amplified by the primer pair: 5'-CTATTCGATGATGAAGATACCCACCA-3' and 5'-GTGAACTTGCGGGGTTTTTCAGTATCTACGA-3'. The identity of cDNA-encoding genes was determined by DNA sequencing and subjected to online alignment.



2.3. Results

2.3.1. The human BSEP polypeptide spanning amino acid 270-815 was used to search the BSEP-interacting proteins through yeast two-hybrid assays.

Most of documented BSEP mutations locate within the third and, especially, the fourth cytoplasmic domains of BSEP (Kubitz, Droge et al. 2012). I used the human BSEP polypeptide spanning amino acids (a.a.) 270-815 (BSEP [270-815]) as the bait to screen a human fetal liver cDNA library by yeast two-hybrid system for BSEP-interacting proteins. The amino acid identity between BSEP (270-815) and rat or mouse Bsep (270-815) homolog is 82.85% and 81.78%, respectively (Figure 8), suggesting this region is highly conserved. The findings from this genetic assay may be feasibly studied in rodent models.

The DNA encoding the human BSEP (270-815) was cloned from a total liver cDNA, which was derived from a patient with biliary atresia, into the vector pGBKT7 (pGBKT7-ABCB11). The cloned BSEP (270-815)-expressing gene contains a common *ABCB11* c.1331T>C (p.V444A) polymorphism in Taiwanese people (Chen, Liu et al. 2008). The plasmid pGBKT7-ABCB11 was supposed to express the BSEP (270-815) fusion protein with the yeast GAL4 DNA-binding domain (BD) as well as a c-Myc tag (Figure 9A). However, this fusion protein could not be detected in immunoblotting through anti-Myc antibodies (Figure 9B). The BSEP (270-815)-encoding gene was sub-cloned into the pBTM116 vector, another bait vector expressing LexA BD (Figure 10A). Two yeast competent cells, AH109 and L40, transformed with pBTM116-ABCB11 could expressed the LexA BD-BSEP (270-815) fusion protein (Figure 10B) and no yeast colony grew in the 3-AT supplementary condition (data not shown). Notably, the chimeric BSEP protein was not stable (Figure 10B).

For testing the efficiency of the human fetal liver cDNA library, approximate one thousand independent yeast colonies were obtained from 100 nanograms of the cDNA transformation, suggesting transformation with one milligram of the cDNA plasmid would obtain 1×10^7 independent colonies and achieve the coverage at least three times of total cDNA library.

2.3.2. Approximate 15% of yeast colonies identified from yeast two-hybrid screening reveals strong β -galactosidase activity.

Figure 11 illustrates the procedure of BSEP-interacting proteins searched through yeast two-hybrid screening. Total seven hundred and fifty-seven yeast colonies were obtained from yeast two-hybrid screening. The β -galactosidase (β -gal) filter assay was used to confirm the interaction between the BSEP bait and the candidate proteins. Lamin was used as the negative control for β -gal assays. Since thirty-eight yeast clones did not grow on the interaction plates, seven hundred and nineteen yeast colonies were assayed. After being incubated with the X-gal at 30°C, colonies on NC membranes were classified as the level 1 to the level 6 according to the appearance of blue in 0.5, 1, 2, 4, 5 hours, or overnight.

Table 6 summarized the statistic result of yeast two-hybrid screening and β -gal filter assays (Figure 12). Approximate 40% (n = 286) of the yeast clones assayed did not turn blue after overnight incubation of X-gal. In all yeast clones assayed by X-gal, 14.4% (n = 103) of yeast colonies revealed blue color within 2 hours (levels 1-3) (Table 6). Hence, those colonies with β -gal activity of levels 1-to-3 were subjected to further analysis.

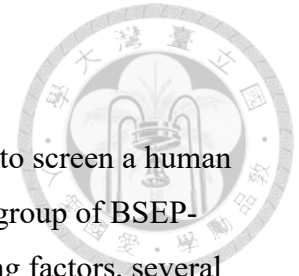
2.3.3. Analysis of yeast plasmid inserts by polymerase chain reaction

Plasmids from yeast clones with levels 1-to-3 β -gal activity was extracted, and the cDNA insert was analyzed through PCR amplification and electrophoresis. For avoiding to the same clones being chosen, the PCR product with different lengths was subjected to Sanger's sequencing for gene identity. Total sixty-eight clones were sequenced and aligned with online data banks.

In sixty-eight clones sequenced, 36 transcripts together with the mitochondrial genome were identified, in which chromatin-remodeling factors were abundant. Except of chromatin-remodeling factors, several transcripts were frequently identified, including serpin peptidase inhibitor clade A (SERPINA) member 1 (*SERPINA1*, *a.k.a.* anti-trypsin), *SERPINA3* (*a.k.a.* anti-chymotrypsin), hexokinase domain containing 1 (*HKDC1*), and hemoglobin genes (*HBA1* and *HBG1*) from 5, 9, 6 and 6 clones, respectively. Additionally, two clones were identified to encode cellular coat proteins, the charged multivesicular body protein 5 (CHMP5) and the coatomer protein complex subunit α (COPA). The sequencing findings were summarized in Table 7.

2.4. Summary

In this study, the human BSEP (270-815) polypeptide was used to screen a human fetal liver cDNA library through the yeast two-hybrid system, and a group of BSEP-interacting candidates was identified. Except of chromatin-remodeling factors, several transcripts are known to be expressed in liver- or fetal liver-specific manner. There transcripts include *SERPINA1* (*a.k.a.* anti-trypsin), *SERPINA3* (*a.k.a.* anti-chymotrypsin), *HKDC1*, *HBA1*, and *HBG1*. Besides, two clones encoding cellular coat protein transcripts were identified *i.e.* *CHMP5* and *COPA*. Both *CHMP5* and *COPA* have been known to participate in subcellular sorting.



Chapter 3 The ESCRT machinery participates the post-Golgi trafficking of BSEP



3.1. Introduction

BSEP is a canalicular transporter with 12 transmembrane segments. Targeting to the apical/canalicular membrane and sustaining the membrane abundance are critical for BSEP functions. Newly synthesized canalicular proteins go through two different routes to the canalicular membrane of hepatocytes (Gissen and Arias 2015). Most apical proteins, such as DPPIV, traffic via the indirect targeting, in which proteins are transferred initially to the basolateral membrane and then undergo transcytosis to the apical membrane. Others, including BSEP and MDR1, target to the canalicular membrane without transcytosis (Kipp and Arias 2000, Kipp, Pichetshote et al. 2001). Before trafficking to the canalicular membrane, BSEP first transfers to the Rab11-positive intermediate pool/subapical compartment (SAC), and then constitutively cycles between SACs and the canalicular membrane (Kipp and Arias 2000, Wakabayashi, Lippincott-Schwartz et al. 2004). This two-stepped direct targeting of BSEP suggests a complicated regulation at SACs.

Chen *et al.* have reported the subcellular distribution of BSEP in human fetal hepatoblasts is different from that in adult hepatocytes (Chen, Chen et al. 2005). The partially intracellular and partially canalicular distribution of BSEP in fetal livers suggested some regulations during BSEP trafficking. Besides, increased intracellular retention of BSEP is the main character of BSEP associated cholestasis (Crocenzi, Zucchetti et al. 2012) (Appendix Figure 1). The BSEP apical targeting may use some common mechanisms shared between developmental livers and cholestatic liver diseases. The mechanisms of disturbed BSEP targeting and functions that cause cholestasis have been elucidated for only a small proportion of BSEP mutational defects, and effective treatments are lacking (Hayashi, Takada et al. 2005, Chen, Liu et al. 2008, Strautnieks, Byrne et al. 2008, Wang, Dong et al. 2008, Byrne, Strautnieks et al. 2009). Hence, I attempted to study the apical targeting of BSEP and pathogenic BSEP mutations found in human cholestasis patients. In this study, I discovered that charged multivesicular body protein 5 (CHMP5), a key endosomal protein complex

required for transport subcomplex-III (ESCRT-III), is essential for the post-Golgi trafficking of BSEP. The aberrant association between CHMP5 and BSEP mutants may cause the intracellular retention of BSEP mutants occurred in PFIC2.



3.2. Materials and Methods

3.2.1. Human liver samples

Liver samples were obtained from three adult living-related liver donors, four infants with non-cholestatic metabolic diseases, and twenty-one fetal liver samples at gestational ages from 13 to 22 weeks from elective terminations of pregnancy for medical indications under informed consent. Liver samples from 5 patients with cholestatic liver diseases were analyzed, including one 4-year-old boy with transient cholestasis; eight infants with neonatal cholestasis and subsequent recovery; one infant with severe cholestasis with a heterozygous c.1460G>A (p.R487H) BSEP mutation; one PFIC2 infant with compound heterozygous c.1478G>A (p.W483X) and c.3011G>A (p.G1004N) BSEP mutations (Chen, Liu et al. 2008, Chen, Li et al. 2019). Informed consent was obtained from each subject, and the protocol was approved by the Institutional Review Board, National Taiwan University.

3.2.2. Plasmid construction and transfection

Human BSEP-expressing constructs were cloned from pTRE-tight-SPGP, a kindly gift of Dr. Victor Ling (The University of British Columbia, Vancouver, Canada). The cryptic prokaryotic promoter in human BSEP coding sequence (Noe, Stieger et al. 2002) was first inactivated via site-directed mutagenesis and then sub-cloned into Hind III/Kpn I site of p3XFLAG-CMV-10 and pEGFP-C2 to yield p3XFLAG-BSEP and pEGFP-BSEP, respectively. A synthetic poly-nucleotide encoding a (GGGGS)₃ polypeptide linker was further inserted in Bgl II/Hind III of pEGFP-BSEP to generate pEGFP-LK-BSEP. All the other plasmids expressing full-length or fragmental BSEP and BSEP mutants were cloned from pEGFP-LK-BSEP.

The open-reading frame (ORF) of *CHMP5* (NM_016410.5), *VPS4A* (NM_013245.2), *VPS4B* (NM_004869.4), and *Rab11A* (NM_004663) was cloned from the cDNA of Hep G2 cells into pCMV6-AC-3HA, pmCherry-C1 or pEGFP-C1 to obtain pCHMP5-3HA, pmCherry-CHMP5, pmCherry-VPS4A, pmCherry-VPS4B, and

pEGFP-Rab11A. Site-directed mutagenesis was further used to generate plasmids expressing the dominant-negative mutants of VPS4A-E228Q (VPS4A-EQ), VPS4B-E235Q (VPS4B-EQ), or Rab11A-S25N (Rab11A-SN). A (GGGS)₃-coding linker was inserted into Bgl II/Hind III of pmCherry-CHMP5 to generate pmCherry-LK-CHMP5.

The plasmid pcDNA3.1 (+)-Mem-DsRed-Monomer was obtained from the Biomedical Resource Core and the Imaging Core at the First Core Lab, National Taiwan University College of Medicine. Plasmids expressing HA-tagged ubiquitin (HA-Ub) mutants were obtained from Addgene, including pRK5-HA-Ubiquitin-WT (#17608), -K48 (#17605), -K48R (#17604), and -K63 (#17606) (Lim, Chew et al. 2005). The plasmid pRK5-HA-Ub-K63R was constructed using site-directed mutagenesis from pRK5-HA-Ubiquitin-WT. Plasmids expressing short hairpin RNA (shRNA) targeting mouse *Chmp5* (TRCN0000009719 and TRCN0000009721) and the paired scramble control (pLAS-Void) were purchased from National RANi Core Facility Platform, Academia Sinica, Taiwan. The target sequences for mouse *Chmp5* were as follows (coding strand sequence indicated): TRCN0000009719, 5'-CCAACCAGATTTAGGTTTCTT-3' and TRCN0000009721, 5'-CCTGCTAAGAACATGGTCAAA-3'. The shRNA scramble sequence of pLAS-Void was 5'-AGTTCAGTTACGATATCATGTCTCGAGACATTCGCGA
GTAAGTGAAGTCTTTTGTG-3'. All primer sequences used for cloning and site-directed mutagenesis were listed in Appendix Table 1. All constructs were confirmed via sequencing and listed in Appendix Table 2. The deliveries of plasmid DNA and small interference RNA (siRNA) were performed using Lipofectamine™ 3000 and Lipofectamine™ RNAiMAX (Thermo Fisher Scientific, Waltham, MA), respectively.

3.2.3. Hydrodynamic injection of mice

Seven- to ten-week-old mice with targeted inactivation of the *Bsep* (*spgp*) gene on an FVB/NJ genetic background (Wang, Salem et al. 2001) and wild-type male FVB/NJ mice (8-week-old) were used for hydrodynamic injection study. Twenty micrograms of plasmid DNA in PBS was injected hydrodynamically through mouse tail veins. Three to four mice were used for each experimental injection. Mice were sacrificed in indicated experimental times. Sera and liver samples were collected for biochemical and immunolabeling assays. Experiments were conducted according to the approved protocols from the Committee on Animal Care, National Taiwan University College of

Medicine.



3.2.4. Yeast two-hybrid screen and interaction assay

The yeast two-hybrid screen and interaction assay were performed using the “interaction-trap” system (Li, Chiang et al. 2007). The human fetal liver cDNA library (Clontech, Mountain View, CA) was screened using amino acid residues 491-680 of human BSEP as bait. Plasmids encoding different BSEP protein fragments for interacting-domain mapping were cloned and subjected to the same assay system of yeast two-hybrid.

3.2.5. Cell culture

Human hepatoma cell lines Hep G2 [HEPG2] (ATCC® HB-8065TM), Huh-7, and Mahlavu were cultured in DMEM with high glucose supplement with 10% fetal bovine serum, MEM-nonessential amino acids, sodium pyruvate, GlutaMAX, and antibiotics. All cell-culture related reagents were purchased from Thermo Fisher Scientific. The cell lines were routinely checked for mycoplasma contamination using EZ-PCR Mycoplasma Test Kit (Cat#20-700-20, Biological Industries, Cromwell, CT).

3.2.6. Temperature shift assay

The temperature shift assay was modified from the protocol described previously (Presley, Cole et al. 1997). In brief, Hep G2 cells were sequentially incubated at 40°C, 20°C, and 32°C to synchronize proteins at ER, Golgi’s apparatus, and to release into the post-Golgi network, respectively. Since incubation at 20°C, cells were refreshed with pre-warmed medium supplement with 100 µg/mL cycloheximide. The detail protocol is indicated in each Figure.

3.2.7. Protein extraction and subcellular fractionation

For the extraction of total cell lysates, cultured cells were washed using cold PBS and lysed using denaturing lysis buffer (150 mM NaCl; 50 mM Tris-Cl, pH 8.0; 1% NP-40; 0.5% sodium deoxycholate; 0.1% SDS; 5 mM EDTA) or non-denaturing n-dodecyl β-D-maltoside (β-DDM) lysis buffer (150 mM NaCl; 20 mM HEPES, pH 7.4; 0.1% β-DDM; and 1 mM EDTA) supplement with protease and phosphatase inhibitor cocktail (Thermo Fisher Scientific). All ubiquitination-related experiments were further supplement with 20 mM N-ethylmaleimide in lysis buffers or reagents. To collect the supernatant, lysed cells were centrifuged at 4°C with 13,000 xg for 10 minutes. For

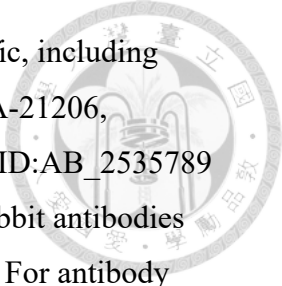
subcellular fractionation, the Mem-PERTM Plus Membrane Protein Extraction Kit (Thermo Fisher Scientific) and Trident Membrane Protein Extraction Kit (GeneTex, HsinChu, Taiwan) were used.



3.2.8. Antibodies, immunoprecipitation, Western blotting and immunostaining

For immunoprecipitation, antibodies against CHMP5 (Cat#sc-67230, RRID:AB_10608611 and Cat# sc-374338, RRID:AB_10989738, Santa Cruz Biotechnology, Dallas, TX), FLAG (Cat# F3165, RRID:AB_259529, Sigma-Aldrich, St. Louis, MO) were used. For Western blotting, the primary antibodies against the following proteins were used: BSEP (Cat# GTX102608, RRID:AB_2036139), COX4 (Cat# GTX114330, RRID:AB_10625002), EGFP (Cat# GTX628894, RRID:AB_2773724), GAPDH (Cat# GTX100118, RRID:AB_1080976), mCherry (Cat# GTX128508, RRID:AB_2721247), and α -Tubulin (Cat# GTX628802, RRID:AB_2716636) from GeneTex; CHMP5 (Cat# sc-374338), HA (Cat# sc-805, RRID:AB_631618), LIP5 (Cat# sc-374012, RRID:AB_10918292), Na⁺/K⁺-ATPase α (Cat# sc-48345, RRID:AB_626712), Rab11A (Cat# sc-166912, RRID:AB_10611645) and VPS4A (Cat# sc-393428, RRID:AB_2773025) from Santa Cruz Biotechnology; FLAG (Cat# F3165) from Sigma-Aldrich; K48-linkage specific ubiquitin (Cat# ab140601, RRID:AB_2783797, Abcam) and K63-linkage specific ubiquitin (Cat# ab192489, RRID:AB_2737584, Abcam, Cambridge, UK) from Abcam. The HRP-conjugated secondary antibodies are EasyBlot anti Mouse IgG (HRP) antibody (Cat# GTX221667-01, RRID:AB_10728926) from GeneTex; goat anti-rabbit IgG, Fc Fragment Specific antibody (Cat# 111-035-046, RRID:AB_2337939); goat anti-mouse IgG, Light Chain Specific antibody (Cat# 115-035-174, RRID:AB_2338512), and goat anti-mouse IgG (subclasses 1+2a+2b+3), Fc-Fragment Specific antibody (Cat# 115-035-164, RRID:AB_2338510) from Jackson ImmunoResearch Labs (West Grove, PA).

For immunofluorescence staining, the primary antibodies against the following proteins were used: BSEP (Cat# sc-74500, RRID:AB_2242103, Santa Cruz Biotechnology), CHMP5 (Cat#sc-67230), FLAG (Cat# F3165), HA (Cat# sc-805), LIP5 (Cat# sc-374012), and mCherry (Cat# GTX128508). The rabbit anti-FLAG (Cat# 20543-1-AP, RRID:AB_11232216, Proteintech Group, Rosemont, IL) antibody was used for immunohistochemical staining. The Alexa Fluor 594 or 488 conjugated



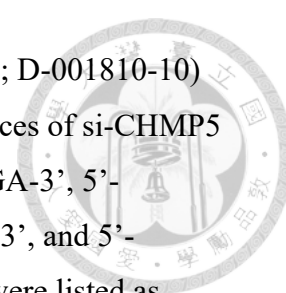
secondary antibodies were all purchased from Thermo Fisher Scientific, including donkey anti-rabbit IgG (Cat# A-21207, RRID:AB_141637 and Cat# A-21206, RRID:AB_2535792) and donkey anti-mouse IgG (Cat# A-21203, RRID:AB_2535789 and Cat# A-21202, RRID:AB_141607); the biotinylated horse anti-rabbit antibodies (Cat# BA-1100, RRID:AB_2336201) were from Vector Laboratories. For antibody labeling, CF350 Mix-n-Stain Antibody Labeling Kits (Cat#92270, Biotium, Fremont, CA) were used.

Immunoprecipitation was performed using Dynabeads Protein G (Thermo Fisher Scientific) conjugated with antibodies or normal immunoglobulins (Cat# sc-2027, RRID:AB_737197 and Cat# sc-2025, RRID:AB_737182, Santa Cruz Biotechnology). GFP-Trap (Cat# GTM-20, ChromoTek, Planegg-Martinsried, Germany) and anti-HA magnetic beads (Thermo Fisher Scientific) were used to immunocapture EGFP-tagged and HA-tagged proteins, respectively. All protein samples were eluted in reducing Bolt™ LDS Sample Buffer; separated in 4-12% Bolt™ gels (Thermo Fisher Scientific), and electro-transferred to PVDF membranes for immunoblotting of targeting proteins. The signal density was quantified using Image Lab (Bio-Rad, Hercules, CA).

Cryopreserved human and mouse liver tissues were sectioned in 6 µm and fixed in cold acetone. For in vitro cell samples, cells were fixed and permeabilized using 4% paraformaldehyde and 0.5% Triton X-100. After serum blocking, samples were incubated with primary antibodies and visualized by fluorochrome-conjugated secondary antibodies. Samples were counter-stained and mounted using ProLong Diamond Antifade Mountant with DAPI (Cat# P36965, Thermo Fisher Scientific). For immunohistochemical staining, paraffin-embedded mouse liver samples were sectioned in 4 µm and then subjected to de-wax, rehydrate, and antigen retrieval. Endogenous peroxidase activity and biotins were quenched using hydrogen peroxide and Avidin/Biotin Blocking Kit (SP-2001, Vector Laboratories, Burlingame, CA), respectively. After incubation of the primary and secondary antibodies, tissue samples were visualized using VECTASTAIN Elite ABC HRP Kit (Cat# PK-6100; Vector Laboratories) and VECTOR NovaRed Peroxidase Substrate Kit (Cat# SK-4800, Vector Laboratories). Cell nuclei were stained using hematoxylin.

3.2.9. RNA interference and quantitative RT-PCR

Pre-designed small interference RNA (siRNA) pool targeting human *CHMP5* (si-



CHMP5; L-004697-01) and the paired non-targeting control (si-CTL; D-001810-10) were purchased from Dharmacon (Lafayette, CO). The target sequences of si-CHMP5 were listed as follows: si-CHMP5, 5'-ACAAGCAAGTGAAGATCGA-3', 5'-GGTATTATAGGTTGGTTAA-3', 5'-GGAATTATCACTACTGTAT-3', and 5'-TAGTGAAGTATAAGGATCA-3'. The target sequences of si-CTL were listed as follows: 5'-UGGUUUACAUGUCGACUAA-3', 5'-UGGUUUACAUGUUGUGUGA-3', 5'-UGGUUUACAUGUUUCUGA-3', and 5'-UGGUUUACAUGUUUCCUA-3'. Hep G2 cells on 6-well plate were reverse transfected with 10 nM siRNA (25 pmol per well). The mRNA and protein of treated cells were harvested and subjected to quantitative PCR and immunoblotting, respectively. Total RNA was extracted through TRIzol® reagent (Thermo Fisher Scientific). Two micrograms of total RNA were reverse transcribed using SuperScript III® (Thermo Fisher Scientific) with oligo-dT primers, and subjected to duplex quantitative PCR using TaqMan™ Gene Expression Assays (Thermo Fisher Scientific) for *CHMP5* (Hs00995158_g1) and *GAPDH* (Hs02758991_g1).

3.2.10. Determination of total bile acids

Hep G2 cells were pre-treated with siRNA for 48 hours, and then transfected with pEGFP-LK-BSEP plus pmCherry-LK-CHMP5 or its vector pmCherry-C1 48 hours. Conditional medium was collected for determining total bile acids using Total Bile Acids Assay Kit (DZ042A; Diazyme Laboratories, Poway, CA).

3.2.11. Image acquisition and processing

Immunostaining samples were imaged using ZEISS Observer. D1 fluorescence microscope (Carl ZEISS, Jena, Germany) equipped with EC Plan-Neofluar 10x/0.30 M27, LD Plan-Neofluar 20x/0.4 Korr Ph2 M27, and LD Plan-Neofluar 40x/0.6 Korr Ph2 M27 objectives; DAPI, FITC, and TRITC filters. AxioCam mRM r3.1 CCD camera and the microscope software AxioVision were used to image acquisition. For confocal microscopy, ZEISS LSM 880 with the Airyscan mode and ZEN software were used. All images were processed by Adobe Photoshop CS6.

3.2.12. Subcellular distribution index and canalicular targeting index

Subcellular distribution index was calculated from images obtained from examined Hep G2 cells after temperature shift assay and immunostaining of FLAG-BSEP proteins

and Mem-DsRed. The numbers of cells with both FLAG-BSEP and Mem-DsRed signals (FLAG-BSEP + Mem-DsRed) and, from these double-positive cells, with FLAG-BSEP signals at the plasma membrane (pFLAG-BSEP) were counted and then calculated as followed:

Subcellular distribution index (%)

$$= \frac{\text{No. of cells with pFLAG - BSEP}}{\text{No. of cells with FLAG - BSEP + Mem - DsRed}}$$

Canalicular targeting index was calculated from images obtained from hydrodynamically injected mouse liver samples with FLAG-BSEP staining. The number of canalicular FLAG-BSEP (cFLAG-BSEP) was manually calculated, and the area of the mouse live tissue in each image was determined by ImageJ program. The canalicular targeting index was calculated as followed:

$$\text{Canalicular targeting index} = \frac{\text{No. of cells with cFLAG - BSEP}}{\text{Area of the mouse liver tissue in images}}$$

3.2.13. Statistical analysis

All experiments are represented as mean \pm SD of independently triplicated or quadruplicated experiments. Statistical significance was determined using two-tailed unpaired *Student's t*-test, and *p* values ≤ 0.05 were consider significant (* $P \leq 0.05$). Data were analyzed using GraphPad Prism (GraphPad Software, San Diego, CA).

3.3. Results

3.3.1. The ESCRT-III CHMP5 interacts with BSEP.

I hypothesized that aberrant BSEP retention in the SACs of cholestatic hepatocytes is likely caused by apical trafficking defects (Appendix Figure 1). To address the hypothesis, I first identified cellular BSEP-binding partners involving in membrane trafficking by using the human BSEP amino acids (a.a.) 491-630 as a bait to screen human fetal liver cDNA library via yeast two-hybrid system. Charged multivesicular body protein 5 (CHMP5), a subunit of the endosomal protein complex required for transport subcomplex-III (ESCRT-III), was found to be one of the BSEP interacting candidates (Figure 13A). By mapping with different fragments of BSEP via the yeast

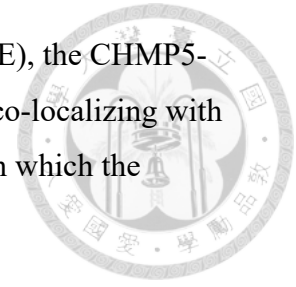
two-hybrid assay, the CHMP5 interacting domain of BSEP mainly located within a.a. 484-558, which is harbored in the first nucleotide-binding fold (NBF1; a.a. 414-610) of human BSEP (Figure 13B).

The interaction between BSEP and CHMP5 was validated via co-immunoprecipitation using three hepatoma cell lines, Hep G2, Huh-7, and Mahlavu. As shown in Figure 13C, endogenous BSEP was co-immunoprecipitated with CHMP5 in these cell lines. In addition to BSEP, other ESCRT subunits, including VPS4A, LIP5, and VPS25, were co-captured with CHMP5 from Hep G2 cell lysate (Appendix Figure 2A). BSEP is a transmembrane protein, whereas CHMP5 is a cytoplasmic protein distributed as either cytosolic monomers or cytoplasmic vesicle-membrane associated polymers. Total membrane-protein fractionation was used to study the subcellular interaction site of BSEP and CHMP5. After total membrane-protein fractionation, BSEP was found to distribute in the total membrane-protein (tM) fraction, which consists of plasma membrane (PM) and organelle-membrane (OM) protein fractions (Figure 13D and Appendix Figure 3). Consistent with previous studies, endogenous and mCherry-tagged CHMP5 was predominantly expressed in the cytosol (Cyt), with less in the tM fractions (Figure 13D and Appendix Figure 3). Immunoprecipitation using anti-EGFP antibodies revealed endogenous and mCherry-tagged CHMP5 formed complexes with EGFP-BSEP within the tM fraction (Figure 13D). These data suggest that only membrane-associated CHMP5 interacts with BSEP.

3.3.2. Subapical BSEP localizes in CHMP5-positive subapical compartments.

To study the interaction between BSEP and CHMP5 *in vivo*, adult human liver samples were analyzed and a hydrodynamic injection-based mouse model was established (Liu, Song et al. 1999). Immunofluorescence assay of BSEP and CHMP5 in adult human liver sections revealed that CHMP5 co-localized with subapical BSEP (Figure 13E). In addition to CHMP5, the subapical BSEP vesicles were also co-localized with the CHMP5 interacting ESCRT protein LIP5 (Appendix Figure 2B). I applied hydrodynamic injection to co-express FLAG-BSEP and haemagglutinin (HA)-tagged CHMP5 (CHMP5-3HA) in *Bsep* knockout mice livers (Wang, Salem et al. 2001). The liver sections of these mice were analyzed through immunofluorescence assays. In line with the total membrane-protein fractionation results *in vitro* and the

observation in adult human liver sections (Figure 13D and Figure 13E), the CHMP5-3HA signal displayed a mainly cytoplasmic distribution as speckles co-localizing with subapical BSEP (Figure 13F). Therefore, the SACs of hepatocytes, in which the subapical BSEP localizes, are CHMP5 positive.

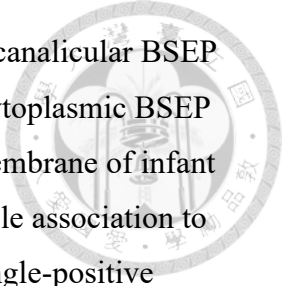


3.3.3. Cholestatic human livers demonstrate aberrant subapical BSEP vesicles.

To study the subcellular distribution of BSEP and CHMP5 in cholestatic human hepatocytes, two cholestatic human liver samples with BSEP mutations were analyzed via immunofluorescence assays. One liver sample is from a severe cholestatic infant harboring heterozygous BSEP-R487H mutation (BSEP-R487H/+) and the other is a PFIC2 infant with compound heterozygous BSEP mutations (BSEP-W493X/G1004D). In comparison with the age-matched infant control liver sample (Figure 14A; the left panel), the level of canalicular BSEP was reduced in both cholestatic livers, a character in BSEP associated cholestasis. On the other hand, abnormally enlarged or scattered puncta with BSEP-positive signals were formed in the subapical area in the cholestatic hepatocytes, which were different from that in the control liver (Figure 14B, and C; the left panel). Besides, these BSEP-associated signals were CHMP5 positive. To confirm the findings of aberrant subapical BSEP distribution in cholestatic hepatocytes, I further analyzed three neonatal hepatitis and one transient cholestasis liver samples. Similarly, huge cytoplasmic compartments or aggregated vesicles with BSEP positive signals was observed in the transient cholestasis (Figure 14D) and neonatal hepatitis (Figure 14E) liver samples, respectively. In these cholestatic hepatocytes, the aberrant subapical BSEP puncta were all CHMP5 positive. The findings of BSEP localizing in aberrant SACs suggest that the polarized trafficking of BSEP may be perturbed in cholestasis livers.

3.3.4. The canalicular targeting of BSEP is developmentally associated with CHMP5.

My observation on cholestatic liver samples raised a question: whether the different BSEP-expressing patterns in fetal and adult hepatocytes (Chen, Chen et al. 2005) may associate with different CHMP5 distribution. I examined the association of BSEP and CHMP5 in human liver development. The expression and distribution of BSEP and CHMP5 in the human liver samples of fetus at gestational age 13-22 weeks,

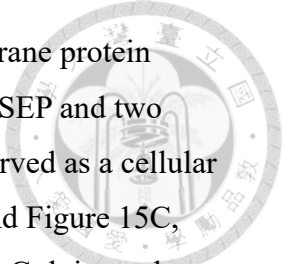


infant, and adult were analyzed. As shown in Appendix Figure 5, the canalicular BSEP signals were gradually increased during hepatocyte maturation; the cytoplasmic BSEP gradually formed clear puncta at the SACs beneath the canalicular membrane of infant and adult human hepatocytes. The CHMP5 signals revealed remarkable association to the cytoplasmic/subapical BSEP signals. Moreover, some CHMP5 single-positive vesicles aligned with the canalicular BSEP were observed in fetal hepatoblasts, especially in the fetal livers at gestational age 18-22 weeks (Appendix Figure 5). Hence, the apical trafficking of BSEP is developmentally regulated, which is also very likely associated with the ESCRT-III CHMP5.

3.3.5. Aberrant interaction between BSEP mutants and CHMP5 affects the polarized trafficking of BSEP mutants.

I uncovered that BSEP was developmentally associated with CHMP5 and aberrant subapical BSEP compartments in cholestatic livers were all CHMP5 positive. These results suggested that the defective targeting of BSEP in cholestatic hepatocytes may be caused by impaired CHMP5-associated ESCRT functions. The ESCRT complex participates in the endocytic pathway (Christ, Raiborg et al. 2017); however, whether the ESCRT machinery involving the apical membrane trafficking is unknown. To dissect the interaction between human BSEP mutants and CHMP5, I constructed plasmids expressing FLAG-tagged BSEP-R487H or BSEP-N490D, another PFIC2-causing BSEP mutant that could express on the canalicular but may be functionally defected (Byrne, Strautnieks et al. 2009), for *in vitro* and *in vivo* studies.

I first tested whether both BSEP mutants at the steady state indeed had disturbances in canalicular targeting *in vivo* by hydrodynamic injection-mediated mouse models. Immunofluorescence assay of the liver samples from hydrodynamically injected mice displayed decreased canalicular FLAG signals of FLAG-BSEP-R487H and FLAG-BSEP-N490D in comparison with wild-type FLAG-BSEP. Moreover, strong cytoplasmic signals were observed in the hepatocytes of mice injected with p3XFLAG-BSEP-R487H (Figure 15A). The glycosylation profile of both BSEP mutants was analyzed in BSEP mutant-expressing cell lysates with PNGase F or tunicamycin treatment. Aberrant glycosylation patterns of both BSEP mutants (Appendix Figure 6) further suggested the apical sorting of BSEP-R487H and BSEP-N490D was disturbed in a different degree. Temperature shift assays to probe post-Golgi trafficking of plasma



membrane proteins, combined with immunostaining or plasma membrane protein fractionation, were performed with Hep G2 cells expressing FLAG-BSEP and two FLAG-BSEP mutants (Presley, Cole et al. 1997). Mem-DsRed was served as a cellular membrane marker for cell image analysis. As shown in Figure 15B and Figure 15C, both BSEP mutants, especially BSEP-R487H, revealed defective post-Golgi membrane targeting in Hep G2 cells. Similarly, immunoblotting demonstrated decreased plasma membrane targeting of the two BSEP mutants in fractionated cell samples (Figure 15D). Taken together, these results suggest the apical targeting of both BSEP-R487H and BSEP-N490D mutants is indeed impaired and as the same as the observation in Figure 14B and in the literature (Byrne, Strautnieks et al. 2009).

I hypothesized that abnormal association with ESCRT molecules caused the impaired apical targeting of both BSEP mutants. I examined whether both mutants could interact with CHMP5 using yeast two-hybrid assay. CHMP5 together with either BSEP(484-558)-R487H or BSEP (484-558)-N490D was co-expressed in yeast cells and analyzed through nutritional selection as well as β -gal filter assays. BSEP (484-558) and BSEP (351-454) was used as positive and negative CHMP5-interaction control, respectively. As shown in Figure 16A, BSEP (484-558) harboring either R487H or N490D mutations could interact with CHMP5.

Total membrane-protein fractionation and co-immunoprecipitation were used to dissect the interaction between CHMP5 and the two BSEP mutants in Hep G2 cells. Immunoblotting of the fractionated samples revealed the decreased expression of BSEP-R487H mutant (Figure 16B, the input control panel). Immunoprecipitation via anti-FLAG antibodies was performed with the tM fractions of Hep G2 cells co-expressing CHMP5-3HA and either FLAG-BSEP mutant constructs. As the same as the wild-type FLAG-BSEP, FLAG-BSEP-R487H and FLAG-BSEP-N490D mutants formed complexes with CHMP5-3HA and two ESCRT molecules LIP5 and VPS4. However, more CHMP5-3HA was co-captured with FLAG-BSEP-R487H and FLAG-BSEP-N490D through densitometry analysis of CHMP5-3HA and FLAG-BSEP signals (Figure 16B, the right panel and the bar graph). Hence, the defective apical targeting of BSEP-R487H and BSEP-N490D may be caused by the altered affinity between the mutant BSEP and the ESCRT-III CHMP5.

3.3.6. CHMP5 regulates the apical targeting of BSEP and BSEP-mediated bile acid secretion.

BSEP-R487H and BSEP-N490D suggested an increased association with CHMP5 but decreased apical trafficking. I hypothesized that CHMP5 and the ESCRT machinery may participate in the post-Golgi trafficking of BSEP. To explore whether CHMP5 indeed affects the apical trafficking of BSEP, small interference RNA (siRNA) and short hairpin RNA (shRNA) targeting to *CHMP5/Chmp5* mRNA were used in Hep G2 cells and in a hydrodynamic injection-based mouse model, respectively. Both the mRNA and protein levels of CHMP5 can be knocked down and sustained at steady-state from 48 to 96 hours post-transfection (Figure 17A and Figure 17B). Hence, further studies using exogenously expressed BSEP with CHMP5 knockdown were performed 48 hours after 10-nM siRNA delivery. Besides, the protein level of endogenous BSEP was unaffected by CHMP5 knockdown (Figure 17C-E), which indicates that CHMP5 does not affect the protein expression or turnover of BSEP.

Temperature shift assays were performed with Hep G2 cells expressing FLAG-BSEP for evaluating its post-Golgi targeting in CHMP5 depletion. Hep G2 cells, pre-treated with 10 nM of si-CHMP5 or si-CTL, were co-expressed with FLAG-BSEP and Mem-DsRed. In CHMP5 depleted Hep G2, plasma membrane targeting of FLAG-BSEP was significantly decreased and FLAG-BSEP was accumulated in the cytoplasm, especially the perinuclear region (Figure 18A and Figure 18B). CHMP5-mediated BSEP apical-targeting was further examined *in vivo* via the hydrodynamic injection-mediated mouse model (Figure 18C). The plasmid pool expressing shRNA against mouse *Chmp5* (sh-*Chmp5*) was injected into FVB mice. In comparison with sh-CTL treated mice, reduced canalicular FLAG-BSEP and accumulated subapical FLAG-BSEP were observed in mice treated with sh-*Chmp5* (Figure 18C and Figure 18D). The results from the *CHMP5/Chmp5* knockdown Hep G2 cells and mouse livers showed that CHMP5 is required for the membrane targeting of BSEP *in vitro* and *in vivo*.

I next addressed the question that whether CHMP5 could impact the bile acid export function of BSEP. Compared to si-CTL pre-treated Hep G2 cells ($1.269 \pm 0.189 \mu\text{M}$), the concentration of total bile acids in the conditioned medium of the si-CHMP5 pre-treated cells ($0.855 \pm 0.225 \mu\text{M}$, $P = 0.0093$) was significantly reduced, which could be rescued through ectopically expressed CHMP5 ($1.377 \pm 0.317 \mu\text{M}$) (Figure 19).

Hence, CHMP5 could affect BSEP-mediated bile acid secretion possibly through influencing the membrane targeting of BSEP.

3.3.7. K63-linked ubiquitination of BSEP is required for the BSEP apical-targeting via CHMP5 associated ESCRT machinery.

K63-linked ubiquitination, the covalent bonding of ubiquitin (Ub) to its targets via its K63 residue, is a specific signal for cargo sorting in the ESCRT machinery (Lauwers, Jacob et al. 2009). Hence, I speculated that BSEP was also ubiquitinated with K63 linkage for its ESCRT-mediated apical targeting. To approach the speculation, HA-tagged ubiquitinated proteins were immunoprecipitated from the lysate of Hep G2 cells co-expressing FLAG-BSEP and HA-tagged wild-type ubiquitin (HA-Ub-Wt) or lysine-to-arginine-substituted Ub mutants (HA-Ub-K48, -K48R, -K63, and -K63R) (Lim, Chew et al. 2005). HA-tagged ubiquitinated FLAG-BSEP (Ub-FLAG-BSEP) greatly increased with HA-Ub-K63 co-expression, but reduced with HA-Ub-K63R co-expression. In contrast, Ub-FLAG-BSEP decreased in HA-Ub-K48 but increased in HA-Ub-K48R (Figure 20A). These results suggest that BSEP is mainly polyubiquitinated via K63 linkage.

I further dissected the role of K63-linked ubiquitination in CHMP5-mediated membrane targeting of BSEP. The PM fractions were isolated from Hep G2 cells ectopically expressing FLAG-BSEP, mCherry-CHMP5 and either HA-Ub-K63 or HA-Ub-K63R. In Ub-K63 expressing cells, FLAG-BSEP signals were detected earlier and more abundantly in the PM fractions compared with that in the Ub-K63R expressing cells (Figure 20B). FLAG-BSEP staining on the plasma membrane was hardly detected in Ub-K63R co-expression. On the other hand, FLAG-BSEP signals could be detected on the plasma membrane in Ub-K63 expressing Hep G2 pre-treated with si-CTL, but reduced in CHMP5 depleted cells (Figure 20C).

The influence of K63-linked ubiquitination on BSEP canalicular-targeting was *in vivo* analyzed in the hydrodynamic injection-based mouse model. As shown in Figure 20D and Figure 20E, more canalicular FLAG-BSEP staining was observed in mouse livers with Ub-K63 co-expression in comparison with those with Ub-K63R co-expression. These data further support that K63-linked ubiquitination of BSEP is required for CHMP5-mediated BSEP apical sorting.



3.3.8. The ESCRT machinery affects the polarized trafficking of BSEP.

VPS4, the only ESCRT molecule harboring enzyme activity, disassembles and recycles ESCRT-III complexes to complete ESCRT involved processes (Caillat, Maity et al. 2019). CHMP5 and other ESCRT-III proteins could recruit and regulate VPS4 through LIP5 (Norgan, Davies et al. 2013, Vild, Li et al. 2015). Mammalian cells express two non-allelic VPS4 paralogs, VPS4A and VPS4B (Scheuring, Rohricht et al. 2001). I co-expressed either mCherry-tagged VPS4A (mCherry-VPS4A) or its dominant negative mutant VPS4A-E228Q (mCherry-VPS4A-EQ) with FLAG-BSEP to assess whether the ESCRT machinery affected BSEP trafficking in Hep G2 cells via temperature shift assay. As shown in Figure 21A, the abundance of FLAG-BSEP in the PM fraction was reduced in the cells co-expressing VPS4A-EQ in comparison with the cells co-expressing wild-type VPS4A after release from the Golgi temperature block. Similarly, dominant negative mutant VPS4B-E235Q (mCherry-VPS4B-EQ), in contrast to mCherry-VPS4B, also impaired post-Golgi trafficking of BSEP (Figure 21B). These results inferred that the ESCRT machinery indeed affected the post-Golgi-trafficking of BSEP.

3.3.9. The ESCRT machinery is upstream of Rab11A to affect the post-Golgi trafficking of BSEP.

Post-Golgi trafficking of BSEP has been known to pass through the endosomal intermediates (Prekeris, Klumperman et al. 2000, Wakabayashi, Lippincott-Schwartz et al. 2004, Wakabayashi, Dutt et al. 2005, Zeigerer, Gilleron et al. 2012, Treyer and Musch 2013, Welz, Wellbourne-Wood et al. 2014). The biogenesis and maturation of endosomes are regulated by the small GTPase Rab proteins, including Rab5 (the early/sorting endosome) and Rab11 (the recycling endosome) (Donaldson, Johnson et al. 2016). Bsep was significantly reduced at the canalicular membrane and retained in the cytoplasm in a mouse model of liver-specific Rab5 knockdown (Zeigerer, Gilleron et al. 2012). At steady state, BSEP constitutively cycled between Rab11-positive compartments and the canalicular membrane in polarized hepatic cells (Wakabayashi, Lippincott-Schwartz et al. 2004, Wakabayashi, Dutt et al. 2005). ESCRTs regulating BSEP trafficking being up- or down-stream of Rab11 was of interest. I co-expressed mCherry-VPS4 or mCherry-VPS4-EQ together with either EGFP-Rab11A or dominant negative EGFP-Rab11A-S25N (EGFP-Rab11A-SN) in Hep G2 cells, which were

followed by temperature shift assay and subcellular fractionation. In the cells expressing dominant negative VPS4 proteins, the FLAG-BSEP signals in PM fractions, regardless of Rab11A or Rab11A-SN, were significantly reduced in comparison of the wild-type VPS4 proteins expressing cells (Figure 22). Therefore, ESCRTs affecting BSEP trafficking was upstream of Rab11A.

ESCRTs molecules have been referred to co-localize with Rab proteins at early/sorting endosomes, which are an internal hub for protein sorting to different subcellular destination (Scott, Vacca et al. 2014). I hypothesized that those BSEP-and-CHMP5 double positive SACs observed in adult human livers (Figure 13E) were the sorting endosomes. Adult human liver samples were co-immunofluorescently stained for BSEP, CHMP5, and Rab5 or Rab11. As shown in Figure 23, BSEP-and-CHMP5 positive SACs in hepatocytes are also with Rab5 and Rab11 signals, suggesting BSEP-resident SACs are the sorting endosome.

3.4. Summary

In this study, I provide the first example that ESCRT-III is essential for polarized trafficking of the apical membrane protein BSEP. The ESCRT-III subunits CHMP5 and LIP5 co-localized with BSEP in hepatocytes at the SACs, which were further evidenced to be the sorting endosome. Defective canalicular targeting of BSEP in cholestatic human livers was accompanied with aberrant morphology of subapical BSEP vesicles, which are CHMP5 positive. Altered affinity of BSEP mutants, such as R487H or N490D, with CHMP5 may cause the intracellular retention and defective apical expression, and lead to cholestatic diseases. Both CHMP5 and VPS4 of the ESCRT-III machinery affected the post-Golgi trafficking of BSEP, which was upstream of Rab11A-mediated BSEP sorting. ESCRT-III regulated BSEP targeting required BSEP to be ubiquitinated via K63 linkages. Taken together, CHMP5 indirectly influenced BSEP-mediated bile salt secretion. Human liver samples at different stages demonstrated the association and co-localization of BSEP with CHMP5 in the cytoplasm, indicating the canalicular trafficking of BSEP is developmentally regulated and possibly mediated through CHMP5-associated ESCRT-III machinery.



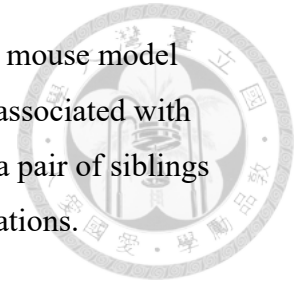
Chapter 4 Plectin mutations in progressive familial intrahepatic cholestasis

4.1. Introduction

The cytoskeleton network is composed of three major cytoskeletons, *i.e.* actin microfilaments, intermediate filaments (IFs), and microtubules, and their associated proteins, which are dynamically regulated. An appropriate organization among these proteins is necessary to physiological functions, survival of adherent cells, cell or tissue integrity, and protection of cells from cellular stress or injuries (Jacob, Coulombe et al. 2018, Hohmann and Dehghani 2019). That is why some cytoskeleton mutations reveal significant symptoms in stressed conditions but no or minor phenotype in physiological status (Fickert, Fuchsbichler et al. 2009, Chen, Guldiken et al. 2015, Omary 2017, Goldmann 2018). Organized cytoskeleton networks and cytoskeleton-associated proteins are also critical to subcellular cargo sorting (Jacob, Coulombe et al. 2018). In the liver, canalicular targeting and retrieval of BSEP/Bsep are microtubule dependent, and BSEP/Bsep internalization additionally requires polymerized actin microfilaments (Misra, Ujhazy et al. 1998, Wakabayashi, Lippincott-Schwartz et al. 2004). Mutations in the actin-based motor protein MYO5B, resulted in cholestasis with BSEP mis-localization (Girard, Lacaille et al. 2014, Gonzales, Taylor et al. 2017). Besides, aberrant cytoskeleton aggregates are frequently observed in chronic liver diseases. For example, the Mallory-Denk body, consisting of the IFs keratin (K) 8 and K18, is a representative hepatic inclusions observed in alcoholic and non-alcoholic steatohepatitis, chronic cholestasis, metabolic disorders and hepatocellular neoplasms (Strnad, Zatloukal et al. 2008).

Neonates and infants are susceptible to cholestatic liver diseases. At least six genes have been identified as causative for progressive familial intrahepatic cholestasis (PFIC), and more genetic defects are known to cause infant cholestasis (Bull and Thompson 2018). Approximately one-third of PFIC patients do not have mutations in these known cholestasis-associated genes (Chen, Li et al. 2019). To search unidentified disease-causing or -associated genes became more feasible due to advances in sequencing technology. The cytoskeleton linker plectin (PLEC) was recently found to

protect the liver from cholestatic injuries in a liver-specific knockout mouse model (Jirouskova, Nepomucka et al. 2018). However, the *PLEC* mutation associated with PFIC has not been reported in human patients. In this study, I report a pair of siblings who had severe cholestasis with compound heterozygous *PLEC* mutations.



4.2. Materials and Methods

4.2.1. Antibodies and Reagents

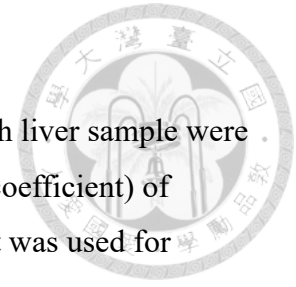
Primary antibodies specific for BSEP (Cat# HPA0195035, RRID:AB_1844429, Sigma-Aldrich), Keratin 8/K8 (Cat# ab53280, RRID:AB_869901, Abcam), MRP2 (Cat# ALX-801-016-C250, RRID:AB_2051908, Enzo Life Sciences), *PLEC* (Cat# sc-33649, RRID:AB_628155, Santa-Cruz) and ZO-1 (Cat# GTX108613, RRID:AB_1952257, GeneTex) were commercially available. Fluorochrome-conjugated secondary antibodies and biotinylated secondary antibodies were purchased from Thermo (Waltham, MA) and Vector Laboratories (Burlingame, CA), respectively. CF568-labelled streptavidin was from Biotium (Fremont, CA), and the ProLong Diamond Mounting Media with DAPI was from Thermo.

4.2.2. Immunofluorescence staining

Paraffin-embedded liver sections were dewaxed, rehydrated and followed by heat-induced antigen retrieval through xylene, graded ethanol and Tris-EDTA buffer (10 mM Tris, 1 mM EDTA, pH 9.0), respectively. After serum blocking, liver sections were incubated with primary antibodies and subsequently with fluorochrome-conjugated secondary antibodies. Endogenous biotin quenching and CF568-conjugated streptavidin were performed when biotinylated secondary antibodies were used. All sections were mounted using ProLong Diamond Mounting Media with DAPI.

4.2.3. Image acquisition

The images of epifluorescence microscopy were acquired by ZEISS Observer. D1 equipped with AxioCam mRm r3.1 as well as filters for DAPI, FITC, and TRITC fluorochrome (Carl ZEISS, Jena, Germany). AxioVision software was used. For confocal microscopy, ZEISS LSM 880 and ZEN software were used.



4.2.4. Analysis and Statistics of PLEC-K8 colocalization

Twenty images of epifluorescent microscopy acquired from each liver sample were subjected to analyze the colocalization index (Pearson's correlation coefficient) of PLEC and K8 using Fiji program. Two-tailed, unpaired Student *t* test was used for statistical analysis.

4.3. Results

4.3.1. Case description

Patient 1 had prolonged jaundice after birth, which subsided after phototherapy. However, she had jaundice and clay stools since 2 months of age. Clinic-pathologic workups revealed giant-cell transformation, bile stasis, and cholestasis due to bile sludge in her liver sample. Although her stool color returned to normal, jaundice got worse. Patient 1 was referred to National Taiwan University Children's Hospital at 2 years old to receive liver transplantation because of liver cirrhosis. During evaluation, computed tomography and magnetic resonance cholangio-pancreatography (MRCP) revealed no definite focal lesion in the liver parenchyma, patent distal common bile duct, but uneven hepatic surface and minimal ascites were observed. Patient 1's liver histology showed end-stage biliary cirrhosis with micronodules, cholestasis, feathery degeneration and necrosis. The patient maintained normal growth after transplantation when followed up to 15 years old.

Patient 2 is Patient 1's younger brother who was born when Patient 1 turned to 4 years old. Fever, jaundice, and thrombocytopenia were noted when he was 5 days old. Brain ultrasonography revealed right intraventricular hemorrhage with bilateral ventriculomegaly. The results of bacterial culture and congenital viral infection were negative. He was developed into hyperbilirubinemia together with elevated levels of aspartate transaminase (AST) and alanine transaminase (ALT). Prothrombin time and γ -glutamyl transferase (GGT) were normal. MRCP revealed invisible distal common bile duct and the gallbladder; nuclear imaging suggested biliary atresia. Patient 2's liver was biopsied and histologically analyzed. Neonatal hepatitis with marked hepatocyte ballooning, multinucleated giant cells formation was observed in his liver sample. Neither portal area expansion nor ductular proliferation was noted. Nevertheless, his

bilirubin and transaminase levels gradually decreased but GGT elevated. Patient 2 was diagnosed with chronic intrahepatic cholestasis, and liver fibrosis persisted on follow-up. Ursodeoxycholic acids and lipid soluble vitamins supplement are used regularly. The laboratory and pathology results of both patients are summarized in Table 9.

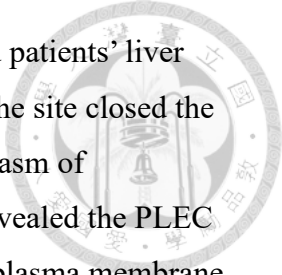
4.3.2. Plectin mutations are associated to PFIC

Suspecting PFIC, I analyzed both patients using target enrichment next-generation sequencing for 42 cholestasis-associated genes (Table 10), but with negative results. (Chen, Li et al. 2019) The DNA from the family was subjected to whole-exome sequencing. Nine thousand and five hundred eighty-two alleles in six thousand and eleven genes were analyzed (Figure 25). Because the parents are unaffected, I assumed (1) the genetic inheritance to be autosomal recessive, and (2) the same disease-causing variant(s) to be existing and heterozygous in the parents in the parents. Twenty-one alleles in five genes, *CUBN* (NM_001081), *MUC19* (NM_173600), *OTOG* (NM_001292063), *PLEC* (NM_00045), and *PSKHI* (NM_006742), were retained. The variant and predictive influences of the five genes identified in the family are summarized in Table 11; the cellular functions, tissue expression, and disease association of the five genes are summarized in Table 12.

Among the five candidates, the gene that neither expressing in the liver nor having liver-associated functions was further excluded. The retained candidate was confirmed using Sangers' sequencing (Figure 26A). I discovered that both patients had compound heterozygous mutations of the *PLEC* (NM_000445) gene—c.2558A>G (p.D853G) and c.6179C>T (p.A2060V)—that were inherited from the mother and father, respectively (Figure 26A and Figure 26B). Both *PLEC* variants are rare in the population: 0.0052% for c.2558A>G and 0.014% for c.6179C>T according to the Genome Aggregation Database.

4.3.3. Decreased colocalization of PLEC and Keratin 8 (K8) in the liver samples of PLEC mutations

PLEC, encoded by the *PLEC* gene, connects the plasm membrane-bound junctional complexes and the intermediate filaments (IFs), such as keratin 8 (K8), to maintain cell and tissue integrity (Wiche, Osmanagic-Myers et al. 2015). The PLEC mutations D853G and A2060V locate within the Src homology 3 (SH3) and the rod domains of PLEC, respectively (Figure 26C). I stained both PLEC and K8



immunofluorescence for investigating their distribution in control and patients' liver samples. In the control liver, PLEC and K8 dominantly expressed at the site closed the plasma membrane and formed some condensed speckles in the cytoplasm of hepatocytes (Figure 27A). Confocal images with higher magnitude revealed the PLEC signals are condensed cytoplasmic puncta associating with K8 at the plasma membrane (Figure 27B). Contrastingly, PLEC and K8 signals were scattered in the cytoplasm of both patients' hepatocytes (Figure 27A and Figure 27B). Besides, the PLEC in the patients' hepatocytes distributed in a fine-sanded way rather than condensed spots observed in the control liver (Figure 27B). I analyzed patients' PLEC and K8 colocalization using the program Fiji. The PLEC-K8 colocalization index (Pearson's correlation coefficient) of the control, patient 1 and patient 2 were 0.93 ± 0.03 , 0.83 ± 0.18 , and 0.64 ± 0.08 , respectively, suggesting reduced colocalization of PLEC and K8 in patients' livers (Figure 27C).

4.3.4. PLEC mutated livers show impaired canalicular expression of BSEP, dilated bile canaliculi, and distorted bile ducts.

Distorted bile ducts were observed in patients' livers (Figure 28A). The bile salt export pump (BSEP) staining showed a reduced and aberrant canalicular pattern and increased cytoplasmic signals. The canalicular multidrug resistance protein 2 (MRP2) was retained, and zona occludens 1 (ZO-1)-labeled bile canaliculi were dilated (Figure 28B).

4.4. Summary

I identified novel cholestasis-associated gene *PLEC* mutations from a pair of siblings manifesting PFIC. The liver samples revealed reduced PLEC-K8 colocalization, disturbed BSEP canalicular targeting, dilated canaliculi, and distorted bile ducts.



Chapter 5 Discussion

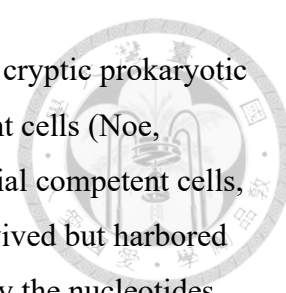
Functional expression of BSEP at the canalicular membrane is necessary to bile and physical homeostasis in humans. So far, the mechanism of how BSEP targeting to the canalicular membrane is not well studied. What molecules possibly interact with BSEP (the BSEP interactome) and affect BSEP sorting is unknown. On the other hand, the underlying molecules may affect canalicular expression of BSEP through indirect mechanisms, such as causing distortion of the cytoskeleton network.

In this study, I addressed these questions by searching BSEP-interacting proteins through genetic approaches and

In this study, I attempted to search BSEP-interacting proteins to explore underlying sorting mechanisms of BSEP. Some potential BSEP-interacting candidates were uncovered from a human fetal liver cDNA library through genetic approaches. One of the BSEP-interacting candidates, the ESCRT-III molecule CHMP5, was dissected in advances. I found that CHMP5 and other ESCRT molecules could regulate the post-Golgi trafficking of BSEP. This ESCRT-mediated mechanism is upstream of Rab11A-involved BSEP trafficking, possibly at the sorting endosome. Moreover, disease-causing BSEP mutations, in the cases of BSEP-R487H and BSEP-N490D, may aberrantly associate with ESCRT molecules, which resulted in cytoplasmic retention. In addition to those known cholestasis genes, I also searched the underlying cholestasis-associated gene from cholestatic patients' samples and the novel cholestasis-associated gene *PLEC* was discovered. Several issues in conducting with these studies are discussed in the following sections.

5.1. Some underlying factors in human *BSEP* cDNA should be concerned.

Different preferences in bile salts suggested that rodent Bsep may not totally behave as the human BSEP, even though these three BSEP/Bsep orthologs are highly homologous (Green, Hoda et al. 2000, Noe, Hagenbuch et al. 2001, Byrne, Strautnieks et al. 2002). However, some intrinsic natures in human *BSEP* cDNA caused human



BSEP to be difficultly dissected. The human *BSEP* cDNA contains a cryptic prokaryotic promoter that makes human *BSEP* cDNA toxic to bacterial competent cells (Noe, Stieger et al. 2002). I also observed the toxic effect on several bacterial competent cells, in which either no colonies grew or few, tolerated colonies were survived but harbored plasmids with insertion/deletion in BSEP-coding sequence, especially the nucleotides spanning 650-1500 of human *BSEP* ORF. Inactivation of the cryptic promoter could increase bacterial tolerance to the toxic human *BSEP* cDNA (Noe, Stieger et al. 2002). However, some observations hinted the existence of underlying factors out of the pseudo-promoter region was toxic to bacterial and yeast hosts. First, I have successfully constructed the plasmid expressing BSEP with N'-terminal fusion of EGFP (EGFP-BSEP) or FLAG (FLAG-BSEP) after inactivating the pseudo-promoter. I have never got a plasmid that could express BSEP with C'-terminal tag, such as BSEP-EGFP and BSEP-FLAG, after screening of hundreds of transformed colonies. Second, the yield of plasmids encoding full-length BSEP in maxi-preparation is always much lower than that of other non-BSEP-encoding plasmids even I could get the BSEP harboring clones.

Third, Stindt *et al.* have reported very low expression level of full-length BSEP in *S. cerevisiae*, and suggested manipulating human BSEP constructs in the yeast *Pichia pastoris* to completely bypass *E. coli* and *S. cerevisiae* as the plasmid host (Stindt, Ellinger et al. 2011). Fourth, I also observed that the BSEP (270-815) bait was no expression or prompt to degradation, which may explain a significant amount of yeast colonies was not growth in β -gal filter assays. These reports and findings suggested unknown factors outside the cryptic promoter region of human *BSEP* cDNA make the *E. coli* or *S. cerevisiae* vulnerable.

5.2. Limited information of BSEP-interacting proteins as well as their mechanisms.

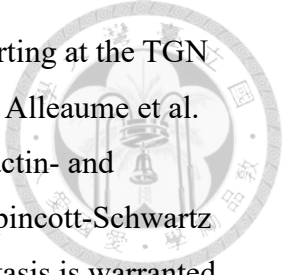
In this study, I used the human BSEP (270-815) polypeptide as the bait to screen a human liver cDNA library through the yeast two-hybrid system, and a group of BSEP-interacting candidates was identified. Irwin M. Arias' group in the US (Ortiz, Moseley et al. 2004, Chan, Calderon et al. 2005) and Lutz Schmitt's in Germany (Przybylla, Stindt et al. 2016) are so far the other two groups that attempted to explore BSEP-interacting proteins and also used similar genetic approaches. Yet, there are several

differences in the screening approaches adapted by me and the other groups, including the ortholog and length of BSEP baits, liver cDNA libraries, yeast two-hybrid systems, and other proteomic strategies.

Human BSEP as the bait was used by me and Schmitt's group, but rBsep by Dr. Arias' groups. The human BSEP (270-815) polypeptide was used in my study. Dr. Arias' group used rBsep spanning amino acids 653-741 (rBsep [653-741]) to screen in a rat liver cDNA library, and Dr. Schmitt's team chose the full-length human BSEP to screen in human liver cDNA. Notably, Przybylla *et al.* from Schmitt's group used the membrane yeast two-hybrid system rather than the traditional one. Besides, they also used co-immunoprecipitation (co-IP) by two different detergents together with MS/MS to explore BSEP interacting candidates.

Arias' group used rBsep (653-741) as the bait to identify two Bsep-interacting proteins HAX-1 (Ortiz, Moseley *et al.* 2004) and MLC2 (Chan, Calderon *et al.* 2005). The region of rBsep (653-741) is covered in the baits that were used in my study as well Schmitt's (Przybylla, Stindt *et al.* 2016). The amino acid identity of this region (a.a. 653-741) between human and rat orthologs is 73% (Figure 8). Except of Arias' group, no other group has reported MLC2 as a BSEP-interaction partner. Neither HAX-1 nor HAX-1-associated AP2 complexes was identified in my studies. By contrast, Przybylla *et al.* had identified AP2 complexes that co-immunoprecipitated with BSEP (Przybylla, Stindt *et al.* 2016), and Kong *et al.* had also reported the interaction between Bsep and HAX-1 in a mouse model of cholesterol-induced cholelithiasis (Kong, Liu *et al.* 2014). Nevertheless, the interaction between HAX-1/AP2 and BSEP seems to be occurred in specific conditions because the complex was preserved in Triton X-100 but disrupted in digitonin (Przybylla, Stindt *et al.* 2016). Besides, mice fed with high cholesterol diet revealed an increase in the interaction of Bsep and HAX-1 and in phosphorylation of the protein kinase C (PKC) isoform α (PKC α) (Kong, Liu *et al.* 2014). PKC α has known to phosphorylate mBsep (Noe, Hagenbuch *et al.* 2001) and trigger rBsep internalization (Kubitz, Saha *et al.* 2004). These findings suggested that the interaction between BSEP and HAX-1 was transient and probably ignored in my studies.

The actin remodeling protein non-muscle cofilin 1 (CFL1) is another BSEP-interacting candidate, which was identified in my study and in in the membrane yeast two-hybrid assays (Przybylla, Stindt *et al.* 2016). In addition to actin remodeling, the

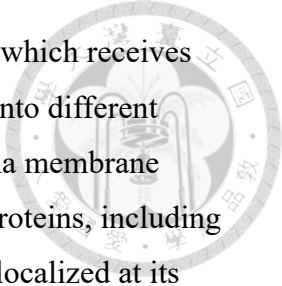


subcellular functions of CFL1 have been referred to regulate cargo sorting at the TGN (von Blume, Duran et al. 2009, Berger and Moeller 2011, von Blume, Alleaume et al. 2011, Curwin, von Blume et al. 2012). BSEP/Bsep internalization is actin- and microtubule-dependent (Misra, Ujhazy et al. 1998, Wakabayashi, Lippincott-Schwartz et al. 2004). Whether CFL1 affects BSEP trafficking or causes cholestasis is warranted to study.

5.3. ESCRTs involve in post-Golgi trafficking of BSEP.

BSEP is the key apical transporter of hepatocytes to generate the major driving force of bile. Defects in BSEP function and canalicular expression are also pivotal events that have caused the failure of many newly developed drugs (Telbisz and Homolya 2016). Since the discovery of HAX-1 as a BSEP-interacting partner, the internalization mechanism of BSEP has been extensively explored in several studies (Ortiz, Moseley et al. 2004, Hayashi and Sugiyama 2007, Hayashi, Inamura et al. 2012, Hayashi, Mizuno et al. 2012, Lam, Xu et al. 2012, Aida, Hayashi et al. 2014). In contrast to the endocytic route of BSEP, the mechanism of post-Golgi targeting of BSEP to apical/canalicular membrane has not been fully characterized so far.

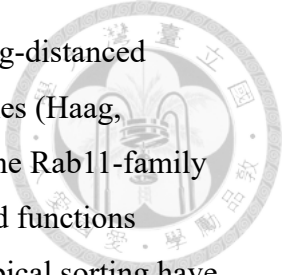
In this study, I provide the first example that ESCRT regulates the post-Golgi trafficking and apical targeting of BSEP. The documented functions of the ESCRT machinery include multivesicular body (MVB) formation; cell polarity establishment; exosome biosynthesis; enveloped virus budding; nuclear and plasma membrane repairmen; autophagy biogenesis and cytokinesis (Lobert and Stenmark 2011, Christ, Raiborg et al. 2017). Recently, some ESCRT molecules have been shown to participate in the unconventional protein secretion of the cystic fibrosis conductance transmembrane regulator (CFTR) mutant (Noh, Gee et al. 2018). Whether ESCRTs participate in the apical trafficking has not been reported in the literatures. Both BSEP and CHMP5 have been identified in human urinary exosomes, implying that BSEP could be an ESCRT cargo and ESCRTs may also involve the endocytic route of BSEP (Gonzales, Pisitkun et al. 2009). On the other hand, the post-Golgi trafficking of rBsep has been studied in rats (Kipp, Pichetshote et al. 2001), mice (Zeigerer, Gilleron et al. 2012), and the polarized WIF-B9 cell model (Wakabayashi, Lippincott-Schwartz et al. 2004, Wakabayashi, Dutt et al. 2005), demonstrating the involvement of the endosomal system and two small G proteins Rab5 and Rab11.



The early/sorting endosome functions as a major sorting station, which receives cargos from the *trans*-Golgi or the plasma membrane and sorts them into different endocytic pathways for degradation or being cycled back to the plasma membrane (Scott, Vacca et al. 2014, Naslavsky and Caplan 2018). Several Rab proteins, including Rab5 and Rab11, are associated with the early/sorting endosome and localized at its distinct membrane domains (Sonnichsen, De Renzis et al. 2000). The Rab5 is a master regulator of endosome biogenesis and serves as an early/sorting endosome marker (Numrich and Ungermann 2014). Rab5 is required to the targeting of ESCRT-III molecules for ESCRT-III mediated membrane abscission (Kumar, Pushpa et al. 2019, Zhou, Wu et al. 2019). Hepatocyte-specific Rab5 knockdown in mice caused Bsep cytoplasmic retention together with a significant reduction (~30% of the control) in canalicular distribution (Zeigerer, Gilleron et al. 2012). On the other hand, the Rab11 protein regulates both secretory pathway and endosomal recycling (Welz, Wellbourne-Wood et al. 2014). Mutations in Rab11-interacting proteins (Zhou and Zhang 2014) and Rab11 effectors (Girard, Lacaille et al. 2014, Gonzales, Taylor et al. 2017) have known to cause cholestasis and abnormal BSEP sorting. Rab11 is located at the *trans*-Golgi network, post-Golgi vesicles, sorting and recycling endosomes (Welz, Wellbourne-Wood et al. 2014). *In vitro* cell-based studies revealed that Bsep and Bsep mutants co-localized with Rab11-positive compartments in polarized WIF-B9 cells (Wakabayashi, Lippincott-Schwartz et al. 2004, Wakabayashi, Dutt et al. 2005) and in nonpolarized HEK293 cells (Lam, Pearson et al. 2007). I also observed the co-localization of intracellular BSEP and Rab11-positive compartments in co-transfected Hep G2 cells (data not shown) and in adult human liver samples. Additionally, Rab5 and the ESCRT-III proteins CHMP5 and LIP5 were located on the intracellular BSEP compartments, indicating these SACs with BSEP signals should be sorting endosomes. Moreover, dominant negative VPS4 affecting BSEP sorting overrode Rab11A influences, suggesting that ESCRTs affected BSEP trafficking from the *trans*-Golgi to the sorting endosome.

5.4. Both ESCRTs and endosomal Rab proteins participate in post-Golgi trafficking of apical proteins.

The ESCRT machinery and the Rab-mediated endosomal system are tangled in many cellular functions and affected by each other. For examples, deletion of the



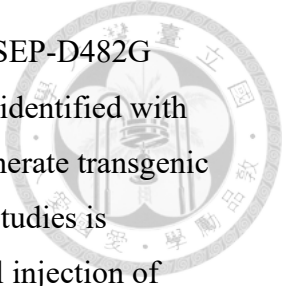
ESCRT-III proteins Did2 in fungi resulted in defective endosomal long-distanced transport, aberrant shuttling and maturation of early and late endosomes (Haag, Pohlmann et al. 2017). The ESCRT-I protein TSG101, which bound the Rab11-family interacting proteins (Rab11-FIPs) to further influence Rab11-mediated functions (Horgan, Hanscom et al. 2012). Defects in cellular polarization and apical sorting have been revealed in *Drosophila* and mammalian cells with manipulations of ESCRT expression (Lobert and Stenmark 2012) (also reviewed in (Lobert and Stenmark 2011)) and in mammalian cells with mutated Rab11 expression (Wakabayashi, Dutt et al. 2005).

In fibroblast cells, ESCRTs mediated cell polarization through regulating the non-muscle myosin II regulatory light chain (MLC2) (Lobert and Stenmark 2012), which is a subunit of the non-muscle myosin II mediating cell polarization, migration, and cell-cell adhesion (Conti and Adelstein 2008). Notably, MLC2 is so far the only Bsep-binding protein known to affect apical targeting of Bsep (Chan, Calderon et al. 2005). However, the role of ESCRTs in hepatic polarization is unclear. How the apical sorting of BSEP is coordinated by ESCRTs, Rab proteins, motor and motor-associated proteins like MLC2 is warranted to further study.

5.5. Defects in canalicular sorting of BSEP mutants may be caused by aberrant association with ESCRTs.

Hundreds of BSEP mutations have been identified, but a few BSEP mutants have been dissected for the disease mechanism (Kubitz, Droge et al. 2012, Droge, Bonus et al. 2017). The disease-causing mechanism of two BSEP mutants, BSEP-R487H and BSEP-N490D, was *in vivo* and *in vitro* dissected in this study and suggested that aberrant association with ESCRT may lead to canalicular sorting defects.

I used hydrodynamic injection of mouse tail veins, rather than *in vitro* cell-based systems, to *in vivo* express both BSEP mutants for studying their canalicular expression at the steady state. For other BSEP mutants that have been studied, the disease mechanisms were studied using *in vitro* cell lines with ectopic expression of human or rodent BSEP/Bsep orthologs harboring a PFIC2/BRIC2 mutation of interest. However, the interpretation of these cell-based results may be controversial. In the case of D482G, the apical targeting were retained in rBsep-D482G (Wang, Soroka et al. 2002), but



strongly impaired in mBsep-D482G (Plass, Mol et al. 2004) and in BSEP-D482G (Hayashi, Takada et al. 2005). Besides, PFIC2 patients are frequently identified with more than one BSEP mutation (Strautnieks, Byrne et al. 2008). To generate transgenic mouse models harboring one Bsep/BSEP mutation for BSEP mutant studies is extremely time-consuming or infeasible. By contrast, hydrodynamical injection of mouse tail veins to express BSEP mutants is a very powerful and efficient strategy to study BSEP mutations *in vivo*. After searching the literatures, it is the first time to apply this strategy to study BSEP and other membrane proteins.

My studies revealed that these two BSEP mutants had different degrees of apical targeting defects, *i.e.* BSEP-R487H revealed fewer canalicular expression and more cytoplasmic retention in comparison with BSEP-N490D. These findings are supported by the clinical observations on a BSEP mutant with substitutions of either Arg at 487 or Asn at 490 (Goto, Sugiyama et al. 2003, Chen, Liu et al. 2008, Strautnieks, Byrne et al. 2008, Liu, Wang et al. 2018). Except of the BSEP-R487L being a non-disease associated variant (Kim, Saito et al. 2009), the other mutations at the a.a. 487 of BSEP, all identified from PFIC2 or patients with severe cholestasis, had no canalicular BSEP expression in their liver samples, including R487P/R487P (Strautnieks, Byrne et al. 2008), V330X/R487H (Goto, Sugiyama et al. 2003), +/R487H (Chen, Liu et al. 2008), and R487H/R1057X (Liu, Wang et al. 2018). On the other hand, patients with a heterozygous BSEP-N490D mutation (+/N490D) retained normal BSEP staining pattern even though they died within one year after birth and were probably caused by functional defects of BSEP mutations (Strautnieks, Byrne et al. 2008). These clinical observations implied that the degree of canalicular targeting in BSEP-R487H mutant should be less and more disturbed at the steady state than that in BSEP-N490D. The results from both BSEP mutants expressed in hydrodynamically injected mouse livers in my studies were in accordance with the implication.

The cell-based results of BSEP-R487H and BSEP-N490D further supported these *in vivo* findings of these two BSEP mutants, and were linked to ESCRT functions. First, BSEP-R487H and BSEP-N490D revealed different degrees of glycosylation abnormalities. Changes in glycosylation profiles have been reported in other BSEP mutants with apical targeting defectiveness, such as E297G and D482G (Plass, Mol et al. 2004, Hayashi, Takada et al. 2005, Hayashi and Sugiyama 2007). Incomplete glycosylation of BSEP has been referred to protein degradation (Mochizuki, Kagawa et

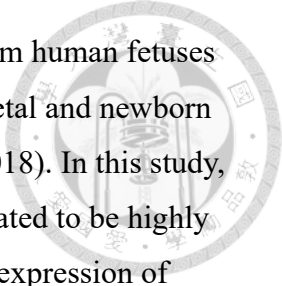
al. 2007). Second, the disturbance of post-Golgi trafficking in transfected cells was minor in BSEP-N490D but severe in BSEP-R487H, which is in accordance with the trend of both BSEP mutants demonstrated in hydrodynamically injected mouse livers. Finally, the BSEP mutant with more ESCRT association might be resulted in less canalicular or plasma membrane targeting.

ESCRTs together with autophagy components have been reported to participate in the unconventional protein trafficking of the cystic fibrosis transmembrane conductance regulator (CFTR, encoded by the *ABCC7* gene) with the deletion of phenylalanine at 508 (CFTR Δ F508) (Noh, Gee et al. 2018). CFTR Δ F508 also demonstrates altered glycosylation compared to the wild type CFTR (Glozman, Okiyoneda et al. 2009). Besides of CFTR Δ F508, other ABC-transporters have been reported to use unconventional proteins secretion for targeting plasma membranes (reviewed in (Rabouille, Malhotra et al. 2012)). Whether BSEP in diseased conditions and/or BSEP mutant-caused cellular stress is also capable to route through unconventional protein secretion to apical sorting as in the case of CFTR Δ F508 is so far unknown.

Another question is whether autophagy components are also involved in the sorting of BSEP and BSEP mutants. Some BSEP mutants, such as E297G and D482G, could not be folded appropriately and caused endoplasmic reticulum (ER) stress (Wang, Dong et al. 2008), which induces autophagy (Song, Tan et al. 2018). The defect in canalicular expression of BSEP-E297G and -D482G mutants could be restored by 4-phenylbutyrate (4-PB also known as BuphenylTM) (Hayashi and Sugiyama 2007, Naoi, Hayashi et al. 2014). 4-PB is a chaperon drug and has been used to restore the apical sorting of CFTR Δ F508 (Rubenstein, Egan et al. 1997). Besides, *ABCB11/Abcb11* gene expression in cultured cells and mouse livers was upregulated by chemical-induced ER stress (Henkel, LeCuyer et al. 2017), and an increased expression of autophagy genes was observed in PFIC2 and *Abcb11b* KO zebrafish livers (Ellis, Bove et al. 2018). The role of ESCRTs and autophagy in BSEP sorting is required to explore in advance.

5.6. A proposed model of ESCRTs regulating the apical targeting of BSEP

The subcellular distribution of BSEP revealed different patterns in fetal and adult human livers (Chen, Chen et al. 2005). Van Groen *et al.* had extensively conducted the



mRNA and protein expression levels of BSEP in the liver samples from human fetuses and newborn infants. However, the BSEP staining pattern in human fetal and newborn livers was not shown in their report (van Groen, van de Steeg et al. 2018). In this study, the polarized distribution of BSEP and CHMP5 was further demonstrated to be highly associated in fetal, infant and adult human livers. The developmental expression of Bsep in rodent models is not comparable to that in humans because rodent Bsep is expressed shortly before birth or parturition (Gao, St Pierre et al. 2004, Cheng, Buckley et al. 2007). Besides, systemic *Chmp5* knockout in mice was early embryonic lethal at approximately embryonic day 10 (Shim, Xiao et al. 2006), which is much earlier than the time of rodent Bsep expression. The rodent model is thus not suitable for studying the developmental expression of BSEP and CHMP5. Hence, a compatible development model to dissect ESCRT functions in BSEP is warranted.

Combined with the findings in this study and the results in the literature, I proposed a model of the ESCRT machinery in the post-Golgi sorting of BSEP (Figure 24). After transcription and translation, BSEP is glycosylated in the ER and Golgi, and subsequently undergoes post-Golgi trafficking through vesicle carriers to target the canalicular membrane of hepatocytes. BSEP is modified with K63-linked polyubiquitin chain and transported via CHMP5-associated ESCRT mechanism to the sorting endosome. VPS4 is recruited to the sorting endosomes and possibly dissociates CHMP5-and-LIP5 bound ESCRT complexes from BSEP. From the sorting endosome, BSEP may enter the Rab11-regulated vesical transport to target canalicular membrane, in which BSEP mediates bile salt secretion. Finally, canalicular BSEP undergoes the Rab11-regulated apical cycling (Wakabayashi, Lippincott-Schwartz et al. 2004).

5.7. Cholestatic liver diseases may be tangled with cytoskeleton disorganization and mis-sorting of canalicular transporters.

BSEP sorting between the SACs and the canalicular membrane is microtubule dependent, and polymerized actin microfilaments are additionally required to internalize BSEP (Misra, Ujhazy et al. 1998, Wakabayashi, Lippincott-Schwartz et al. 2004). Discoveries of MLC2 (Chan, Calderon et al. 2005) and MYO5B (Girard, Lacaille et al. 2014, Gonzales, Taylor et al. 2017) involving in BSEP trafficking suggested that defects in canalicular targeting of BSEP may be caused by mutations of cytoskeletons or

cytoskeleton-associated proteins. I discovered novel mutations of the cytoskeleton linker *PLEC* gene (NM_201384) from a pair of siblings suspected PFIC.

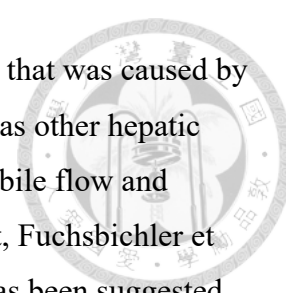
Plectin (PLEC, encoded by the *PLEC* gene) is a Plakin family protein with tremendous molecular weight (~ 500 kD) (Hu, Huang et al. 2018). Alternative splicing of the 5'-end of the *Plec* gene transcript directly into the common exon 2 gives rise to eleven mouse *Plec* isoforms (1-1j), nine of which have been identified in humans (Liu, Maercker et al. 1996). In addition to 5' splicing diversity, the *PLEC/Plec* transcripts additionally lacking exon 31, which encodes the entire rod domain, have been identified in rodents and humans. The *PLEC/Plec* proteins encoded by these *PLEC/Plec* isoforms without exon 31 have been referred to “rodless PLEC” (Elliott, Becker et al. 1997, Fuchs, Spazierer et al. 2005, Steinboeck and Kristufek 2005). PLEC is a tripartite protein composed of N- and C-terminal globular domains and the central coiled-coil rod domain (Wiche, Becker et al. 1991). The N-terminal domain contains an actin-binding domain (ABD) composed of two calponin homology domains, and a plakin domain formed by nine spectrin repeats (SRs). An SH3 motif (a.a. 749-918) is embedded in SR5. The C-terminal globular domain is composed of five type-B and one type-C plakin repeats. The intermediate filament binding domain (IFBD, a.a. 4140-4190) locates in the carboxyl end of the fifth type-B plakin repeat (Nikolic, Mac Nulty et al. 1996, Bouameur, Favre et al. 2014). The central rod domain mediates PLEC dimerization through coiled-coil interaction. The N- and C-terminal globular domains connect all three major cytoskeletons and plasma membrane-bound junctional complexes (hemidesmosomes) to maintain cell and tissue integrity (Svitkina, Verkhovsky et al. 1996, Winter and Wiche 2013). The different N'-terminal alternative sequence preceding ABD dictate the subcellular distribution and interaction partners of *PLEC/Plec* isoforms (Rezniczek, Abrahamsberg et al. 2003, McInroy and Maatta 2011). Each tissue and cell type expresses a unique composition of *PLEC* isoforms in physiological and diseased conditions (Winter and Wiche 2013).

PLEC mutations (OMIM: 601282) cause epidermolysis bullosa simplex (EBS) that is probably combined with muscle dystrophy (EBS-MD), pyloric atresia (EBS-PA), or none (EBS-Ogna) (Natsuga 2015). Systemic *Plec* knockout mouse models revealed many EBS-like phenotypes such as skin blistering and abnormal architectures of muscles and the heart (Andra, Lassmann et al. 1997). *Plec* isoform-specific mouse models further suggested that each *Plec* isoforms involved different cellular and tissue

functions (Winter and Wiche 2013, Staszewska, Fischer et al. 2015, Winter, Kuznetsov et al. 2015). However, the role of PLEC in the liver was first demonstrated in liver-specific *Plec* knockout (*Plec^{Alb}*) mice (Jirouskova, Nepomucka et al. 2018).

The two *PLEC* mutated siblings whom I assayed in this study shared some similarities to the finding of *Plec^{Alb}* mice challenged with cholestatic stress, including scattered K8 signals in the cytoplasm of hepatocytes, distorted bile ducts, and dilated bile canaliculi. The impaired BSEP canalicular expression accompanied with an increase in bile acid levels suggested that the *PLEC* mutations may affect BSEP targeting and cause cholestasis. The colocalization of PLEC and K8 was decreased in *PLEC* mutated patients' liver samples. Hepatocytes majorly express the acidic type I keratin K8 and the basic type II keratin K18, which form obligate heteropolymers (Yi, Yoon et al. 2018). The expression and distribution of K18 was in accordance with that of PLEC in several studies using hepatoma cell lines (Liu, Cheng et al. 2008, Liu, Cheng et al. 2011, Liu, Ho et al. 2011, Cheng, Lai et al. 2015). Besides, PLEC was tightly associated with keratin filaments of the hepatocytes in human liver samples, which has been revealed by electron microscopy (Wiche, Krepler et al. 1983) and immunofluorescence confocal microscopy (Svitkina, Verkhovsky et al. 1996). Hence, the co-localization of PLEC and K8 may serve as a functional indicator of PLEC.

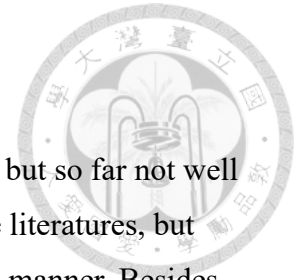
D853G and A2060V mutations of PLEC have not been reported in literatures (Natsuga 2015) and the online database (<https://databases.lovd.nl/shared/genes/PLEC>). Whether both *PLEC* mutants will result in *PLEC* functional defects is unknown. The D853G mutation of *PLEC* locates in the SH3 motif of SR5. The SH3 domain embedded in a SR is conserved in Plakin family proteins (Hu, Huang et al. 2018) and mediates the protein-protein interaction (Daday, Kolsek et al. 2017). The SH3 domain of *PLEC* has been suggested to antagonize the microtubule-stabilizing and assembly-promoting function of microtubule-associated proteins (Valencia, Walko et al. 2013). On the other hand, the A2060V mutation locating in the rod domain of *PLEC* may not be so virulent to *PLEC* functions because the rodless *PLEC* is a natural variant identified in humans and rodent *PLEC/Plec* (Elliott, Becker et al. 1997, Fuchs, Spazierer et al. 2005, Steinboeck and Kristufek 2005). A mouse model with systemic deletion of the rod domain encoding exon further suggested that the rod domain of *Plec* was not functionally essential (Ketema, Secades et al. 2015). Therefore, functional characterization of *PLEC*-D853G is warranted to future studies.



It could be ruled out the possibility of altered BSEP distribution that was caused by altered K8 distribution because canalicular targeting of Bsep as well as other hepatic transporters was unaffected in either K8 or K18 knockout mice. The bile flow and composition in K8 or K18 knockout mice were also retained (Fickert, Fuchsbichler et al. 2009). Notably, myosin II or a myosin II-associated component has been suggested to involve in PLEC mediated interaction of IFs with actin microfilaments (Svitkina, Verkhovsky et al. 1996). As discussed in Section 5.4., the subunit of myosin II, MLC2, may be functionally disturbed and subsequently affect BSEP trafficking in the hepatocytes with *PLEC* mutations.

I could not rule out the possibility of PLEC being a disease modifier. Similar to keratin-associated transgenic mouse models (Yi, Yoon et al. 2018), *Plec^{Alb}* mice in the physiological condition revealed subtle changes in the liver architecture unless the liver was challenged by cholestatic stimuli (Jirouskova, Nepomucka et al. 2018). There may be some unknown factors that caused cholestasis, which was aggravated by mutated PLEC. Further experiments will clarify this possibility.

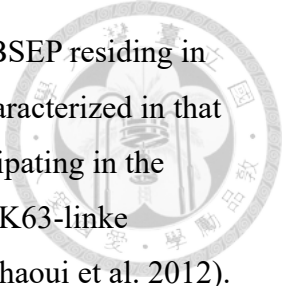
Chapter 6 Perspectives



The trafficking mechanism of BSEP is an important, interesting but so far not well studied field. Hundreds of BSEP mutations have been reported in the literatures, but disease mechanisms of these BSEP mutants were elucidated in a rare manner. Besides, defects in transport activity and canalicular expression of BSEP may cause failure of drug development. In this study, I attempted to dissect the mechanism of BSEP apical targeting and to search novel cholestasis-associated genes that may affect canalicular expression of BSEP. I provided ESCRT-mediated mechanism of BSEP sorting and the cytoskeleton linker PLEC that may cause defective targeting of BSEP and result in PFIC when *PLEC* was mutated. Extending from my studies, there are still many questions in the BSEP field that require more studies to resolve and answer. A part of these questions is the extent of my studies; others are the dilemma or predicament that I faced during the my investigation.

6.1. Ubiquitination and deubiquitination of BSEP

Ubiquitination is a process mediated by a group of ubiquitination enzymes, including E1 Ub-activating enzymes, E2 Ub-conjugating enzymes, and E3 Ub-ligases, that sequentially transfer ubiquitin molecules to targets (Komander 2009). In this study, I discovered that ESCRT-mediated apical targeting of BSEP required K63-linked ubiquitination of BSEP, suggesting the involvement of unidentified E3 ligases. Besides, I have dissected the ubiquitination pattern of BSEP in CHMP5 knockdown cells. The ubiquitination pattern of BSEP in CHMP5 knockdown cells was the same, but more ubiquitinated BSEP was observed in contrast to that in si-CTL pretreated cells (Appendix Figure 7A), suggesting the accumulation of K63-linked ubiquitinated BSEP in CHMP5 depletion. This accumulation of K63-linked ubiquitinated BSEP was also revealed in CHMP5 knockdown Hep G2 with p3XFLAG-BSEP transfection. With the pre-treatment of si-CHMP5 or si-CTL, FLAG-BSEP isolated via anti-FLAG antibodies was bonded with K63-linked ubiquitin chains detected by K63-linkage specific anti-ubiquitin antibodies. The Ub-K63-linked FLAG-BSEP signals in the CHMP5 knockdown samples were reduced slower than that in si-CTL samples (Appendix Figure 7B). The result supported that CHMP5 knockdown caused the accumulation of ubiquitinated BSEP, suggesting CHMP5 may regulate the de-ubiquitination of BSEP.



Ubiquitination has been reported to affect the internalization of BSEP residing in the plasma membrane; however, the linkage of ubiquitination is uncharacterized in that study (Aida, Hayashi et al. 2014). After discoveries of ESCRTs participating in the trafficking of newly synthesized BSEP, it is reasonable to assume the K63-linked ubiquitination involved (Lauwers, Jacob et al. 2009, Erpapazoglou, Dhaoui et al. 2012). Some BSEP mutants were found to be more ubiquitinated, but the linkage is unidentified (Hayashi and Sugiyama 2009). It is unknown that the ubiquitination pattern of BSEP-R487H and BSEP-N490D is also increased or dominant in linkages other than K63 ubiquitination, which causes both mutants target membrane improperly. Besides, some deubiquitylases (DUBs) interact to ESCRTs directly (Wright, Berlin et al. 2011) and CHMP5 has been documented to recruit and interact with the DUB, USP15 (Greenblatt, Park et al. 2015). In accordance with my findings that more K63-linked ubiquitinated FLAG-BSEP was detected in CHMP5 knockdown cells, I speculated that CHMP5 may be indirectly involved in the deubiquitination of BSEP through unknown DUBs. Hence, to dissect the mechanisms of BSEP ubiquitination and deubiquitination will not only clarify the role of ubiquitination in subcellular sorting of BSEP, but also provide a new aspect of treatment development to BSEP-associated diseases.

6.2. The role of autophagy in canalicular expression of BSEP

An interesting question is whether autophagy is involved in the canalicular targeting of BSEP. Autophagy, like ESCRT complexes assembled sequentially, is also activated in a sequential manner, and ESCRT proteins as well as ubiquitination are also involved in the formation process of autophagosomes (Grumati and Dikic 2018, Song, Tan et al. 2018, Allaire, Rautou et al. 2019). Autophagy had been regarded as an intracellular “scavenger” or a self-protective mechanism to eliminate the organelles or to survive on starvation (Ge, Baskaran et al. 2014, Hurley and Schulman 2014). Accumulated evidences suggest that the function of autophagy is more than engulfment of intracellular materials for cell survival. In the case of CFTR Δ 508, the apical targeting of CFTR Δ 508 mutant has been referred to involvement of autophagy and ESCRTs for unconventional protein secretion (Noh, Gee et al. 2018). Besides, autophagy genes were upregulated in PFIC2 and in Abcb11 KO zebrafish livers (Ellis, Bove et al. 2018). CFTR Δ 508 may possibly serve as a model of transmembrane protein mutants to be applied to study other apical transporter like BSEP.

6.3. COPA may mediate BSEP between ER and Golgi.

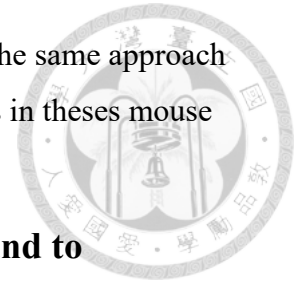
Among those BSEP-interacting candidates discovered in this study, COPA is one of interesting targets. COPA is a subunit of the COP-I complex and participates vesicular trafficking between ER and the Golgi (Beck, Rawet et al. 2009, Szul and Sztul 2011). Gene mutations in COPA have linked to Alzheimer's disease (Bettayeb, Hooli et al. 2016) and autoimmune diseases (Watkin, Jessen et al. 2015). The tertiary structure of COP-I complex is very like to that of the AP2 adaptor complex (Popoff, Adolf et al. 2011). BSEP has been shown to undergo endocytic pathways through the AP2 machinery (Hayashi, Inamura et al. 2012). COPA is highly possible to interact with BSEP and regulate its sorting between the ER and the Golgi's apparatus.

6.4. The cytoskeleton network and cytoskeleton-associated proteins in BSEP trafficking

In addition to COPA that involves the vesicle sorting at the ER-and-Golgi trafficking, the impact of the cytoskeleton network on BSEP trafficking is not well studied although polymerized microtubules and actin microfilaments are known to be essential to BSEP sorting (Misra, Ujhazy et al. 1998, Wakabayashi, Lippincott-Schwartz et al. 2004). The non-muscle cofilin 1 (CFL1) is a BSEP-interacting candidate that was identified in my study and in in the membrane yeast two-hybrid assays (Przybylla, Stindt et al. 2016). Functions of CFL1 have been referred to actin remodeling and regulate cargo sorting at the TGN (von Blume, Duran et al. 2009, Berger and Moeller 2011, von Blume, Alleaume et al. 2011, Curwin, von Blume et al. 2012). Whether CFL1 affects BSEP trafficking or causes cholestasis is warranted to study.

For the cytoskeleton linker PLEC, the functional defectiveness of both PLEC PLEC-D853G and PLEC-A2060V should be elucidated, especially the D853G mutation. Due to the tremendous molecular weight of PLEC, construction of a plasmid expressing the N'-terminal domain of PLEC harboring D853G mutation is supposedly feasible for further cell-based studies. Besides, the role of PLEC in BSEP apical targeting could be assayed in through hydrodynamically injected mouse models with liver- or hepatocyte-specific *Plec* knockdown. The shRNA targeting to mouse *Plec* or individual *Plec* isoforms could be either expressed by the plasmid directly injected or by viral transduction such as the recombinant adenovirus (AV) or the adeno-associated

virus (AAV). Exogenous human BSEP is further expressed through the same approach to dissect the impact of Plec on BSEP sorting. Cholestatic challenges in these mouse models may be required to reveal more phenotypes or mechanisms.

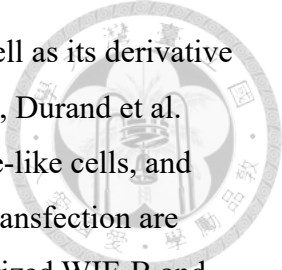


6.5. To search underlying cholestasis-associated genes and to generate *in vitro* and *in vivo* models for studying BSEP and cholestasis are essential not only to disease mechanism but also to drug screening.

Approximately one-third of PFIC patients do not have mutations in those known cholestasis-associated genes (Chen, Li et al. 2019). To search unidentified disease-causing or -associated genes became more feasible due to advances in sequencing technology. In addition to searching BSEP-interacting proteins, the next-generation sequencing (NGS)-based assays could be used to search unidentified cholestasis-causing or -associated genes from cholestatic patients. These findings from the NGS-based assay should be further validated in the laboratory. *In vitro* and *in vivo* polarized model systems are required to validation of the clinical findings.

A lack of *in vitro* and *in vivo* polarized model systems is a fundamental predicament for BSEP studies. Most of epithelial cells such as intestinal cells have one apical domain locating at the cell apex and one basolateral domain corresponding to the remaining plasma membrane. This type of polarity is so-called simple polarity. By contrast, hepatocytes organized in the livers have several apical and basolateral poles (Decaens, Durand et al. 2008, Treyer and Musch 2013). Hepatocyte polarity is affected by several factors including cytoskeletons, adhesion molecules, Rab proteins, and chemicals (Warskulat, Kubitz et al. 1999, Decaens, Durand et al. 2008, Homolya, Fu et al. 2014, Porat-Shliom, Tietgens et al. 2016, Xie, Miao et al. 2018).

Several cell-based systems have been used to study hepatic polarity and polarized trafficking in hepatocytes. Primary hepatocytes isolated from perfused livers are not a good system for BSEP/Bsep studies because the hepatocytes polarity and BSEP/Bsep expression were lost within one week. The preparation and genetic manipulation of primary hepatocytes are not easy. The human hepatic cell lines that are frequently used are either poorly (such as Huh-7) or partially (such as Hep G2) polarized. The human



hepatic cell line HepaRG and the human-rat hybrid cells WIF-B as well as its derivative WIB-B9 could be polarized upon induction for several days (Decaens, Durand et al. 2008). However, about half HepaRG will differentiate into hepatocyte-like cells, and commonly used transfection methods such Lipofectamine mediated transfection are infeasible to deliver plasmids or siRNA into polarized HepaRG. Polarized WIF-B and WIB-B9 also need transduction to ectopically express the proteins of interests even though WIF-B lineage cells are so far the hepatic cell line being able to fully polarize (Decaens, Durand et al. 2008). Moreover, the WIF-B lineage is a hybrid cell line obtained by fusion of rat hepatoma cells and human fibroblasts (Ihrke, Neufeld et al. 1993). The knockdown of target genes in WIF-B lineage cells must be conducted by RNAi targeting to human genes and rat orthologs at the same time. Besides, WIF-B cell lines does not express BSEP/Bsep (Wakabayashi, Lippincott-Schwartz et al. 2004). Hence, to generate a human hepatic cell line that could mimic *in vivo* hepatocytes is necessary to the studies of BSEP as well as other hepatic proteins.

Before a new human hepatic cell line being established, further genetic manipulation of WIF-B lineage cells for BSEP studies may be feasible. The human BSEP-coding sequence could be cloned into lentivirus-based plasmids with a drug-controlling promoter such as by tetracycline. WIF-B/WIF-B9 cells are infected by the lentiviruses harboring the BSEP gene and drug-regulated promoter to establish a BSEP inducible WIF-B/WIF-B9 cell line. The expression of BSEP is induced for trafficking studies after this stable line is fully polarized. A similar approach to control BSEP expression could be applied *in vivo* by either generate a human *BSEP* knock-in mouse model or a mouse model with a BSEP-inducible gene delivered by AAV. I believe that these approaches be benefit to BSEP studies and drug screening.

References

- Adachi, Y., H. Kobayashi, Y. Kurumi, M. Shouji, M. Kitano and T. Yamamoto (1991). "ATP-dependent taurocholate transport by rat liver canalicular membrane vesicles." Hepatology **14**(4 Pt 1): 655-659.
- Aida, K., H. Hayashi, K. Inamura, T. Mizuno and Y. Sugiyama (2014). "Differential roles of ubiquitination in the degradation mechanism of cell surface-resident bile salt

export pump and multidrug resistance-associated protein 2." Mol Pharmacol **85**(3): 482-491.

Allaire, M., P. E. Rautou, P. Codogno and S. Lotersztajn (2019). "Autophagy in liver diseases: Time for translation?" J Hepatol **70**(5): 985-998.

Alnouti, Y. (2009). "Bile Acid sulfation: a pathway of bile acid elimination and detoxification." Toxicol Sci **108**(2): 225-246.

Andra, K., H. Lassmann, R. Bittner, S. Shorny, R. Fassler, F. Propst and G. Wiche (1997). "Targeted inactivation of plectin reveals essential function in maintaining the integrity of skin, muscle, and heart cytoarchitecture." Genes Dev **11**(23): 3143-3156.

Ballatori, N., W. V. Christian, S. G. Wheeler and C. L. Hammond (2013). "The heteromeric organic solute transporter, OSTalpha-OSTbeta/SLC51: a transporter for steroid-derived molecules." Mol Aspects Med **34**(2-3): 683-692.

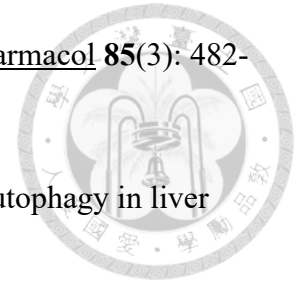
Ballatori, N., J. F. Rebbeor, G. C. Connolly, D. J. Seward, B. E. Lenth, J. H. Henson, P. Sundaram and J. L. Boyer (2000). "Bile salt excretion in skate liver is mediated by a functional analog of Bsep/Spgp, the bile salt export pump." Am J Physiol Gastrointest Liver Physiol **278**(1): G57-63.

Beck, R., M. Rawet, F. T. Wieland and D. Cassel (2009). "The COPI system: molecular mechanisms and function." FEBS Lett **583**(17): 2701-2709.

Berger, K. and M. J. Moeller (2011). "Cofilin-1 in the podocyte: a molecular switch for actin dynamics." Int Urol Nephrol **43**(1): 273-275.

Bettayeb, K., B. V. Hooli, A. R. Parrado, L. Randolph, D. Varotsis, S. Aryal, J. Gresack, R. E. Tanzi, P. Greengard and M. Flajolet (2016). "Relevance of the COPI complex for Alzheimer's disease progression in vivo." Proc Natl Acad Sci U S A **113**(19): 5418-5423.

Bezerra, J. A., R. G. Wells, C. L. Mack, S. J. Karpen, J. H. Hoofnagle, E. Doo and R. J. Sokol (2018). "BILIARY ATRESIA: Clinical and Research Challenges for the 21(st) Century." Hepatology **68**(3): 1163-1173.



Bohme, M., M. Muller, I. Leier, G. Jedlitschky and D. Keppler (1994). "Cholestasis caused by inhibition of the adenosine triphosphate-dependent bile salt transport in rat liver." Gastroenterology **107**(1): 255-265.

Bolder, U., H. T. Ton-Nu, C. D. Scheingart, E. Frick and A. F. Hofmann (1997). "Hepatocyte transport of bile acids and organic anions in endotoxemic rats: impaired uptake and secretion." Gastroenterology **112**(1): 214-225.

Bonifacino, J. S. (2014). "Adaptor proteins involved in polarized sorting." J Cell Biol **204**(1): 7-17.

Bossard, R., B. Stieger, B. O'Neill, G. Fricker and P. J. Meier (1993). "Ethinylestradiol treatment induces multiple canalicular membrane transport alterations in rat liver." J Clin Invest **91**(6): 2714-2720.

Bouameur, J. E., B. Favre, L. Fontao, P. Lingasamy, N. Begre and L. Borradori (2014). "Interaction of plectin with keratins 5 and 14: dependence on several plectin domains and keratin quaternary structure." J Invest Dermatol **134**(11): 2776-2783.

Bremmelgaard, A. and J. Sjovall (1980). "Hydroxylation of cholic, chenodeoxycholic, and deoxycholic acids in patients with intrahepatic cholestasis." J Lipid Res **21**(8): 1072-1081.

Bull, L. N. and R. J. Thompson (2018). "Progressive Familial Intrahepatic Cholestasis." Clin Liver Dis **22**(4): 657-669.

Bull, L. N., M. J. van Eijk, L. Pawlikowska, J. A. DeYoung, J. A. Juijn, M. Liao, L. W. Klomp, N. Lomri, R. Berger, B. F. Scharschmidt, A. S. Knisely, R. H. Houwen and N. B. Freimer (1998). "A gene encoding a P-type ATPase mutated in two forms of hereditary cholestasis." Nat Genet **18**(3): 219-224.

Byrne, J. A., S. S. Strautnieks, G. Ihrke, F. Pagani, A. S. Knisely, K. J. Linton, G. Mieli-Vergani and R. J. Thompson (2009). "Missense mutations and single nucleotide polymorphisms in ABCB11 impair bile salt export pump processing and function or disrupt pre-messenger RNA splicing." Hepatology **49**(2): 553-567.

Byrne, J. A., S. S. Strautnieks, G. Mieli-Vergani, C. F. Higgins, K. J. Linton and R. J. Thompson (2002). "The human bile salt export pump: characterization of substrate specificity and identification of inhibitors." Gastroenterology **123**(5): 1649-1658.

Cai, S. Y., L. Wang, N. Ballatori and J. L. Boyer (2001). "Bile salt export pump is highly conserved during vertebrate evolution and its expression is inhibited by PFIC type II mutations." Am J Physiol Gastrointest Liver Physiol **281**(2): G316-322.

Caillat, C., S. Maity, N. Miguet, W. H. Roos and W. Weissenhorn (2019). "The role of VPS4 in ESCRT-III polymer remodeling." Biochem Soc Trans **47**(1): 441-448.

Chan, J. and J. L. Vandeberg (2012). "Hepatobiliary transport in health and disease." Clin Lipidol **7**(2): 189-202.

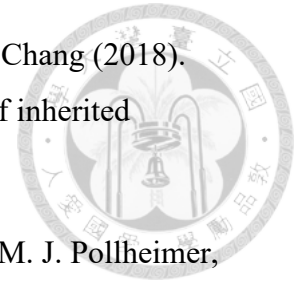
Chan, W., G. Calderon, A. L. Swift, J. Moseley, S. Li, H. Hosoya, I. M. Arias and D. F. Ortiz (2005). "Myosin II regulatory light chain is required for trafficking of bile salt export protein to the apical membrane in Madin-Darby canine kidney cells." J Biol Chem **280**(25): 23741-23747.

Chen, H. L., P. S. Chang, H. C. Hsu, Y. H. Ni, H. Y. Hsu, J. H. Lee, Y. M. Jeng, W. Y. Shau and M. H. Chang (2002). "FIC1 and BSEP defects in Taiwanese patients with chronic intrahepatic cholestasis with low gamma-glutamyltranspeptidase levels." J Pediatr **140**(1): 119-124.

Chen, H. L., H. L. Chen, Y. J. Liu, C. H. Feng, C. Y. Wu, M. K. Shyu, R. H. Yuan and M. H. Chang (2005). "Developmental expression of canalicular transporter genes in human liver." J Hepatol **43**(3): 472-477.

Chen, H. L., H. Y. Li, J. F. Wu, S. H. Wu, H. L. Chen, Y. H. Yang, Y. H. Hsu, B. Y. Liou, M. H. Chang and Y. H. Ni (2019). "Panel-Based Next-Generation Sequencing for the Diagnosis of Cholestatic Genetic Liver Diseases: Clinical Utility and Challenges." J Pediatr **205**: 153-159 e156.

Chen, H. L., Y. J. Liu, Y. N. Su, N. Y. Wang, S. H. Wu, Y. H. Ni, H. Y. Hsu, T. C. Wu and M. H. Chang (2008). "Diagnosis of BSEP/ABCB11 mutations in Asian patients with cholestasis using denaturing high performance liquid chromatography." J Pediatr **153**(6): 825-832.



Chen, H. L., S. H. Wu, S. H. Hsu, B. Y. Liou, H. L. Chen and M. H. Chang (2018).

"Jaundice revisited: recent advances in the diagnosis and treatment of inherited cholestatic liver diseases." J Biomed Sci **25**(1): 75.

Chen, Y., N. Guldiken, M. Spurny, H. H. Mohammed, J. Haybaeck, M. J. Pollheimer, P. Fickert, N. Gassler, M. K. Jeon, C. Trautwein and P. Strnad (2015). "Loss of keratin 19 favours the development of cholestatic liver disease through decreased ductular reaction." J Pathol **237**(3): 343-354.

Cheng, C. C., Y. C. Lai, Y. S. Lai, Y. H. Hsu, W. T. Chao, K. C. Sia, Y. H. Tseng and Y. H. Liu (2015). "Transient knockdown-mediated deficiency in plectin alters hepatocellular motility in association with activated FAK and Rac1-GTPase." Cancer Cell Int **15**: 29.

Cheng, X., D. Buckley and C. D. Klaassen (2007). "Regulation of hepatic bile acid transporters Ntcp and Bsep expression." Biochem Pharmacol **74**(11): 1665-1676.

Cheng, Y., S. Chen, C. Freeden, W. Chen, Y. Zhang, P. Abraham, D. M. Nelson, W. G. Humphreys, J. Gan and Y. Lai (2017). "Bile Salt Homeostasis in Normal and Bsep Gene Knockout Rats with Single and Repeated Doses of Troglitazone." J Pharmacol Exp Ther **362**(3): 385-394.

Cheng, Y., C. Freeden, Y. Zhang, P. Abraham, H. Shen, D. Wescott, W. G. Humphreys, J. Gan and Y. Lai (2016). "Biliary excretion of pravastatin and taurocholate in rats with bile salt export pump (Bsep) impairment." Biopharm Drug Dispos **37**(5): 276-286.

Chiang, J. Y. (2002). "Bile acid regulation of gene expression: roles of nuclear hormone receptors." Endocr Rev **23**(4): 443-463.

Chiang, J. Y. L. and J. M. Ferrell (2019). "Bile Acids as Metabolic Regulators and Nutrient Sensors." Annu Rev Nutr **39**: 175-200.

Childs, S., R. L. Yeh, E. Georges and V. Ling (1995). "Identification of a sister gene to P-glycoprotein." Cancer Res **55**(10): 2029-2034.

Childs, S., R. L. Yeh, D. Hui and V. Ling (1998). "Taxol resistance mediated by transfection of the liver-specific sister gene of P-glycoprotein." Cancer Res **58**(18): 4160-4167.

Christ, L., C. Raiborg, E. M. Wenzel, C. Campsteijn and H. Stenmark (2017). "Cellular Functions and Molecular Mechanisms of the ESCRT Membrane-Scission Machinery." Trends Biochem Sci **42**(1): 42-56.

Claro da Silva, T., J. E. Polli and P. W. Swaan (2013). "The solute carrier family 10 (SLC10): beyond bile acid transport." Mol Aspects Med **34**(2-3): 252-269.

Conti, M. A. and R. S. Adelstein (2008). "Nonmuscle myosin II moves in new directions." J Cell Sci **121**(Pt 1): 11-18.

Cresawn, K. O., B. A. Potter, A. Oztan, C. J. Guerriero, G. Ihrke, J. R. Goldenring, G. Apodaca and O. A. Weisz (2007). "Differential involvement of endocytic compartments in the biosynthetic traffic of apical proteins." Embo j **26**(16): 3737-3748.

Crocenzi, F. A., A. E. Zucchetti, A. C. Boaglio, I. R. Barosso, E. J. Sanchez Pozzi, A. D. Mottino and M. G. Roma (2012). "Localization status of hepatocellular transporters in cholestasis." Front Biosci (Landmark Ed) **17**: 1201-1218.

Curwin, A. J., J. von Blume and V. Malhotra (2012). "Cofilin-mediated sorting and export of specific cargo from the Golgi apparatus in yeast." Mol Biol Cell **23**(12): 2327-2338.

Daday, C., K. Kolsek and F. Grater (2017). "The mechano-sensing role of the unique SH3 insertion in plakin domains revealed by Molecular Dynamics simulations." Sci Rep **7**(1): 11669.

Dawson, P. A., M. L. Hubbert and A. Rao (2010). "Getting the mOST from OST: Role of organic solute transporter, OSTalpha-OSTbeta, in bile acid and steroid metabolism." Biochim Biophys Acta **1801**(9): 994-1004.

de Vree, J. M., E. Jacquemin, E. Sturm, D. Cresteil, P. J. Bosma, J. Aten, J. F. Deleuze, M. Desrochers, M. Burdelski, O. Bernard, R. P. Oude Elferink and M. Hadchouel

(1998). "Mutations in the MDR3 gene cause progressive familial intrahepatic cholestasis." Proc Natl Acad Sci U S A **95**(1): 282-287.

Decaens, C., M. Durand, B. Grosse and D. Cassio (2008). "Which in vitro models could be best used to study hepatocyte polarity?" Biol Cell **100**(7): 387-398.

Delacour, D. and R. Jacob (2006). "Apical protein transport." Cell Mol Life Sci **63**(21): 2491-2505.

Deutschmann, K., M. Reich, C. Klindt, C. Droge, L. Spomer, D. Haussinger and V. Keitel (2018). "Bile acid receptors in the biliary tree: TGR5 in physiology and disease." Biochim Biophys Acta Mol Basis Dis **1864**(4 Pt B): 1319-1325.

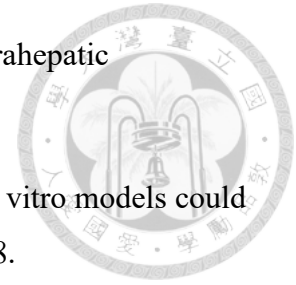
Donaldson, J. G., D. L. Johnson and D. Dutta (2016). "Rab and Arf G proteins in endosomal trafficking and cell surface homeostasis." Small GTPases **7**(4): 247-251.

Droge, C., M. Bonus, U. Baumann, C. Klindt, E. Lainka, S. Kathemann, F. Brinkert, E. Grabhorn, E. D. Pfister, D. Wenning, A. Fichtner, D. N. Gotthardt, K. H. Weiss, P. McKiernan, R. D. Puri, I. C. Verma, S. Kluge, H. Gohlke, L. Schmitt, R. Kubitz, D. Haussinger and V. Keitel (2017). "Sequencing of FIC1, BSEP and MDR3 in a large cohort of patients with cholestasis revealed a high number of different genetic variants." J Hepatol **67**(6): 1253-1264.

Elliott, C. E., B. Becker, S. Oehler, M. J. Castanon, R. Hauptmann and G. Wiche (1997). "Plectin transcript diversity: identification and tissue distribution of variants with distinct first coding exons and rodless isoforms." Genomics **42**(1): 115-125.

Ellis, J. L., K. E. Bove, E. G. Schuetz, D. Leino, C. A. Valencia, J. D. Schuetz, A. Miethke and C. Yin (2018). "Zebrafish *abcb11b* mutant reveals strategies to restore bile excretion impaired by bile salt export pump deficiency." Hepatology **67**(4): 1531-1545.

Erpapazoglou, Z., M. Dhaoui, M. Pantazopoulou, F. Giordano, M. Mari, S. Leon, G. Raposo, F. Reggiori and R. Haguenauer-Tsapis (2012). "A dual role for K63-linked ubiquitin chains in multivesicular body biogenesis and cargo sorting." Mol Biol Cell **23**(11): 2170-2183.



Esteller, A. (2008). "Physiology of bile secretion." World J Gastroenterol **14**(37): 5641-5649.

Fickert, P., A. Fuchsbichler, M. Wagner, D. Silbert, K. Zatloukal, H. Denk and M. Trauner (2009). "The role of the hepatocyte cytokeratin network in bile formation and resistance to bile acid challenge and cholestasis in mice." Hepatology **50**(3): 893-899.

Fickert, P. and M. Wagner (2017). "Biliary bile acids in hepatobiliary injury - What is the link?" J Hepatol **67**(3): 619-631.

Folsch, H., P. E. Mattila and O. A. Weisz (2009). "Taking the scenic route: biosynthetic traffic to the plasma membrane in polarized epithelial cells." Traffic **10**(8): 972-981.

Fu, D., J. Lippincott-Schwartz and I. M. Arias (2011). "Cellular mechanism of bile acid-accelerated hepatocyte polarity." Small GTPases **2**(6): 314-317.

Fuchs, C. D., G. Paumgartner, A. Wahlstrom, P. Schwabl, T. Reiberger, N. Leditznig, T. Stojakovic, N. Rohr-Udilova, P. Chiba, H. U. Marschall and M. Trauner (2017). "Metabolic preconditioning protects BSEP/ABCB11(-/-) mice against cholestatic liver injury." J Hepatol **66**(1): 95-101.

Fuchs, P., D. Spazierer and G. Wiche (2005). "Plectin rodless isoform expression and its detection in mouse brain." Cell Mol Neurobiol **25**(7): 1141-1150.

Fujiwara, R., M. Haag, E. Schaeffeler, A. T. Nies, U. M. Zanger and M. Schwab (2018). "Systemic regulation of bilirubin homeostasis: Potential benefits of hyperbilirubinemia." Hepatology **67**(4): 1609-1619.

Gao, B., M. V. St Pierre, B. Stieger and P. J. Meier (2004). "Differential expression of bile salt and organic anion transporters in developing rat liver." J Hepatol **41**(2): 201-208.

Ge, L., S. Baskaran, R. Schekman and J. H. Hurley (2014). "The protein-vesicle network of autophagy." Curr Opin Cell Biol **29**: 18-24.

Gerloff, T., B. Stieger, B. Hagenbuch, J. Madon, L. Landmann, J. Roth, A. F. Hofmann and P. J. Meier (1998). "The sister of P-glycoprotein represents the canalicular bile salt export pump of mammalian liver." J Biol Chem **273**(16): 10046-10050.

Girard, M., F. Lacaille, V. Verkarre, R. Mategot, G. Feldmann, A. Grodet, F. Sauvat, S. Irtan, A. Davit-Spraul, E. Jacquemin, F. Ruemmele, D. Rainteau, O. Goulet, V. Colomb, C. Chardot, A. Henrion-Caude and D. Debray (2014). "MYO5B and bile salt export pump contribute to cholestatic liver disorder in microvillous inclusion disease." Hepatology **60**(1): 301-310.

Gissen, P. and I. M. Arias (2015). "Structural and functional hepatocyte polarity and liver disease." J Hepatol **63**(4): 1023-1037.

Gissen, P., L. Tee, C. A. Johnson, E. Genin, A. Caliebe, D. Chitayat, C. Clericuzio, J. Denecke, M. Di Rocco, B. Fischler, D. FitzPatrick, A. Garcia-Cazorla, D. Guyot, S. Jacquemont, S. Koletzko, B. Leheup, H. Mandel, M. T. Sanseverino, R. H. Houwen, P. J. McKiernan, D. A. Kelly and E. R. Maher (2006). "Clinical and molecular genetic features of ARC syndrome." Hum Genet **120**(3): 396-409.

Glozman, R., T. Okiyoneda, C. M. Mulvihill, J. M. Rini, H. Barriere and G. L. Lukacs (2009). "N-glycans are direct determinants of CFTR folding and stability in secretory and endocytic membrane traffic." J Cell Biol **184**(6): 847-862.

Golachowska, M. R., D. Hoekstra and I. S. C. van (2010). "Recycling endosomes in apical plasma membrane domain formation and epithelial cell polarity." Trends Cell Biol **20**(10): 618-626.

Goldmann, W. H. (2018). "Intermediate filaments and cellular mechanics." Cell Biol Int **42**(2): 132-138.

Gomez-Ospina, N., C. J. Potter, R. Xiao, K. Manickam, M. S. Kim, K. H. Kim, B. L. Shneider, J. L. Picarsic, T. A. Jacobson, J. Zhang, W. He, P. Liu, A. S. Knisely, M. J. Finegold, D. M. Muzny, E. Boerwinkle, J. R. Lupski, S. E. Plon, R. A. Gibbs, C. M. Eng, Y. Yang, G. C. Washington, M. H. Porteus, W. E. Berquist, N. Kambham, R. J. Singh, F. Xia, G. M. Enns and D. D. Moore (2016). "Mutations in the nuclear bile acid receptor FXR cause progressive familial intrahepatic cholestasis." Nat Commun **7**: 10713.

Gonzales, E., S. A. Taylor, A. Davit-Spraul, A. Thebaut, N. Thomassin, C. Guettier, P. F. Whittington and E. Jacquemin (2017). "MYO5B mutations cause cholestasis with

normal serum gamma-glutamyl transferase activity in children without microvillous inclusion disease." Hepatology **65**(1): 164-173.

Gonzales, P. A., T. Pisitkun, J. D. Hoffert, D. Tchapyjnikov, R. A. Star, R. Kleta, N. S. Wang and M. A. Knepper (2009). "Large-scale proteomics and phosphoproteomics of urinary exosomes." J Am Soc Nephrol **20**(2): 363-379.

Goto, K., K. Sugiyama, T. Sugiura, T. Ando, F. Mizutani, K. Terabe, K. Ban and H. Togari (2003). "Bile salt export pump gene mutations in two Japanese patients with progressive familial intrahepatic cholestasis." J Pediatr Gastroenterol Nutr **36**(5): 647-650.

Green, R. M., F. Hoda and K. L. Ward (2000). "Molecular cloning and characterization of the murine bile salt export pump." Gene **241**(1): 117-123.

Greenblatt, M. B., K. H. Park, H. Oh, J. M. Kim, D. Y. Shin, J. M. Lee, J. W. Lee, A. Singh, K. Y. Lee, D. Hu, C. Xiao, J. F. Charles, J. M. Penninger, S. Lotinun, R. Baron, S. Ghosh and J. H. Shim (2015). "CHMP5 controls bone turnover rates by dampening NF-kappaB activity in osteoclasts." J Exp Med **212**(8): 1283-1301.

Groen, A., M. R. Romero, C. Kunne, S. J. Hoosdally, P. H. Dixon, C. Wooding, C. Williamson, J. Seppen, K. Van den Oever, K. S. Mok, C. C. Paulusma, K. J. Linton and R. P. Oude Elferink (2011). "Complementary functions of the flippase ATP8B1 and the floppase ABCB4 in maintaining canalicular membrane integrity." Gastroenterology **141**(5): 1927-1937 e1921-1924.

Grumati, P. and I. Dikic (2018). "Ubiquitin signaling and autophagy." J Biol Chem **293**(15): 5404-5413.

Haag, C., T. Pohlmann and M. Feldbrugge (2017). "The ESCRT regulator Did2 maintains the balance between long-distance endosomal transport and endocytic trafficking." PLoS Genet **13**(4): e1006734.

Hayashi, H., K. Inamura, K. Aida, S. Naoi, R. Horikawa, H. Nagasaka, T. Takatani, T. Fukushima, A. Hattori, T. Yabuki, I. Horii and Y. Sugiyama (2012). "AP2 adaptor complex mediates bile salt export pump internalization and modulates its hepatocanalicular expression and transport function." Hepatology **55**(6): 1889-1900.

Hayashi, H., T. Mizuno, R. Horikawa, H. Nagasaka, T. Yabuki, H. Takikawa and Y. Sugiyama (2012). "4-Phenylbutyrate modulates ubiquitination of hepatocanalicular MRP2 and reduces serum total bilirubin concentration." J Hepatol **56**(5): 1136-1144.

Hayashi, H. and Y. Sugiyama (2007). "4-phenylbutyrate enhances the cell surface expression and the transport capacity of wild-type and mutated bile salt export pumps." Hepatology **45**(6): 1506-1516.

Hayashi, H. and Y. Sugiyama (2009). "Short-chain ubiquitination is associated with the degradation rate of a cell-surface-resident bile salt export pump (BSEP/ABCB11)." Mol Pharmacol **75**(1): 143-150.

Hayashi, H., T. Takada, H. Suzuki, H. Akita and Y. Sugiyama (2005). "Two common PFIC2 mutations are associated with the impaired membrane trafficking of BSEP/ABCB11." Hepatology **41**(4): 916-924.

Hayashi, H., T. Takada, H. Suzuki, R. Onuki, A. F. Hofmann and Y. Sugiyama (2005). "Transport by vesicles of glycine- and taurine-conjugated bile salts and tauroolithocholate 3-sulfate: a comparison of human BSEP with rat Bsep." Biochim Biophys Acta **1738**(1-3): 54-62.

Henkel, A. S., B. LeCuyer, S. Olivares and R. M. Green (2017). "Endoplasmic Reticulum Stress Regulates Hepatic Bile Acid Metabolism in Mice." Cell Mol Gastroenterol Hepatol **3**(2): 261-271.

Hiebl, V., A. Ladurner, S. Latkolik and V. M. Dirsch (2018). "Natural products as modulators of the nuclear receptors and metabolic sensors LXR, FXR and RXR." Biotechnol Adv **36**(6): 1657-1698.

Hofmann, A. F. (1999). "The continuing importance of bile acids in liver and intestinal disease." Arch Intern Med **159**(22): 2647-2658.

Hofmann, A. F., L. R. Hagey and M. D. Krasowski (2010). "Bile salts of vertebrates: structural variation and possible evolutionary significance." J Lipid Res **51**(2): 226-246.

Hohmann, T. and F. Dehghani (2019). "The Cytoskeleton-A Complex Interacting Meshwork." Cells **8**(4).

Homolya, L., D. Fu, P. Sengupta, M. Jarnik, J. P. Gillet, L. Vitale-Cross, J. S. Gutkind, J. Lippincott-Schwartz and I. M. Arias (2014). "LKB1/AMPK and PKA control ABCB11 trafficking and polarization in hepatocytes." PLoS One **9**(3): e91921.

Horgan, C. P., S. R. Hanscom, E. E. Kelly and M. W. McCaffrey (2012). "Tumor susceptibility gene 101 (TSG101) is a novel binding-partner for the class II Rab11-FIPs." PLoS One **7**(2): e32030.

Hu, L., Z. Huang, Z. Wu, A. Ali and A. Qian (2018). "Mammalian Plakins, Giant Cytolinkers: Versatile Biological Functions and Roles in Cancer." Int J Mol Sci **19**(4).

Hunt, C. M., J. I. Papay, V. Stanulovic and A. Regev (2017). "Drug rechallenge following drug-induced liver injury." Hepatology **66**(2): 646-654.

Hurley, J. H. and B. A. Schulman (2014). "Atomistic autophagy: the structures of cellular self-digestion." Cell **157**(2): 300-311.

Ihrke, G., E. B. Neufeld, T. Meads, M. R. Shanks, D. Cassio, M. Laurent, T. A. Schroer, R. E. Pagano and A. L. Hubbard (1993). "WIF-B cells: an in vitro model for studies of hepatocyte polarity." J Cell Biol **123**(6 Pt 2): 1761-1775.

Ikegami, T. and A. Honda (2018). "Reciprocal interactions between bile acids and gut microbiota in human liver diseases." Hepatol Res **48**(1): 15-27.

Jacob, J. T., P. A. Coulombe, R. Kwan and M. B. Omary (2018). "Types I and II Keratin Intermediate Filaments." Cold Spring Harb Perspect Biol **10**(4).

Jansen, P. L., S. S. Strautnieks, E. Jacquemin, M. Hadchouel, E. M. Sokal, G. J. Hooiveld, J. H. Koning, A. De Jager-Krieken, F. Kuipers, F. Stellaard, C. M. Bijleveld, A. Gouw, H. Van Goor, R. J. Thompson and M. Muller (1999). "Hepatocanalicular bile salt export pump deficiency in patients with progressive familial intrahepatic cholestasis." Gastroenterology **117**(6): 1370-1379.

Jirouskova, M., K. Nepomucka, G. Oyman-Eyrilmez, A. Kalendova, H. Havelkova, L. Sarnova, K. Chalupsky, B. Schuster, O. Benada, P. Miksatkova, M. Kuchar, O. Fabian, R. Sedlacek, G. Wiche and M. Gregor (2018). "Plectin controls biliary tree architecture and stability in cholestasis." J Hepatol **68**(5): 1006-1017.

Jurica, J., G. Dovrtelova, K. Noskova and O. Zendulka (2016). "Bile acids, nuclear receptors and cytochrome P450." Physiol Res **65**(Supplementum 4): S427-S440.

Keitel, V., M. Burdelski, U. Warskulat, T. Kuhlkamp, D. Keppler, D. Haussinger and R. Kubitz (2005). "Expression and localization of hepatobiliary transport proteins in progressive familial intrahepatic cholestasis." Hepatology **41**(5): 1160-1172.

Keppler, D. (2014). "The roles of MRP2, MRP3, OATP1B1, and OATP1B3 in conjugated hyperbilirubinemia." Drug Metab Dispos **42**(4): 561-565.

Ketema, M., P. Secades, M. Kreft, L. Nahidiazar, H. Janssen, K. Jalink, J. M. de Pereda and A. Sonnenberg (2015). "The rod domain is not essential for the function of plectin in maintaining tissue integrity." Mol Biol Cell **26**(13): 2402-2417.

Kim, S. R., Y. Saito, M. Itoda, K. Maekawa, M. Kawamoto, N. Kamatani, S. Ozawa and J. Sawada (2009). "Genetic variations of the ABC transporter gene ABCB11 encoding the human bile salt export pump (BSEP) in a Japanese population." Drug Metab Pharmacokinet **24**(3): 277-281.

Kipp, H. and I. M. Arias (2000). "Intracellular trafficking and regulation of canalicular ATP-binding cassette transporters." Semin Liver Dis **20**(3): 339-351.

Kipp, H. and I. M. Arias (2000). "Newly synthesized canalicular ABC transporters are directly targeted from the Golgi to the hepatocyte apical domain in rat liver." J Biol Chem **275**(21): 15917-15925.

Kipp, H. and I. M. Arias (2002). "Trafficking of canalicular ABC transporters in hepatocytes." Annu Rev Physiol **64**: 595-608.

Kipp, H., N. Pichetshote and I. M. Arias (2001). "Transporters on demand: intrahepatic pools of canalicular ATP binding cassette transporters in rat liver." J Biol Chem **276**(10): 7218-7224.

Komander, D. (2009). "The emerging complexity of protein ubiquitination." Biochem Soc Trans **37**(Pt 5): 937-953.

Kong, J., B. B. Liu, S. D. Wu, Y. Wang, Q. Q. Jiang and E. L. Guo (2014). "Enhancement of interaction of BSEP and HAX-1 on the canalicular membrane of

hepatocytes in a mouse model of cholesterol cholelithiasis." Int J Clin Exp Pathol **7**(4): 1644-1650.

Kubitz, R., C. Droge, J. Stindt, K. Weissenberger and D. Haussinger (2012). "The bile salt export pump (BSEP) in health and disease." Clin Res Hepatol Gastroenterol **36**(6): 536-553.

Kubitz, R., N. Saha, T. Kuhlkamp, S. Dutta, S. vom Dahl, M. Wettstein and D. Haussinger (2004). "Ca²⁺-dependent protein kinase C isoforms induce cholestasis in rat liver." J Biol Chem **279**(11): 10323-10330.

Kullak-Ublick, G. A., B. Stieger, B. Hagenbuch and P. J. Meier (2000). "Hepatic transport of bile salts." Semin Liver Dis **20**(3): 273-292.

Kumar, H., K. Pushpa, A. Kumari, K. Verma, R. Pergu and S. V. S. Mylavarapu (2019). "The exocyst complex and Rab5 are required for abscission by localizing ESCRT III subunits to the cytokinetic bridge." J Cell Sci **132**(14): jcs226001.

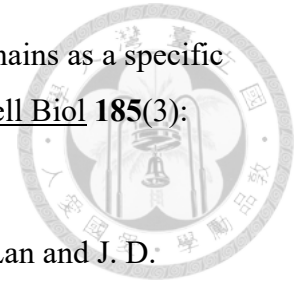
Kuroki, S., K. Shimazu, M. Kuwabara, M. Une, K. Kihira, T. Kuramoto and T. Hoshita (1985). "Identification of bile alcohols in human bile." J Lipid Res **26**(2): 230-240.

Lam, P., C. L. Pearson, C. J. Soroka, S. Xu, A. Mennone and J. L. Boyer (2007). "Levels of plasma membrane expression in progressive and benign mutations of the bile salt export pump (Bsep/Abcb11) correlate with severity of cholestatic diseases." Am J Physiol Cell Physiol **293**(5): C1709-1716.

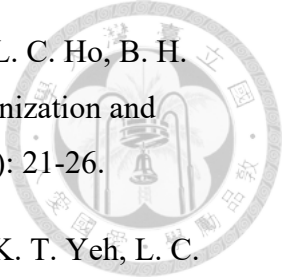
Lam, P., C. J. Soroka and J. L. Boyer (2010). "The bile salt export pump: clinical and experimental aspects of genetic and acquired cholestatic liver disease." Semin Liver Dis **30**(2): 125-133.

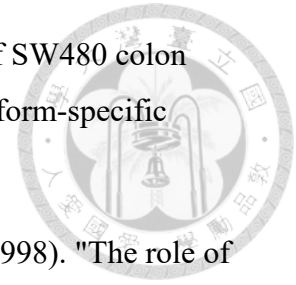
Lam, P., R. Wang and V. Ling (2005). "Bile acid transport in sister of P-glycoprotein (ABCB11) knockout mice." Biochemistry **44**(37): 12598-12605.

Lam, P., S. Xu, C. J. Soroka and J. L. Boyer (2012). "A C-terminal tyrosine-based motif in the bile salt export pump directs clathrin-dependent endocytosis." Hepatology **55**(6): 1901-1911.



- Lauwers, E., C. Jacob and B. Andre (2009). "K63-linked ubiquitin chains as a specific signal for protein sorting into the multivesicular body pathway." J Cell Biol **185**(3): 493-502.
- Lecureur, V., D. Sun, P. Hargrove, E. G. Schuetz, R. B. Kim, L. B. Lan and J. D. Schuetz (2000). "Cloning and expression of murine sister of P-glycoprotein reveals a more discriminating transporter than MDR1/P-glycoprotein." Mol Pharmacol **57**(1): 24-35.
- Lee, C. S., A. Kimura, J. F. Wu, Y. H. Ni, H. Y. Hsu, M. H. Chang, H. Nittono and H. L. Chen (2017). "Prognostic roles of tetrahydroxy bile acids in infantile intrahepatic cholestasis." J Lipid Res **58**(3): 607-614.
- Li, C. C., T. C. Chiang, T. S. Wu, G. Pacheco-Rodriguez, J. Moss and F. J. Lee (2007). "ARL4D recruits cytohesin-2/ARNO to modulate actin remodeling." Mol Biol Cell **18**(11): 4420-4437.
- Lim, K. L., K. C. Chew, J. M. Tan, C. Wang, K. K. Chung, Y. Zhang, Y. Tanaka, W. Smith, S. Engelender, C. A. Ross, V. L. Dawson and T. M. Dawson (2005). "Parkin mediates nonclassical, proteasomal-independent ubiquitination of synphilin-1: implications for Lewy body formation." J Neurosci **25**(8): 2002-2009.
- Linton, K. J. (2015). "Lipid flopping in the liver." Biochem Soc Trans **43**(5): 1003-1010.
- Liu, C. G., C. Maercker, M. J. Castanon, R. Hauptmann and G. Wiche (1996). "Human plectin: organization of the gene, sequence analysis, and chromosome localization (8q24)." Proc Natl Acad Sci U S A **93**(9): 4278-4283.
- Liu, F., Y. Song and D. Liu (1999). "Hydrodynamics-based transfection in animals by systemic administration of plasmid DNA." Gene Ther **6**(7): 1258-1266.
- Liu, T., R. X. Wang, J. Han, C. Z. Hao, Y. L. Qiu, Y. Y. Yan, L. T. Li, N. L. Wang, J. Y. Gong, Y. Lu, M. H. Zhang, X. B. Xie, J. C. Yang, Y. J. You, J. Q. Li, A. S. Knisely, C. H. Borchers, V. Ling and J. S. Wang (2018). "Comprehensive bile acid profiling in hereditary intrahepatic cholestasis: Genetic and clinical correlations." Liver Int **38**(9): 1676-1685.

- 
- Liu, Y. H., C. C. Cheng, C. C. Ho, W. T. Chao, R. J. Pei, Y. H. Hsu, L. C. Ho, B. H. Shiu and Y. S. Lai (2011). "Plectin deficiency on cytoskeletal disorganization and transformation of human liver cells in vitro." Med Mol Morphol **44**(1): 21-26.
- Liu, Y. H., C. C. Cheng, C. C. Ho, W. T. Chao, R. J. Pei, Y. H. Hsu, K. T. Yeh, L. C. Ho, M. C. Tsai and Y. S. Lai (2008). "Degradation of plectin with modulation of cytokeratin 18 in human liver cells during staurosporine-induced apoptosis." In Vivo **22**(5): 543-548.
- Liu, Y. H., C. C. Ho, C. C. Cheng, W. T. Chao, R. J. Pei, Y. H. Hsu and Y. S. Lai (2011). "Cytokeratin 18-mediated disorganization of intermediate filaments is induced by degradation of plectin in human liver cells." Biochem Biophys Res Commun **407**(3): 575-580.
- Ljubuncic, P., I. Yousef and A. Bomzon (2004). "Cholemic transgenic mice: a novel animal model to investigate the effects of bile acids." J Pharmacol Toxicol Methods **50**(3): 231-235.
- Lobert, V. H. and H. Stenmark (2011). "Cell polarity and migration: emerging role for the endosomal sorting machinery." Physiology (Bethesda) **26**(3): 171-180.
- Lobert, V. H. and H. Stenmark (2012). "The ESCRT machinery mediates polarization of fibroblasts through regulation of myosin light chain." J Cell Sci **125**(Pt 1): 29-36.
- Lu, F. T., J. F. Wu, H. Y. Hsu, Y. H. Ni, M. H. Chang, C. I. Chao and H. L. Chen (2014). "gamma-Glutamyl transpeptidase level as a screening marker among diverse etiologies of infantile intrahepatic cholestasis." J Pediatr Gastroenterol Nutr **59**(6): 695-701.
- Malhi, H. and M. Camilleri (2017). "Modulating bile acid pathways and TGR5 receptors for treating liver and GI diseases." Curr Opin Pharmacol **37**: 80-86.
- Martinot, E., L. Sedes, M. Baptissart, J. M. Lobaccaro, F. Caira, C. Beaudoin and D. H. Volle (2017). "Bile acids and their receptors." Mol Aspects Med **56**: 2-9.
- Matsubara, T., F. Li and F. J. Gonzalez (2013). "FXR signaling in the enterohepatic system." Mol Cell Endocrinol **368**(1-2): 17-29.



- McInroy, L. and A. Maatta (2011). "Plectin regulates invasiveness of SW480 colon carcinoma cells and is targeted to podosome-like adhesions in an isoform-specific manner." Exp Cell Res **317**(17): 2468-2478.
- Misra, S., P. Ujhazy, Z. Gatmaitan, L. Varticovski and I. M. Arias (1998). "The role of phosphoinositide 3-kinase in taurocholate-induced trafficking of ATP-dependent canalicular transporters in rat liver." J Biol Chem **273**(41): 26638-26644.
- Misra, S., L. Varticovski and I. M. Arias (2003). "Mechanisms by which cAMP increases bile acid secretion in rat liver and canalicular membrane vesicles." Am J Physiol Gastrointest Liver Physiol **285**(2): G316-324.
- Mochizuki, K., T. Kagawa, A. Numari, M. J. Harris, J. Itoh, N. Watanabe, T. Mine and I. M. Arias (2007). "Two N-linked glycans are required to maintain the transport activity of the bile salt export pump (ABCB11) in MDCK II cells." Am J Physiol Gastrointest Liver Physiol **292**(3): G818-828.
- Molinaro, A., A. Wahlstrom and H. U. Marschall (2018). "Role of Bile Acids in Metabolic Control." Trends Endocrinol Metab **29**(1): 31-41.
- Morotti, R. A., F. J. Suchy and M. S. Magid (2011). "Progressive familial intrahepatic cholestasis (PFIC) type 1, 2, and 3: a review of the liver pathology findings." Seminars in liver disease **31**(1): 3-10.
- Moseley, R. H., W. Wang, H. Takeda, K. Lown, L. Shick, M. Ananthanarayanan and F. J. Suchy (1996). "Effect of endotoxin on bile acid transport in rat liver: a potential model for sepsis-associated cholestasis." Am J Physiol **271**(1 Pt 1): G137-146.
- Muhlfeld, S., O. Domanova, T. Berlage, C. Stross, A. Helmer, V. Keitel, D. Haussinger and R. Kubitz (2012). "Short-term feedback regulation of bile salt uptake by bile salts in rodent liver." Hepatology **56**(6): 2387-2397.
- Muller, M., T. Ishikawa, U. Berger, C. Klunemann, L. Lucka, A. Schreyer, C. Kannicht, W. Reutter, G. Kurz and D. Keppler (1991). "ATP-dependent transport of taurocholate across the hepatocyte canalicular membrane mediated by a 110-kDa glycoprotein binding ATP and bile salt." J Biol Chem **266**(28): 18920-18926.

Muller, T., M. W. Hess, N. Schiefermeier, K. Pfaller, H. L. Ebner, P. Heinz-Erian, H. Ponstingl, J. Partsch, B. Rollinghoff, H. Kohler, T. Berger, H. Lenhartz, B. Schlenck, R. J. Houwen, C. J. Taylor, H. Zoller, S. Lechner, O. Goulet, G. Utermann, F. M. Ruemmele, L. A. Huber and A. R. Janecke (2008). "MYO5B mutations cause microvillus inclusion disease and disrupt epithelial cell polarity." Nat Genet **40**(10): 1163-1165.

Murphy, G. M. and E. Signer (1974). "Bile acid metabolism in infants and children." Gut **15**(2): 151-163.

Musch, A. (2014). "The unique polarity phenotype of hepatocytes." Exp Cell Res **328**(2): 276-283.

Muthuswamy, S. K. and B. Xue (2012). "Cell polarity as a regulator of cancer cell behavior plasticity." Annu Rev Cell Dev Biol **28**: 599-625.

Naoi, S., H. Hayashi, T. Inoue, K. Tanikawa, K. Igarashi, H. Nagasaka, M. Kage, H. Takikawa, Y. Sugiyama, A. Inui, T. Nagai and H. Kusuhara (2014). "Improved liver function and relieved pruritus after 4-phenylbutyrate therapy in a patient with progressive familial intrahepatic cholestasis type 2." J Pediatr **164**(5): 1219-1227 e1213.

Naslavsky, N. and S. Caplan (2018). "The enigmatic endosome - sorting the ins and outs of endocytic trafficking." J Cell Sci **131**(13): jcs216499.

Natsuga, K. (2015). "Plectin-related skin diseases." J Dermatol Sci **77**(3): 139-145.

Nikolic, B., E. Mac Nulty, B. Mir and G. Wiche (1996). "Basic amino acid residue cluster within nuclear targeting sequence motif is essential for cytoplasmic plectin-vimentin network junctions." J Cell Biol **134**(6): 1455-1467.

Nishida, T., Z. Gatmaitan, M. Che and I. M. Arias (1991). "Rat liver canalicular membrane vesicles contain an ATP-dependent bile acid transport system." Proc Natl Acad Sci U S A **88**(15): 6590-6594.

Noe, J., B. Hagenbuch, P. J. Meier and M. V. St-Pierre (2001). "Characterization of the mouse bile salt export pump overexpressed in the baculovirus system." Hepatology **33**(5): 1223-1231.

Noe, J., B. Stieger and P. J. Meier (2002). "Functional expression of the canalicular bile salt export pump of human liver." Gastroenterology **123**(5): 1659-1666.

Noh, S. H., H. Y. Gee, Y. Kim, H. Piao, J. Kim, C. M. Kang, G. Lee, I. Mook-Jung, Y. Lee, J. W. Cho and M. G. Lee (2018). "Specific autophagy and ESCRT components participate in the unconventional secretion of CFTR." Autophagy **14**(10): 1761-1778.

Norgan, A. P., B. A. Davies, I. F. Azmi, A. S. Schroeder, J. A. Payne, G. M. Lynch, Z. Xu and D. J. Katzmann (2013). "Relief of autoinhibition enhances Vta1 activation of Vps4 via the Vps4 stimulatory element." J Biol Chem **288**(36): 26147-26156.

Numrich, J. and C. Ungermann (2014). "Endocytic Rabs in membrane trafficking and signaling." Biol Chem **395**(3): 327-333.

Omary, M. B. (2017). "Intermediate filament proteins of digestive organs: physiology and pathophysiology." Am J Physiol Gastrointest Liver Physiol **312**(6): G628-G634.

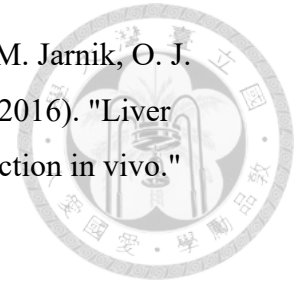
Ortiz, D. F., J. Moseley, G. Calderon, A. L. Swift, S. Li and I. M. Arias (2004). "Identification of HAX-1 as a protein that binds bile salt export protein and regulates its abundance in the apical membrane of Madin-Darby canine kidney cells." J Biol Chem **279**(31): 32761-32770.

Ortiz, D. F., M. V. St Pierre, A. Abdulmessih and I. M. Arias (1997). "A yeast ATP-binding cassette-type protein mediating ATP-dependent bile acid transport." J Biol Chem **272**(24): 15358-15365.

Patel, M., M. Johnson, C. J. Sychterz, G. J. Lewis, C. Watson, H. Ellens, J. W. Polli and M. J. Zamek-Gliszczynski (2018). "Hepatobiliary Disposition of Atovaquone: A Case of Mechanistically Unusual Biliary Clearance." J Pharmacol Exp Ther **366**(1): 37-45.

Plass, J. R., O. Mol, J. Heegsma, M. Geuken, J. de Bruin, G. Elling, M. Muller, K. N. Faber and P. L. Jansen (2004). "A progressive familial intrahepatic cholestasis type 2 mutation causes an unstable, temperature-sensitive bile salt export pump." J Hepatol **40**(1): 24-30.

Popoff, V., F. Adolf, B. Brugger and F. Wieland (2011). "COPI budding within the Golgi stack." Cold Spring Harb Perspect Biol **3**(11): a005231.



Porat-Shliom, N., A. J. Tietgens, C. M. Van Itallie, L. Vitale-Cross, M. Jarnik, O. J. Harding, J. M. Anderson, J. S. Gutkind, R. Weigert and I. M. Arias (2016). "Liver kinase B1 regulates hepatocellular tight junction distribution and function in vivo." Hepatology **64**(4): 1317-1329.

Prekeris, R., J. Klumperman and R. H. Scheller (2000). "A Rab11/Rip11 protein complex regulates apical membrane trafficking via recycling endosomes." Mol Cell **6**(6): 1437-1448.

Presley, J. F., N. B. Cole, T. A. Schroer, K. Hirschberg, K. J. Zaal and J. Lippincott-Schwartz (1997). "ER-to-Golgi transport visualized in living cells." Nature **389**(6646): 81-85.

Przybylla, S. and L. Schmitt (2014). "Posttranslational regulation of the bile salt export pump." European Journal of Medical Research **19**(S1).

Przybylla, S., J. Stindt, D. Kleinschrodt, J. Schulte Am Esch, D. Haussinger, V. Keitel, S. H. Smits and L. Schmitt (2016). "Analysis of the Bile Salt Export Pump (ABCB11) Interactome Employing Complementary Approaches." PLoS One **11**(7): e0159778.

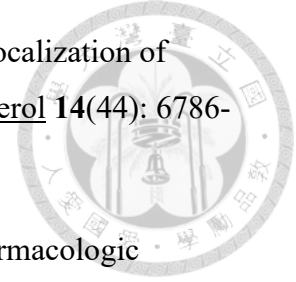
Rabouille, C., V. Malhotra and W. Nickel (2012). "Diversity in unconventional protein secretion." J Cell Sci **125**(Pt 22): 5251-5255.

Reschly, E. J., N. Ai, S. Ekins, W. J. Welsh, L. R. Hagey, A. F. Hofmann and M. D. Krasowski (2008). "Evolution of the bile salt nuclear receptor FXR in vertebrates." J Lipid Res **49**(7): 1577-1587.

Reshetnyak, V. I. (2013). "Physiological and molecular biochemical mechanisms of bile formation." World J Gastroenterol **19**(42): 7341-7360.

Rezniczek, G. A., C. Abrahamsberg, P. Fuchs, D. Spazierer and G. Wiche (2003). "Plectin 5'-transcript diversity: short alternative sequences determine stability of gene products, initiation of translation and subcellular localization of isoforms." Hum Mol Genet **12**(23): 3181-3194.

Roberts, E. A. (2003). "Neonatal hepatitis syndrome." Seminars in Neonatology **8**(5): 357-374.



Roma, M. G., F. A. Crocenzi and A. D. Mottino (2008). "Dynamic localization of hepatocellular transporters in health and disease." World J Gastroenterol **14**(44): 6786-6801.

Rubenstein, R. C., M. E. Egan and P. L. Zeitlin (1997). "In vitro pharmacologic restoration of CFTR-mediated chloride transport with sodium 4-phenylbutyrate in cystic fibrosis epithelial cells containing delta F508-CFTR." J Clin Invest **100**(10): 2457-2465.

Russell, D. W. (2003). "The enzymes, regulation, and genetics of bile acid synthesis." Annu Rev Biochem **72**: 137-174.

Sai, Y., A. T. Nies and I. M. Arias (1999). "Bile acid secretion and direct targeting of mdrl-green fluorescent protein from Golgi to the canalicular membrane in polarized WIF-B cells." J Cell Sci **112** (Pt 24): 4535-4545.

Sambrotta, M., S. Strautnieks, E. Papouli, P. Rushton, B. E. Clark, D. A. Parry, C. V. Logan, L. J. Newbury, B. M. Kamath, S. Ling, T. Grammatikopoulos, B. E. Wagner, J. C. Magee, R. J. Sokol, G. Mieli-Vergani, G. University of Washington Center for Mendelian, J. D. Smith, C. A. Johnson, P. McClean, M. A. Simpson, A. S. Knisely, L. N. Bull and R. J. Thompson (2014). "Mutations in TJP2 cause progressive cholestatic liver disease." Nat Genet **46**(4): 326-328.

Samyn, M. and G. Mieli-Vergani (2007). "Liver and biliary disease in infancy." Medicine **35**(2): 61-66.

Scheuring, S., R. A. Rohricht, B. Schoning-Burkhardt, A. Beyer, S. Muller, H. F. Abts and K. Kohrer (2001). "Mammalian cells express two VPS4 proteins both of which are involved in intracellular protein trafficking." J Mol Biol **312**(3): 469-480.

Scott, C. C., F. Vacca and J. Gruenberg (2014). "Endosome maturation, transport and functions." Semin Cell Dev Biol **31**: 2-10.

Sedlak, T. W., M. Saleh, D. S. Higginson, B. D. Paul, K. R. Juluri and S. H. Snyder (2009). "Bilirubin and glutathione have complementary antioxidant and cytoprotective roles." Proc Natl Acad Sci U S A **106**(13): 5171-5176.

Shim, J. H., C. Xiao, M. S. Hayden, K. Y. Lee, E. S. Trombetta, M. Pypaert, A. Nara, T. Yoshimori, B. Wilm, H. Erdjument-Bromage, P. Tempst, B. L. Hogan, I. Mellman and S. Ghosh (2006). "CHMP5 is essential for late endosome function and down-regulation of receptor signaling during mouse embryogenesis." J Cell Biol **172**(7): 1045-1056.

Song, S., J. Tan, Y. Miao and Q. Zhang (2018). "Crosstalk of ER stress-mediated autophagy and ER-phagy: Involvement of UPR and the core autophagy machinery." J Cell Physiol **233**(5): 3867-3874.

Sonnichsen, B., S. De Renzis, E. Nielsen, J. Rietdorf and M. Zerial (2000). "Distinct membrane domains on endosomes in the recycling pathway visualized by multicolor imaging of Rab4, Rab5, and Rab11." J Cell Biol **149**(4): 901-914.

Staszewska, I., I. Fischer and G. Wiche (2015). "Plectin isoform 1-dependent nuclear docking of desmin networks affects myonuclear architecture and expression of mechanotransducers." Hum Mol Genet **24**(25): 7373-7389.

Steinboeck, F. and D. Kristufek (2005). "Identification of the cytolinker protein plectin in neuronal cells - expression of a rodless isoform in neurons of the rat superior cervical ganglion." Cell Mol Neurobiol **25**(7): 1151-1169.

Sticova, E. and M. Jirsa (2013). "New insights in bilirubin metabolism and their clinical implications." World J Gastroenterol **19**(38): 6398-6407.

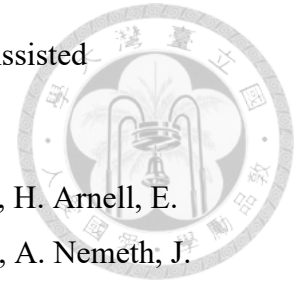
Sticova, E., M. Jirsa and J. Pawlowska (2018). "New Insights in Genetic Cholestasis: From Molecular Mechanisms to Clinical Implications." Can J Gastroenterol Hepatol **2018**: 2313675.

Stieger, B., K. Fattinger, J. Madon, G. A. Kullak-Ublick and P. J. Meier (2000). "Drug- and estrogen-induced cholestasis through inhibition of the hepatocellular bile salt export pump (Bsep) of rat liver." Gastroenterology **118**(2): 422-430.

Stieger, B., B. O'Neill and P. J. Meier (1992). "ATP-dependent bile-salt transport in canalicular rat liver plasma-membrane vesicles." Biochem J **284** (Pt 1)(1): 67-74.

Stindt, J., P. Ellinger, C. Stross, V. Keitel, D. Haussinger, S. H. Smits, R. Kubitz and L. Schmitt (2011). "Heterologous overexpression and mutagenesis of the human bile salt

export pump (ABCB11) using DREAM (Directed REcombination-Assisted Mutagenesis)." PLoS One **6**(5): e20562.



Strautnieks, S. S., L. N. Bull, A. S. Knisely, S. A. Kocoshis, N. Dahl, H. Arnell, E. Sokal, K. Dahan, S. Childs, V. Ling, M. S. Tanner, A. F. Kagalwalla, A. Nemeth, J. Pawlowska, A. Baker, G. Mieli-Vergani, N. B. Freimer, R. M. Gardiner and R. J. Thompson (1998). "A gene encoding a liver-specific ABC transporter is mutated in progressive familial intrahepatic cholestasis." Nat Genet **20**(3): 233-238.

Strautnieks, S. S., J. A. Byrne, L. Pawlikowska, D. Cebecauerova, A. Rayner, L. Dutton, Y. Meier, A. Antoniou, B. Stieger, H. Arnell, F. Ozcay, H. F. Al-Hussaini, A. F. Bassas, H. J. Verkade, B. Fischler, A. Nemeth, R. Kotalova, B. L. Shneider, J. Cielecka-Kuszyk, P. McClean, P. F. Whittington, E. Sokal, M. Jirsa, S. H. Wali, I. Jankowska, J. Pawlowska, G. Mieli-Vergani, A. S. Knisely, L. N. Bull and R. J. Thompson (2008). "Severe bile salt export pump deficiency: 82 different ABCB11 mutations in 109 families." Gastroenterology **134**(4): 1203-1214.

Strautnieks, S. S., A. F. Kagalwalla, M. S. Tanner, A. S. Knisely, L. Bull, N. Freimer, S. A. Kocoshis, R. M. Gardiner and R. J. Thompson (1997). "Identification of a locus for progressive familial intrahepatic cholestasis PFIC2 on chromosome 2q24." Am J Hum Genet **61**(3): 630-633.

Strnad, P., K. Zatloukal, C. Stumptner, H. Kulaksiz and H. Denk (2008). "Mallory-Denk-bodies: lessons from keratin-containing hepatic inclusion bodies." Biochim Biophys Acta **1782**(12): 764-774.

Suga, T., H. Yamaguchi, T. Sato, M. Maekawa, J. Goto and N. Mano (2017). "Preference of Conjugated Bile Acids over Unconjugated Bile Acids as Substrates for OATP1B1 and OATP1B3." PLoS One **12**(1): e0169719.

Svitkina, T. M., A. B. Verkhovsky and G. G. Borisy (1996). "Plectin sidearms mediate interaction of intermediate filaments with microtubules and other components of the cytoskeleton." J Cell Biol **135**(4): 991-1007.

Szul, T. and E. Sztul (2011). "COPII and COPI traffic at the ER-Golgi interface." Physiology (Bethesda) **26**(5): 348-364.

Telbisz, A. and L. Homolya (2016). "Recent advances in the exploration of the bile salt export pump (BSEP/ABCB11) function." Expert Opin Ther Targets **20**(4): 501-514.

Thakare, R., J. A. Alamoudi, N. Gautam, A. D. Rodrigues and Y. Alnouti (2018). "Species differences in bile acids I. Plasma and urine bile acid composition." J Appl Toxicol **38**(10): 1323-1335.

Thakare, R., J. A. Alamoudi, N. Gautam, A. D. Rodrigues and Y. Alnouti (2018). "Species differences in bile acids II. Bile acid metabolism." J Appl Toxicol **38**(10): 1336-1352.

Tomer, G., M. Ananthanarayanan, A. Weymann, N. Balasubramanian and F. J. Suchy (2003). "Differential developmental regulation of rat liver canalicular membrane transporters Bsep and Mrp2." Pediatr Res **53**(2): 288-294.

Trauner, M. (1997). "Molecular alterations of canalicular transport systems in experimental models of cholestasis: possible functional correlations." Yale J Biol Med **70**(4): 365-378.

Treyer, A. and A. Musch (2013). "Hepatocyte polarity." Compr Physiol **3**(1): 243-287.

Valencia, R. G., G. Walko, L. Janda, J. Novacek, E. Mihailovska, S. Reipert, K. Andra-Marobela and G. Wiche (2013). "Intermediate filament-associated cytolinker plectin 1c destabilizes microtubules in keratinocytes." Mol Biol Cell **24**(6): 768-784.

van Groen, B. D., E. van de Steeg, M. G. Mooij, M. M. H. van Lipzig, B. A. E. de Koning, R. M. Verdijk, H. M. Wortelboer, R. Gaedigk, C. Bi, J. S. Leeder, R. H. N. van Schaik, J. van Rosmalen, D. Tibboel, W. H. Vaes and S. N. de Wildt (2018). "Proteomics of human liver membrane transporters: a focus on fetuses and newborn infants." Eur J Pharm Sci **124**: 217-227.

van Mil, S. W., W. L. van der Woerd, G. van der Brugge, E. Sturm, P. L. Jansen, L. N. Bull, I. E. van den Berg, R. Berger, R. H. Houwen and L. W. Klomp (2004). "Benign recurrent intrahepatic cholestasis type 2 is caused by mutations in ABCB11." Gastroenterology **127**(2): 379-384.

Vasiliou, V., K. Vasiliou and D. W. Nebert (2009). "Human ATP-binding cassette (ABC) transporter family." Hum Genomics **3**(3): 281-290.

Vijayvargiya, P. and M. Camilleri (2018). "Update on Bile Acid Malabsorption: Finally Ready for Prime Time?" Curr Gastroenterol Rep **20**(3): 10.

Vild, C. J., Y. Li, E. Z. Guo, Y. Liu and Z. Xu (2015). "A novel mechanism of regulating the ATPase VPS4 by its cofactor LIP5 and the endosomal sorting complex required for transport (ESCRT)-III protein CHMP5." J Biol Chem **290**(11): 7291-7303.

Vitale, G., S. Gitto, R. Vukotic, F. Raimondi and P. Andreone (2019). "Familial intrahepatic cholestasis: New and wide perspectives." Dig Liver Dis **51**(7): 922-933.

von Blume, J., A. M. Alleaume, G. Cantero-Recasens, A. Curwin, A. Carreras-Sureda, T. Zimmermann, J. van Galen, Y. Wakana, M. A. Valverde and V. Malhotra (2011). "ADF/cofilin regulates secretory cargo sorting at the TGN via the Ca²⁺ ATPase SPCA1." Dev Cell **20**(5): 652-662.

von Blume, J., J. M. Duran, E. Forlanelli, A. M. Alleaume, M. Egorov, R. Polishchuk, H. Molina and V. Malhotra (2009). "Actin remodeling by ADF/cofilin is required for cargo sorting at the trans-Golgi network." J Cell Biol **187**(7): 1055-1069.

Wakabayashi, Y., P. Dutt, J. Lippincott-Schwartz and I. M. Arias (2005). "Rab11a and myosin Vb are required for bile canalicular formation in WIF-B9 cells." Proc Natl Acad Sci U S A **102**(42): 15087-15092.

Wakabayashi, Y., H. Kipp and I. M. Arias (2006). "Transporters on demand: intracellular reservoirs and cycling of bile canalicular ABC transporters." J Biol Chem **281**(38): 27669-27673.

Wakabayashi, Y., J. Lippincott-Schwartz and I. M. Arias (2004). "Intracellular trafficking of bile salt export pump (ABCB11) in polarized hepatic cells: constitutive cycling between the canalicular membrane and rab11-positive endosomes." Mol Biol Cell **15**(7): 3485-3496.





Wang, L., H. Dong, C. J. Soroka, N. Wei, J. L. Boyer and M. Hochstrasser (2008).

"Degradation of the bile salt export pump at endoplasmic reticulum in progressive familial intrahepatic cholestasis type II." Hepatology **48**(5): 1558-1569.

Wang, L., C. J. Soroka and J. L. Boyer (2002). "The role of bile salt export pump mutations in progressive familial intrahepatic cholestasis type II." J Clin Invest **110**(7): 965-972.

Wang, R., H. L. Chen, L. Liu, J. A. Sheps, M. J. Phillips and V. Ling (2009).

"Compensatory role of P-glycoproteins in knockout mice lacking the bile salt export pump." Hepatology **50**(3): 948-956.

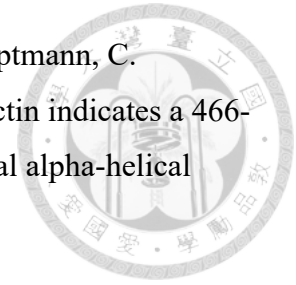
Wang, R., M. Salem, I. M. Yousef, B. Tuchweber, P. Lam, S. J. Childs, C. D. Helgason, C. Ackerley, M. J. Phillips and V. Ling (2001). "Targeted inactivation of sister of P-glycoprotein gene (spgp) in mice results in nonprogressive but persistent intrahepatic cholestasis." Proc Natl Acad Sci U S A **98**(4): 2011-2016.

Warskulat, U., R. Kubitz, M. Wettstein, B. Stieger, P. J. Meier and D. Haussinger (1999). "Regulation of bile salt export pump mRNA levels by dexamethasone and osmolarity in cultured rat hepatocytes." Biol Chem **380**(11): 1273-1279.

Watkin, L. B., B. Jessen, W. Wiszniewski, T. J. Vece, M. Jan, Y. Sha, M. Thamsen, R. L. Santos-Cortez, K. Lee, T. Gambin, L. R. Forbes, C. S. Law, A. Stray-Pedersen, M. H. Cheng, E. M. Mace, M. S. Anderson, D. Liu, L. F. Tang, S. K. Nicholas, K. Nahmod, G. Makedonas, D. L. Canter, P. Y. Kwok, J. Hicks, K. D. Jones, S. Penney, S. N. Jhangiani, M. D. Rosenblum, S. D. Dell, M. R. Waterfield, F. R. Papa, D. M. Muzny, N. Zaitlen, S. M. Leal, C. Gonzaga-Jauregui, G. Baylor-Hopkins Center for Mendelian, E. Boerwinkle, N. T. Eissa, R. A. Gibbs, J. R. Lupski, J. S. Orange and A. K. Shum (2015). "COPA mutations impair ER-Golgi transport and cause hereditary autoimmune-mediated lung disease and arthritis." Nat Genet **47**(6): 654-660.

Weisz, O. A. and E. Rodriguez-Boulan (2009). "Apical trafficking in epithelial cells: signals, clusters and motors." J Cell Sci **122**(Pt 23): 4253-4266.

Welz, T., J. Wellbourne-Wood and E. Kerkhoff (2014). "Orchestration of cell surface proteins by Rab11." Trends Cell Biol **24**(7): 407-415.



Wiche, G., B. Becker, K. Lubber, G. Weitzer, M. J. Castanon, R. Hauptmann, C. Stratowa and M. Stewart (1991). "Cloning and sequencing of rat plectin indicates a 466-kD polypeptide chain with a three-domain structure based on a central alpha-helical coiled coil." J Cell Biol **114**(1): 83-99.

Wiche, G., R. Krepler, U. Artlieb, R. Pytela and H. Denk (1983). "Occurrence and immunolocalization of plectin in tissues." J Cell Biol **97**(3): 887-901.

Wiche, G., S. Osmanagic-Myers and M. J. Castanon (2015). "Networking and anchoring through plectin: a key to IF functionality and mechanotransduction." Curr Opin Cell Biol **32**: 21-29.

Winter, L., A. V. Kuznetsov, M. Grimm, A. Zeold, I. Fischer and G. Wiche (2015). "Plectin isoform P1b and P1d deficiencies differentially affect mitochondrial morphology and function in skeletal muscle." Hum Mol Genet **24**(16): 4530-4544.

Winter, L. and G. Wiche (2013). "The many faces of plectin and plectinopathies: pathology and mechanisms." Acta Neuropathol **125**(1): 77-93.

Wolters, H., F. Kuipers, M. J. Slooff and R. J. Vonk (1992). "Adenosine triphosphate-dependent taurocholate transport in human liver plasma membranes." J Clin Invest **90**(6): 2321-2326.

Wright, M. H., I. Berlin and P. D. Nash (2011). "Regulation of endocytic sorting by ESCRT-DUB-mediated deubiquitination." Cell Biochem Biophys **60**(1-2): 39-46.

Wu, S. H., J. S. Hsu, H. L. Chen, M. M. Chien, J. F. Wu, Y. H. Ni, B. Y. Liou, M. C. Ho, Y. M. Jeng, M. H. Chang, P. L. Chen and H. L. Chen (2019). "Plectin Mutations in Progressive Familial Intrahepatic Cholestasis." Hepatology.

Xie, Y., H. Miao and J. T. Blankenship (2018). "Membrane trafficking in morphogenesis and planar polarity." Traffic.

Yi, H., H. N. Yoon, S. Kim and N. O. Ku (2018). "The role of keratins in the digestive system: lessons from transgenic mouse models." Histochem Cell Biol **150**(4): 351-359.

Zeigerer, A., J. Gilleron, R. L. Bogorad, G. Marsico, H. Nonaka, S. Seifert, H. Epstein-Barash, S. Kuchimanchi, C. G. Peng, V. M. Ruda, P. Del Conte-Zerial, J. G. Hengstler,

Y. Kalaidzidis, V. Koteliansky and M. Zerial (2012). "Rab5 is necessary for the biogenesis of the endolysosomal system in vivo." Nature **485**(7399): 465-470.

Zhou, F., Z. Wu, M. Zhao, R. Murtazina, J. Cai, A. Zhang, R. Li, D. Sun, W. Li, L. Zhao, Q. Li, J. Zhu, X. Cong, Y. Zhou, Z. Xie, V. Gyurkovska, L. Li, X. Huang, Y. Xue, L. Chen, H. Xu, H. Xu, Y. Liang and N. Segev (2019). "Rab5-dependent autophagosome closure by ESCRT." J Cell Biol **218**(6): 1908-1927.

Zhou, Y. and J. Zhang (2014). "Arthrogyryposis-renal dysfunction-cholestasis (ARC) syndrome: from molecular genetics to clinical features." Ital J Pediatr **40**: 77.

Tables

Table 1 Progressive familial intrahepatic cholestasis (PFIC)*

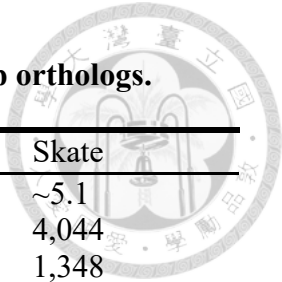
| | PFIC1 | PFIC2 | PFIC3 | PFIC4 | PFIC5 | PFIC |
|--------------|---|--|--|---|---|---|
| Gene (locus) | <i>ATP11</i> (18q21-22) | <i>ABCB11</i> (2q24) | <i>ABCB4</i> (7q21) | <i>TJP2</i> (9q21.11) | <i>NR1H4</i> (12q23.1) | <i>MyosinVB</i> (18q21.1) |
| Protein | FIC1 | BSEP | MDR3 | ZO-2 | FXR | MYO5B |
| Function | flippase | Bile salt transport | floppase | adhesion | Nuclear receptor | Motor protein |
| Laboratory | | | | | | |
| BA | High | Very high | High | High | High | High |
| GGT | Low or normal | Low or normal | High | Normal or mild elevation | Normal | Normal |
| AST/ALT | Mild elevation | Moderate elevation | Mild elevation | Elevation | Moderate elevation | Mild or moderate elevation |
| AFP | Normal | High | Normal | High | High | Normal |
| Histology | Mild cholestasis, mild lobular fibrosis and inflammation with giant cells | Canalicular cholestasis, lobular/portal fibrosis and inflammation with giant cells | Loss of MDR3 expression, portal inflammation, portal fibrosis, cholestasis, ductular proliferation | Centrolobular cholestasis; mislocalization of claudin | Cholestasis, loss of BSEP expression | Cholestasis, Inflammation with giant cells, BSEP and MDR3 tissue expression, MYO5B and RAB11 A canalicular staining |
| Clinics | Early onset; severe jaundice/itching; growth retardation; | Early onset, severe jaundice/itching; leads to LT; | Childhood/young adulthood onset; can be drug-triggered; hepatomegaly, | Early severe cholestasis onset; Progression to liver failure in childhood; No | Neonatal onset, rapid progression to ESLD, vitK-independent; coagulopathy | Onset < 2 years: ± MVID, jaundice/itching; hepatomegaly |

| PFIC1 | PFIC2 | PFIC3 | PFIC4 | PFIC5 | PFIC6 |
|---|------------------------------|---|------------------------------|-------|-------|
| diarrhea, pancreatitis, deafness; leads to LT | potential post-LT recurrence | growth retardation, HCC risk; leads to LT | post-LT recurrence; HCC risk | | |
| Gene-associated non-PFIC | | | | | |
| BRIC, ICP | BRIC, ICP, DIC | ICP, DIC, LPAC | ICP | ICP | BRIC |

Abbreviations: PFIC, progressive familial intrahepatic cholestasis; BRIC, benign recurrent intrahepatic cholestasis; ICP, intrahepatic cholestasis of pregnancy; DILI: drug induced cholestasis; LPAC: low-phospholipid-associated cholelithiasis; BSEP: biliary salt export pump; MDR-3, class III multidrug resistance P-glycoprotein; TJP-2, tight junctions protein-2; zo-2: zona occludens-2; FXR: farnesoid X receptor; MVID, microvillous Inclusion Disease; MYO5B: myosin VB protein; RAB11A: RAS-related protein RAB11 A; LT: liver transplantation; ESLD, end-stage liver disease; vit. K, vitamin K; AST, aspartate aminotransferase; ALT, alanine aminotransferase; GGT, gamma-glutamyl transferase; AFP, alpha-1-fetoprotein; BA, bile acids.

This table is adapted from (Vitale, Gitto et al. 2019).

Table 2 A comparison of human, rat, mouse and skate BSEP/Bsep orthologs.



| | Human | Rat | Mouse | Skate |
|-------------------------------------|---|---|--|-------------------------|
| cDNA (kb) | ~5.3 | ~5.0 | ~4.8 | ~5.1 |
| ORF (b.p.) | 3,963 | 3,963 | 3,963 | 4,044 |
| Protein (a.a.) | 1,321 | 1,321 | 1,321 | 1,348 |
| <i>N</i> -glycosylation site (a.a.) | 109, 116, 122, and 125 | 109, 116, 122, and 125 | 109, 116, 122, and 125 | 126, 133, and 142 |
| Reference | (Strautnieks, Bull et al. 1998, Byrne, Strautnieks et al. 2002, Noe, Stieger et al. 2002) | (Childs, Yeh et al. 1998, Gerloff, Stieger et al. 1998) | (Green, Hoda et al. 2000, Lecureur, Sun et al. 2000, Noe, Hagenbuch et al. 2001) | (Cai, Wang et al. 2001) |

Abbreviations: a.a., amino acid; b.p., base pair; kb, kilobase pair; ORF, open reading frame.

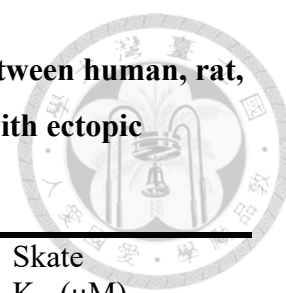


Table 3 Comparison of Km/*Ki values and bile salt transport between human, rat, mouse and skate membrane vesicles from the liver and the cell with ectopic BSEP/Bsep expression.

| | Human | | Rat | | Mouse | | Skate | |
|------|--------------------------------------|--|---|---|---------------------|--------------------------------------|---------------------|------------------|
| | K _m /*K _i (μM) | | K _m (μM) | | K _m (μM) | | K _m (μM) | |
| | cLPM | BSEP | cLPM | Bsep | cLPM | Bsep | cLPM | Bsep |
| TC | 4.2 ^e | 4.25 ^j 7.9 ^k 6.2 ^o | 47 ^a 5.7 ^b 26 ^c 2.1 ^{d, h} | 5.3 ^{f, h} 9.7 ^o | - | 11 ^g 30.3 ⁱ | 40 ^l | 15 ^m |
| TCDC | - | 28 ^{i*} 4.8 ^k 6.6 ^o | 3.6 ^h | 2.2 ^h 10.2 ^o | - | 5.7 ⁱ | - | - |
| TUDC | - | 11.9 ^k | 6.2 ^h | 4.1 ^h | - | - | - | - |
| GC | - | 11 ^{j*} 11.1 ^k 21.7 ^o | 3.8 ^h | 25.7 ^o | - | 19.5 ⁱ | - | - |
| GCDC | - | 7 ^{j*} 7.5 ^o | - | 5.6 ^o | - | - | - | - |
| ScyS | - | - | - | - | - | - | 23 ^l | 14 ^{m*} |

Abbreviations: cLPM, canalicular liver plasma membrane; N.D., not detectable; ScyS, scymnol sulfate; TC, taurocholate; TCDC, taurochenodeoxycholate; TUDC, tauroursodeoxycholate; GC, glycocholate; GCDC, glycochenodeoxycholate.

^a(Adachi, Kobayashi et al. 1991); ^b(Muller, Ishikawa et al. 1991); ^c(Nishida, Gatmaitan et al. 1991); ^d(Stieger, O'Neill et al. 1992); ^e(Wolters, Kuipers et al. 1992); ^f(Gerloff, Stieger et al. 1998); ^g(Green, Hoda et al. 2000); ^h(Stieger, Fattinger et al. 2000); ⁱ(Noe, Hagenbuch et al. 2001); ^j(Byrne, Strautnieks et al. 2002); ^k(Noe, Stieger et al. 2002); ^l(Ballatori, Rebbeor et al. 2000); ^m(Cai, Wang et al. 2001); ^o(Hayashi, Takada et al. 2005)

Table 4 The rank order of different bile salts transported by the Bsep ortholog of human, rat, mouse, and skate.

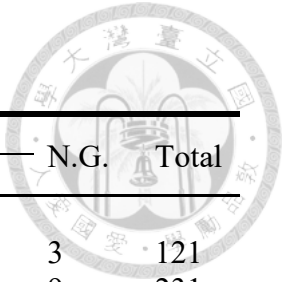
| Bsep ortholog | Rank | Reference |
|---------------|--|--|
| Human | TC > GCDC > GC > TCDC | #1(Byrne, Strautnieks et al. 2002)(Byrne, Strautnieks et al. 2002) |
| | TCDC > TC ≡ GC ≡ TUDC *CA was not transported. | #2 |
| | TCDC > GCDC > TDC ≡ TUDC > TC > GUDC > TLC- S > GC > CA | #3 |
| Rat | TCDC > TC ≡ TUDC | #4 |
| | *GC and CA were not detectable in uptake assays. | |
| | TCDC > GCDC > TC > TDC ≡ TUDC > GC | #5 |
| | *TLSC was not transported | |
| | TCDC > ScyS ≥ TC ≥ TDC > CA > TLC ≡ GLC > GC ≡ UDC > LC ≡ TUDC | #6 |
| | TCDC > GCDC ≡ TC ≡ TDC ≡ TUDC > GUDC > GC > CA ≡ TLC-S | #3 |
| Mouse | TDC > CDC > TCDC > CA ≡ UDC | #7 |
| | TCDC > GC > TC | #8 |
| Skate | ScyS ≥ TDC ≥ TCDC > TC > CA > GC ≡ TLC ≡ TUDC ≡ UDC > GLC ≫ LC | #6 |

Abbreviations: CA, cholic acid; CDC, chenodeoxycholate; GC, glycocholate; GCDC, glycochenodeoxycholate acid; GUDC, glyoursodeoxycholate; GLC, glycolithocholate; LC, lithocholate; ScyS, scymnol sulfate; TC, taurocholate; TCDC, taurochenodeoxycholate; TDC, taurodeoxycholate; TLC- S, tauroolithocholate 3-sulfate; TLSC, tauroolithosulfocholate; TLC, tauroolithocholate; TUDC, taurooursodeoxycholate; UDC, ursodeoxycholate.

#1 (Byrne, Strautnieks et al. 2002); #2 (Noe, Stieger et al. 2002); #3 (Hayashi, Takada et al. 2005); #4 (Gerloff, Stieger et al. 1998); #5 (Stieger, Fattinger et al. 2000); #6 (Cai, Wang et al. 2001); #7 (Green, Hoda et al. 2000); and #8(Noe, Hagenbuch et al. 2001).

Table 5 A comparision of *Abcb11/abcb11b* knockout (KO) animal models

| | <i>Abcb11</i> KO mice | <i>Abcb11</i> KO rat | <i>abcb11b</i> KO zebrafish |
|-----------|--|---|---|
| Approach | Homologous recombination with targeting vectors to delete a 1.4-kb fragment containing the coding region of a.a. 454-478 of mBsep | Zinc finger nuclease technology to specifically Delete 8 base-pair nuclear acids from rat <i>Bsep</i> mRNA to introduce a premature stop codon in exon 5 | CRISPR/Cas9-based genome editing on the <i>abcb11b</i> gene of zebrafish |
| Phenotype | Viable, fertile, but growth retardation Enlarged livers Impaired excretion of conjugated bile salts Mild and nonprogressive cholestasis Increase in the excretion of cholesterol and phospholipids | Low expression of rBsep proteins (15% of that in wild type), which may come from an identified rBsep variant. Nearly normal A decrease in the liver efflux of taurocholate Some transporters may upregulate at RNA levels. | Premature death Enlarged livers Increase in liver injuries and hepatocyte death PFIC2-like phenotypes Impaired bile flow and cytoplasmic aggregation of Mdr1 in hepatocytes, which could be restored by rapamycin administration. |
| Reference | (Wang, Salem et al. 2001, Lam, Wang et al. 2005, Wang, Chen et al. 2009) | (Cheng, Freeden et al. 2016, Cheng, Chen et al. 2017, Patel, Johnson et al. 2018) | (Ellis, Bove et al. 2018) |

Table 6 Statistics and classification of β -galactosidase assays

| Yeast colonies | Levels of β -galactosidase activity | | | | | | N.S. | N.G. | Total |
|----------------|---|-----|-----|------|------|------|------|------|-------|
| | 1 | 2 | 3 | 4 | 5 | 6 | | | |
| Growth on | | | | | | | | | |
| Day 3 | 2 | 3 | 3 | 9 | 36 | 14 | 51 | 3 | 121 |
| Day 4 | 4 | 7 | 24 | 25 | 38 | 36 | 88 | 9 | 231 |
| Day 5 | 1 | 5 | 23 | 18 | 19 | 55 | 68 | 3 | 192 |
| Day 6 | 0 | 7 | 6 | 24 | 5 | 27 | 40 | 9 | 118 |
| Day 7 | 0 | 6 | 12 | 10 | 3 | 11 | 39 | 14 | 95 |
| Total | 7 | 28 | 68 | 86 | 101 | 143 | 286 | 38 | 757 |
| Ratio (%) | 1.0 | 3.9 | 9.5 | 12.0 | 14.0 | 19.9 | 39.8 | | |

The levels 1 to 6 represent the permeabilized yeasts with blue appearance in 0.5, 1, 2, 4, 5 hours, or overnight, respectively, after X-gal incubation. The level N.S. is the yeast colony which did not turn blue after overnight X-gal incubation. Abbreviation: N.G., no growth of yeast colonies when these yeast cells were re-seeded on selection plate for β -galactosidase assays from the master plate. N.S., colonies did not turn blue. The ratio is calculated from the yeast colony number of each level of β -galactosidase activity divided by the total number of growth yeast colonies.

Table 7 Classification of the cDNA inserts identified from the yeast two-hybrid screen for BSEP-interacting proteins.

| Functions | cDNA identity | Levels* of β -gal |
|--|---|----------------------------|
| Protease inhibition | Serpin peptidase inhibitor clade A member 1 (SERPINA1, anti-trypsin) | 2, 3 |
| | Serpin peptidase inhibitor clade A member 3 (SERPINA3, anti-chymotrypsin) | 3 |
| | Alpha-1-microglobulin/bikunin precursor (AMBP) | 3 |
| Protein sorting | Charged multivesicular body protein 5 (CHMP5) | 2 |
| | Coatomer protein complex, subunit alpha (COPA) | 3 |
| Glycosylation | Hexokinase domain containing 1 (HKDC1), mRNA | 2, 3 |
| | Proteoglycan 4 (PRG4) | 3 |
| Cytoskeleton remodeling | Cofilin 1 (non-muscle) (CFL1), mRNA | 3 |
| Protein folding and degradation | DnaJ (Hsp40) homolog, subfamily C, member 9 | 3 |
| | DDB1 and CUL4 associated factor 11 (DCAF11), transcript variant 5, non-coding RNA | 2 |
| | Proteasome subunit beta type 6 (PSMB6), mRNA | 3 |
| | Proteasome subunit beta type, 10 (PSMB10) | 2 |
| | Amyloid beta (A4) precursor-like protein 2 (APLP2) | 2 |
| Metabolism | Farnesyl-diphosphate farnesyltransferase 1 (FDFT1), mRNA | 3 |
| | Inter-alpha-trypsin inhibitor heavy chain 2 (ITI2) | 2 |
| Physical homeostasis | Albumin (ALB) | 2, 3 |
| | Hemoglobin, alpha 1 (HBA1) | 2, 3 |
| | Hemoglobin, gamma A (HBG1), mRNA | 2 |
| Chromatin modification | Centromere protein A (CENPA) | 1 |
| | H2A histone family, member J (H2AFJ) | 2, 3 |
| | H3 histone, family 3A, pseudogene 4 (H3F3AP4) | 2, 3 |
| | H3 histone, family 3B (H3F3B) | 2, 3 |
| | HIST1H2AC histone cluster 1 (H2ac) | 2, 3 |
| | HIST1H2BG histone cluster 1, (H2bg) | 2, 3 |
| | HIST1H2BK histone cluster 1, (H2bk) | 2, 3 |
| | HIST1H2BD transcript variant 1, mRNA | 2, 3 |
| | HIST1H2BG, mRNA | 2, 3 |
| | HIST2H2BE, mRNA | 2, 3 |
| | HIRA interacting protein 3 (HIRIP3), | 2, 3 |
| | SET domain containing 1A (SETD1A) | 2, 3 |
| | Homologous Alu RNA binding protein (SRP14) | 2, 3 |
| | X-ray repair complementing defective repair in Chinese hamster cells 6 (XRCC6) | 2, 3 |
| | Zinc finger and BTB domain containing 16 (ZBTB16) | 2, 3 |
| Transcription, translation, or mRNA processing | MT-RNR2-like 8 (MTRNR2L8) | 2 |
| | POLM polymerase (DNA directed), mu | 3 |
| | Serine/arginine-rich splicing factor 4 (SRSF4), mRNA | 2 |
| Others | Mitochondrion, complete genome | 2 |

The levels 1, 2, and 3 of β -gal represent the permeabilized yeasts with blue appearance in 0.5, 1, and 2 hours, respectively, after X-gal incubation.



Table 8 Classification of the cDNA inserts identified from the yeast two-hybrid screen for BSEP-interacting proteins.

| Name | Aliases | Functions |
|----------------------------|--|--|
| CHMP5 (NP_057494) | Vps60; CGI-34; PNAS-2; C9orf83; HSPC177; SNF7DC2 | Components of ESCRT-III (endosomal sorting complex required for transport III) involved in degradation of surface receptor proteins and formation of endocytic multivesicular bodies (MVBs) |
| COPA (NP_001091868) | HEP-COP; a-COPA | Vesicle transportation |
| SERPINA1 (NP_001121179) | PI; A1A; AAT; PI1; A1AT; PRO2275; alpha1AT | Protease inhibitors |
| SERPINA3 (NP_001076) | ACT; AACT; GIG24; GIG25 | Protease inhibitors |
| Cofilin 1 (NP_005498) | | Actin polymerization |



Table 9 Clinical characteristics with serial laboratory data

| | Patient 1 | | Patient 2 | | |
|----------------------|--|----------|--|----------|----------|
| Sex | Female | | Male | | |
| Age | 2 years | 15 years | 15 days | 5 months | 11 years |
| Serum tests | | | | | |
| T-Bil (mg/dL) | 30.10 | 0.78 | 21.69 | 0.83 | 3.25 |
| D-Bil (mg/dL) | 19.81 | 0.26 | 15.87 | 0.56 | 1.92 |
| GGT (U/L) | 15 | 41 | 68 | 548 | 585 |
| ALP (U/L) | 840 | 133 | 500 | 950 | 713 |
| AST (U/L) | 207 | 41 | 584 | 130 | 213 |
| ALT (U/L) | 105 | 28 | 400 | 225 | 242 |
| PT/INR | 1.45 | ND | 1.07 | ND | 0.99 |
| BA _s (μM) | 196.80 | 40.81 | 96.71 | ND | 131.94 |
| Liver histology | End-stage biliary cirrhosis with micronodules, cholestasis, feathery degeneration and necrosis, and ductular reaction. | | Neonatal hepatitis with marked hepatocyte ballooning and multinucleated giant cells. | | |

Abbreviations (and reference ranges): ALP, alkaline phosphatase (34-104 U/L); ALT, alanine aminotransferase (0-41 U/L); AST, aspartate aminotransferase (8-31 U/L); BA_s, bile acids (<30 μM); D-Bil, direct bilirubin (0.03-0.18 mg/dl); GGT, γ-glutamyl transpeptidase (9-64 U/L); ND, no data available; PT/INR, prothrombin time/international normalized ratio (0.92-1.09); T-Bil, total bilirubin (0.30-0.10 mg/dL).

This table is adapted from (Wu, Hsu et al. 2019).

Table 10 Jaundice-associated gene panel for target-gene enriched next-generation sequencing

| Diseases | Gene (alias) |
|---|--|
| PFIC (5 genes) | ATP8B1 (FIC1), ABCB11 (BSEP), ABCB4 (MDR3), TJP2 (ZO2), NR1H4 (FXR)* |
| Syndromic cholestasis (3 genes) | JAG1, NOTCH2, VPS33B |
| Metabolic liver disease (4 genes) | SERPINA1, CFTR, SLC25A13 (CITRIN), ATP7B |
| Bile acid metabolic defects (8 genes) | CYP27A1, HSD3B7, AKR1D1, CYP7B1, BAAT, EPHX1, CYP7A1, AMACR |
| Mitochondrial disorder (8 genes) | TWNK (C10orf2), DGUOK, MPV17, POLG, BCS1L, RRM2B, SCO1, SUCLG1 |
| Neonatal sclerosing cholangitis (1 gene) | CLDN1 |
| Polycystic diseases (5 genes) | PKD1, PKD2, PRKCSH, SEC63, PKHD1 |
| Bilirubin metabolism (8 genes) | ABCC2 (MRP2), G6PD, UGT1A1, SLCO1B1 (OATP1B1), SLCO1B3 (OATP1B3), HBA1, HBA2, HBB |
| Bile metabolism related genes not reported to cause human disease before (10 genes) | ABCB1 (MDR1), ABCC3 (MRP3), ABCC4 (MRP4), FGF19, NR1H4 (FXR)*, SLC10A1 (NTCP), SLC51A (OSTalpha, OSTA), SLC51B (OSTbeta, OSTB), SLCO1A2 (OATP1A2), SLCO2B1 (OATP2B1) |

*This gene is associated with two categories. This table is adapted from (Chen, Li et al.

2019).

Table 11 The Variants of the Five Genes Identified Using the Whole-Exome Sequencing from the Family Suspected of PFIC

| Gene (Accession No.) | Inherited from | Variants | Mutation type | Functional prediction SIFT | PolyPhen |
|-------------------------|------------------|--|------------------|----------------------------------|--------------------|
| CUBN (NM_001081) | Father (predict) | c.2932C>A (p.H978N); No available | Missense | tolerated | benign |
| | Mother | c.2745T>C (p.S915S); 0.03% | Synonymous | potential alteration of splicing | |
| MUC19 (NM_173600) | Father (predict) | c.C17912ins+A (p.T5971ins?) | | Unknown | |
| | Mother | c.19632G>C (p.A6382A); c.19636G>A (p.G6383R); c.9639T>A (p.S6384T); c.20184C>T (p.N6566N); c.20185A>G (p.N6566D); c.20318C>T (p.A6611V); c.20324G>C (p.G6613A); c.20325C>T (p.G6613G); c.20337C>T (p.A6617A); c.20395A>G (p.I6636V); c.20393A>G (p.N6636S); c.20394C>T (p.N6636N) | | Unknown | |
| OTOG (NM_001292063) | Mother | c.916G>A (p.A306T); 0.06% | Missense | tolerated | benign |
| | Father (predict) | c.3178C>T (p.H1060Y); 0.43% | Missense | tolerated | benign |
| PLEC (NM_000445) | father | c.6179C>T (p.A2060V); No available | Missense | tolerated | benign |
| | Mother | c.2558A>G (p.D853G); 0.27% | Missense | deleterious | possible damage |
| PSKH1 (NM_006742) | Father (predict) | c.273C>A (p.D91E); No available | Missense | tolerated | benign |
| | Mother | c.957+1G>A; No available | Splicing | most probably affecting splicing | |

Abbreviation: SIFT, Sorting Intolerant From Tolerant (<https://sift.bii.a-star.edu.sg>); PolyPhen, Polymorphism Phenotyping v2 (<http://genetics.bwh.harvard.edu/pph2/index.shtml>)

Table 12 The Protein Encoded, Functions, Tissue Expression and Disease Association of the Gene Variants Identified in The Family of Progressive Familial Intrahepatic Cholestasis.



| Gene/Protein | Cellular functions | Disease association | Expression |
|---|---|---|---|
| <i>CUBN</i> /Cubilin | A receptor for intrinsic factor-vitamin B12 complexes | Imerslund-Gräsbeck syndrome Megaloblastic anemia | Only in the kidney and the small intestine |
| <i>MUC19</i> /Mucin 19, oligomeric <i>OTOG</i> /Otogelin | | Sjogren syndrome Deafness | Unknown Only in testis |
| <i>PLEC</i> /Plectin | Linker between desmosomes and intermediate filament | Epidermolysis bullosa (with pyloric atresia) congenital myasthenic syndrome; HCC | Universally, medium in liver |
| <i>PSKH1</i> /Protein Ser Kinase H1 | Interaction with CDC6, a protein initiating DNA replication | Maintenance of the Golgi apparatus splice factor compartment | Universally, medium in livers and the gallbladder |



Figures

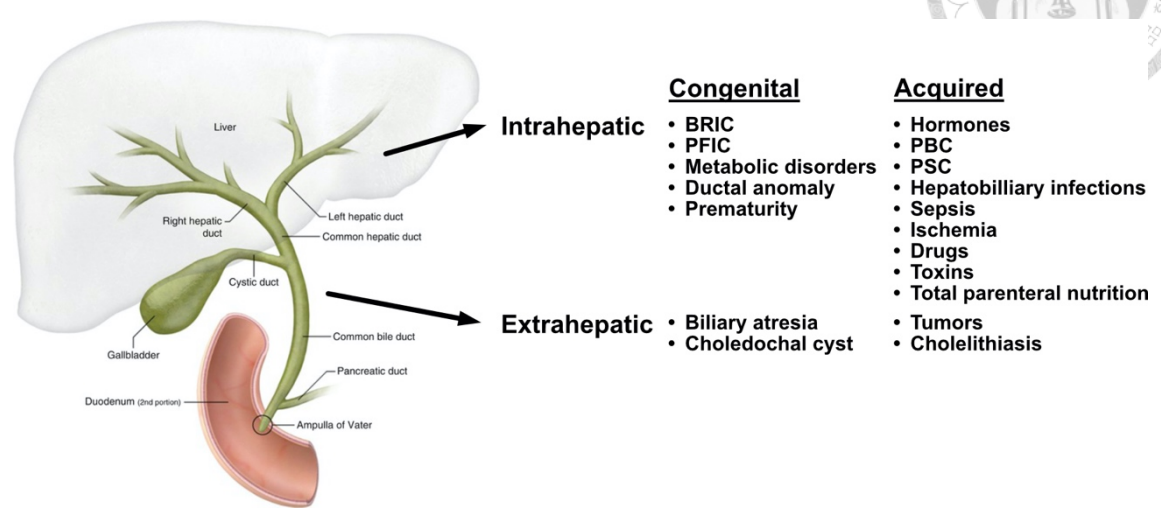


Figure 1 Etiologies of intrahepatic and extrahepatic cholestasis of congenital or acquired causes.

Cholestasis is a disease caused by disturbance in bile flow. Cholestasis is anatomically divided into intrahepatic and extrahepatic cholestasis. Intrahepatic cholestasis arises from genetic mutations or acquired inhibition of biliary epithelial transporters or metabolic enzymes, developmental anomaly, and destruction of small bile ducts. Extrahepatic cholestasis results from extrahepatic bile ducts that are developmentally aberrant or obstructed by tumors or stones. Abbreviations: BRIC, benign recurrent intrahepatic cholestasis; PBC, primary biliary cholangitis or primary biliary cirrhosis; PFIC, progressive familial intrahepatic cholestasis; and PSC, primary sclerosing cholangitis. The figure is modified from (Chen, Wu et al. 2018), and the image of the biliary system is adapted from <https://radiologykey.com/the-biliary-tree/>.

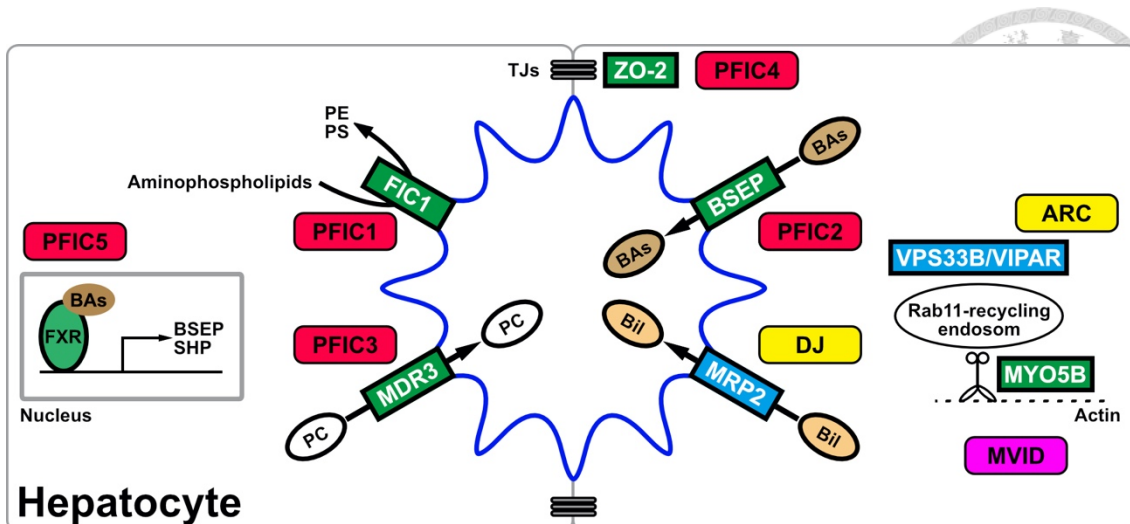


Figure 2 Functions of PFIC- and other cholestasis-associated proteins.

Hepatocytes are polarized epithelial cells. The adhesion molecule tight junction complex (TJs) defines the apical/canalicular domain (the line in blue) and the basolateral/sinusoidal domain of the plasma membrane of hepatocytes. Bile canaliculi is the space surrounded by the canalicular membrane of hepatocytes. Bile is an amalgam of water, bile acids (BAs), ions, phospholipids (phosphatidylcholine [PC]), cholesterol, bilirubin (Bil), proteins, and xenobiotics. Among these ingredients, BAs, PC, cholesterol, and Bil are transported by bile salt export pump (BSEP), multidrug resistance P-glycoprotein 3 (MDR3), ABCG5/G8, and multidrug resistance-associated protein 2 (MRP2), respectively. Extraction of PC by BAs is accompanied with the flop of phosphatidylserine (PS), which causes injuries of the canalicular membrane. The flippase FIC1 flips PS back to stabilize the canalicular membrane. Expression of these transporters is regulated by the nuclear receptor farnesoid X receptor (FXR). The apical targeting of some canalicular transporters, such as BSEP, requires the coordination of the Rab11-positive endosome and the actin-based motor protein myosin 5B (MYO5B). Mutations in these transporters, regulatory proteins and TJ proteins (i.e. zonula occludens protein 2 [ZO-2]) are associated with several cholestatic diseases, including progressive familial intrahepatic cholestasis (PFIC), Dubin-Johnson syndrome (DJ), arthrogyrosis-renal dysfunction-cholestasis (ARC) syndrome, and microvillus inclusion disease (MVID). MVID has been referred to PFIC6. This figure is modified from (Chen, Wu et al. 2018).

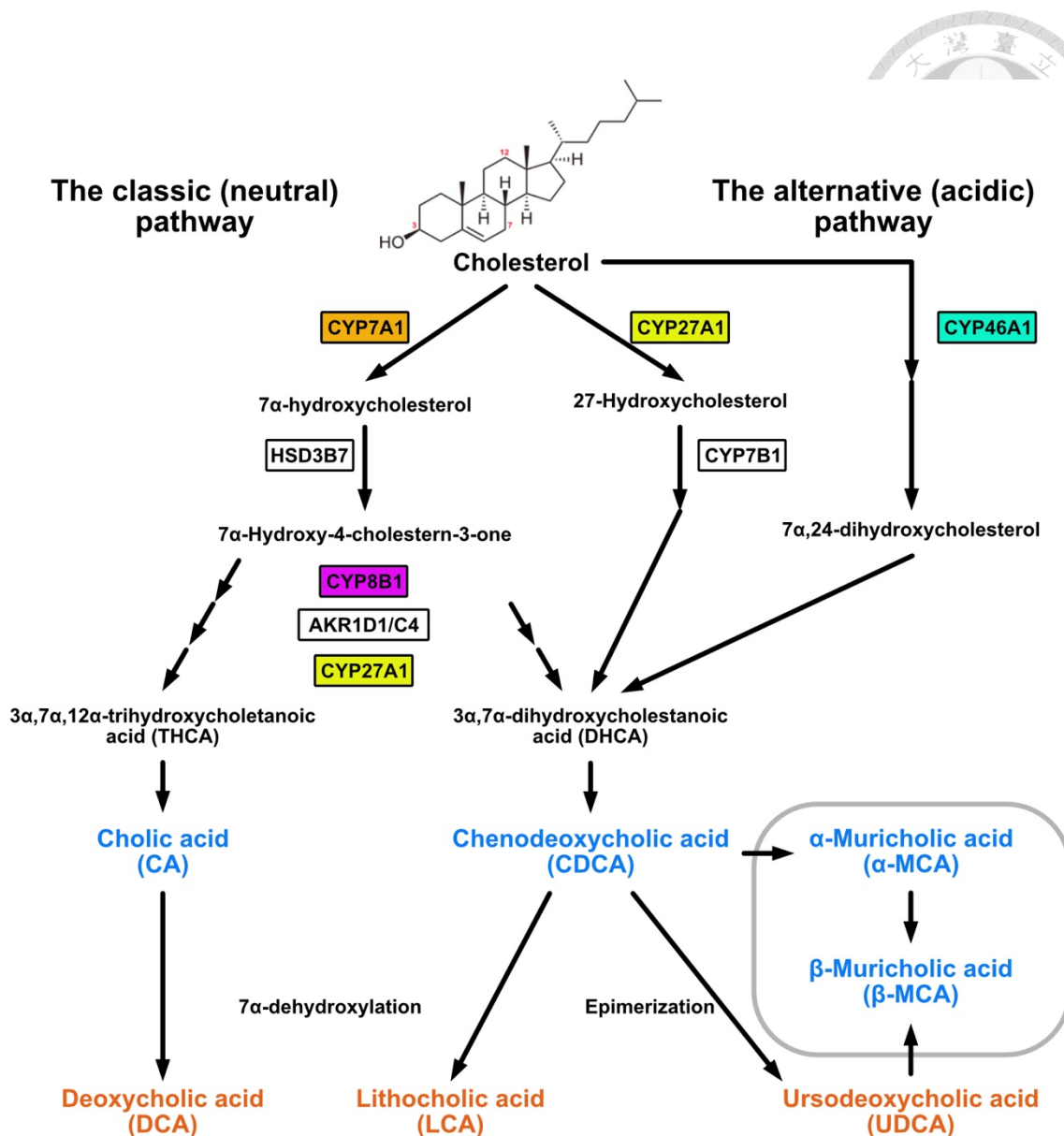


Figure 3 The synthesis pathways of bile acids.

Cholesterol is converted to bile acids through two pathways: the classic (neutral) pathway and the alternative (acidic) pathway. The classic pathway is initiated by CYP7A1 in the liver, and followed by HSD3B7 to generate 7α-hydroxy-4-cholestern-3-one. CYP8B1 determines that 7α-hydroxy-4-cholestern-3-one is converted into either cholic acid (CA) or chenodeoxycholic acid (CDCA). The alternative pathway is initiated by CYP27A1 in the liver, macrophages, and adrenal glands, and by CYP46A1 in the brain. Through alternative pathway, cholesterol is finally converted to CDCA in the hepatocytes. CA and CDCA are the primary bile acids (words in blue) in humans. Mice contain two additional primary bile acids, α-muricholic acid (α-MCA) and β-muricholic acid (β-MCA), which are resulted from CDCA converted by rodent-specific enzymes. The primary bile acids are conjugated with either taurine or glycine, and then secreted in bile. Conjugated primary bile acids are deconjugated, dehydroxylated, and epimerized by intestinal bacteria to generate the secondary bile acids (words in orange). The figure is modified from (Chiang and Ferrell 2019).

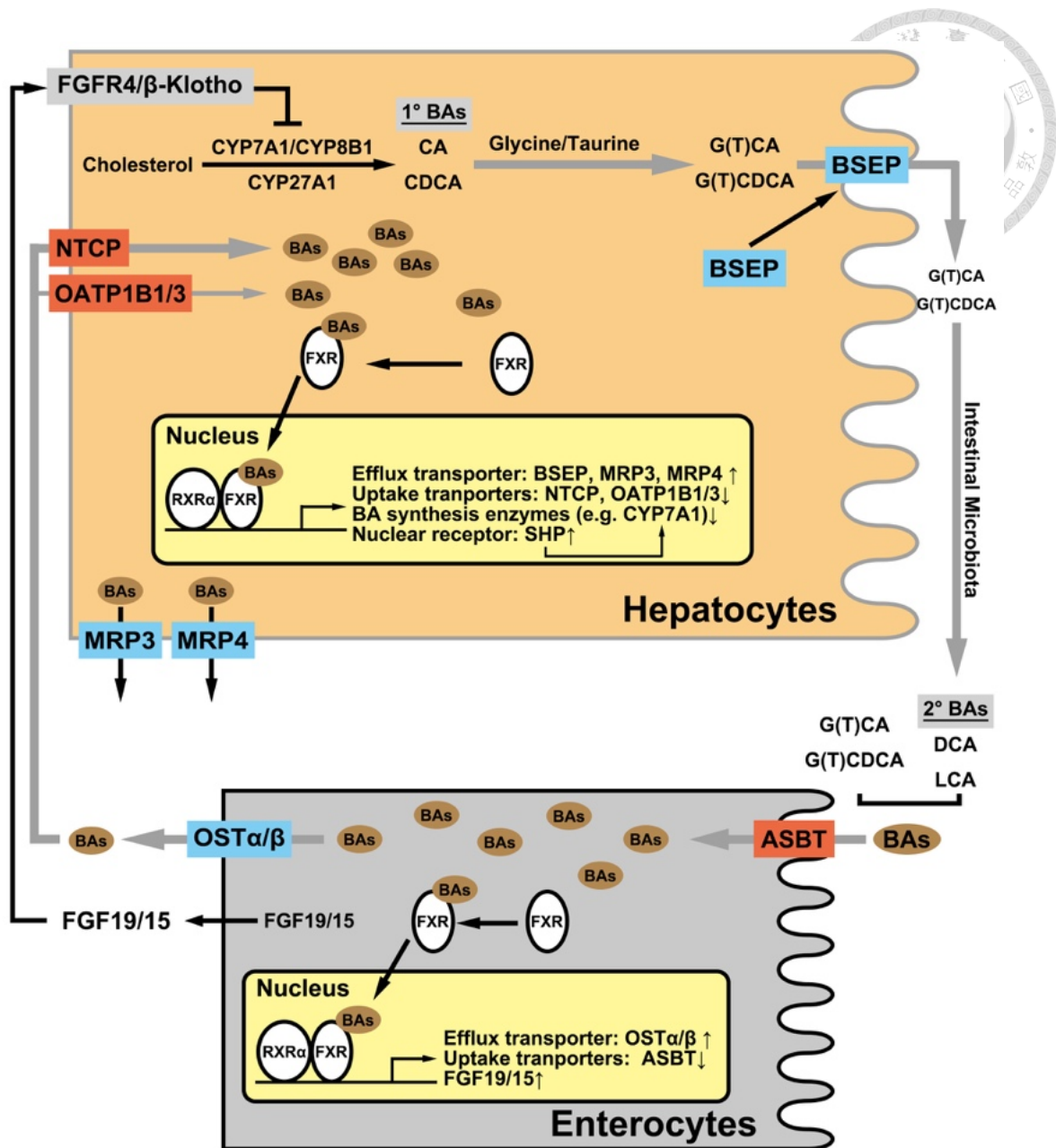
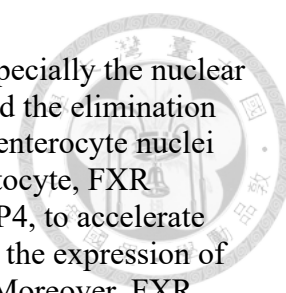


Figure 4 The enterohepatic circulation and homeostasis of bile acids.

Bile acids (BAs) are synthesized from cholesterol in hepatocytes through CYP7A1/CYP8B1 and CYP27A1 to generate the primary BAs CA and CDCA, respectively, which are further conjugated with glycine (G) or taurine (T). The conjugated primary BAs, G(T)CA and G(T)CDCA, are excreted by BSEP into bile canaliculi. After drained into intestines, intestinal microbiota processes series chemical reactions to convert G(T)CA and G(T)CDCA into the secondary BAs DCA and LCA, respectively. Most of these BAs enter enterocytes through the BA uptake transporter ASBT at the apical membrane and then delivered into the circulation system via BA efflux transporter OSTα/β in the basolateral membrane. BAs are absorbed from the circulation system into hepatocytes via BA influx transporters NTCP, majorly, and OATP1B1/3. Hepatocytes secrete these BAs and *de novo* synthesized BAs, which enter the next cycle. This process is called the enterohepatic circulation of bile acids.



The bile acid pool is maintained by a group of bile acid receptors, especially the nuclear receptor FXR. FXR regulates the BA homeostasis at the synthesis and the elimination levels. After binding with BAs, FXR translocates into hepatocyte or enterocyte nuclei and heterodimerizes with another nuclear receptor RXR α . In the hepatocyte, FXR upregulates bile efflux transporters, including BSEP, MRP3 and MRP4, to accelerate the clearance of intracellular BAs. On the other hand, FXR represses the expression of uptake transporters (NTCP and OATP1B1/3) to reduce BA loading. Moreover, FXR downregulates BA synthesis pathways, especially the rate-limiting enzyme CYP7A1. FXR activates another nuclear receptor SHP, which also represses the BA synthesis system. In enterocytes, FXR upregulates enteral BA efflux via the transporter OST α/β and downregulates BA uptake via ASBT. FXR activates the hormone FGF19/15 expression. FGF19/15 is the ligand of the hepatic receptor FGFR4/ β -Klotho at the basolateral domain of hepatocytes. After binding with FGF19/15, downstream signaling of FGFR4/ β -Klotho represses CYP7A1 to attenuate BA synthesis machinery.

Abbreviations: 1 $^{\circ}$ BAs, primary bile acids; 2 $^{\circ}$ BAs, secondary bile acids; ASBT, apical sodium dependent bile acid transporter; BAs, bile acids; BSEP, bile salt export pump; CA, cholic acid; CDCD, chenodeoxycholic acid; DCA, deoxycholic acid; FGFR4, fibroblast growth factor receptor 4; FXR, farnesoid X receptor; G(T)CA, glyco- or tauro-cholic acid; G(T)CDCA, glyco- or tauro-chenodeoxycholic acid; LCA, lithocholic acid; MRP3, multidrug resistance-associated protein 3; MRP4, multidrug resistance-associated protein 4; NTCP, sodium/taurocholate co-transporting polypeptide; OATP1B1/3, organic-anion-transporting polypeptide 1B1 and 1B3; OST α/β , organic solute transporter- α/β ; RXR α , retinoid X receptor α ; SHP, small heterodimer partner; UDCA, ursodeoxycholic acid. This figure is modified from (Chen, Wu et al. 2018).

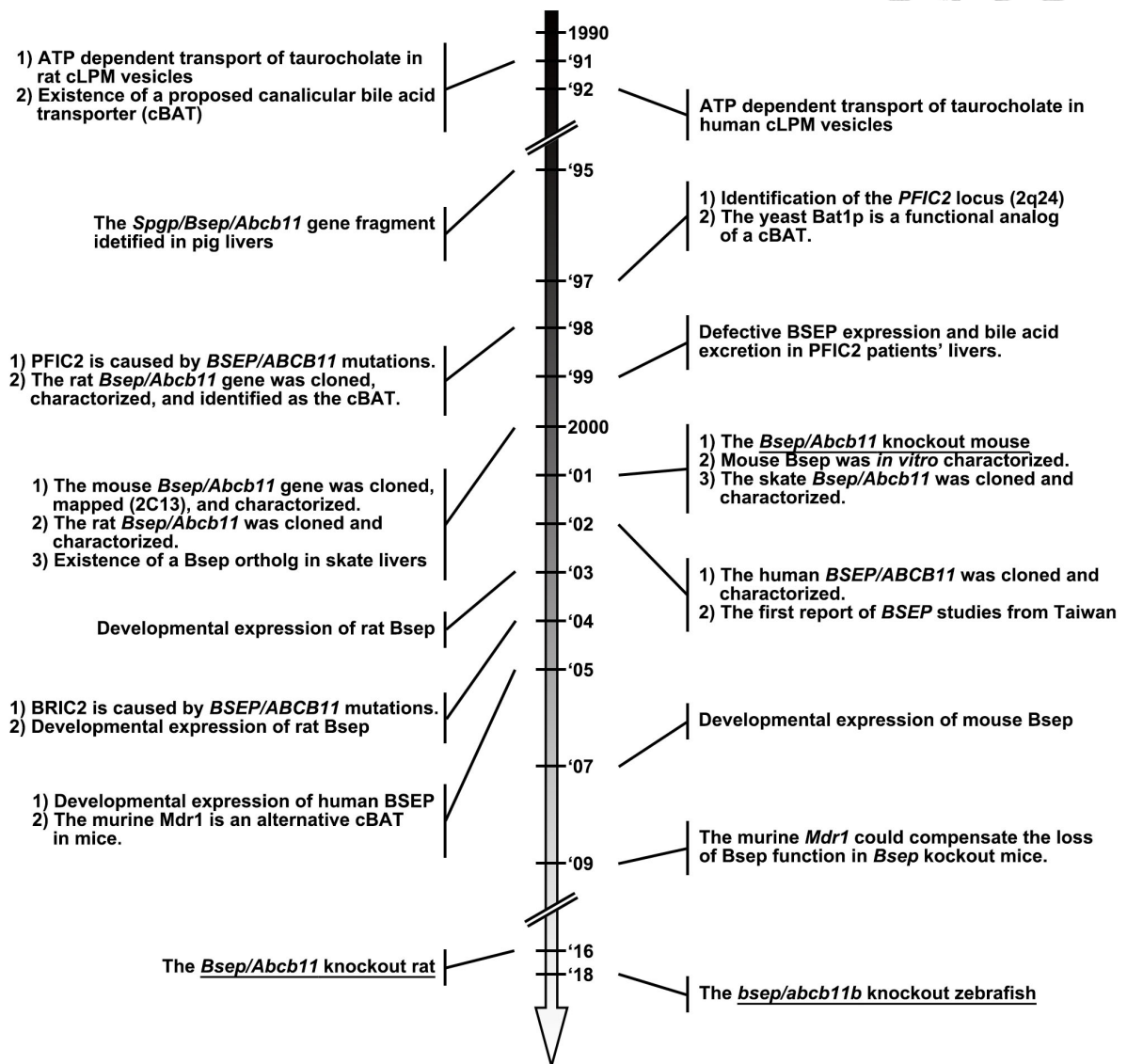


Figure 5 Milestones of BSEP/Bsep being characterized as the canalicular bile acid transporter (cBAT).

In early 1990s, the canalicular transport of bile salts requiring ATP consumption was evidenced by uptake of radio-active taurocholate in rat and human liver canalicular membrane (cLPM) vesicles, and suggested the existence of a putative canalicular bile acid transporter (cBAT) (Adachi, Kobayashi et al. 1991, Muller, Ishikawa et al. 1991, Nishida, Gatmaitan et al. 1991, Stieger, O'Neill et al. 1992, Wolters, Kuipers et al. 1992, Bossard, Stieger et al. 1993, Moseley, Wang et al. 1996). The *Sister gene of P-glycoprotein (Spgp)*, which was latter denominated as *Bsep/Abcb11*, was first isolated in pig livers, mapped to human chromosome 2q31, exclusively expressed in rat and human livers, and finally recognized as the cBAT in the year 1998 (Childs, Yeh et al. 1995, Childs, Yeh et al. 1998, Gerloff, Stieger et al. 1998). In the same and the next years, the *PFIC2* (2q24)-linked *PFIC* patients was identified with mutations of the human *ABCB11* gene (Strautnieks, Kagalwalla et al. 1997, Strautnieks, Bull et al. 1998), and these patients' livers revealed functional defects in canalicular expression of BSEP as well as in biliary excretion of bile salts (Jansen, Strautnieks et al. 1999, Byrne, Strautnieks et al. 2002, Noe, Stieger et al. 2002). In a latter study, mutations in the

ABCB11 gene linked the benign recurrent intrahepatic cholestasis type 2 (BRIC2) (van Mil, van der Woerd et al. 2004). The first BSEP study conducting Taiwanese PFIC patients further reported novel *ABCB11* mutations in the year 2002 (Chen, Chang et al. 2002). The *ABCB11/Abcb11* ortholog has been cloned and assayed its biochemical properties and/or developmental expression in several vertebrates, including mice (Green, Hoda et al. 2000, Lecreur, Sun et al. 2000, Cheng, Buckley et al. 2007), rats (Stieger, Fattinger et al. 2000, Tomer, Ananthanarayanan et al. 2003) (Gao, St Pierre et al. 2004), humans (Byrne, Strautnieks et al. 2002, Noe, Stieger et al. 2002, Chen, Chen et al. 2005), the skate (Ballatori, Rebbeor et al. 2000, Cai, Wang et al. 2001), and zebrafish (Ellis, Bove et al. 2018). The *Abcb11* knockout animal has been generated in mice (Wang, Salem et al. 2001), rats (Cheng, Freeden et al. 2016), and zebrafish (Ellis, Bove et al. 2018). Unexpectedly, the mouse *Mdr1* could compensate the loss of Bsep functions (Lam, Wang et al. 2005, Wang, Chen et al. 2009). Assays of these BSEP/Bsep orthologs suggested that BSEP/Bsep is an evolutionally conserved cBAT.

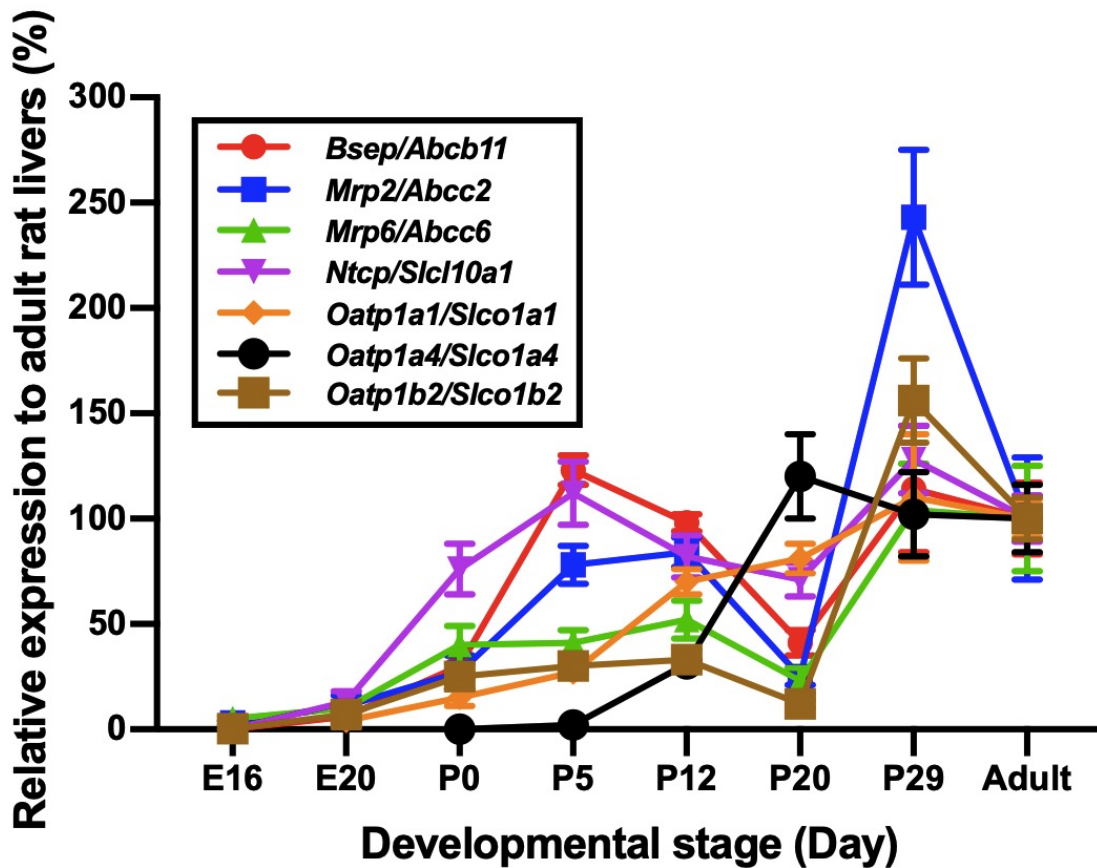


Figure 6 The line graph illustrates developmental expression of rat hepatic transporters.

The relative mRNA levels of hepatic transporters in rat livers at the different developmental stage, from the embryonic day (E) 16 to the post-natal day (P) 29, were plotted. The mRNA level of each transporter in adult rat livers was defined as 100%. The original data was adapted from (Gao, St Pierre et al. 2004).

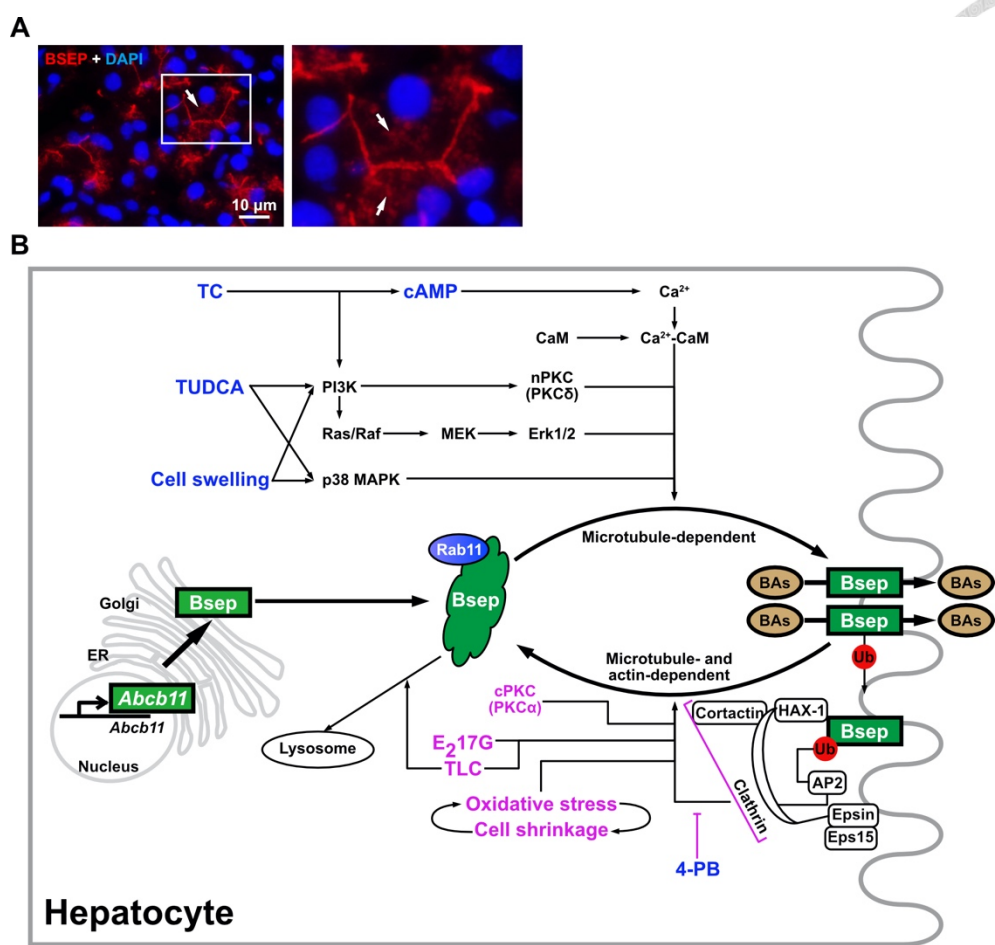
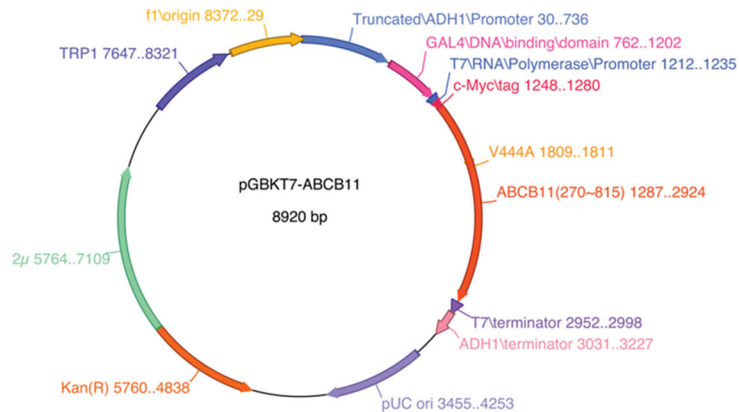


Figure 7 Graphic illustration of subcellular trafficking of BSEP in hepatocytes.

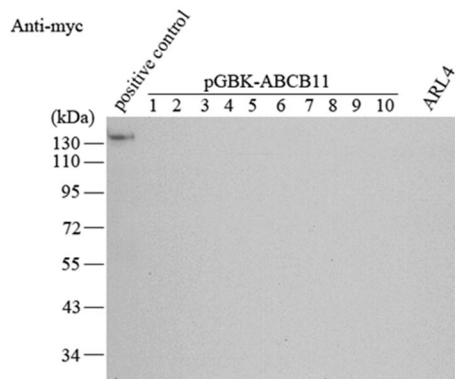
(A) Representative immunofluorescence image of adult human livers demonstrates that BSEP localizes at the subapical compartments (SACs) in the cytoplasm and at the canalicular membrane of hepatocytes in the adult human livers. Cryosection of adult human liver samples was immunostained for BSEP (red). The liver nuclei were stained with DAPI. For clarity, the image of the right panel is the enlarged version of the white open rectangle. The arrow indicates the cytoplasmic BSEP localizing at the SACs of hepatocytes. (B) Graphic illustration of subcellular trafficking of BSEP in hepatocytes. After transcription and translation, BSEP is glycosylated in the ER and Golgi, and then transferred to SACs in hepatocytes before targeting to the canalicular membrane. The SACs were further evidenced with Rab11 co-localization (Wakabayashi, Lippincott-Schwartz et al. 2004). Approximate half of newly synthesized BSEP at SACs would further target to the canalicular membrane in a microtubule dependent manner. By contrast, BSEP retrieval requires polymerized microtubules and actin microfilaments. BSEP constitutively cycled between Rab11-positive SACs and the canalicular membrane of hepatocyte before being delivered into lysosomal/proteosomal degradation. Several physical stimuli, bile salts, hormone, and BSEP-interacting proteins such as HAX-1 could trigger apical targeting (words in blue) and canalicular retrieval (words in purple) of BSEP. Some signaling pathways are shared by stimuli- or chemical substance-induced trafficking mechanisms of BSEP. (Kipp and Arias 2002, Roma, Crocenzi et al. 2008, Lam, Soroka et al. 2010, Hayashi, Inamura et al. 2012, Lam, Xu et al. 2012, Muhlfield, Domanova et al. 2012).

A

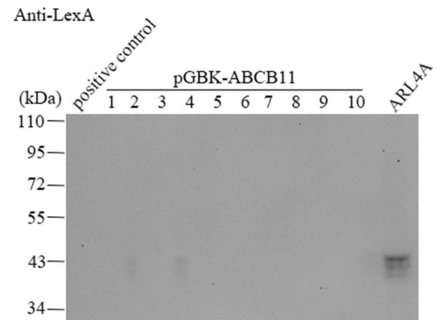


B

AH109



Anti-LexA



L40

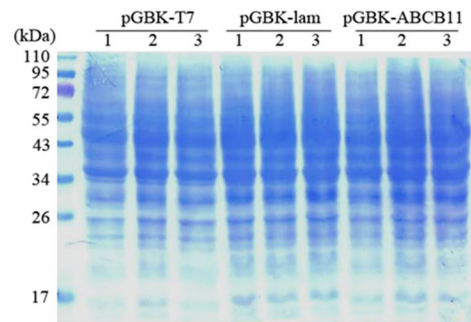
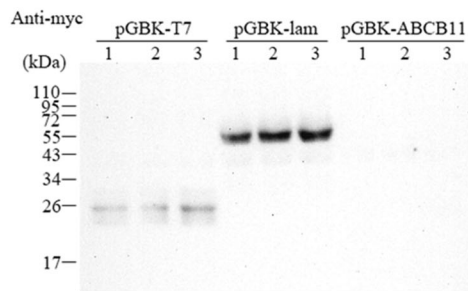


Figure 9 The bait protein, BSEP (270-815), is unstable in yeast competent cells.

(A) The plasmid map of pGBKT7-ABCB11. The gene encoding the human BSEP polypeptide spanning amino acid residues 250-815 (BSEP [270-815]) was cloned into the vector pGBKT7. A common BSEP variant, V444A, exists in BSEP (270-815). (B) Western blotting and Coomassie Blue staining for BSEP (270-815) expressed by pGBKT7-ABCB11 in two yeast competent cells AH109 and L40.

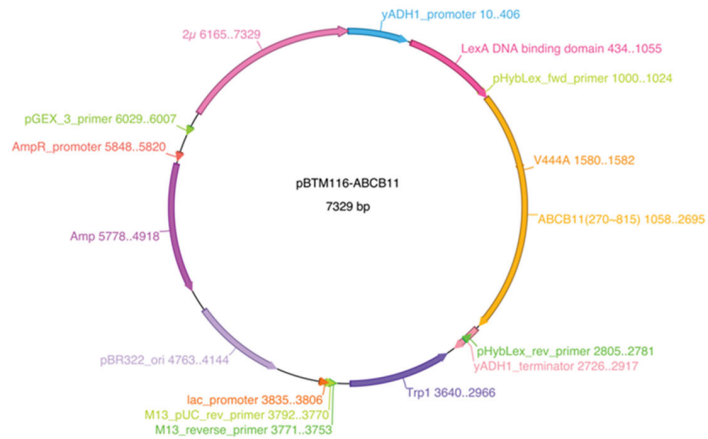
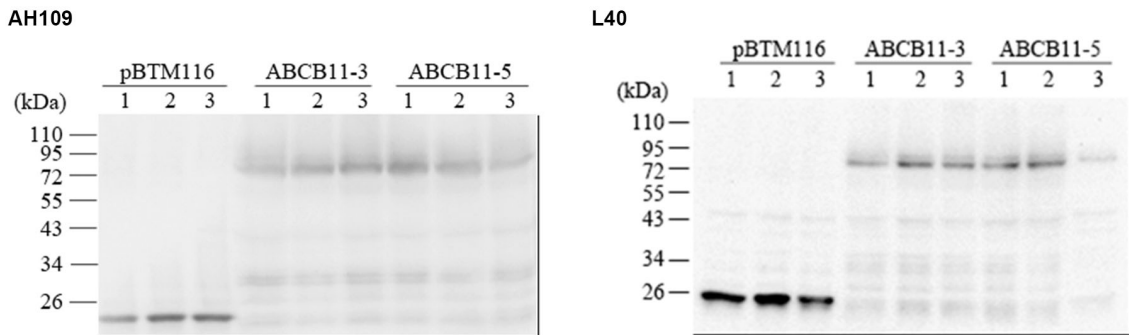
A**B**

Figure 10 The bait protein, BSEP (270-815), is unstable in yeast competent cells.

(A) The plasmid map of pBTM116-ABCB11. The gene encoding the human BSEP polypeptide spanning amino acid residues 250-815 (BSEP [270-815]) was cloned into the vector pBTM116. A common BSEP variant, V444A, exists in BSEP (270-815). (B) Western blotting for BSEP (270-815) expressed by two pBTM116-ABCB11 clones, pBTM116-ABCB11-3 and pBTM116-ABCB11-5, in two yeast competent cells AH109 and L40.

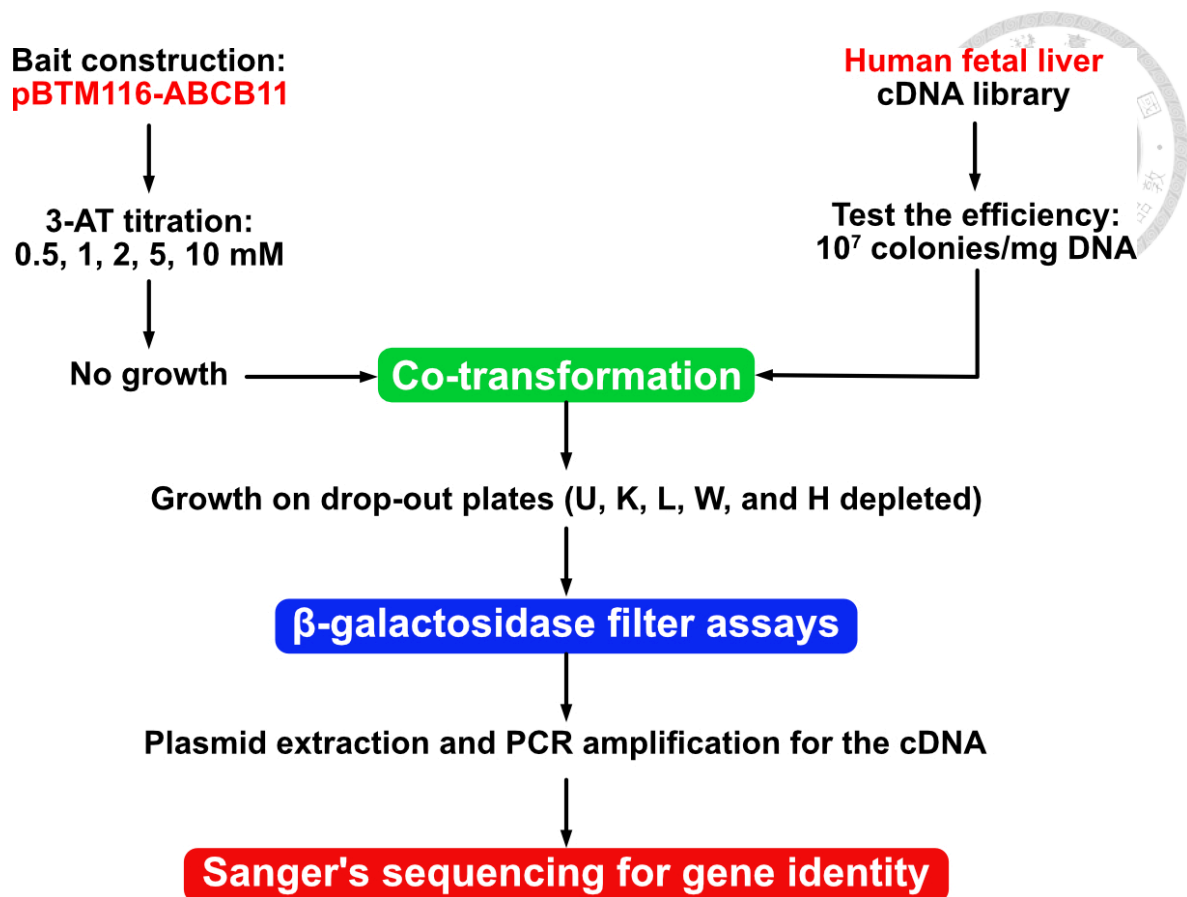


Figure 11 The flow chart illustrates the search of BSEP-interacting proteins.

The pBTM116-ABCB11 plasmid expressed a BSEP (270-815) protein, which was used as the bait to screen a human fetal liver cDNA library via yeast two-hybrid assays. To suppress background growth on His deficient condition, the concentration of 3-amino-1,2,4-triazole (3-AT) was titrated. Yeast cells with co-transformation of the bait and the cDNA library were cultured on drop-out plates, in which uracil, tyrosine, leucine, tryptophan, and histidine were absent. Yeas colonies growing on drop-out plates were subjected to β -galactosidase filter assays. Those colonies turning blue within 2 hours in β -galactosidase filter assays would further identify the cDNA through Sanger's sequencing.

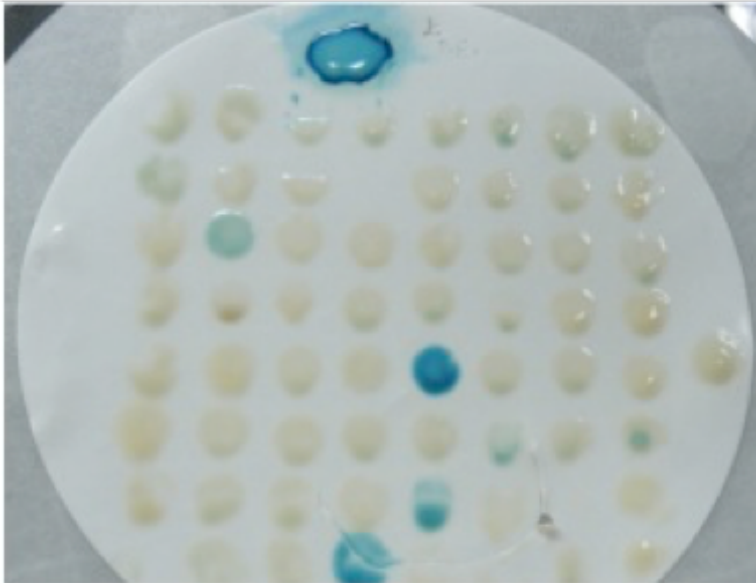
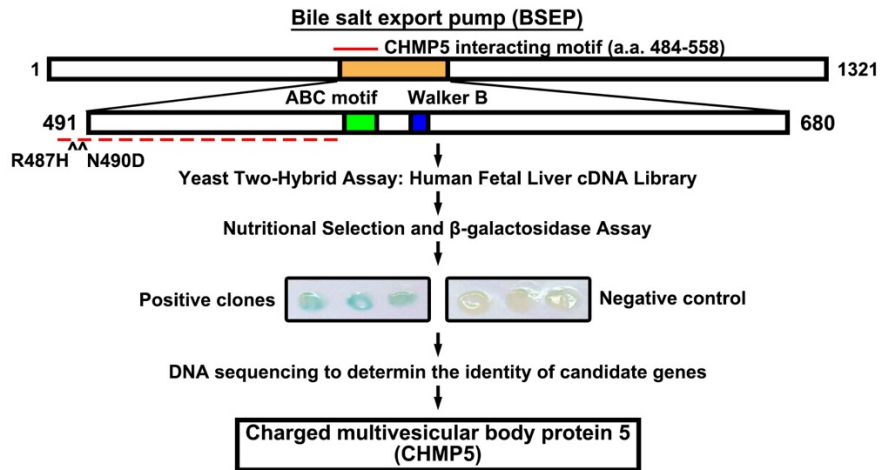


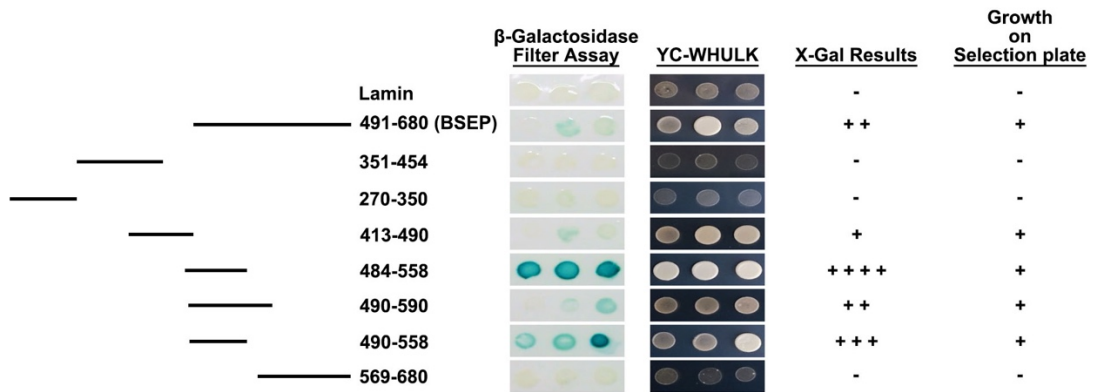
Figure 12 A representative result of β -galactosidase filter assays.

Yeast clones obtained through yeast two-hybrid assays were subjected to β -galactosidase filter assays. Yeast colonies were classified into 6 levels (levels 1 to 6) according to the blue appearance after being incubated with the β -gal substrate, X-gal. From levels 1 to 6, each represented the colony turn into blue in 0.5, 1, 2, 4, 5 hours, or overnight, respectively.

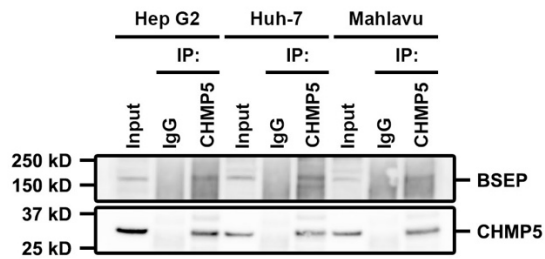
A



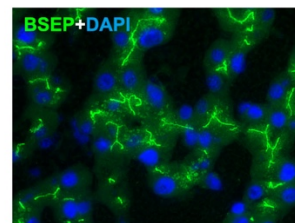
B



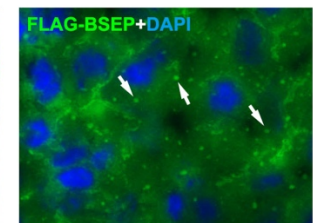
C



E



F



D

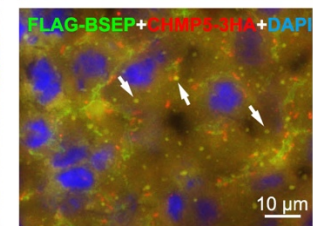
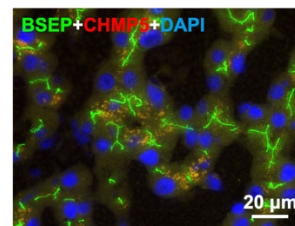
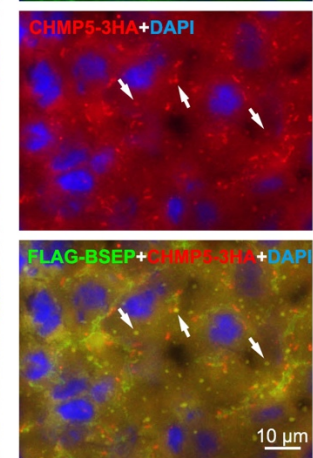
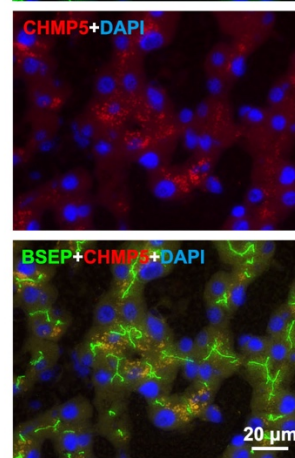
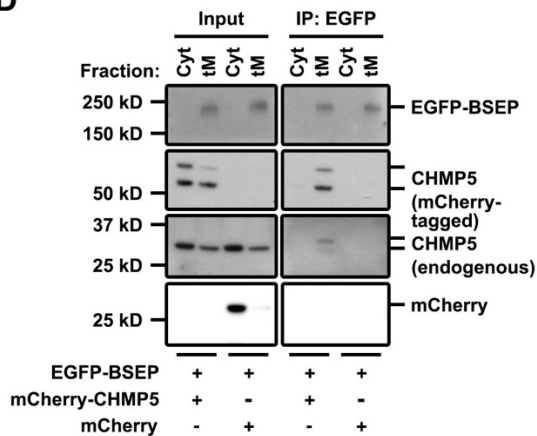


Figure 13 The ESCRT-III subunit CHMP5 co-localizes with BSEP in the subapical compartments of hepatocytes.

(A) The flow chart illustrates the identification of CHMP5 as a BSEP-interacting protein via yeast two-hybrid screening. A positive β -galactosidase assay indicates a polypeptide derived from CHMP5 interacting with the BSEP bait. Lamin was used as a negative control. The red line and dashed line represent the CHMP5 interacting motif (amino acid [a.a.] 484-558) of human BSEP. (B) CHMP5 interacted with the polypeptide spanning a.a. 484-558 of human BSEP. The CHMP5-interacting domain of BSEP was mapped via yeast two-hybrid screening. BSEP fragments, together with CHMP5, were co-expressed in competent yeast cells and analyzed by nutritional depletion and β -galactosidase filter assays. (C) BSEP was co-immunoprecipitated with CHMP5 from three hepatoma cell lines, Hep G2, Huh-7, and Mahlavu. Total cell lysate (25 μ g) were loaded as an input control; normal mouse immunoglobulins (IgG) as a negative control. (D) Endogenous and mCherry-tagged CHMP5 were co-immunoprecipitated with EGFP-BSEP in the total membrane-protein fraction. Hep G2 cells co-expressing EGFP-BSEP and mCherry-CHMP5 or mCherry were fractionated into cytosolic (Cyt) and total membrane-protein (tM) fractions. The two fractions were subjected to immunoprecipitation and immunoblotting via the antibodies indicated. The tM fraction contains the transmembrane and membrane-associated proteins (referred to Appendix Figure 3). (E) Representative immunofluorescence images demonstrate that CHMP5 co-localizes with BSEP in the subapical compartments (SACs) in the adult human livers. Cryosection of adult human liver samples was stained for BSEP (green) and CHMP5 (red). (F) Representative immunofluorescence images reveal the co-localization of CHMP5-3HA and FLAG-BSEP in the SACs in *Bsep* knockout mouse livers. CHMP5-3HA and FLAG-BSEP were co-expressed in *Bsep* knockout mice via hydrodynamic injection. Cryosections of the mouse liver samples were stained by anti-FLAG and anti-HA antibodies for FLAG-BSEP (green) and CHMP5-3HA (red), respectively. Arrows indicate the SACs with both FLAG-BSEP and CHMP5-3HA signals. The liver cell nuclei were stained by DAPI.

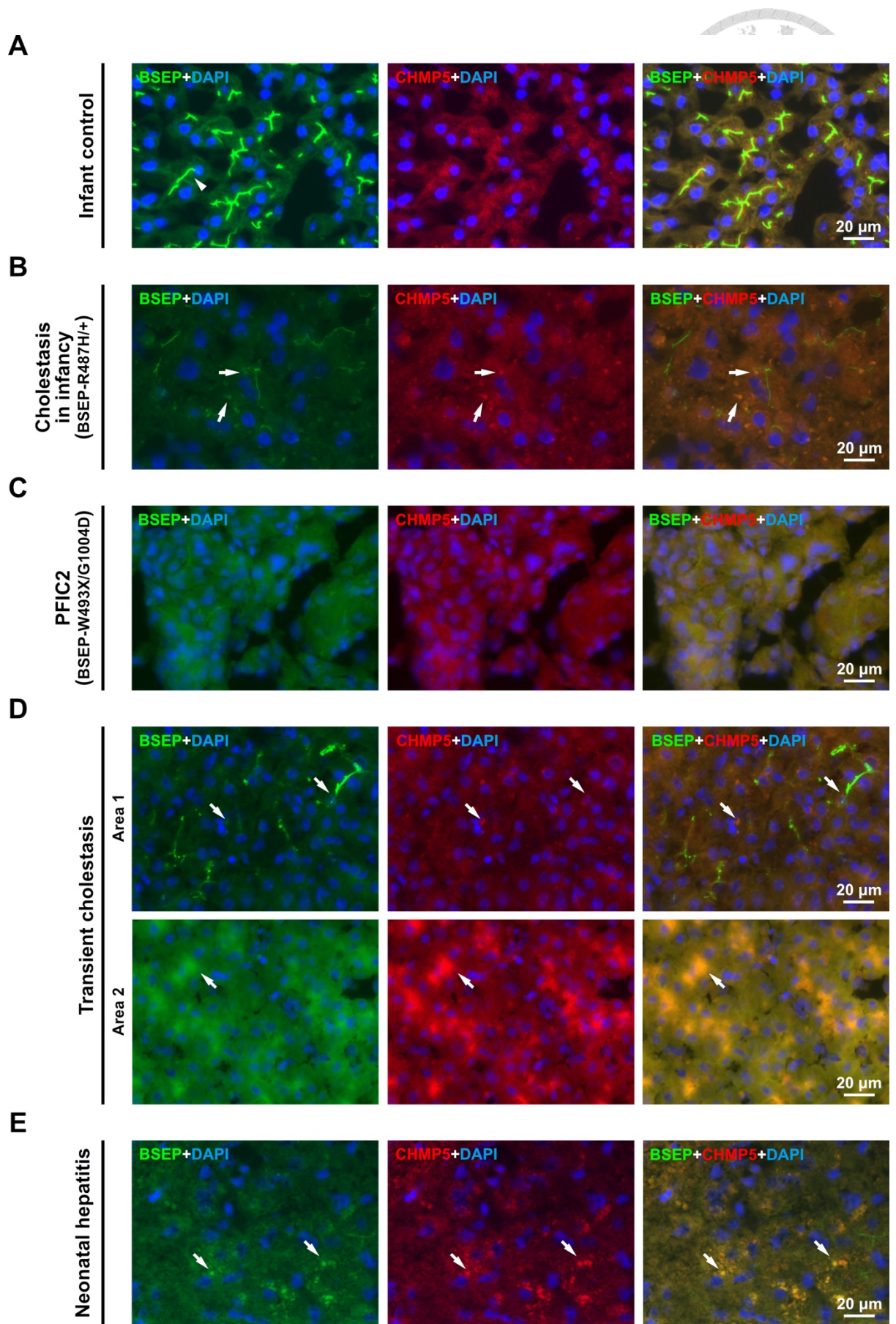


Figure 14 Aberrant subapical BSEP compartments in cholestatic human livers are CHMP5 positive.

Immunofluorescence staining demonstrated BSEP and the ESCRT-III CHMP5 in the SACs of hepatocytes in human liver samples from **(A)** a representative infant control; **(B)** a patient with cholestasis in infancy harboring heterozygous BSEP-R487H mutation (BSEP-R487H/+); **(C)** a PFIC2 infant with BSEP-W493X/G1004D mutations; **(D)** a diseased child with transient cholestasis; and **(E)** a representative patient with neonatal hepatitis. Cryosection of human livers samples were stained for BSEP (green) and CHMP5 (red). The liver nuclei were stained with DAPI. The arrowhead indicates the apical/canalicular membrane of hepatocytes, where the apical/canalicular BSEP localizes; arrows indicate the aberrant BSEP vesicles in the cytoplasm of cholestatic livers. Notably, two different patterns of BSEP and CHMP5 were observed in the transient cholestasis sample **(D)** and referred to Appendix Figure 4.

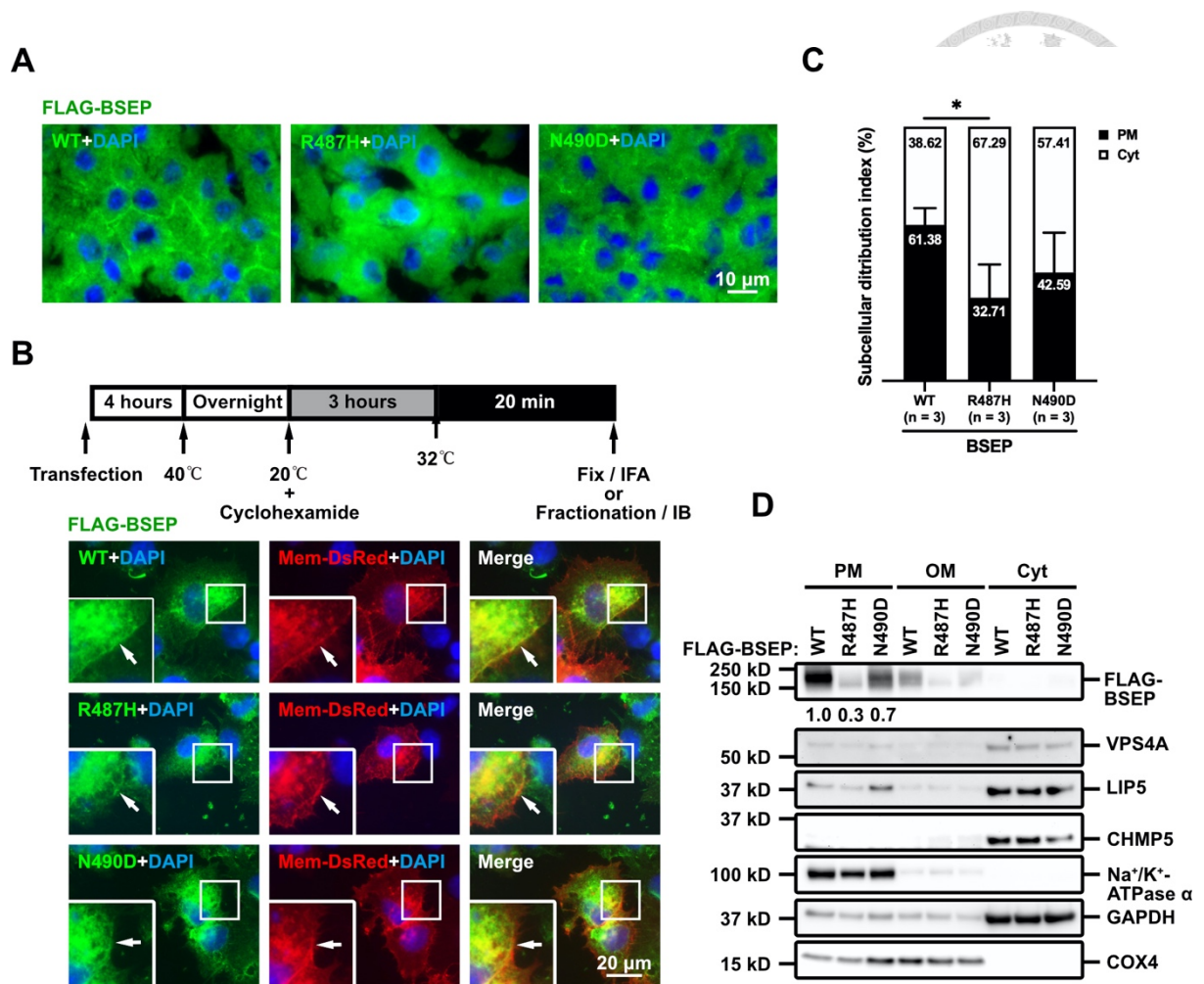
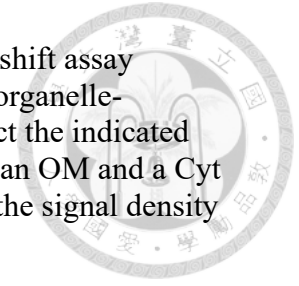


Figure 15 Impaired polarized trafficking of BSEP-R487H and BSEP-N490D mutants *in vivo* and *in vitro*.

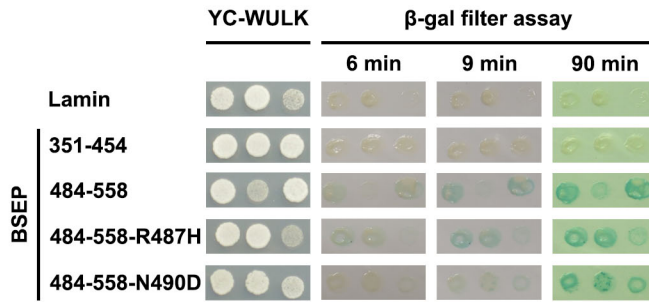
(A) Representative immunostaining demonstrates the impaired canalicular targeting of BSEP-R487H and BSEP-N490D mutants at the steady state *in vivo*. FLAG-tagged BSEP wild type or either mutants were expressed in *Bsep* knockout mouse livers for 7 days via hydrodynamic injection. Cryosections of the injected mouse livers were stained using anti-FLAG antibodies for FLAG-BSEPs (green). The liver cell nuclei were stained with DAPI. (B) Representative images demonstrate the impaired post-Golgi and plasma membrane trafficking of BSEP-R487 and BSEP-N490D mutants. Temperature shift assay was performed with Hep G2 cells transiently expressing the membrane marker Mem-DsRed plus FLAG-tagged BSEP, BSEP-R487H, or BSEP-N490D. FLAG-BSEPs and Mem-DsRed were stained with anti-FLAG and anti-mCherry antibodies, respectively. DAPI was used to stain cell nuclei. For clarity, the squared images are enlarged versions of the white open squares. Arrows indicate the plasma membrane. (C) A bar graph (n = 3, mean \pm SD) illustrates the subcellular distribution of FLAG-tagged BSEP and the two BSEP mutations after temperature shift assays. The images obtained from the experiment described in (B) were independently triplicated and analyzed for the subcellular distribution index (the detail in 3.2.12). The number of total cells counted for FLAG-BSEP-WT, -R487H, and -N490D is 131, 99, and 98, respectively. Two-tailed unpaired *Student's t*-test was used ($*P \leq 0.05$). The *P*-value is 0.0434. (D) Representative immunoblotting reveals the decreased plasma-membrane targeting of BSEP-R487H and BSEP-N490D. Hep G2 cells were transfected with p3XFLAG-BSEP,

-BSEP-R487H, or -BSEP-N490D and then subjected to temperature shift assay followed by subcellular fractionation. The plasma-membrane (PM), organelle-membrane (OM) and cytosolic (Cyt) fractions were analyzed to detect the indicated proteins. Na⁺/K⁺-ATPase α , COX4 and GAPDH were used as a PM, an OM and a Cyt fractionation control. Numbers are the relative ratio calculated from the signal density of FLAG-BSEPs in the PM normalized to that of Na⁺/K⁺-ATPase α .





A



B

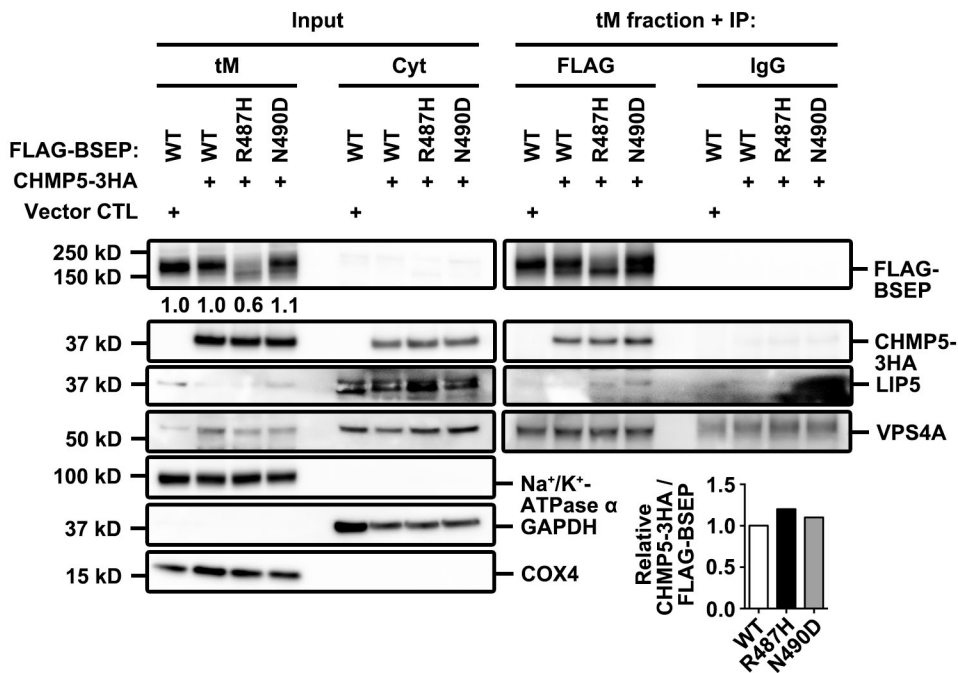


Figure 16 Aberrant association between CHMP5 and the two BSEP-R487H and BSEP-N490D mutants.

(A) BSEP polypeptides (amino acids [a.a.] 484-558) harboring either R487H or N490D mutant could interact with CHMP5 in yeast two-hybrid assays. BSEP fragments, together with CHMP5, were co-expressed in competent yeast cells and analyzed by β-galactosidase filter assays. The BSEP-484-55 and BSEP-351-454 fragments were used as the positive and negative CHMP5-interaction control, respectively. Lamin was used as a negative control. (B) Immunoblotting demonstrates aberrant association between the two BSEP mutants and ESCRT-III molecules. Hep G2 cells were expressed CHMP5-3HA together with FLAG-BSEP, FLAG-BSEP-R487H, or -N490D mutants for 24 hours and then fractionated into total membrane (tM) and cytosolic (Cyt) fractions. The tM fractions were subjected to co-immunoprecipitation using anti-FLAG antibodies. The pCMV6-AC-3HA was the vector control (Vector CTL). FLAG-BSEPs, CHMP5-3HA were detected by using anti-FLAG and anti-CHMP5 antibodies, respectively. The others were detected via indicated antibodies. Na⁺/K⁺-ATPase α, COX4 and GAPDH were used as a PM, an OM and a Cyt fractionation control. The numbers in the Input panel are the relative densitometry ratio of FLAG-BSEPs normalized to Na⁺/K⁺-ATPase α. The bar graph illustrates the relative signal density of CHMP5-3HA normalized to FLAG-BSEPs of the “tM fraction + IP” panel.

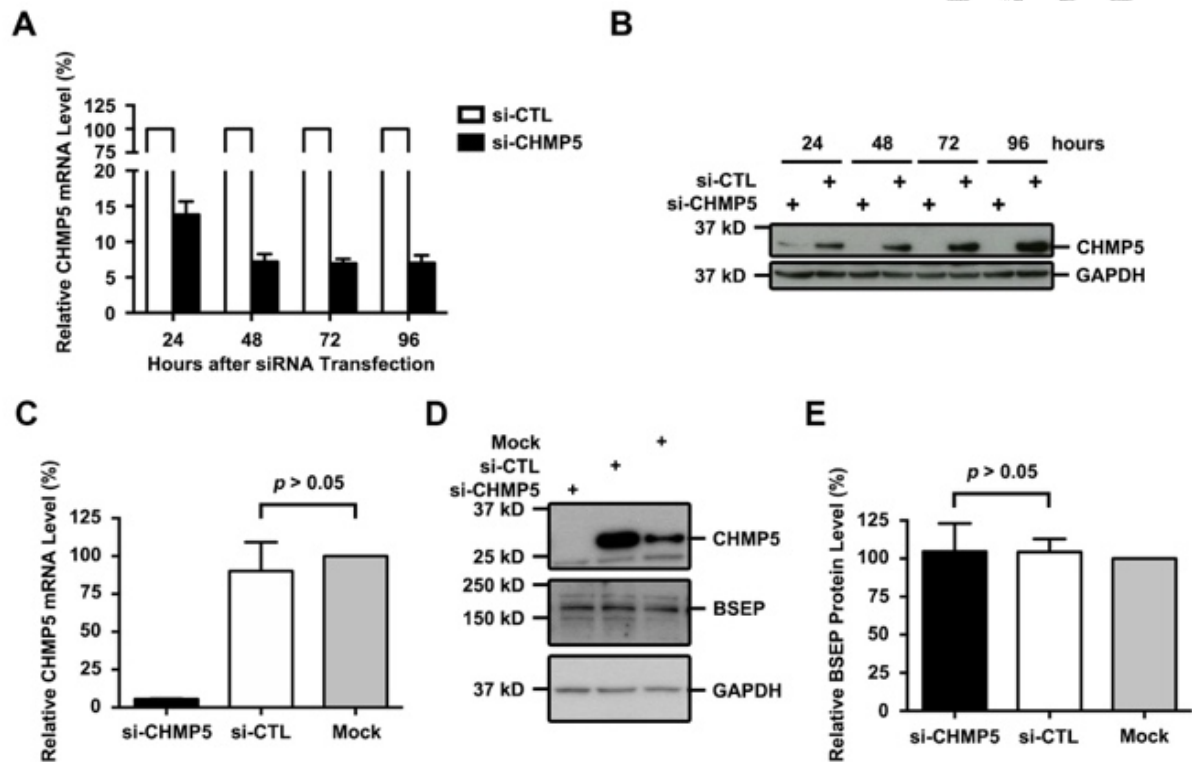


Figure 17 The protein expression and turnover of BSEP is unaffected with CHMP5 knockdown.

(A and B) Endogenous CHMP5 in Hep G2 cells was knocked down and sustained in steady state by small interference RNA (siRNA) in 48 hours. Hep G2 cells were reverse transfected with 10 nM of a *CHMP5*-targeting (si-CHMP5) or a non-targeting (si-CTL) pools for the indicated times. (A) Bar graph (n = 3, mean ± SD) demonstrates the quantitative PCR results of the relative *CHMP5* mRNA levels, which were normalized to *GAPDH*, and the si-CTL group at each corresponding time point was defined as 100%. (B) Representative immunoblots of CHMP5 and GAPDH demonstrate CHMP5 knockdown at the protein level. The protein GAPDH was used as a loading control. (C and D) Hep G2 cells were reverse transfected with si-CHMP5 or si-CTL for 48 hours. (C) Bar graph (n = 3, mean ± SD) demonstrates the quantitative PCR result of the relative *CHMP5* mRNA level, which were normalized to *gapdh*. The Mock group was defined as 100%. (D) Representative immunoblot of BSEP, CHMP5 and GAPDH demonstrates CHMP5 knockdown and BSEP at the protein level. GAPDH was used as a loading control. (E) The bar graph (n = 3, mean ± SD) illustrates the relative BSEP protein levels, which were unaffected by *CHMP5* knockdown. Densitometry was applied to quantify the signal densities of BSEP and GAPDH from (D). The Mock group was defined as 100%. The *P*-value was calculated by *Student's t*-test.

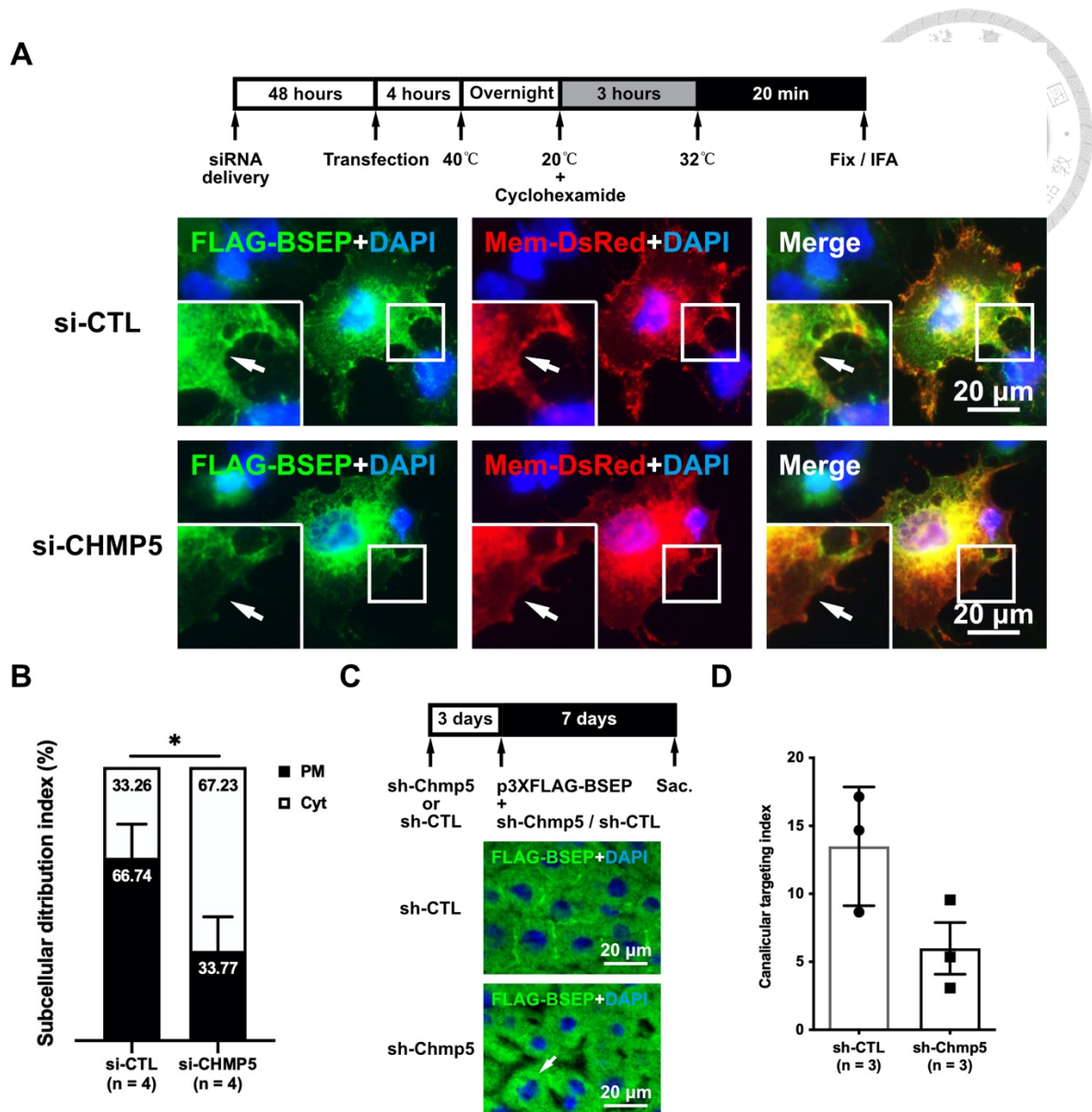


Figure 18 CHMP5 regulates the apical targeting of BSEP *in vivo* and *in vitro*.

(A) Representative images demonstrate the defective post-Golgi trafficking and membrane targeting of BSEP in CHMP5 knockdown Hep G2 cells. Hep G2 cells were pretreated with *CHMP5*-targeting (si-CHMP5) or non-targeting (si-CTL) siRNA pools and then co-expressed FLAG-BSEP and the membrane marker Mem-DsRed for temperature shift assays. FLAG-BSEP and Mem-DsRed were detected with anti-FLAG and anti-mCherry antibodies, respectively. DAPI was used to stain the cell nuclei. For clarity, the squared images are enlarged versions of the white open squares. Arrows indicate the FLAG-BSEP on the plasma membrane. (B) A bar graph ($n = 3$, mean \pm SD) illustrates the subcellular distribution of FLAG-BSEP in CHMP5 knockdown Hep G2 cells after temperature shift assays. The images obtained from the experiment described in (A) were independently triplicated and analyzed for the subcellular distribution index (the detail in 3.2.12). The number of total cells counted for FLAG-BSEP in si-CTL and in si-CHMP5 pretreated Hep G is 121 and 96, respectively. Two-tailed unpaired *Student's t*-test was used ($*P \leq 0.05$). The *P*-value is 0.0286. (C) Representative images reveal defective apical targeting of BSEP in *Chmp5* knockdown mouse livers. The plasmid pool expressing shRNA targeting to mouse *Chmp5* (sh-Chmp5) or to the

scramble shRNA (sh-CTL) was hydrodynamically injected into FVB/NJ mouse livers twice. In the second time of injection, p3XFLAG-BSEP was con-injected. The mouse liver samples were analyzed for the distribution of FLAG-BSEP (green) through immunostaining with anti-FLAG antibodies. The arrow indicates the accumulated subapical BSEP. **(D)** A bar graph (n = 3, mean \pm SD) illustrates the canalicular distribution of FLAG- BSEP in *Chmp5* knockdown mouse livers. The images obtained from the experiment described in **(C)** were analyzed for the canalicular targeting index (the detail in 3.2.12). More than 10 images per mice and total mice in each group were analyzed.

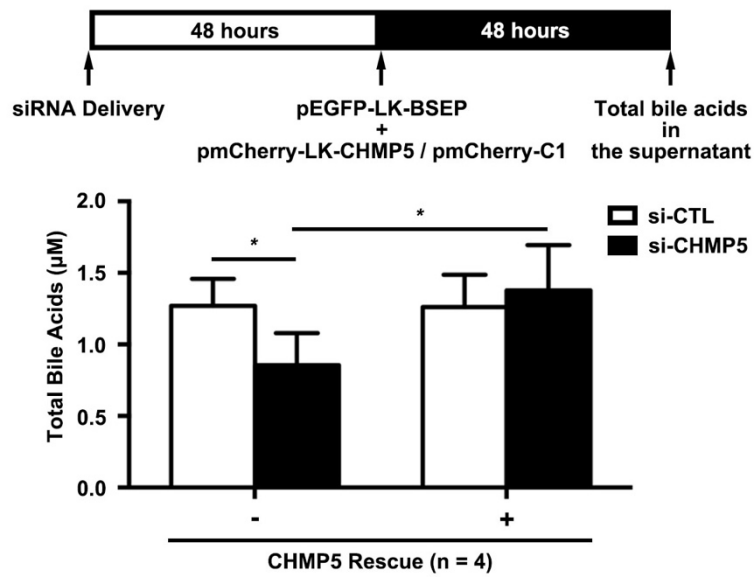


Figure 19 CHMP5 indirectly regulates BSEP-mediated bile acid secretion.

The bar graph (n = 4; mean \pm SD) illustrates that CHMP5 knockdown decreased the bile acid secretion mediated by BSEP, which could be rescued through overexpressing CHMP5. The total bile acids concentrations were determined from the conditional medium of Hep G2 cells that were pre-treated with si-CHMP5 or si-CTL, and then co-transfected with EGFP-BSEP and mCherry-CHMP5 expressing plasmids. The plasmid pmCherry-C1 was used as a negative control for CHMP5 rescue. Two-tailed unpaired *Student's t*-test was used ($*P \leq 0.05$). The *P*-value is 0.0314 and 0.0402 of the left and the right analysis, respectively.

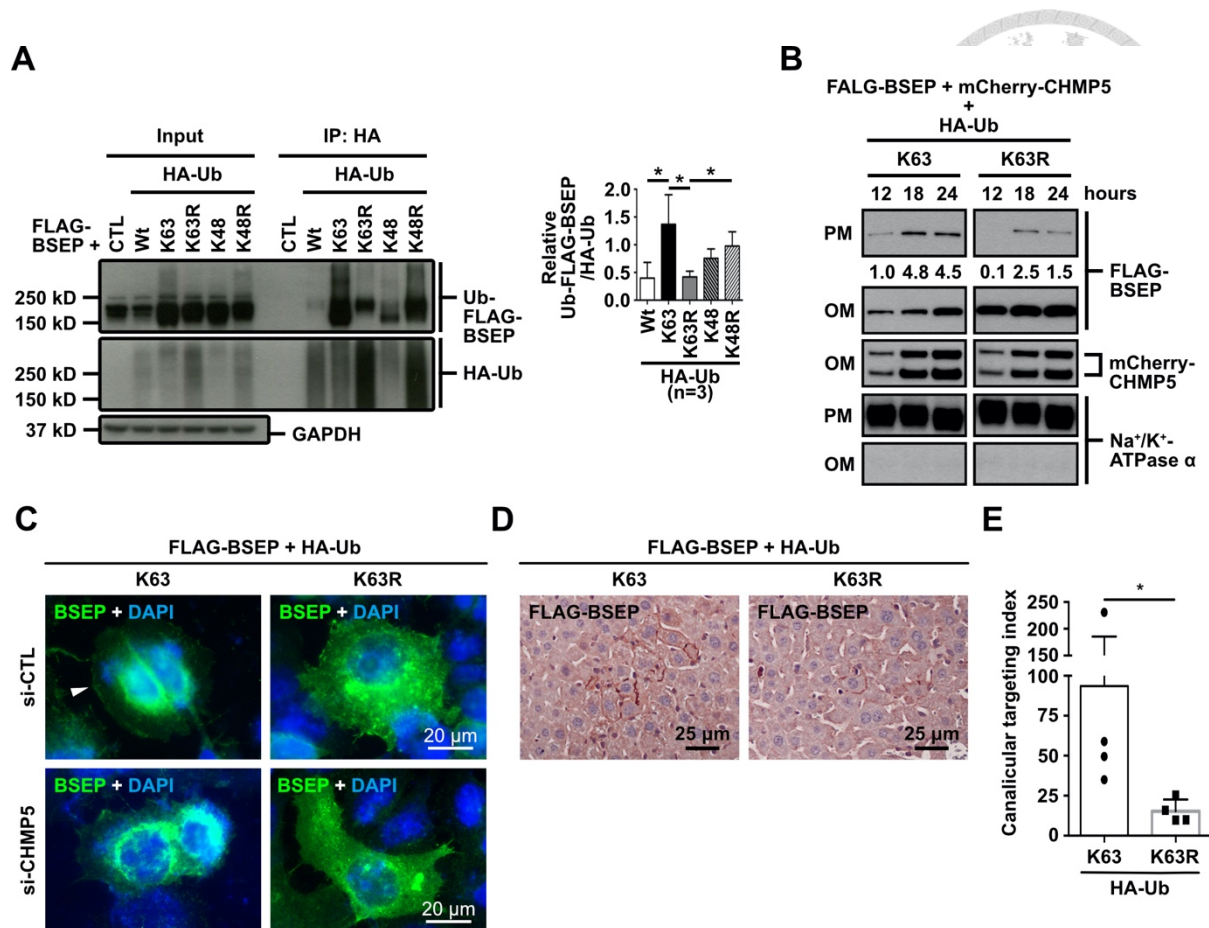


Figure 20 BSEP is abundantly modified with K63-linked ubiquitination.

(A) Representative immunoblotting demonstrates BSEP was abundantly modified with K63-linked ubiquitin (Ub) chains. Hep G2 cells were co-transfected with p3XFLAG-BSEP and HA-Ub mutants or the control plasmid pcDNA3.1 (+) for 24 hours. The HA-tagged ubiquitinated proteins were isolated through anti-HA antibodies, from which ubiquitinated FLAG-BSEP (Ub-FLAG-BSEP) and HA-Ub were probed via anti-FLAG and anti-HA antibodies, respectively. The total lysate was loaded as an input control; GAPDH was used as a loading control. The bar graph ($n = 3$, mean \pm SD) represents the Ub-FLAG-BSEP signals normalized to HA-Ub. Two-tailed unpaired *Student's t*-test was used ($*P \leq 0.05$). The *P*-value, from the left to the right, is 0.0495, 0.0380, and 0.0253, respectively. (B) Hep G2 cells were co-transfected with p3XFLAG-BSEP, pmCherry-LK-CHMP5 and either pRK5-HA-Ub-K63 or pRK5-HA-Ub-K63R, and then fractionated at the indicated times. The plasma-membrane (PM) and organelle-membrane (OM) protein fractions were analyzed via immunoblotting assays to detect FLAG-BSEP and mCherry-CHMP5 using anti-FLAG and anti-CHMP5 antibodies, respectively. Na⁺/K⁺-ATPase was used as a PM fractionation control. The number was relative FLAG-BSEP signals normalized the PM control quantified via densitometry. (C) Representative immunofluorescence images demonstrate Ub-K63 is essential for CHMP5-regulated membrane trafficking of BSEP *in vitro*. Hep G2 cells with indicated siRNA pre-treatment were co-expressed FLAG-BSEP and HA-Ub-K63 or HA-Ub-K63R for temperature shift assay followed by immunostainings of FLAG-BSEP (green). Cell nuclei were stained via DAPI. The arrowhead indicates the FLAG-BSEP signal the plasma membrane. (D) Immunohistochemical staining shows the strong canaliculi targeting FLAG-BSEP in Ub-K63 co-expression *in vivo*. FLAG-BSEP and HA-Ub-

K63 or -K63R were expressed in FVB/NJ mouse livers via hydrodynamic injection. The FLAG-BSEP in paraffin-embedded sections were immunochemically labeled through anti-FLAG antibodies, and visualized the HRP substrate NovaRed. The cell nuclei were stained by hematoxylin. **(E)** A bar graph (n = 1, mean \pm SD) illustrates the canalicular distribution of FLAG- BSEP in Ub-K63 or -K63R expressed mouse livers. The images obtained from the experiment described in **(D)** were analyzed for the canalicular targeting index (the detail in 3.2.12). Four images per mice and total mice in each group were analyzed. Two-tailed unpaired *Student's t*-test was used ($*P \leq 0.05$). The *P*-value, from the left to the right, is 0.0286.

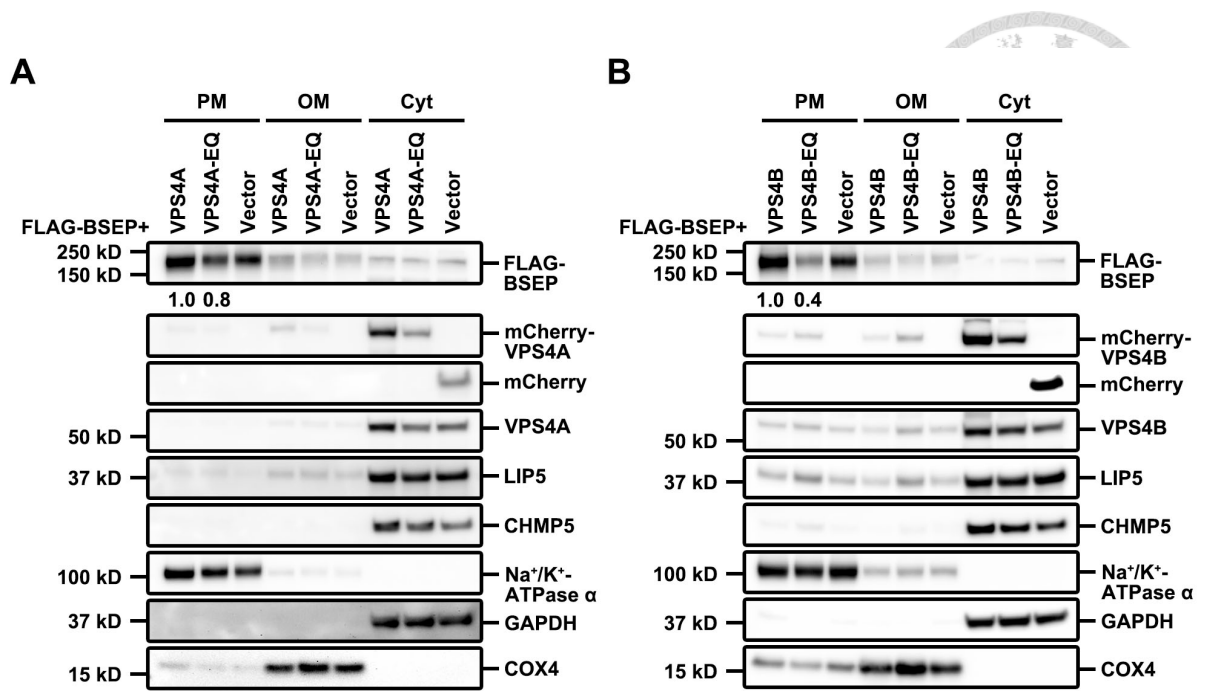


Figure 21 Both VPS4 molecules affect post-Golgi trafficking of BSEP.

Disturbed membrane targeting of BSEP in dominant-negative VPS4A or VPS4B mutant co-expressing cells was revealed through temperature shift assay followed by subcellular fractionation and immunoblotting. Hep G2 cells co-expressing FLAG-BSEP and either mCherry-tagged (A) VPS4A, VPS4A-E228Q (VPS4A-EQ), (B) VPS4B, or VPS4B-E235Q (VPS4B-EQ) were subjected to temperature shift assay. VPS4A-EQ and VPS4B-EQ are the dominant negative VPS4A and VPS4B mutants, respectively. The plasmid pmCherry-C1 was used as the vector control. A representative immunoblotting reveals the plasma-membrane (PM), organelle-membrane (OM) and cytosolic (Cyt) fractions detected by the indicated protein antibodies. Na⁺/K⁺-ATPase α , COX4 and GAPDH were used as a PM, an OM and a Cyt fractionation controls. The values are the relative FLAG-BSEP signal normalized to the corresponding fractionation control signal.

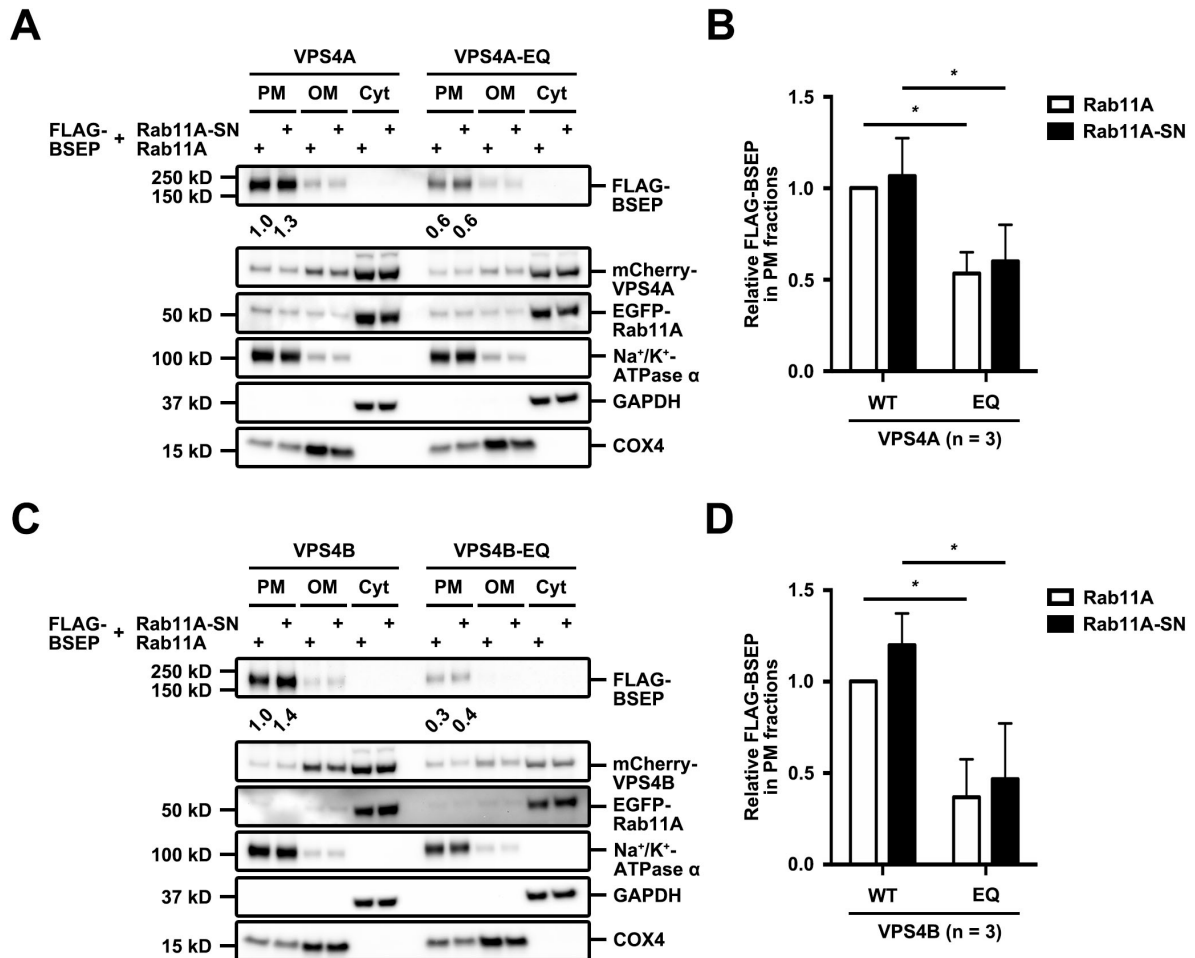


Figure 22 VPS4 affecting apical targeting of BSEP is upstream of Rab11a.

Membrane targeting of BSEP in VPS4 paralog and Rab11A co-expressing cells was revealed through temperature shift assay followed by subcellular fraction and immunoblotting. Hep G2 cells co-expressing FLAG-BSEP, EGFP-Rab11A or EGFP-Rab11A-S25N (EGFP-Rab11A-SN) together with (A) mCherry-VPS4A or -VPS4A-E228Q (VPS4A-EQ) or (C) mCherry-VPS4B or -VPS4B-E235Q (VPS4B-EQ) were subjected to temperature shift assay. The plasmid pmCherry-C1 was used as the vector control. A representative immunoblotting reveals the plasma-membrane (PM), organelle-membrane (OM) and cytosolic (Cyt) fractions detected by the indicated protein antibodies. Na⁺/K⁺-ATPase α , COX4 and GAPDH were used as a PM, an OM and a Cyt fractionation controls. These experiments, described in (A) and (C), have been independently triplicated. The values are the relative FLAG-BSEP signals normalized to the corresponding fractionation control signals. The independently triplicated results were illustrated in (B) and (D).

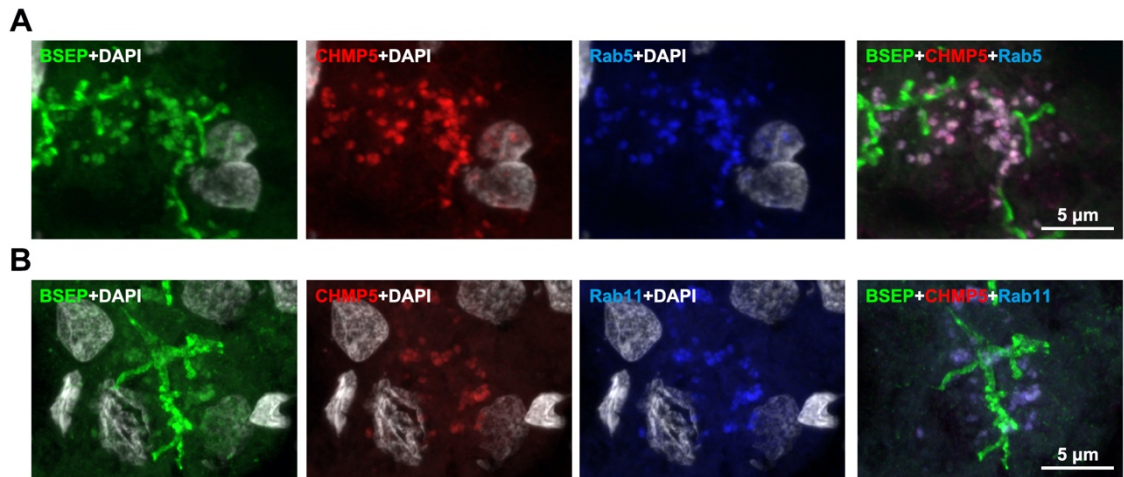


Figure 23 The subapical compartments at which BSEP and CHMP5 are colocalized are Rab5 and Rab11 positive.

Confocal microscopy demonstrates the BSEP-and-CHMP5 colocalized SACs are also positive with **(A)** the early/sorting endosome marker Rab5 and **(B)** the recycling endosome maker Rab11. Adult human liver samples were co-immunofluorescently stained for BSEP (green), CHMP5 (red), and either Rab5 (blue pseudo-color) or Rab11 (blue pseudo-color). DAPI (white pseudo-color) stained the nuclei of hepatocytes.

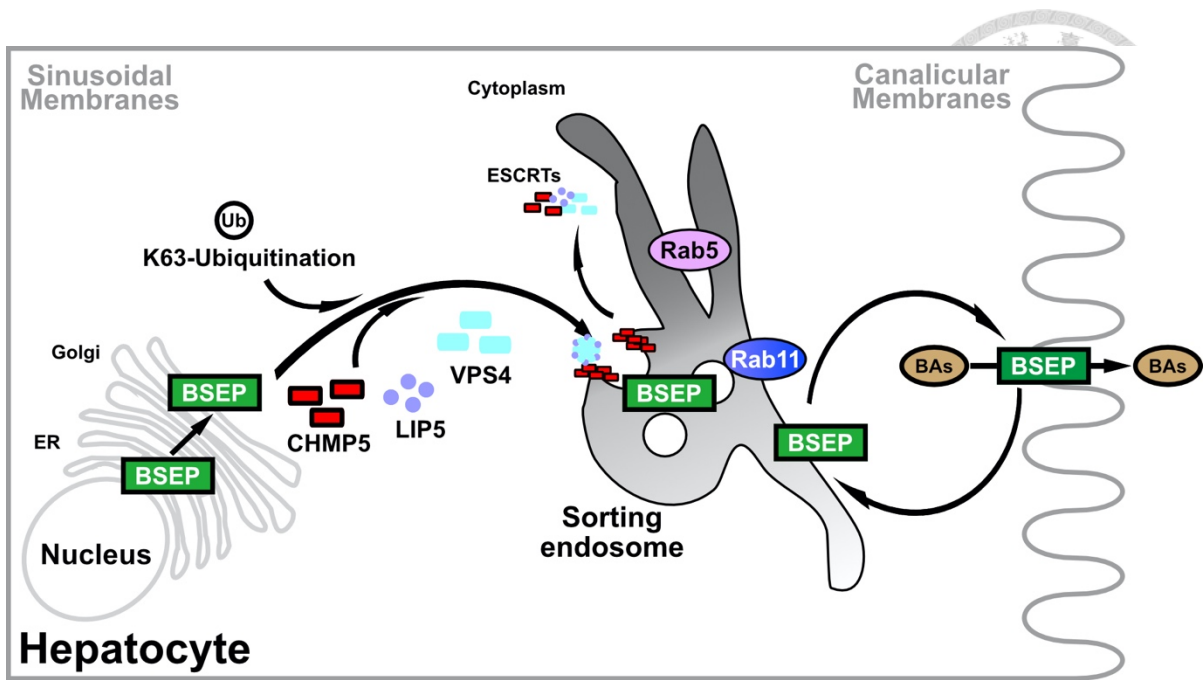


Figure 24 Proposed model of CHMP5-associated ESCRTs in BSEP canalicular-targeting.

After transcription and translation, BSEP undergoes core- and complete-glycosylation in the ER and Golgi, respectively, and subsequent post-Golgi trafficking. BSEP is poly-ubiquitinated via K63 linkages and bound with CHMP5 further targets to the sorting endosomes. The sorting endosome is an internal trafficking hub enriched with the small GTPase Rab5 proteins. Other ESCRT molecules, at least LIP5, may co-localize with BSEP and CHMP5 at the sorting endosome. VPS4 disassembles ESCRTs on the sorting endosomes, from which BSEP is transferred to the canalicular membrane via Rab11-mediated targeting and then cycles between the Rab11-recycling endosomes.

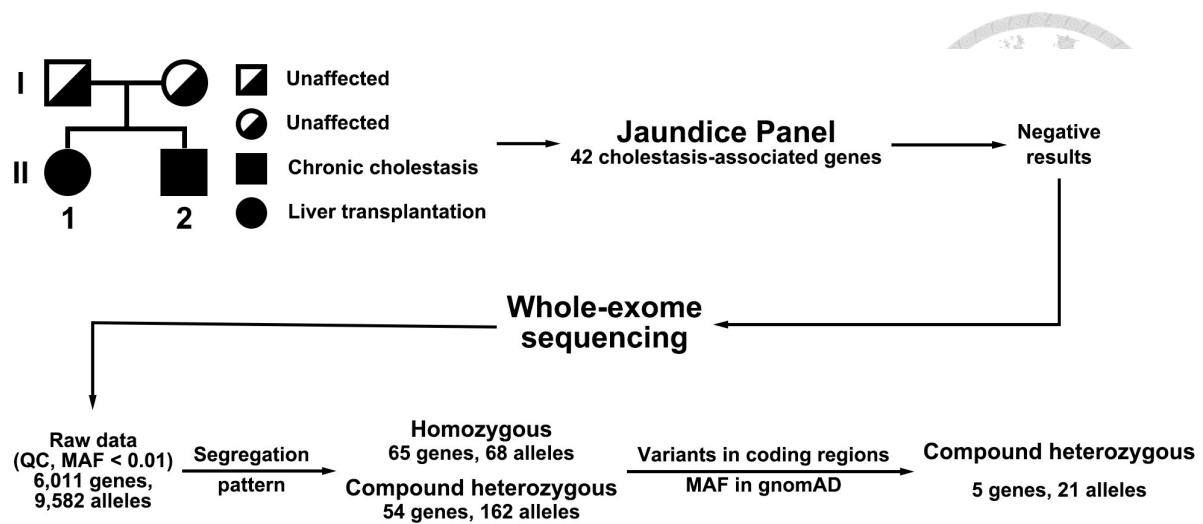


Figure 25 The flow chart of whole-exome sequencing to explore novel PFIC-associated candidate genes.

Patient 1 and patient 2, from the same family, were diagnosed with cholestasis. Patient 1 received liver transplantation at the age of 2 years. Patient 2 demonstrates chronic cholestasis. Suspecting PFIC, I analyzed both patients using target enrichment next-generation sequencing for 42 cholestasis-associated genes but with negative results (Chen, Li et al. 2019). The DNA from the family was subjected to whole-exome sequencing. Because the parents are unaffected, I assumed: (i) the disease inheritance should be autosomal recessive, and (ii) the same disease-causing variant(s) should exist(s) and be heterozygous in the parents. Twenty-one alleles in five genes were retained.

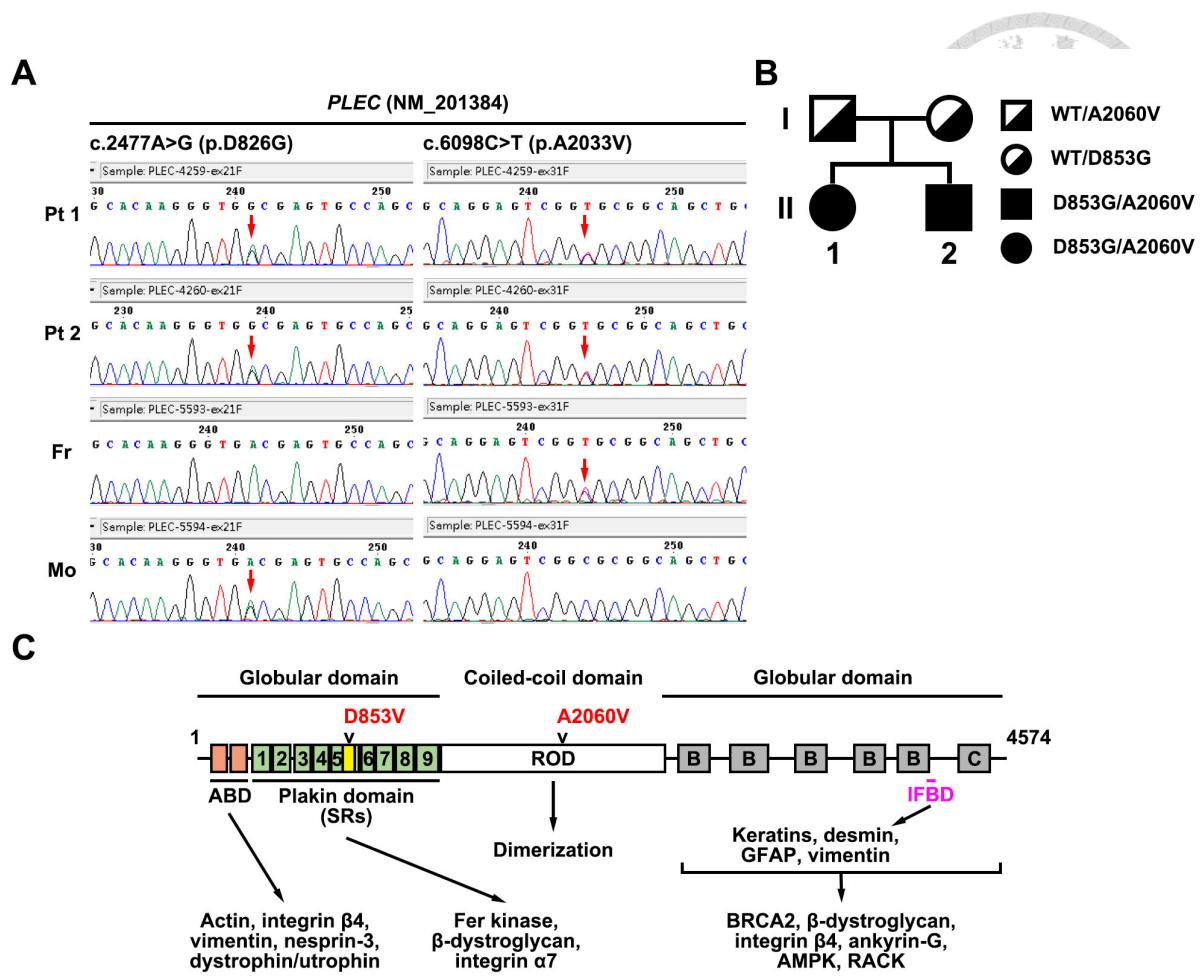


Figure 26 The *PLEC* (NM_000436) mutations identified from the PFIC family.

(A) The *PLEC* mutations, c2477A>G and c.6098C>T, were inherited from the mother and father, respectively. Sanger's sequencing confirmed the two *PLEC* mutations identified in whole-exome sequencing. The red arrow indicates the two different nucleotide residues in Sanger's sequencing data. (B) Pedigree of the family with *PLEC* mutations. (C) Schematic illustration of the structure of human *PLEC*, *PLEC*-interacting proteins, and the two *PLEC* mutations identified in this study. The *PLEC* is an approximate 500-kDa, tripartite protein composed of N- and C-terminal globular domains and the central coiled-coil rod domain. The N-terminal domain contains an ABD composing of two calponin homology domains (orange), and a plakin domain formed by nine spectrin repeats (SRs; green). An SH3 motif (a.a. 749-918; yellow) is embedded in SR5. The C-terminal globular domain is composed of five type-B and one type-C plakin repeats (grey). The IFBD (a.a. 4140-4190; purple) locates in the carboxyl end of the fifth type-B plakin repeat. The central rod domain mediates *PLEC* dimerization through coiled-coil interaction. The N- and C-terminal globular domains connect various cytoskeletal molecules and plasma membrane-bound junctional complexes to maintain cell and tissue integrity (modified from (Winter and Wiche 2013)). Abbreviations: ABD, actin-binding domain; AMPK, AMP-activated protein kinase; BRCA2, breast cancer type 2 susceptibility protein; CTL, control liver sample; Fr, father; GFAP, glial fibrillary acidic protein; IFBD, intermediate filament-binding domain; m, month; Mo, mother; *PLEC*, plectin; Pt, patient; RACK, the receptor for activated C kinase 1; SR, spectrin repeat; y, years. A part of this figure has been published in (Wu, Hsu et al. 2019).

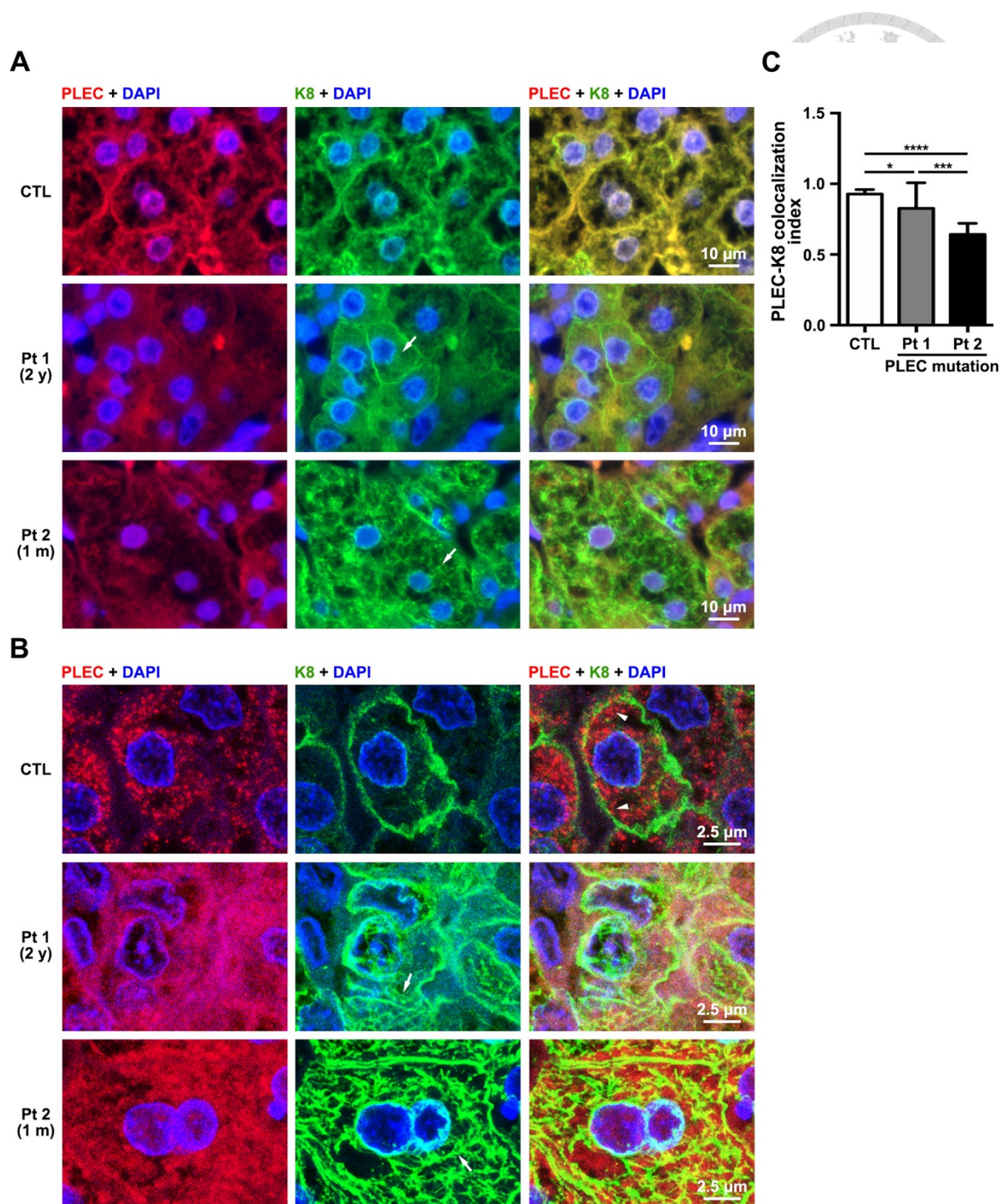


Figure 27 Decreased colocalization of PLEC and K8 in the cholestatic liver samples of *PLEC* mutations.

(A) Epifluorescence microscopy and, for clarity, (B) confocal microscopy demonstrate PLEC-and-K8 distribution in the cholestatic liver samples of *PLEC* mutations. Paraffin-embedded liver sections were co-immunofluorescently labeled with PLEC and K8, and DAPI was used to stain cell nuclei. The arrow indicates the scattered K8 signals in the cytoplasm of the patients' hepatocytes; the arrowhead indicates PLEC signals close to peripheral K8 in the control hepatocytes. (C) Reduced colocalization of PLEC and K8 in *PLEC* mutated livers. Twenty images of epifluorescent microscopy acquired from each liver sample were analyzed

the co-localization index (Pearson's correlation coefficient) of PLEC and K8 using ImageJ program. The bar graph illustrates that the co-localization index (mean \pm SD) of the control, Patient 1, and Patient 2 were 0.93 ± 0.03 , 0.83 ± 0.18 , and 0.64 ± 0.08 , respectively. Two-tailed, unpaired Student *t* test was used to calculate **P* < 0.05, ****P* < 0.001, and *****P* < 0.0001. Abbreviations: CTL, control liver sample; DAPI, 4'6-diamidino-2-phenylindole; K8, (cyto)keratin 8; m, month; PLEC, plectin; Pt, patient; y, years.

A part of this figure has been published in (Wu, Hsu et al. 2019).

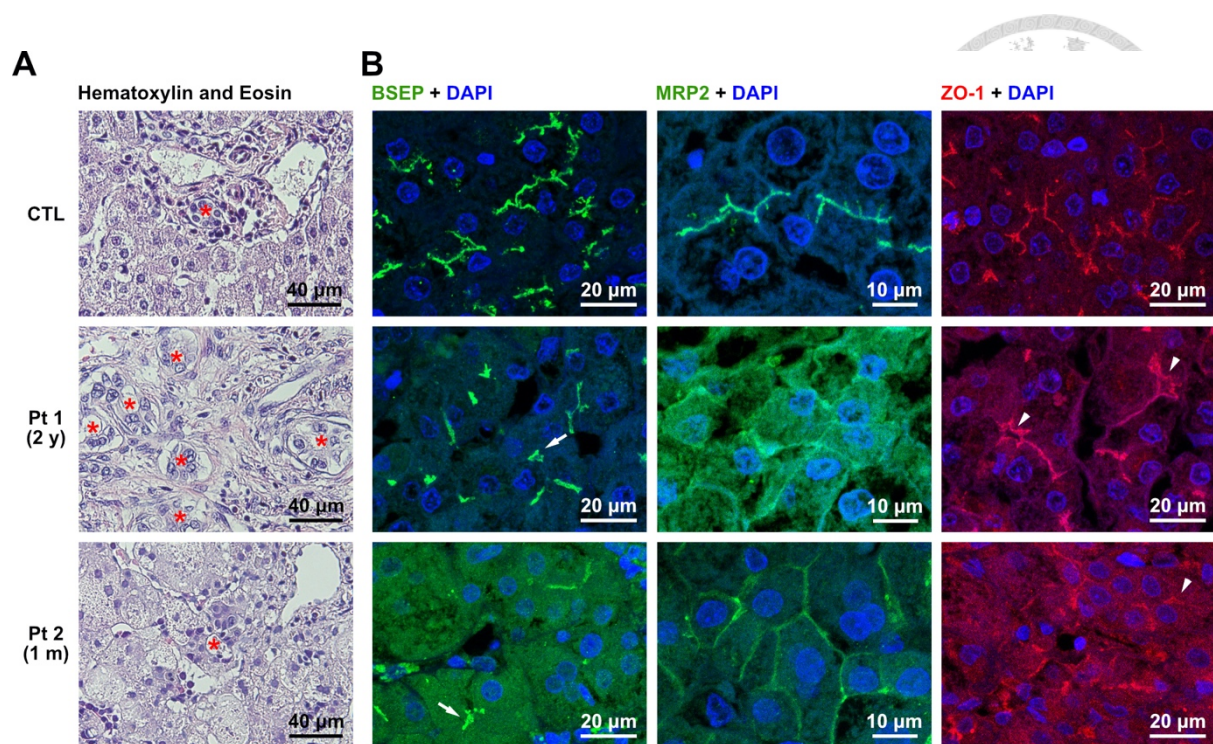
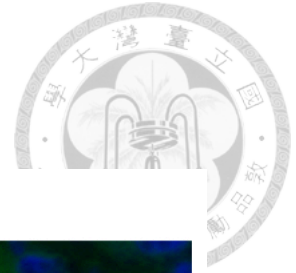


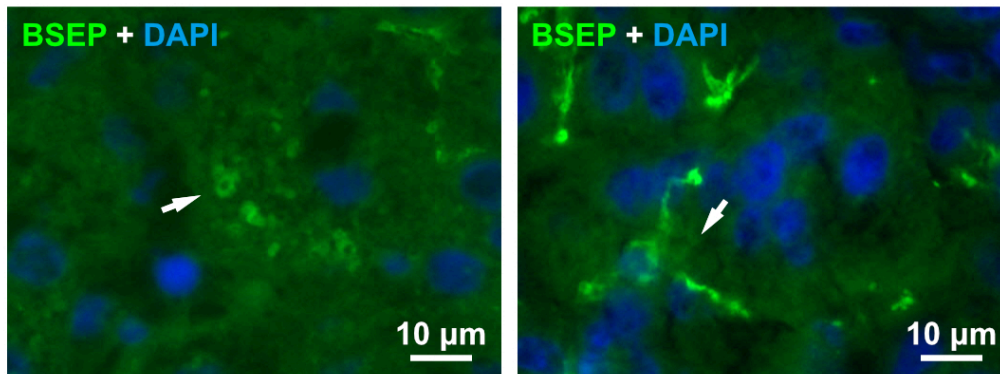
Figure 28 The distorted bile ducts, disturbed canalicular targeting of BSEP and dilated ZO-1 positive bile canaliculi in the livers with *PLEC* mutation.

(A) The distorted bile ducts in the cholestatic liver samples of *PLEC* mutations. Hematoxylin and eosin stained these two cholestatic patients' and control liver samples. The asterisk indicates the bile duct. (B) Impaired canalicular targeting of BSEP and dilated ZO-1-positive bile canaliculi in the hepatocytes with *PLEC* mutations. The paraffin-embedded liver sample sections were immunofluorescently stained for BSEP, MRP2, and ZO-1. The arrow indicates the aberrant canalicular BSEP and significantly increased cytoplasmic BSEP; the arrowhead indicates the dilated ZO-1-labeled bile canaliculi and increased cytoplasmic ZO-1 signals. Canalicular MRP2 staining was retained, and increased cytoplasmic signals were noted. Abbreviations: BSEP, bile salt export pump; CTL, control liver sample; DAPI, 4'-diamidino-2-phenylindole; m, month; MRP2, multidrug resistance protein 2; Pt, patient; y, years; ZO-1, zona occludens 1. This figure has been published in (Wu, Hsu et al. 2019).

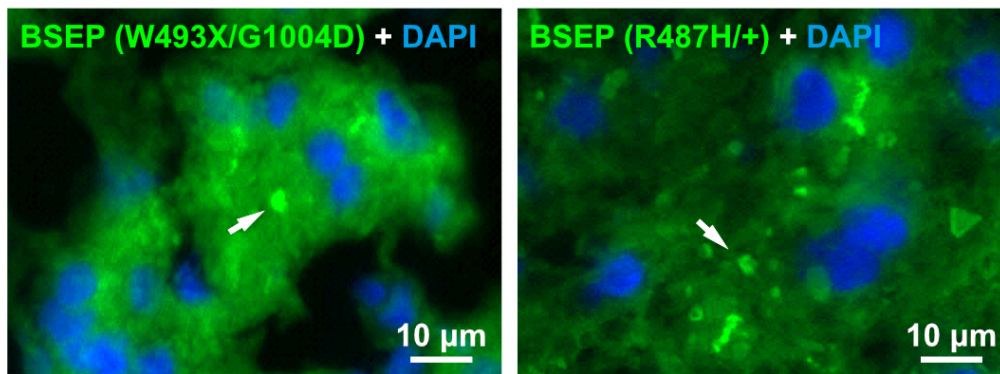


Appendix

A



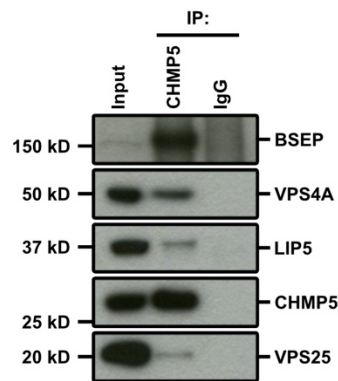
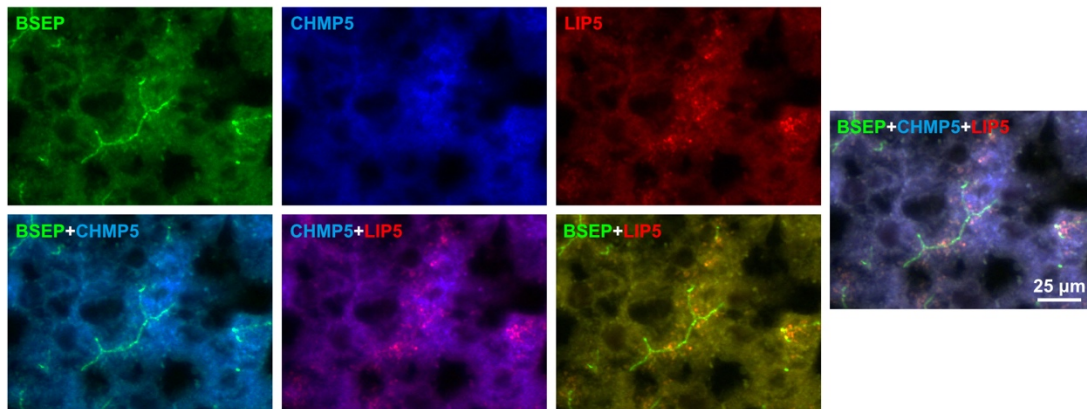
B



Appendix Figure 1 Aberrant subapical BSEP compartments in a patient's liver of neonatal hepatitis.

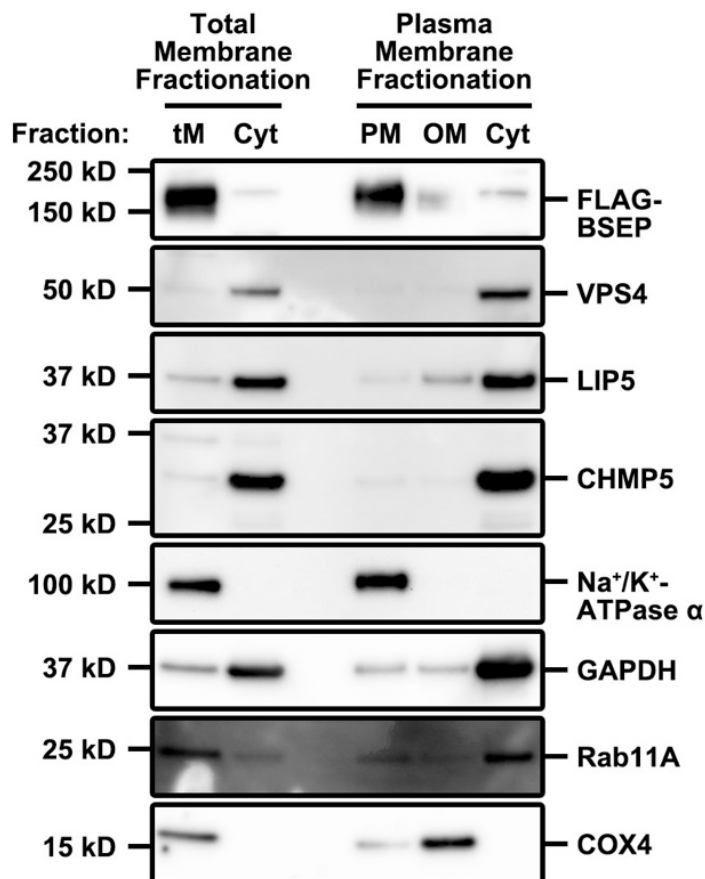
Immunofluorescence staining demonstrated BSEP in the human liver samples from (A) two patients with neonatal hepatitis and (B) two patients with BSEP mutations.

Cryosection of adult human liver samples was immunostained for BSEP (green). The liver nuclei were stained with DAPI. The arrow indicates the aberrant BSEP vesicles in the cytoplasm of these cholestatic liver samples.

A**B**

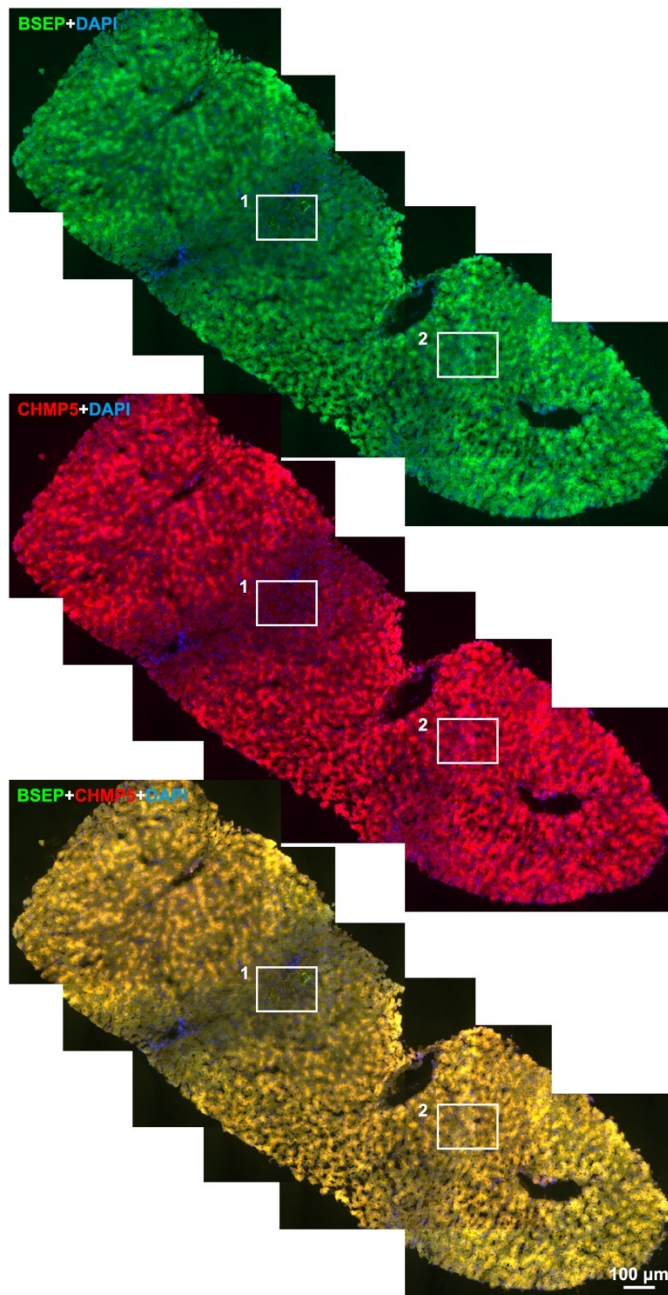
Appendix Figure 2 The ESCRT-III subunits CHMP5 and LIP5 co-localizes with BSEP-resident subapical compartments in adult human hepatocytes.

(A) BSEP was co-immunoprecipitated with CHMP5 and other ESCRT molecules from Hep G2 cells. Total cell lysate (25 μg) were loaded as an input control; normal mouse immunoglobulins (IgG) as a negative control. (B) Cryosections of the adult human livers were immunofluorescently stained for BSEP (green), CHMP5 (blue), and the CHMP5-interacting protein LIP5 (red).



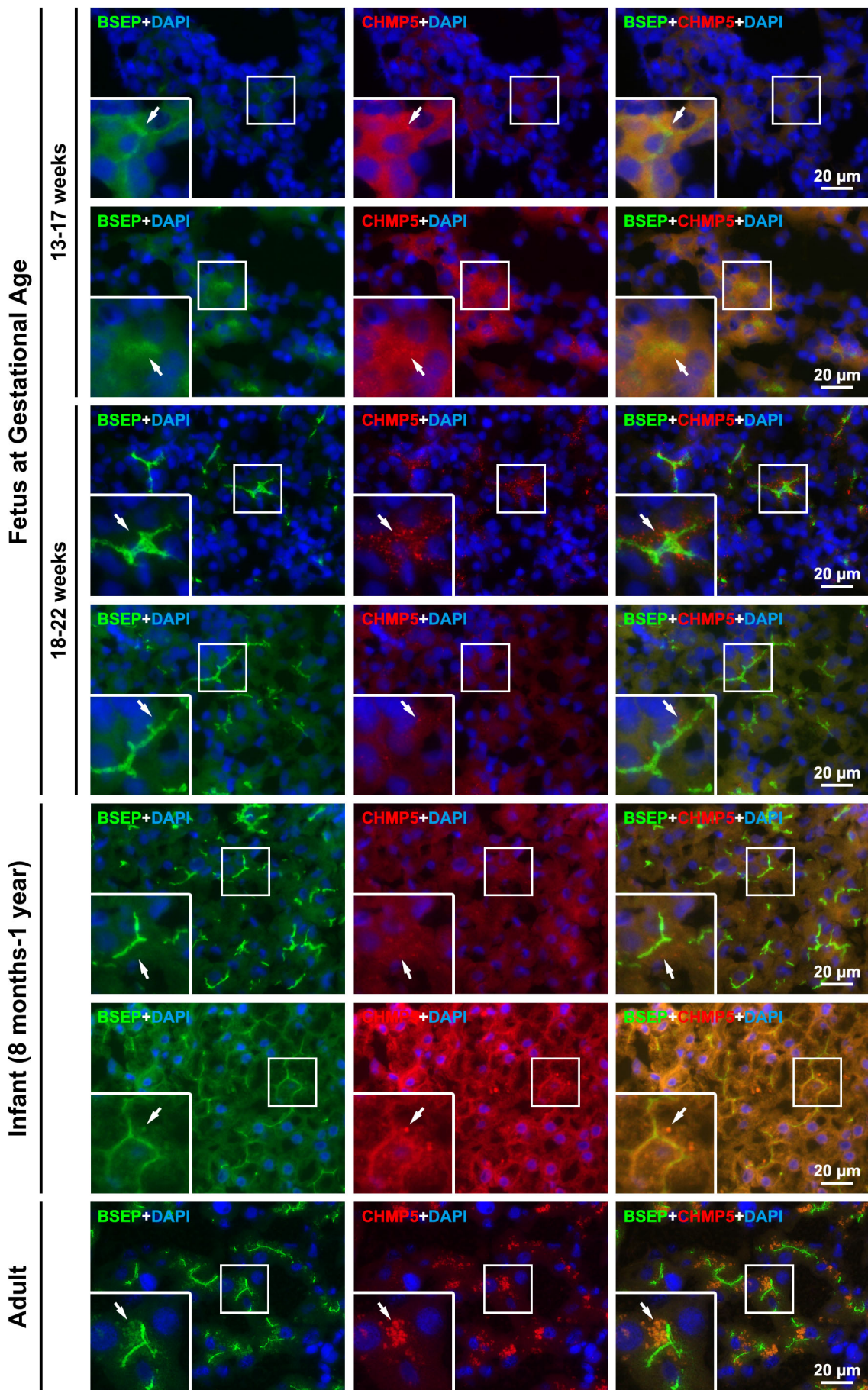
Appendix Figure 3 The total membrane-protein fraction contains the plasma-membrane plus organelle-membrane protein fractions.

Hep G2 cells were transfected with p3XFLAG-BSEP and then fractionated through two different fractionation methods. One is to isolate the total membrane-protein (tM) and the cytosolic (Cyt) fractions. The other is to fractionated into the plasma-membrane (PM), the organelle-membrane (OM), the cytosolic (Cyt) and the nuclear protein fractions. Each protein was probed via indicated antibodies. Na⁺/K⁺-ATPase α, COX4, and GAPDH were used as a PM, an OM, and a Cyt fractionation controls.



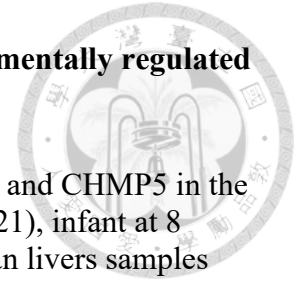
Appendix Figure 4 BSEP is retained at aberrant CHMP5-positive subapical compartments in a transient cholestatic human liver sample. (Related to Figure 14D)

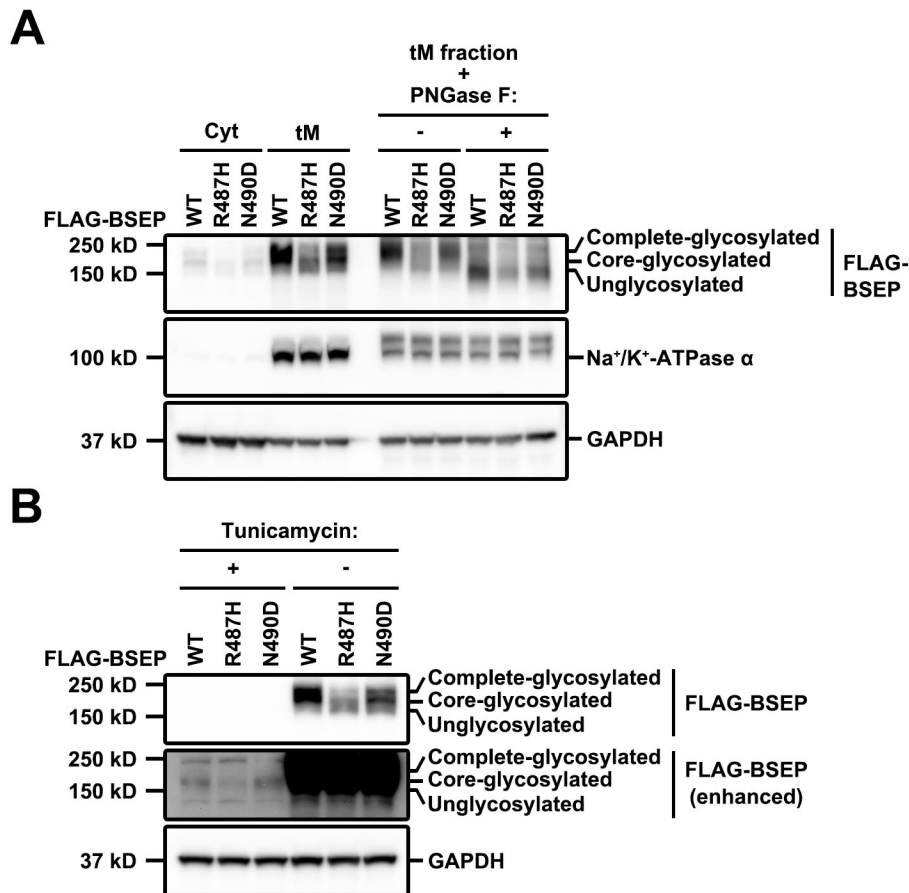
Immunofluorescence staining demonstrated the co-localization of subapical BSEP and CHMP5 in the cytoplasm of hepatocytes in a transient cholestatic liver sample. Cryosections of the human liver were immunofluorescently labeled with BSEP (green) and CHMP5 (red). The liver cell nuclei were stained with DAPI. Notably, a small region of hepatocytes reveals canalicular BSEP, but others show aggregated signals of BSEP and CHMP5 in the cytoplasm. The 200x images were manually integrated using the program Adobe Photoshop CS6. The white rectangles numbered are the similar area of the 400x images shown in Figure 14D.



Appendix Figure 5 The canalicular targeting of BSEP is developmentally regulated and very likely associated with CHMP5 in human livers.

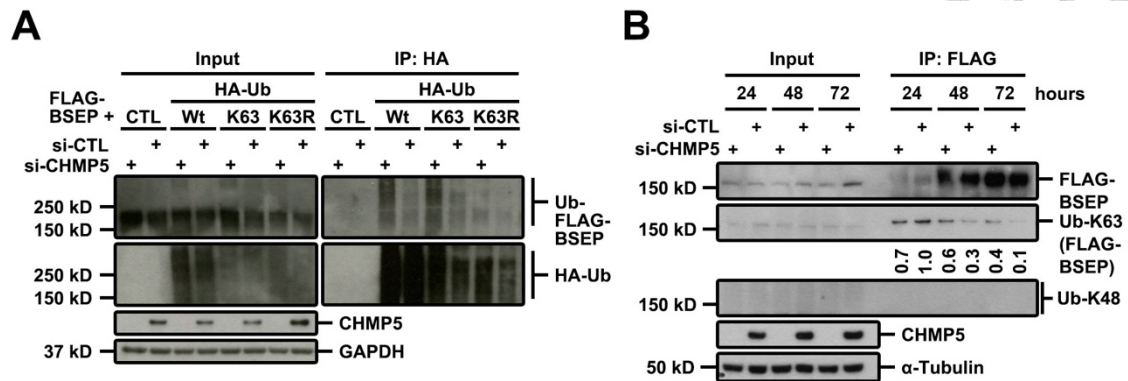
Immunofluorescence staining demonstrated the distribution of BSEP and CHMP5 in the human liver samples from fetus at gestational age 13-22 weeks (n = 21), infant at 8 months-1year (n = 4), and adult control (n = 3). Cryosection of human livers samples were immunostained for BSEP (green) and CHMP5 (red). The liver nuclei were stained with DAPI. Arrows indicate the different degree of CHMP5 that co-localizes with subapical BSEP.





Appendix Figure 6 The glycosylation patterns of BSEP-R487H and BSEP-N490D are different from that of wild type BSEP.

The *N*-linked glycosylation profiles of BSEP, BSEP-R487H and BSEP-N490D mutants were determined by **(A)** PNGase F and **(B)** tunicamycin treatments. **(A)** BSEP-R487H and BSEP-N490D harbored reduced complete-glycosylation. Hep G2 cells were ectopically expressed 3XFLAG-tagged BSEP wild type, R487H or N490D mutant for 24 hours and then fractionated into total membrane (tM) and cytosolic (Cyt) fractions. The tM fractions were subjected to PNGase F treatment. FLAG-tagged BSEP proteins were probed using anti-FLAG antibodies. Na⁺/K⁺-ATPase α and GAPDH were used as a membrane and a cytosolic control, respectively. **(B)** Immunoblotting reveals the *N*-linked glycosylation of BSEP and both BSEP mutants. Hep G2 cells were transfected with a plasmid expressing FLAG-BSEP, FLAG-BSEP-R487H, or BSEP-N490D and treated with tunicamycin (10 μg/mL) for 24 hours. Tunicamycin is an *N*-linked glycosylation inhibitor. Cell lysates were collected and analyzed via Western blot to detect FLAG-BSEPs using anti-FLAG antibodies. GAPDH was used as a loading control.



Appendix Figure 7 CHMP5 might regulate BSEP ubiquitination in an indirect manner.

(A) Immunoblotting reveals the accumulation of ubiquitinated BSEP in CHMP5 depleted cells. Hep G2 cells were pre-treated with a CHMP5-targeting (si-CHMP5) or the non-targeting control (si-CTL) siRNA pool, and subsequently subjected to the same experiment procedure described in Figure 20A. **(B)** Immunoblotting reveals the retarded de-ubiquitination of K63-linked ubiquitinated BSEP in CHMP5 depleted cells. Hep G2 with si-CHMP5 or si-CTL pre-treatment was transfected with p3XFLAG-BSEP for indicated times. Together with total cell lysate as input controls, FLAG-BSEP isolated via anti-FLAG antibodies was detected FLAG-BSEP, its K63-linked (Ub-K63) and K48-linked (Ub-K48) ubiquitin by using anti-FLAG, anti-K63- and anti-K48-linkage specific antibodies, respectively. Alpha-tubulin was the loading control. The values indicate the relative signal densities of Ub-K63 over FLAG-BSEP in immunoprecipitation results.

Appendix Table 1. The primer list

| Name | Sequence (5' to 3') |
|-------------------------|---|
| 3XFLAG-CHMP5-F | CAAGGATGACGATGACAAGCTTATGAACCGACTC TTCGGG |
| 3XFLAG-CHMP5-R | TAGAGTCGACTGGTACCCTATGAAGCAGGGATCT GTG |
| 3XFLAG-CHMP5-F | GATGACAAGCTTATGAACCGACTCTTCGGG |
| 3XFLAG-CHMP5-R | GACTGGTACCGACTATGAAGCAGGGATCTG |
| 3XFLAG-F | GATTACAAGGATGACGACGATAAGATCGATTACA AGGATGACGACGATAAGGTTTAAACGG |
| 3XFLAG-R | TCCCTTATCGTCGTCATCCTTGTAATCCTCGAGCG GCCGCGTACG |
| 3XFLAG-STOP-F | TAATAGTGAGGATCCCGGGTGG |
| 3XFLAG-STOP-R | TCACTATTAAAGCTTGTCATCGTCATCCT |
| 3XFLAG-F | GATGACAAGCTTTCTGACTCAGTAATTCTT |
| 3XFLAG-R | GACTGGTACCGATCAACTGATGGGGGATCC |
| ABCB11-61-99-F | GAGTCAGATAAATCATAACAATGATAAGAAAT CAAGG |
| ABCB11-61-99-R | CCTTGATTTCTTATCATTGTTGTATGATTTATCTGA CTC |
| ABCB11-eGFP-F | TCAGATCTCGAGCTCAAGCTTATGTCTGACTCAGT AATTCTTCG |
| ABCB11-eGFP-R | CCGGGCCCGCGGTACCGTACTGATGGGGGATCCA GTG |
| ABCB11-FP1 | GGGAGCTGAATACAAGATTCTCTG |
| ABCB11-FP2 | TGCAACTCATTTCAGCGATTC |
| ABCB11-FP3 | GTGCAGGAAGAAGTTGAACC |
| ABCB11-FP4 | TCTGCTTCCTACAGATATGG |
| ABCB11-FP5 | TTGTCATTGCCATCGCTTGTC |
| ABCB11(1122-1141)- R | CCAAACAAGGAGAGGCATTG |
| ABCB11(1448-1467)-F | GCCATGACATTCGCTCTCTT |
| ABCB11(1905-1924)-R | CTTCATGGGTCCCTCTTCC |
| ABCB11(2245-2264)-F | GCTCCAGAATGGCCCTACAT |
| ABCB11(2718-2737)- R | AAGCCAAGAAGGGGAAGAAG |
| ABCB11(3052-3072)-F | TTCAGGGTGATCTCTGCAGTT |
| ABCB11(3482-3501)- R | GGCAAACAACACTGGTTCCT |
| ABCB11(3666-3685)-F | GGAGAAACAACGCATTGCTA |
| ABCB11(372-391)-R | ACCCACAACGTGTTCCATTT |
| ABCB11(587-610)-R | CAGAGAATCTTGTATTCAGCTCCC |
| ABCB11(672-691)-F | GACCTCGACCATCTGTGGTT |
| BMRC-12 | CTACAGGAAAGAGTTACTCAAG |
| BMRC-9 | CCTTCGTCAGCAGAGCTTCACC |

| Name | Sequence (5' to 3') |
|--------------------|---|
| BSEP-del490-558-F | ATGAGTGGTGGCCAGAAAC |
| BSEP-del490-558-R | AAGAGAGCGAATGTCATGG |
| BSEP-FP-N-F | GAGCTCAAGCTTATGTCTGACTCAGTAATT |
| BSEP-FP-N-R | GGCCCGCGGTACCGTACTGATGGGGGATCCAGT |
| BSEP(1)-F | TTTGGAGAGGAGAATGATGGT |
| BSEP(1)-R | TTGAAAGAAGCCAACCTCTAACG |
| BSEP(2)-F | CTTCAAGACAGCCATTCAGAAA |
| BSEP(2)-R | CCTCATTGGAGATTAAGTAACCT |
| BSEP(351)-3HA-F | ATCTGCCGCCGCGATCGCCATGGAAGGAGAATAT ACACC |
| BSEP(375)-3HA-F | ATCTGCCGCCGCGATCGCCATGAATGCCTCTCCTT GTTTG |
| BSEP(4)-F | ACATGCTTGCGAGGACCTTTA |
| BSEP(4)-R | GGAGGTTCGTGCACCAGGTA |
| BSEP(413-590)-FN-F | TCAGATCTCGAGCTCAAGCTTCGCCACCATGTTGG ATCGAATCAAGG |
| BSEP(413-590)-FN-R | CCGGGCCCGCGGTACCGTGTTAAGAGAGCGAATG TCATG |
| BSEP(454-558)-FN-F | TCAGATCTCGAGCTCAAGCTTCGCCACCATGGTAG GACCCAGTGGAG |
| BSEP(454-558)-FN-R | CCGGGCCCGCGGTACCGTCTGGCCTCCTCCTTCTC C |
| BSEP(454)-3HA-R | TCGAGCGGCCGCGTACGCGTTACCAGAGCTGTCAT TTC |
| BSEP(484-558)-FN-F | TCAGATCTCGAGCTCAAGCTTCGCCACCATGCATG ACATTCGCTCTC |
| BSEP(484-558)-FN-R | CCGGGCCCGCGGTACCGTCTGGCCTCCTCCTTCTC C |
| BSEP(490-590)-FN-F | TCAGATCTCGAGCTCAAGCTTCGCCACCATGAACA TTCAGTGGCTTAGAGATC |
| BSEP(490-590)-FN-F | TCAGATCTCGAGCTCAAGCTTCGCCACCATGAACA TTCAGTGGCTTAGAG |
| BSEP(490-590)-FN-R | CCGGGCCCGCGGTACCGTGTCCAGAGCTGAGGTG GC |
| BSEP(490-590)-FN-R | CCGGGCCCGCGGTACCGTGTCCAGAGCTGAGGTG G |
| BSEP(5)-F | GGGCCATTGTACGAGATCCTAA |
| BSEP(5)-R | TGCACCGTCTTTTCACTTTCTG |
| BSEP(569-815)-FN-F | TCAGATCTCGAGCTCAAGCTTCGCCACCATCGCCA GAGCCCTCATC |
| BSEP(569-815)-FN-F | TCAGATCTCGAGCTCAAGCTTCGCCACCATGATCG CCAGAGCCCTC |
| BSEP(569-815)-FN-R | CCGGGCCCGCGGTACCGTTAGAAATTGGGTGAAA AGAGATACAC |
| BSEP(569)-3HA-F | ATCTGCCGCCGCGATCGCCATGATCGCCAGAGCCC TC |

| Name | Sequence (5' to 3') |
|--------------------|--|
| BSEP(680)-3HA-R | TCGAGCGGCCGCGTACGCGTCCTCGCAAGCATGTC ATC |
| BSEP(815)-3HA-R | TCGAGCGGCCGCGTACGCGTTAGAAATTGGGTGA AAAGAGATACAC |
| BSEP(N490D)-EGFP-F | TCAGATCTCGAGCTCAAGCTTCGCCACCATGCATG ACATTCGCTCTCTTGAC |
| BSEP(N490D)-EGFP-R | CCGGGCCCGCGGTACCGTCTGGCCTCCTCCTTCTC C |
| BSEP#413-490-F | ATCTGCCGCCGCGATCGCCATGTTGGATCGAATCA AGG |
| BSEP#413-490-R | TCGAGCGGCCGCGTACGCGTTAAGAGAGCGAATG TCATG |
| BSEP#413-490-R-2 | TCGAGCGGCCGCGTACGCGTGTTAAGAGAGCGAA TGTCATG |
| BSEP#454-558-F | ATCTGCCGCCGCGATCGCCATGGTAGGACCCAGT GGAG |
| BSEP#454-558-R | TCGAGCGGCCGCGTACGCGTCTGGCCTCCTCCTTC TCC |
| BSEP#484-558-F | ATCTGCCGCCGCGATCGCCATGCATGACATTCGCT CTC |
| BSEP#484-558-R | TCGAGCGGCCGCGTACGCGTCTGGCCTCCTCCTTC TCC |
| BSEP#490-590-F | ATCTGCCGCCGCGATCGCCATGAACATTCAGTGGC TTAGAGATC |
| BSEP#490-590-R | TCGAGCGGCCGCGTACGCGTGTCAGAGCTGAGG TGGC |
| CHMP5-3'-F | GTGAACTTGCGGGGTTTTTCA |
| CHMP5-3'-R | GATGGAGTTCTGGTGGATGAA |
| CHMP5-3XDDK-F | ATCTGCCGCCGCGATCGCCATGAACCGACTCTTCG GG |
| CHMP5-3XDDK-R | TCGAGCGGCCGCGTACGCGTTGAAGCAGGGATCT GTGG |
| CHMP5-5'-F | TTCATCCACCAGAACTCCATC |
| CHMP5-5'-R | CTATTCGATGATGAAGATAACCCCA |
| CHMP5-FP-N-F | GAGCTCAAGCTTATGAACCGACTCTTCGGG |
| CHMP5-FP-N-R | GGCCCGCGGTACCGTTGAAGCAGGGATCTGTGG |
| CHMP5-HcRed-F | TCAGATCTCGAGCTCAAGCTTATGAACCGACTCTT CGG |
| CHMP5-HcRed-R | CCGGGCCCGCGGTACCGTTGAAGCAGGGATCTGT GG |
| ECFP-C1-F | GATCCGCTAGCGCTACCGGTCGCCACCATGGTGA GCAAGGGCGAG |
| ECFP-C1-R | CCGCCTCCGCCTCGAGATCTTCCGGACTCCTTGTA CAGCTCGTCCATGC |
| ECFP/Venus-R | ATCCGAGCTCGGTACCTTACTTGTACAGCTCGTCC ATGC |
| eGFP-ABCB11-F | TCAGATCTCGAGCTCAAGCTTCATGTCTGACTCAG TAATTCTTC |

| Name | Sequence (5' to 3') |
|---------------------|--|
| eGFP-ABCB11-R | CCGGGCCCGCGGTACCCTCAACTGATGGGGGATCC |
| EGFP-BSEP-F | AGCTCAAGCTTCATGTCTGACTCAGTAATT |
| EGFP-BSEP-R | CCCGCGGTACCGACTGATGGGGGATCCAGT |
| EGFP-BSEP(N490D)-F | TCAGATCTCGAGCTCAAGCTTCGCATGACATTCGC TCTCTTGAC |
| EGFP-BSEP(N490D)-R | CCGGGCCCGCGGTACCCTGGCCTCCTCCTTCTCC |
| EGFP-BSEP(R487H)-F | GACATTCACTCTCTTAACATTCAGTGG |
| EGFP-BSEP(R487H)-R | AAGAGAGTGAATGTCATGCGAAG |
| EGFP-C-F | CACATGGTCCTGCTGGAGTTC |
| EGFP-C-R | GAACTCCAGCAGGACCATGTG |
| EGFP-CHMP5-F | AGCTCAAGCTTCATGAACCGACTCTTCGGG |
| EGFP-CHMP5-R | CCCGCGGTACCGTGAAGCAGGGATCTGTGG |
| EGFP-Kozak-ABCB11-F | TCAGATCTCGAGCTCAAGCTTCGCCACCATGTCTG ACTC |
| EGFP-Kozak-ABCB11-R | CCGGGCCCGCGGTACCGTACTGATGGGGGATCCA GTG |
| EGFP-N-F | CGACGTAAACGGCCACAAGT |
| EGFP-N-R | ACTTGTGGCCGTTTACGTCG |
| FN-C1-ABCB11-F | TCAGATCTCGAGCTCAAGCTTCGATGTCTGACTCA GTAATTCTTC |
| FN-LK-C1-ABCB11-F | TGGCGGCTCCGCTCAAGCTTCGATGTCTGACTCAG TAATTCTTC |
| FP-BSEP-270-F | TCAGATCTCGAGCTCAAGCTTCGGAGCTGAAGGC CTATGCC |
| FP-BSEP-350-R | CCGGGCCCGCGGTACCATCCAGGACAAGTGTGGA G |
| FP-BSEP-351-F | TCAGATCTCGAGCTCAAGCTTCGGAAGGAGAATA TACACCAGG |
| FP-BSEP-375-F | TCAGATCTCGAGCTCAAGCTTCGAATGCCTCTCCT TGTTTG |
| FP-BSEP-413-F | TCAGATCTCGAGCTCAAGCTTCGTTGGATCGAATC AAGGGTG |
| FP-BSEP-454-F | TCAGATCTCGAGCTCAAGCTTCGGTAGGACCCAGT GGAGCT |
| FP-BSEP-454-R | CCGGGCCCGCGGTACCTACCAGAGCTGTCATTTTC |
| FP-BSEP-484-F | TCAGATCTCGAGCTCAAGCTTCGCATGACATTCGC TCTCTTAACATTC |
| FP-BSEP-490-F | TCAGATCTCGAGCTCAAGCTTCGAACATTCAGTGG CTTAGAGATCAG |
| FP-BSEP-490-R | CCGGGCCCGCGGTACCGTTAAGAGAGCGAATGTC ATG |
| FP-BSEP-490-R | CCGGGCCCGCGGTACCGTTAAGAGAGCGAATGTC ATG |
| FP-BSEP-491-F | TCAGATCTCGAGCTCAAGCTTCGATTCAGTGGCTT AGAGATCAG |

| Name | Sequence (5' to 3') |
|-------------------|--|
| FP-BSEP-558-R | CCGGGCCCGCGGTACCCTGGCCTCCTCCTTCTCC |
| FP-BSEP-569-F | TCAGATCTCGAGCTCAAGCTTCGATCGCCAGAGCC CTCATC |
| FP-BSEP-590-R | CCGGGCCCGCGGTACCGTCCAGAGCTGAGGTGGC |
| FP-BSEP-680-R | CCGGGCCCGCGGTACCCCTCGCAAGCATGTCATC |
| FP-BSEP-815-R | CCGGGCCCGCGGTACCTAGAAATTGGGTGAAAAG AGATACAC |
| FP-Rab11A-F | GGACTCAGATCTCGAGCTCAAGCTTCGATGGGCA CCCGCGACGAC |
| FP-Rab11A-R | GGATCCCGGGCCCGCGGTACCTTAGATGTTCTGAC AGCACTGCACCTTTG |
| FP-VPS4B-F | TCAGATCTCGAGCTCAAGCTTCGATGTCATCCACT TCGCCC |
| FP-VPS4B-R | CCGGGCCCGCGGTACCTTAGCCTTCTTGACCAAAA TC |
| h-BSEP(1)-F | TGGTGAGAAAAGAGAGGTTGA |
| h-BSEP(1)-R | CGAATCCAGTAAAGAATCCCAT |
| h-BSEP(2)-F | CTTCAAGACAGCCATTCAGAAA |
| h-BSEP(2)-R | GAGCCCCTCATTGGAGATTA |
| h-BSEP(3)-F | AAAGGTCACAGATCAATGGT |
| h-BSEP(3)-R | CCCAGATTTAGCAAAGGCATA |
| h-BSEP(paper)-F | TGAGCCTGGTCATCTTGTG |
| h-BSEP(paper)-R | TCCGTAATATTGGCTTTCTG |
| h-CHMP5-F | TATGGTCAAGCAGAAAGCCT |
| h-CHMP5-R | TCCTTCAAAGACTGGATGGTA |
| h-CHMP5(paper)-F | CAGAAAGCCTTGCGAGTT |
| h-CHMP5(paper)-R | ACCGTGGTCTTGGTGTCC |
| h-GAPDH-F | CATTTCTGGTATGACAACG |
| h-GAPDH-R | CAGTGAGGGTCTCTCTCTTC |
| h-β-actin(ACTB)-F | ACCACACCTTCTACAATGAG |
| h-β-actin(ACTB)-R | TAGCACAGCCTGGATAGCAA |
| HcRed-BSEP-F | GCTCAAGCTTCGATGTCTGACTCAGTAATT |
| HcRed-BSEP-R | GCCCCGCGGTACCACTGATGGGGGATCCAGT |
| HcRed-CHMP5-F | GCTCAAGCTTCGATGAACCGACTCTTCGGG |
| HcRed-CHMP5-F | TCAGATCTCGAGCTCAAGCTTCGATGAACCGACTC TTCGGG |
| HcRed-CHMP5-R | GCCCCGCGGTACCTGAAGCAGGGATCTGTGG |
| HcRed-CHMP5-R | CCGGGCCCGCGGTACCGCTATGAAGCAGGGATCT GTG |
| hw-DDX5-F | CTTGTCTTGATGAAGCAGA |
| hw-DDX5-R | AGTCGCACTCCACATTAG |
| mCherry-C-F | ACAACGAGGACTACACCATC |
| mCherry-N-R | CTTGGTCACTTCAGCTTGG |
| mCherry-VPS4A-F | TCAGATCTCGAGCTCAAGCTTCGATGACAACGTCA ACCCTC |

| Name | Sequence (5' to 3') |
|-------------------------------|--|
| mCherry-VPS4A-R | CCGGGCCCGCGGTACCGTAACTCTCTTGCCCAA G |
| mito-ECFP-F | GGCTAGCGTTTAAACTTAAGCTTCGCCACCATGTC CGTCCTGACGCCG |
| myr-Venus-F | GGCTAGCGTTTAAACTTAAGCTTCGCCACCATGGG AAGCAG |
| pACT2-CHMP5-V-F | TGGGGTATCTTCATCATCGAATAG |
| pACT2-CHMP5-V-R | TGAAAAACCCCGCAAGTTCAC |
| pBTM116-BSEP(270)- F | GCTGGAATTCCCGGGGATCCGTGAGCTGAAGGCC TATGCC |
| pBTM116-BSEP(375)- F | GCTGGAATTCCCGGGGATCCGTAATGCCTCTCCTT GTTTG |
| pBTM116- BSEP(484;N490D)-F | GCTGGAATTCCCGGGGATCCGTCATGACATTGCT CTCTTGAC |
| pBTM116- BSEP(484;R487H)-F | GCTGGAATTCCCGGGGATCCGTCATGACATTCCT CTCTTAACATTCAG |
| pBTM116-BSEP(490)- F | GCTGGAATTCCCGGGGATCCGTAACATTCAGTGGC TTAGAGATCAG |
| pBTM116-BSEP(491)- F | GCTGGAATTCCCGGGGATCCGTATTCAGTGGCTTA GAGATCAG |
| pBTM116-BSEP(558)- R | TAGCTTGGCTGCAGGTCGACTCACTGGCCTCCTCC TTCTCC |
| pBTM116-BSEP(569)- F | GCTGGAATTCCCGGGGATCCGTATCGCCAGAGCC CTCATC |
| pBTM116-BSEP(680)- R | TAGCTTGGCTGCAGGTCGACTCACCTCGCAAGCAT GTCATC |
| pCAG-F | TTCCTACTTGGCAGTACATC |
| pcDNA3.1(+)-HA-F | GCCACCATGTACCCATACGATGTTCCGGATTACGC TGGTACCGAGCTCGGATCCACTAG |
| pcDNA3.1(+)-HA-R | AGCGTAATCCGGAACATCGTATGGGTACATGGTG GCAAGCTTAAGTTTAAACGCTAGCCA |
| pCMV6-ABCB11-1 | ATCTGCCGCCGCGATCGCATGTCTGACTCAGTAAT TCTTCG |
| pCMV6-ABCB11-2 | ATCTGCCGCCGCGATCGCCATGTCTGACTCAGTAA TTCTTCG |
| pCMV6-ABCB11-3 | ATCTGCCGCCGCGATCGCCGATGTCTGACTCAGTA ATTCTTCG |
| pCMV6-ABCB11-R | TCGAGCGGCCGCGTACGCGTACTGATGGGGGATC CAGTG |
| pEGFP-ABCB11- linker-F | GATCTCGAGCGGCGGAGGCGGATCCGGTGGTGGC GGCTCTGGAGGTGGCGGCTCCTCA |
| pEGFP-ABCB11- linker-R | AGCTTGAGGAGCCGCCACCTCCAGAGCCGCCACC ACCGGATCCGCCTCCGCCGCTCGA |
| pEGFP-R | AAGCTGCAATAACAAGTTAACAACAACAATT |
| pFP-N-linker-F | CGGGATGGCGGAGGCGGATCCGGTGGTGGCGGCT CTGGAGGTGGCGGCTCCCCA |
| pFP-N-linker-R | CCGGTGGGGAGCCGCCACCTCCAGAGCCGCCACC ACCGGATCCGCCTCCGCCATCCCGGGCC |

| Name | Sequence (5' to 3') |
|--------------------------------|--|
| pHcRed-CHMP5-linker-F | GATCTCGAGGCGGAGGCGGATCCGGTGGTGGCGGCTCTGGAGGTGGCGGCTCCGCTCA |
| pHcRed-CHMP5-linker-R | AGCTTGAGCGGAGCCGCCACCTCCAGAGCCGCCA CCACCGGATCCGCCTCCGCCTCGA |
| pLKO-shRNA-F | ACAAAATACGTGACGTAG |
| pLKO-shRNA-R | CTGTTGCTATTATGTCTAC |
| pTRE-Tightseq-F | TATGTCGAGGTAGGCGTGTACGG |
| SDM-BSEP-559-F | TCTCTTATGAGTGGTGGCCAGAAACAAACAA |
| SDM-BSEP-559-R | ACCACTCATAAGAGAGCGAATGTCATGGCC |
| SDM-BSEP-FL-N490D-F | CTCTCTTGACATTCAGTGGCTTAGAG |
| SDM-BSEP-FL-N490D-R | TGAATGTCAAGAGAGCGAATGTCA |
| SDM-BSEP-FL-R487H-R | AAGAGAGTGAATGTCATGGCCATC |
| SDM-EGFP-LK-ABCB11-F | CGGCTCTGGAGGTGGCGGCTCCTCAAGCTTCATGTCTGACTC |
| SDM-EGFP-LK-ABCB11-R | CCACCACCGGATCCGCCTCCGCCGCTCGAGATCTGAGTCCG |
| SDM-HcRed-LK-CHMP5-F | CGGCTCTGGAGGTGGCGGCTCCGCTCAAGCTTCGATGAAC |
| SDM-HcRed-LK-CHMP5-R | CCACCACCGGATCCGCCTCCGCCTCGAGATCTGAGTCCGGAG |
| SDM-pABCB11-eGFP-F | ACCATGTCTGACTCAGTAATTCTTC |
| SDM-pABCB11-eGFP-R | AAGCTTGAGCTCGAGATC |
| SDM-pBSEP(484-558;R487H)-3HA-R | AAGAGAGTGAATGTCATGCATGGC |
| SDM-pBSEP(484-558)-3HA-F | TCGCTCTCTTGACATTCAGTG |
| SDM-pBSEP(484-558)-3HA-R | ATGTCATGCATGGCGATC |
| SDM-pCHMP5-HcRed-F | ACCATGAACCGACTCTTCGGG |
| SDM-pCHMP5-HcRed-R | AAGCTTGAGCTCGAGATC |
| SDM-Rab11A-Q70L-F | AGCAGGGCTAGAGCGATATCGAGCTATAACATC |
| SDM-Rab11A-Q70L-R | CGCTCTAGCCCTGCTGTGTCCCATATC |
| SDM-Rab11A-S25N-F | TGGAAAGAATAATCTCCTGTCTCGATTTACTCGA |
| SDM-Rab11A-S25N-R | AGATTATTCTTTCCAACACCAGAATCTCCAA |
| SDM-si-CHMP5#12-F | CGTTAAATACAAAGACCAGATCAAGAAGATGAGAGAGGGTCCCTG |
| SDM-si-CHMP5#12-R | TCTTTGTATTTAACGAGCTCAGCATCCAATCGAGAAATC |
| SDM-si-CHMP5#9-F | TAAACAGGTCAAATAGACCAGATTGAGGATTTACAAGACCAGC |

| Name | Sequence (5' to 3') |
|-------------------|--|
| SDM-si-CHMP5#9-R | ATTTTGACCTGTTTATATGCCTTCTTCATTTCCCTTT ACTCCC |
| SDM-TATA-F | CAATGATAAGAAATCAAGGTTACAAGATGAGAAG AAAGGTG |
| SDM-TATA-R | TTGTATGATTTATCTGACTCAAACCATCATTCTC CTCTC |
| SDM-Ub-K29-F | ATCTTCGTGAAGACGTAAACCGGTAAAACC |
| SDM-Ub-K29-R | CGTCTTCACGAAGATCTGCATGGTCGA |
| SDM-Ub-K48R-F | CTTTGCTGGGAGGCAGCTGGAAG |
| SDM-Ub-K48R-R | ATCAACCTCTGCTGGTCAG |
| SDM-Ub-K63R-F | CAACATCCAGAGGGAGTCCACCCTG |
| SDM-Ub-K63R-F | ATTCAGAGGGAGTCCACCCTGCACCTG |
| SDM-Ub-K63R-R | TAGTCAGACAGGGTGCGT |
| SDM-Ub-K63R-R | GGACTCCCTCTGAATGTTGTAATCAGACAG |
| SDM-Ub-L73P-F | CCTCCGTCCCAGAGGTGGTTGAGCGGCC |
| SDM-Ub-L73P-R | CCTCTGGGACGGAGGACCAGGTGCAG |
| SDM-Ub-R48K-F | GCCGGTAAACAGCTCGAGGACGGTAGA |
| SDM-Ub-R48K-R | GAGCTGTTTACCGGCAAAGATCAATCTTTG |
| SDM-VPS4A-Q173K-F | ACAGGGCAATCCTACCTGGCCAAAGCCG |
| SDM-VPS4A-Q173K-R | GTAGGATTGCCCTGTGCCAGGGGGT |
| SDM-VPS4A-Q228E-F | ATCGATCAGGTGGATTCCCTCTGCGG |
| SDM-VPS4A-Q228E-R | ATCCACCTGATCGATGAAGATGATGGAGGGCTTG |
| SDM-VPS4B-K180Q-F | GAACAGGACAGTCCTACTTAGCCAAAGCTGTAGC |
| SDM-VPS4B-K180Q-R | AGGACTGTCCTGTTCCAGGCGGCC |
| SDM-VPS4B-K235Q-F | TCATTGATCAAATTGATTCTCTCTGTGGTTCAAG |
| SDM-VPS4B-K235Q-R | CAATTTGATCAATGAAGATAATGGAGGGCTTG |
| SV40-poly-A-F | GGACAAACCACAACCTAGAATGCAG |
| SV40-poly-A-R | CTGCATTCTAGTTGTGGTTTGTCC |
| Ub-K48R-F | AATGGTGGTGGTGGTGGGTCGACCATGCAGATCTT CGTCAAG |
| Ub-K48R-R | GATCCTTACTTACTTAGCGGCCGCTCAACCACCTC TTAGTCTTAAGAC |
| VP1.5 | GGACTTCCAAAATGTCTG |
| XL39 | ATTAGGACAAGGCTGGTGGG |

Appendix Table 2. All plasmids constructed and used in the dissertation



| Clone | Note |
|-----------------------------|--|
| pBTM116#1 | A bait vector for Y2H |
| pcDNA3.1 (+) | |
| p3XFLAG-CMV10 | |
| pCMV6-AC-3DDK | Cloned from pCMV6-AC-Myc-DDK |
| pCMV6-AC-Myc-DDK | |
| pCMV6-AC-3HA | |
| pECFP-C1 | Cloned from pCAG-mito-ECFP |
| pVenus-C1 | Cloned from pCAG-myr-Venus |
| pEGFP-C1 | |
| pEGFP-C2 | |
| pEGFP-N1/1 | |
| pmCherry-C1 | |
| pmCherry-N1 | |
| pHcRed1-C2 | |
| pHcRed1-N1/1 | |
| p3XFLAG-STOP | SDM of p3XFLAG-CMV10 to remove MCS |
| sh-Chmp5 (TRCN9719) | shRNA targeting mouse Chmp5 from RNAi core |
| sh-Chmp5 (TRCN9720) | shRNA targeting mouse Chmp5 from RNAi core |
| sh-Chmp5 (TRCN9721) | shRNA targeting mouse Chmp5 from RNAi core |
| sh-Chmp5 (TRCN9722) | shRNA targeting mouse Chmp5 from RNAi core |
| sh-Chmp5 (TRCN9723) | shRNA targeting mouse Chmp5 from RNAi core |
| TRC005 | Vector control from RNAi core |
| pLAS-Void | Scramble control from RNAi core |
| sh-Luc | From Dr. Tsue |
| sh-HA | From Dr. Tsue |
| sh-Lamin#1 | From Dr. Tsue |
| sh-CHMP5-1 | Purchased from Quiagen |
| sh-CHMP5-2 | Purchased from Quiagen |
| sh-CHMP5-3 | Purchased from Quiagen |
| sh-CHMP5-4 | Purchased from Quiagen |
| sh-CTL | Purchased from Quiagen |
| pcDNA3.1 (+)-DsRed2-ER | |
| pcDNA3.1 (+)-Mem-DsRed-Mono | |
| pCAG-mito-ECFP | |
| pcDNA3.1(+)-mito-ECFP | |
| pCAG-myr-Venus | |
| pcDNA3.1(+)-myr-Venus | |
| pTOPO- β -Actin | for qPCR |
| pTOPO-DDX5 | for qPCR |
| pTOPO-GAPDH | for qPCR |
| pTOPO-GAPDH-3'UTR | human full-length GAPDH containing 3'UTR |
| pBTM116-ABCB11 (270-350) | |



| Clone | Note |
|--------------------------------|------|
| pBTM116-ABCB11 (270-490) | |
| pBTM116-ABCB11 (270-680) | |
| pBTM116-ABCB11 (270-815) | |
| pBTM116-ABCB11 (351-454) | |
| pBTM116-ABCB11 (375-680) | |
| pBTM116-ABCB11 (413-490) | |
| pBTM116-ABCB11 (484-558) | |
| pBTM116-ABCB11 (484-558;R487H) | |
| pBTM116-ABCB11 (484-558;N490D) | |
| pBTM116-ABCB11 (490-558) | |
| pBTM116-ABCB11 (490-590) | |
| pBTM116-ABCB11 (491-680) | |
| pBTM116-ABCB11 (491-815) | |
| pBTM116-ABCB11 (569-680) | |
| pBTM116-ABCB11 (569-815) | |
| pACT2-CHMP5 | |
| pBSEP (413-490)-Myc-DDK | |
| pBSEP (454-558)-Myc-DDK | |
| pBSEP (484-558)-Myc-DDK | |
| pBSEP (490-590)-Myc-DDK | |
| pBSEP (413-490)-3DDK | |
| pBSEP (454-558)-3DDK | |
| pBSEP (484-558; R487H)-3DDK | |
| pBSEP (484-558; N490D)-3DDK | |
| pBSEP (490-590)-3DDK | |
| pBSEP (351-454)-3HA | |
| pBSEP (375-454)-3HA | |
| pBSEP (413-490)-3HA | |
| pBSEP (484-558)-3HA | |
| pBSEP (484-558; R487H)-3HA | |
| pBSEP (484-558; N490D)-3HA | |
| pBSEP (569-680)-3HA | |
| pBSEP (569-815)-3HA | |
| pBSEP (413-490)-EGFP | |
| pBSEP (454-558)-EGFP | |
| pBSEP (484-558)-EGFP | |
| pBSEP (484-558; N490D) | |
| pBSEP (490-558)-EGFP | |
| pBSEP (490-590)-EGFP | |
| pBSEP (569-815)-EGFP | |
| pEGFP-BSEP (270-350) | |
| pEGFP-BSEP (270-490) | |
| pEGFP-BSEP (270-680) | |
| pEGFP-BSEP (351-454) | |
| pEGFP-BSEP (375-454) | |
| pEGFP-BSEP (375-490) | |
| pEGFP-BSEP (375-680) | |



| Clone | Note |
|-----------------------------|--|
| pEGFP-BSEP (375-815) | |
| pEGFP-BSEP (413-490) | |
| pEGFP-BSEP (454-558) | |
| pEGFP-BSEP (484-558) | |
| pEGFP-BSEP (484-558; R487H) | |
| pEGFP-BSEP (484-558; N490D) | |
| pEGFP-BSEP (490-558) | |
| pEGFP-BSEP (491-680) | |
| pEGFP-BSEP (491-815) | |
| pEGFP-BSEP (569-680) | |
| pEGFP-BSEP (569-815) | |
| pTRE-Tight-Spgp | From Dr. Victor Ling |
| pTRE-ABCB11 | Cryptic promoter inactivated |
| p3XFLAG-ABCB11 | |
| p3XFLAG-BSEP-R487H | |
| p3XFLAG-BSEP-N490D | |
| pEGFP-ABCB11 | |
| pEGFP-LK-ABCB11 | |
| pEGFP-LK-BSEP-R487H | |
| pEGFP-LK-BSEP-N490D | |
| pmCherry-LK-BSEP | |
| pHcRed1-CHMP5 | |
| pCHMP5-HcRed1 | |
| pHcRed1-LK-CHMP5 | |
| pmCherry-CHMP5 | |
| pmCherry-LK-CHMP5 | |
| pmCherry-LK-CHMP5-resc. | si-CHMP5 targeting sequences inactivated |
| pECFP-LK-CHMP5 | |
| pVenus-LK-CHMP5 | |
| pEGFP-CHMP5 | |
| p3XFLAG-CHMP5 | |
| pCHMP5-3DDK | |
| pCHMP5-3HA | |
| pmCherry-VPS4A | |
| pmCherry-VPS4A-E173Q | VPS4A-E173Q |
| pmCherry-VPS4A-K228Q | VPS4A-K228Q |
| pmCherry-VPS4A-K173/E228Q | VPS4A-K173Q+E228Q |
| pEGFP-VPS4B | |
| pEGFP-VPS4B-K180Q | Cloned from pEGFP-VPS4B |
| pEGFP-VPS4B-E235Q | Cloned from pEGFP-VPS4B |
| pmCherry-VPS4B | |
| pmCherry-VPS4B-K180Q | Cloned from pmCherry-VPS4B |
| pmCherry-VPS4B-E235Q | Cloned from pmCherry-VPS4B |
| p3XFLAG-NTCP | |
| pmCherry-NTCP | |
| pCMV-HA-Ub | |
| pMyc-Ub-K48 | |
| pRK5-HA-Ub-WT | Addgene#17608 |
| pRK5-HA-Ub-K11 | Addgene#22901 |

| Clone | Note |
|-------------------------|--------------------------------|
| pRK5-HA-Ub-K29 | Addgene#22903 |
| pRK5-HA-Ub-K29R | Addgene#17602 |
| pRK5-HA-Ub-K48 | Addgene#17605 |
| pRK5-HA-Ub-K48R | Addgene#17604 |
| pRK5-HA-Ub-K63 | Addgene#17606 |
| pRK5-HA-Ub-K63R | Cloned from pRK5-HA-Ub-WT |
| pRK5-HA-Ub-K48/63R | Cloned from pRK5-HA-Ub-K48R |
| pRK5-HA-Ub-K0 | Addgene#17603 |
| pRK5-HA-Ub-L73P | Cloned from pRK5-HA-Ub-WT |
| pRK5-HA-Ub-K48-L73P | Cloned from pRK5-HA-Ub-K48 |
| pRK5-HA-Ub-K48R-L73P | Cloned from pRK5-HA-Ub-K48R |
| pRK5-HA-Ub-K63-L73P | Cloned from pRK5-HA-Ub-K63 |
| pRK5-HA-Ub-K63R-L73P | Cloned from pRK5-HA-Ub-K63R |
| pRK5-HA-Ub-K48/63R-L73P | Cloned from pRK5-HA-Ub-K48/63R |
| pEGFP-Rab11A | |
| pEGFP-Rab11A-S25N | Cloned from pEGFP-Rab11A#4 |
| pEGFP-Rab11A-Q70L | Cloned from pEGFP-Rab11A#4 |
| pmCherry-Rab11A | |
| pmCherry-Rab11A-S25N | Cloned from pmCherry-Rab11A#2 |
| pmCherry-Rab11A-Q70L | Cloned from pmCherry-Rab11A#2 |



Appendix Table 3. The publication during the PhD program



Wu SH, Hsu JS, Chen HL, Chien MM, Wu JF, Ni YH, et al. *Plectin mutations in progressive intrahepatic cholestasis*. Hepatology 2019 Jul 3. doi: 10.1002/hep.30841.

[Epub ahead of print]

Chen HL, **Wu SH**, Hsu SH, Liou BY, Chen HL, Chang MH. *Jaundice revisited: recent advances in the diagnosis and treatment of inherited cholestatic liver diseases*. J Biomed Sci 2018;25:75. **(Review article)**

Chen HL, Li HY, Wu JF, **Wu SH**, Chen HL, Yang YH, et al. *Panel-Based Next-Generation Sequencing for the Diagnosis of Cholestatic Genetic Liver Diseases: Clinical Utility and Challenges*. J Pediatr 2018.

Wu SH, Chen HL, Chen YH, Chien CS, Chen HL, and Chang MH. *Charged multivesicular protein 5, a newly identified bile salt transport pump (BSEP)-interacting protein, involves the membrane targeting of BSEP*. ESPGHAN 2017 Monothematic Conference: Familial Cholestasis. Budapest, Hungary **(Conference Poster)**

Chien CS, Chen YH, Chen HL, Wang CP, **Wu SH**, Ho SL, et al. *Cells responsible for liver mass regeneration in rats with 2-acetylaminofluorene/partial hepatectomy injury*. J Biomed Sci 2018;25:39.

Chen YH, Chen HL, Chien CS, **Wu SH**, Ho YT, Yu CH, Chang MH. *Contribution of Mature Hepatocytes to Biliary Regeneration in Rats with Acute and Chronic Biliary Injury*. PLoS One 2015;10:e0134327.

Chen YH, Chang MH, Chien CS, **Wu SH**, Yu CH, Chen HL. *Contribution of mature hepatocytes to small hepatocyte-like progenitor cells in retrorsine-exposed rats with chimeric livers*. Hepatology 2013;57:1215-1224.

Chen HL, Chen HL, Yuan RH, **Wu SH**, Chen YH, Chien CS, et al. *Hepatocyte transplantation in bile salt export pump-deficient mice: selective growth advantage of donor hepatocytes under bile acid stress*. J Cell Mol Med 2012;16:2679-2689.



Abbreviations

| | |
|-------------|---|
| 3-AT | 3-amino-1,2,4-triazole |
| 5-NT | 5-nucleotidase |
| a.a. | Amino acid |
| ABC | ATP-binding cassette |
| ABCG2 | ATP-binding cassette transporter G2 |
| ABCG5/G8 | ATP-binding cassette transporters G5/G8 |
| ALT | Alanine transaminase |
| ASBT | Apical sodium-dependent bile acid transporter |
| AST | Aspartate transaminase |
| ATP8B1 | ATPase phospholipid transporting 8B1 |
| BAs | Bile acids |
| BAT1 | Bile acid transporter 1 |
| BRIC | Benign recurrent intrahepatic cholestasis |
| BSEP/Bsep | Bile salt export pump |
| CA | Cholic acid |
| cBAT | Canalicular bile acid transporter |
| CDC | Chenodeoxycholate |
| CDCA | Chenodeoxycholic acid |
| CFTR | Cystic fibrosis conductance transmembrane regulator |
| CHMP5/Chmp5 | Charged multivesicular body protein 5 |
| cLPM | Canalicular membrane vesicle prepared from the livers |
| COPA | Coatomer protein complex subunit α |
| CYP | Cytochrome P450 enzymes |
| DCA | Deoxycholic acid |
| DO | Dropout solution. |
| DPPIV | Dipeptidyl peptidase IV |
| ER | Endoplasmic reticulum |
| ESCRT | Endosomal sorting complexes required for transport |
| FXR | Farnesoid X receptor |
| GCDC | Glycochenodeoxycholate |
| GC | Glycocholate |
| GGT | Gamma-glutamyl transferase |

| | |
|--------------------|---|
| GPI | Glycosyl-phosphatidylinositol |
| HA | Haemagglutinin |
| HAX1 | HCLS1-associated protein X-1 |
| HBA1 | Hemoglobin, alpha 1 |
| HBG1 | Hemoglobin subunit gamma-1 |
| HKDC1 | Hexokinase domain containing 1 |
| K8 | Keratin/cytokeratin 8 |
| K18 | Keratin/cytokeratin 18 |
| KO | Knockout |
| LCA | Lithocholic acid |
| mBsep | Mouse/murine Bsep |
| MDR1/Mdr1 | Multidrug resistance protein 1/P-glycoprotein 1 |
| MDR3 | Multidrug resistance protein 3/P-glycoprotein 3 |
| MLC2 | Non-muscle myosin II regulatory light chain |
| MRCP | Magnetic resonance cholangio-pancreatography |
| MRP2 | Multidrug resistance-associated protein 2/cMOAT/ABCC2 |
| MTOC | Microtubule-organizing center |
| mTOR | Mammalian target of rapamycin |
| MVB | Multivesicular body |
| NBF | Nucleotide-binding fold |
| NC | Nitrocellulose membrane |
| NTCP | Na ⁺ -taurocholate co-transporting polypeptide |
| OATP1B1/3 | Organic-anion-transporting polypeptide 1B1/3 |
| OM | Organelle-membrane |
| ORF | Open-reading frame |
| OST α/β | Organic solute transporter α/β |
| PC | Phosphatidylcholine |
| PFIC | Progressive familial intrahepatic cholestasis |
| P-gp | P-glycoprotein |
| pIgA-R | Polymeric immunoglobulin A receptor |
| PLEC/Plec | Plectin |
| PM | Plasma membrane |



| | |
|--------------|--|
| rBsep | Rat Bsep |
| RXR | Retinoid X receptor |
| SAC | Subapical compartment |
| ScyS | Scymnol sulfate |
| SERPINA1 | Serpin peptidase inhibitor clade A (SERPINA) member 1 |
| SERPINA3 | Serpin peptidase inhibitor clade A (SERPINA) member 3 |
| sh-Chmp5 | shRNA against mouse Chmp5 |
| SH3 | SRC homology 3 |
| shRNA | short hairpin RNA |
| si-CHMP5 | Pre-designed siRNA pool targeting human <i>CHMP5</i> |
| si-CTL | Pre-designed siRNA pool of non-targeting control |
| siRNA | small interference RNA |
| sBsep | Skate Bsep |
| Spgp | Sister gene of P-glycoprotein |
| TC | Taurocholate |
| TCDC | Taurochenodeoxycholate |
| TDC | Taurodeoxycholate |
| TGN | <i>Trans</i> -Golgi network |
| TGR5 | Takeda G-protein-coupled receptor 5/G protein-coupled bile acid receptor 1 |
| tM | Total membrane-protein |
| TUDC | Tauroursodeoxycholate |
| Ub | Ubiquitin |
| UDCA | Ursodeoxycholic acid |
| UGT-1A | Uridine diphosphoglucuronosyltransferase 1A1 |
| X-gal | 5-Bromo-4-chloro-3-indolyl- β -D-galactopyranoside |
| YFP | Yellow fluorescence protein |
| YNB | Yeast Nitrogen Base |
| ZO-1 | Zona occludens 1 |
| β -DDM | n-Dodecyl β -D-maltoside |
| β -gal | β -Galactosidase |

